DISTRIBUTED INTELLIGENT SPECTRUM MANAGEMENT IN COGNITIVE RADIO AD HOC NETWORKS

by

Yi Song

A dissertation submitted to the faculty of
The University of North Carolina at Charlotte
in partial fulfillment of the requirements
for the degree of Doctor of Philosophy in
Electrical Engineering

Charlotte

2013

Approved by:

Dr. Jiang (Linda) Xie

Dr. Asis Nasipuri

Dr. Yu Wang

Dr. Wensheng Wu

© 2013
Yi Song
ALL RIGHTS RESERVED

ABSTRACT

YI SONG. Distributed intelligent spectrum management in cognitive radio ad hoc networks.
(Under the direction of DR. JIANG (LINDA) XIE)

The rapid growth of the number of wireless devices has brought an exponential increase in the demand of the radio spectrum. However, according to the Federal Communications Commission (FCC), almost all the radio spectrum for wireless communications has already been allocated. In addition, according to FCC, up to 85% of the allocated spectrum is underutilized due to the current fixed spectrum allocation policy. To alleviate the spectrum scarcity problem, FCC has suggested a new paradigm for dynamically accessing the allocated spectrum. Cognitive radio (CR) technology has emerged as a promising solution to realize dynamic spectrum access (DSA). With the capability of sensing the frequency bands in a time and location-varying spectrum environment and adjusting the operating parameters based on the sensing outcome, CR technology allows an unlicensed user to exploit the licensed channels which are not used by licensed users in an opportunistic manner.

In this dissertation, distributed intelligent spectrum management in CR ad hoc networks is explored. In particular, four spectrum management issues in CR ad hoc networks are investigated: 1) distributed broadcasting in CR ad hoc networks; 2) distributed optimal HELLO message exchange in CR ad hoc networks; 3) distributed protocol to defend a particular network security attack in CR ad hoc networks; and 4) distributed spectrum handoff protocol in CR ad hoc networks. The research in this dissertation has fundamental impact on CR ad hoc network establishment, network functionality, network security, and network performance. In addition, many of the unique challenges of distributed intelligent spectrum management in CR ad hoc networks are addressed for the first time in this dissertation. These challenges are extremely difficult to solve due to the dynamic spectrum environment and they

have significant effects on network functionality and performance. This dissertation is essential for establishing a CR ad hoc network and realizing networking protocols for seamless communications in CR ad hoc networks. Furthermore, this dissertation provides critical theoretical insights for future designs in CR ad hoc networks.

ACKNOWLEDGMENTS

I would like to express my greatest and deepest gratitude to my advisor, Professor Linda Xie, for her guidance and supervision throughout these years. Without her, I would not be where I am today. I consider myself a super-lucky person to have her as my Ph.D. advisor. Not only as an independent researcher, but also as a socially mature person, I have learned a lot from her. Professor Xie, thank you very much for your faith in me even though I have doubted myself a million times.

I would also like to thank my committee members: Dr. Asis Nasipuri, Dr. Yu Wang, and Dr. Wensheng Wu for their time and advice.

This work is dedicated to my beloved parents: Ruoqin Chen and Hanqiao Song, who have always been giving me strength when I am down.

TABLE OF CONTENTS

CHAPTER 1: INTRODUCTION 1

1.1 Background on CR Networks 2

1.2 Broadcasting in CR Ad Hoc Networks 3

1.2.1 Distributed Broadcast Protocols in CR Ad Hoc Networks 3

1.2.2 Analysis of Broadcast Protocols in CR Ad Hoc Networks 6

1.3 Optimal HELLO Message Exchange Scheme in CR Ad Hoc Networks 8

1.4 Fighting Against the FCIE Attacks in CRAHNs 11

1.5 Spectrum Handoff in CR Ad Hoc Networks 13

1.5.1 Proactive Spectrum Handoff Framework in CRAHNs 14

1.5.2 Analysis of Spectrum Handoff in CR Ad Hoc Networks 15

1.6 Overview of the Proposed Intelligent Spectrum Management 17

CHAPTER 2: RELATED WORK 21

2.1 Existing Broadcast Protocols in CRNs 21

2.2 Existing Analytical Model for Broadcast Protocols in CRNs 22

2.3 Background on HELLO Message Exchange 22

2.4 Existing Security Schemes to Defend FCIE Attacks in CRNs 24

2.5 Existing Spectrum Handoff Protocols in CRNs 25

2.6 Existing Analytical Models for Spectrum Handoff in CRNs 26

CHAPTER 3: DISTRIBUTED BROADCAST PROTOCOLS IN CRAHNS 28

3.1 Network Model 28

3.2 Exploring Broadcast Design in CRNs 29

3.2.1 Random Broadcast Scheme 30

3.2.2 Full Broadcast Scheme 31

3.2.3 Remarks 32

3.3 The Basic QB^2IC Scheme 33

3.3.1 The Single-hop Scenario 33
3.3.2 The Multi-hop Scenario 36
3.4 The Enhanced QB^2IC Scheme 38
3.4.1 Analysis of the Channel Availability 38
3.4.2 The Enhanced QB^2IC Scheme 41
3.5 Performance Evaluation 42
3.5.1 The Impact of the Number of SUs and PUs 44
3.5.2 The Impact of the Number of Channels 46
3.5.3 The Impact of the Channel Availability Variation 47
3.5.4 The Impact of Transmission Errors 48
3.6 The Proposed BRACER Protocol 49
3.6.1 Construction of the Broadcasting Sequences 51
3.6.2 The Distributed Broadcast Scheduling Scheme 55
3.6.3 The Broadcast Collision Avoidance Scheme 57
3.6.4 Protocol Flow Chart 61
3.7 The Derivation of the Value of w 62
3.7.1 The Network Model 62
3.7.2 The Derivation of the Value of w 63
3.8 Discussion on the Proposed BRACER Protocol 69
3.8.1 2-hop Location Information 69
3.8.2 Time Synchronization 70
3.9 Performance Evaluation 73
3.9.1 Successful Broadcast Ratio 74
3.9.2 Average Broadcast Delay 75
3.9.3 The Impact of Unsynchronized Time Slots 77
3.9.4 Broadcast Collision Analysis 80
3.9.5 Overhead Analysis 81

CHAPTER 4: ANALYTICAL MODEL FOR BROADCASTS IN CRAHNS 84
4.1 Calculating the Successful Broadcast Ratio 85
4.1.1 The Unique Challenge 85
4.1.2 The Proposed Algorithm 88
4.1.3 An Illustrative Example 90
4.2 Calculating the Average Broadcast Delay 91
4.2.1 The Unique Challenge 92
4.2.2 The Proposed Algorithm 92
4.2.3 An Illustrative Example 96
4.3 Broadcasting in CR Ad Hoc Networks 97
4.3.1 Random Broadcast Scheme 97
4.3.2 QoS-based Broadcast Scheme 100
4.3.3 Distributed Broadcast Scheme 104
4.4 Performance Evaluation 107
4.4.1 Validating Analysis using Hardware Implementation 107
4.4.2 Validating Analysis using Simulation 109
4.4.3 System Parameter Design using the Proposed Analytical Model 114
CHAPTER 5: OPTIMAL HELLO EXCHANGE SCHEME IN CRAHNS 116
5.1 Network Model 117
5.2 The Optimal HELLO Exchange Protocol for Static CRAHNs 117
5.2.1 Problem Formulation 118
5.2.2 The Derivation of SU Throughput 119
5.2.3 The Derivation of the Average SU Waiting Time 123
5.2.4 The Derivation of the Average Channel Busy Duration 124
5.3 The Optimal HELLO Exchange Protocol for Mobile CRAHNs 127
5.3.1 The Adaptive Optimal HELLO Exchange in Mobile CRAHNs 127
5.3.2 The Supplementary HELLO Message Update Scheme 128

5.4 Performance Evaluation 131
5.4.1 Static CR Ad Hoc Networks 132
5.4.2 Mobile CR Ad Hoc Networks 134
CHAPTER 6: SECURITY SCHEMES FOR FCIE ATTACKS IN CRAHNS 136
6.1 The Spatial Correlation of the Channel Availability 136
6.1.1 The Network Model 136
6.1.2 The Spatial Correlation of the Channel Availability 137
6.2 The Proposed Algorithm to Fight Against FCIE Attacks 141
6.2.1 The Basic Approach 142
6.2.2 The Improved Approach with the Assistance of an Honest Node 144
6.3 Performance Evaluation 145
CHAPTER 7: SPECTRUM HANDOFF PROTOCOLS IN CRAHNS 149
7.1 Network Coordination and Assumptions 149
7.1.1 Single Rendezvous Coordination Scheme 149
7.1.2 Multiple Rendezvous Coordination Scheme 150
7.2 Proposed Proactive Spectrum Handoff Protocol 153
7.2.1 Proposed Spectrum Handoff Criteria and Policies 153
7.2.2 Proposed Spectrum Handoff Protocol Details 157
7.3 Distributed Channel Selection Algorithm 162
7.3.1 Procedure of the Proposed Channel Selection Algorithm 162
7.3.2 Fairness of the Proposed Channel Selection Algorithm 165
7.3.3 Scalability of the Proposed Channel Selection Algorithm 166
7.4 Performance Evaluation 166
7.4.1 Simulation Setup 167
7.4.2 Spectrum Handoff Criteria for Biased-Geometric Traffic 168
7.4.3 Spectrum Handoff Criteria for Pareto Traffic 169
7.4.4 The Proposed Proactive Spectrum Handoff Scheme 170

7.4.5 The Proposed Distributed Channel Selection Scheme 176
CHAPTER 8: ANALYSIS ON SPECTRUM HANDOFFS IN CRAHNS 182
8.1 Spectrum Handoff Process 182
8.2 The Proposed Three Dimensional Discrete-time Markov Model 183
8.2.1 The Proposed Markov Model 183
8.2.2 Derivation of Steady-State Probabilities 186
8.2.3 The Probability that at Least One Channel is Idle 190
8.3 The Impact of Different Channel Selection Schemes 191
8.3.1 Random Channel Selection 192
8.3.2 Greedy Channel Selection 196
8.3.3 Pseudo-Random Selecting Sequence based Channel Selection 197
8.3.4 Results Validation 197
8.4 The Impact of Spectrum Sensing Delay 198
8.4.1 Results Validation 200
8.5 Performance Evaluation 201
8.5.1 Collision Probability between SUs and PUs 201
8.5.2 Average Spectrum Handoff Delay 202
CHAPTER 9: END-TO-END CONGESTION CONTROL IN CRAHNS 203
9.1 End-to-End Congestion Control Framework in Multi-hop CRAHNs 207
9.1.1 Related Work 207
9.1.2 End-to-End Congestion Control Framework 208
9.2 Challenges of End-to-End Congestion Control in Multi-hop CRAHNs 211
9.2.1 Network Scenario 211
9.2.2 Challenges of End-to-End Congestion Control 212
9.3 Performance Evaluation 217
9.3.1 Performance of Packet Delay Variation 217
9.3.2 Impact of Channel Errors on Network Performance 218

CHAPTER 10: OPTIMAL POWER CONTROL FOR CRAHNS 220
10.1 System Model and Problem Formulation 222
10.2 Optimal Power Control 224
10.2.1 Feasibility of Optimal Power Control 224
10.2.2 Optimal Power Control for Mobility Scenarios 227
10.2.3 Shadowing Fading Effect 229
10.3 Performance Results 230
10.3.1 Simulation Parameters 230
10.3.2 Simulation Results 231
CHAPTER 11: CONCLUSION 236
11.1 Conclusions 236
11.1.1 Completed Work 239
11.2 Future Work 240
REFERENCES 242
APPENDIX A: PUBLISHED AND SUBMITTED WORKS 254

CHAPTER 1: INTRODUCTION

The rapid growth of the number of wireless devices has brought an exponential increase in the demand of the radio spectrum. However, according to the Federal Communications Commission (FCC), almost all the radio spectrum for wireless communications has already been allocated. In addition, according to FCC, up to 85% of the allocated spectrum is underutilized due to the current fixed spectrum allocation policy [1]. In order to alleviate the spectrum scarcity problem and to overcome the imbalance between the increase in the spectrum access demand and the inefficiency in the spectrum usage, FCC has suggested a new paradigm for dynamically accessing the allocated spectrum [2].

Cognitive radio (CR) technology has emerged as a promising solution to realize dynamic spectrum access (DSA) [3]. Since CR networks are overlaid with a legacy network, there are two types of users in the CR networks: 1) licensed user (or, primary user) who has a license to operate in a certain spectrum band in the legacy network and 2) unlicensed user (or, secondary user) who has no spectrum license to use the spectrum. The access of primary users (PUs) should not be affected by the operations of any secondary user (SU). With the capability of sensing the frequency bands in a time and location-varying spectrum environment and adjusting the operating parameters based on the sensing outcome, CR technology allows a SU to exploit the licensed channels which are not used by primary users in an opportunistic manner [4]. SUs can either form a CR infrastructure-based network or a CR ad hoc network. Recently, CR ad hoc networks have attracted plentiful research attention due to their various applications [5].

1.1 Background on CR Networks

Since SUs need to access the licensed spectrum adaptively, new functionalities are required in CR networks to support this adaptivity [4]. Specifically, the main functionalities for CR networks can be summarized as follows:

1) Spectrum sensing: SUs can sense the unused spectrum and utilize it without harmful interference to PUs. It is an important requirement of CR networks to sense the "spectrum holes". Detecting PUs is the most efficient way to detect "spectrum holes". Spectrum sensing techniques can be classified into three categories: 1) primary transmitter detection: CRs must have the capability to determine a signal from a primary transmitter [6], 2) cooperative spectrum sensing: multiple SUs share sensing information with each other and incorporate for PU detection [7], and 3) interference based detection [8].

2) Spectrum management: SUs capture the best available spectrum to meet communication requirements while not creating harmful interference to other PUs. CRs should decide on the best spectrum band to meet the Quality-of-Service (QoS) requirements over all available spectrum bands, therefore spectrum management functions are required for CRs. These management functions can be classified as: 1) spectrum analysis [4] and 2) spectrum decision.

3) Spectrum mobility: SUs change its operating frequency based on its radio environment. CR technology aims to use the licensed spectrum in a dynamic manner by allowing SUs to operate in the best available frequency band, while maintaining seamless communication requirements during the transition to a better spectrum. This brings about a new type of handoff called spectrum handoff, which refers to the process that a SU determines and switches to a new available channel to continue the transmission when the current spectrum is not available. Based on the moment when the spectrum handoff is carried out, two types of spectrum mobility are introduced: 1) reactive approach and 2) proactive approach.

4) Spectrum sharing: SUs provide a fair spectrum scheduling method. One of the major challenges in open spectrum usage is the spectrum sharing. It can be regarded as the media access control (MAC) issues in existing wireless networks.

Currently, spectrum sensing and spectrum sharing have been studied extensively in the research community [4]. However, spectrum management still lacks sufficient research efforts. In this dissertation, four spectrum management issues in CR ad hoc networks are investigated: 1) distributed broadcasting in CR ad hoc networks; 2) distributed optimal HELLO message exchange in CR ad hoc networks; 3) distributed protocol to defend a particular network security attack in CR ad hoc networks; and 4) distributed spectrum handoff protocol in CR ad hoc networks. This dissertation has fundamental impact on CR ad hoc network establishment, network functionality, network security, and network performance. In addition, many of the unique challenges of distributed intelligent spectrum management in CR ad hoc networks are addressed for the first time in this dissertation. These challenges are extremely difficult to solve due to the dynamic spectrum environment and they have significant effects on network functionality and performance. This dissertation is essential for establishing a CR ad hoc network and realizing networking protocols for seamless communications in CR ad hoc networks. Furthermore, this dissertation provides critical theoretical insights for future designs in CR ad hoc networks.

1.2 Broadcasting in CR Ad Hoc Networks

1.2.1 Distributed Broadcast Protocols in CR Ad Hoc Networks

We first consider the broadcasting issue in CR ad hoc networks. When a CR ad hoc network is initially deployed, each SU only acquires its local network information (e.g., its own channel availability information). Before any control information is exchanged, SUs are unaware of the network information of any other user. However, many networking protocols in CR ad hoc network, such as unicast routing protocols, require certain network information in order to be realized. Therefore, SUs need

to exchange the network information with other nodes. This control information is often sent out as network-wide broadcasts, messages that are sent to all other nodes in a network. In addition, some exigent data packets such as emergency messages and alarm signals are also delivered as network-wide broadcasts [9]. Due to the importance of the broadcast operation, in this research, we address the broadcasting issue in multi-hop CR ad hoc networks. Since broadcast messages often need to be disseminated to all destinations as quickly as possible, we aim to achieve very high successful broadcast ratio and very short broadcast delay.

The broadcasting issue has been studied extensively in traditional ad hoc networks [10, 11, 12, 13]. However, unlike traditional single-channel or multi-channel ad hoc networks where the channel availability is uniform, in CR ad hoc networks, different SUs may acquire different sets of available channels. This non-uniform channel availability imposes special design challenges for broadcasting in CR ad hoc networks. First of all, for traditional single-channel and multi-channel ad hoc networks, due to the uniformity of channel availability, all nodes can tune to the same channel. Thus, broadcast messages can be conveyed through a single common channel which can be heard by all nodes in a network. However, in CR ad hoc networks, the availability of a common channel for all nodes may not exist. More importantly, before any control information is exchanged, a SU is unaware of the available channels of its neighboring nodes. Therefore, broadcasting messages on a global common channel is not feasible in CR ad hoc networks.

To further illustrate the challenges of broadcasting in CR ad hoc networks, we consider a single-hop scenario shown in Figure 1.1(a), where node A is the source node. For traditional single-channel and multi-channel ad hoc networks, as shown in Figure 1.1(a), nodes can tune to the same channel (e.g., channel 1) for broadcasting. Thus, node A only needs one time slot to let all its neighboring nodes receive the broadcast message in an error-free environment. However, in CR ad hoc networks

where the channel availability is heterogeneous and SUs are unaware of the available channels of each other, as shown in Figure 1.1(b), node A may have to use multiple channels for broadcasting and may not be able to finish the broadcast within one time slot. In fact, the exact broadcast delay for all single-hop neighboring nodes to successfully receive the broadcast message in CR ad hoc networks relies on various factors (e.g., channel availability and the number of neighboring nodes) and it is random.

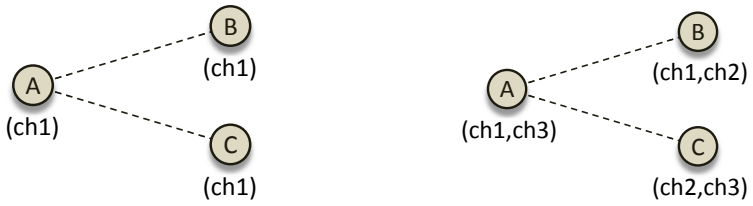

(a) Traditional ad hoc networks.

(b) CR ad hoc networks.

Figure 1.1: The single-hop broadcast scenario.

Furthermore, since multiple channels may be used for broadcasting and the exact time for all single-hop neighboring nodes to successfully receive the broadcast message is random, to avoid broadcast collisions (i.e., a node receives multiple copies of the broadcast message simultaneously) is much more complicated in CR ad hoc networks, as compared to traditional ad hoc networks. In traditional ad hoc networks, numerous broadcast scheduling schemes are proposed to reduce the probability of broadcast collisions while optimizing the network performance [14, 15, 16, 17, 18, 19]. All these proposals are on the basis that all nodes use a single channel for broadcasting and the exact delay for a single-hop broadcast is one time slot. However, in CR ad hoc networks, without the information about the channel used for broadcasting and the exact delay for a single-hop broadcast, to predict when and on which channel a broadcast collision occurs is extremely difficult. Hence, to design a broadcast protocol which can avoid broadcast collisions, as well as provide high successful broadcast ratio and short broadcast delay is a very challenging issue for multi-hop CR ad hoc networks under practical scenarios. Simply extending existing broadcast protocols to CR ad

hoc networks cannot yield the optimal performance.

1.2.2 Analysis of Broadcast Protocols in CR Ad Hoc Networks

In addition, we also study the performance analysis of broadcast protocols in CR ad hoc networks. Even though the broadcasting issue has been studied extensively in traditional mobile ad hoc networks (MANETs) [10, 20, 11, 12, 13], research on broadcasting in multi-hop CR ad hoc networks is still in its infant stage. There are a few papers addressing the broadcasting issue in multi-hop CR ad hoc networks [21, 22, 23, 24]. However, these proposals mainly focus on broadcast protocol designs. The performance analysis of these proposed protocols is simulation-based. Thus, the analytical relationship between these proposals and their performance is not known. More importantly, without analytical analysis, the system parameters in these protocols are not designed to achieve the optimal performance. In fact, analytical analysis is beneficial not only for better understanding the nature of a proposed protocol, but also for better designing the system parameters of a protocol to achieve the optimal performance. It can also provide useful insights to guide the future broadcast protocol designs in CR ad hoc networks. Hence, in this research, we focus on the analytical analysis of broadcast protocols for multi-hop CR ad hoc networks.

Although a vast amount of analytical works on broadcast protocols in traditional MANETs exist [25, 26, 27, 28, 29], currently, there is no analytical work on broadcast protocols in multi-hop CR ad hoc networks. More importantly, all the methods proposed for traditional MANETs cannot be simply applied to multi-hop CR ad hoc networks. This is because that in traditional MANETs, the channel availability is uniform for all nodes, as shown in Figure 1.1(a). However, in CR ad hoc networks, different secondary users (SUs) may acquire different available channel sets, depending on the locations and traffic of primary users (PUs), as shown in Figure 1.1(b). This non-uniform channel availability leads to several significant differences and causes unique challenges when analyzing the performance of broadcast protocols in CR ad

hoc networks.

First of all, unlike in traditional MANETs, in CR ad hoc networks, the single-hop broadcast is not always successful in an error-free environment. The reason can be illustrated using Figure 1.1. If node A is the source node, in traditional MANETs, all its neighboring nodes can tune to the same channel to receive the broadcast message. However, in CR ad hoc networks, such a common available channel for all neighboring nodes may not exist [30, 31, 32, 33, 34]. As a result, the broadcast may fail. More severely, even if a common available channel exists between the source node and its neighboring nodes, they may not be able to tune to that channel at the same time, which will also result in a failed broadcast. In fact, whether the single-hop broadcast is successful depends on the channel availability of each SU which is time-varying and location-varying. Due to the uncertainty of the single-hop broadcast success, the successful broadcast ratio of a network is usually random. Furthermore, since there usually exist multiple message propagation scenarios for all the nodes to successfully receive the broadcast message in a multi-hop CR ad hoc network, it is extremely challenging to identify every possible message propagation scenario for calculating the successful broadcast ratio in a complicated network. An example illustrating this challenge will be given in Section 4.1.1.

Secondly, different from traditional MANETs where the relative locations of the communication pair do not impact the successful receipt of the message as long as they are within the transmission range of each other, in CR ad hoc networks, the probability that a node successfully receives a broadcast message is affected by the relative locations between the sender and the receiver. This is because that the available channels of a SU are obtained based on the sensing outcome from the proximity of the node. Thus, SU nodes that are close to each other have similar available channels and they may have higher successful broadcast ratio, as compared with the SU nodes far away from each other whose available channels are often less similar. These

two differences show that the successful broadcast ratio is affected by various factors and it is random. Currently, there is no straightforward solution to analyze this issue.

Thirdly, the single-hop broadcast delay is usually more than one time slot in CR ad hoc networks, while in traditional MANETs, it is always one time slot. As shown in Figure 1.1(a), node A only needs one time slot to let all its neighboring nodes receive the broadcast message in an error-free environment. However, in CR ad hoc networks, due to the non-uniform channel availability, node A may have to use multiple channels for broadcasting and may not be able to finish the broadcast within one time slot. In fact, the exact broadcast delay for all single-hop neighboring nodes to successfully receive the broadcast message in CR ad hoc networks relies on various factors (e.g., channel availability and the number of neighboring nodes) and it is also random. Moreover, since there may exist multiple message propagation scenarios, to identify which node is the last node in a network to receive the message is very difficult. Thus, the multi-hop broadcast delay is extremely difficult to obtain.

Finally, broadcast collisions are complicated in CR ad hoc networks. Unlike in traditional MANETs where nodes use a common channel for broadcasting, in CR ad hoc networks, nodes may use multiple channels for broadcasting. Without the information about the channel used for broadcasting and the exact delay for a single-hop broadcast, to predict when and on which channel a broadcast collision occurs is extremely difficult. Hence, to mathematically analyze broadcast collisions is very challenging for multi-hop CR ad hoc networks under practical scenarios.

1.3 Optimal HELLO Message Exchange Scheme in CR Ad Hoc Networks

Secondly, we explore the optimal HELLO message exchange issue in CR ad hoc networks. In CR networks, since secondary users (SUs) can only utilize the spectrum when primary users (PUs) are absent, several new functionalities are introduced to increase the spectrum utilization of SUs while avoiding harmful interference to PUs (e.g., spectrum sensing, spectrum sharing, and spectrum mobility [4]). Currently,

research on these functionalities is mostly conducted independently. Very little work has been focused on the interconnection between these functionalities. Figure 1.2 shows how the main functionalities in CR networks are interconnected. One essential component to link these functionalities: control information exchange between SUs, such as spectrum availability information and neighborhood information, is often ignored. However, due to the dynamically changing radio environment of mobile CR ad hoc networks, control information is crucial for networking designs and should be updated in a timely manner to avoid it becoming obsolete. Without such control information update, some networking protocols cannot even be realized. In most networking protocols, control information is often broadcasted to all the neighboring nodes of a SU via periodic updates (e.g., periodic HELLO or beacon messages). Therefore, in this research, we study the design of HELLO message exchange for updating control information in mobile CR ad hoc networks.

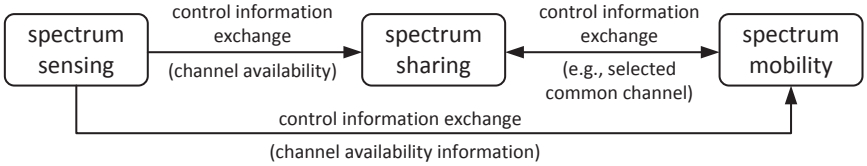

Figure 1.2: The interconnection between the main functionalities in CR networks.

HELLO messages (or, beacon messages) are a fundamental component in both wired and wireless networks. In this research, a HELLO message is not only for node announcement as in some reactive routing protocols [35], but also a control packet that contains important control information (i.e., spectrum availability of SUs, neighborhood relationship, node locations, etc.). In traditional mobile ad hoc networks (MANETs), periodic HELLO message exchange among neighboring nodes helps them to establish and maintain up-to-date neighborhood tables and to cope with any change in the network topology for many networking protocols (e.g., proactive routing protocols [36][37]). However, in mobile CR ad hoc networks, besides the conventional change in the network topology and neighborhood relationship, changes

in SU spectrum availability also occur due to either PU traffic or SU mobility. Hence, the freshness and consistency of the control information has a significant impact on the realization of many networking protocols in CR ad hoc networks [38, 39, 40, 41].

Currently, there is no existing work on the HELLO message exchange protocol design either in static or mobile CR ad hoc networks. In this research, we investigate the optimal HELLO message exchange protocol in mobile CR ad hoc networks. To address this issue, two questions need to be answered: 1) how often should a SU broadcast a HELLO message? and 2) how to guarantee all neighboring nodes to receive the HELLO message from the sender? The second question is related to channel rendezvous schemes, which can be addressed by existing protocols [42, 31, 30, 33, 34, 24]. Thus, in the rest of this research, we mainly investigate the first question.

To design a proper HELLO message exchange interval for mobile CR ad hoc networks is very challenging. If the HELLO message exchange interval is too long, control information is likely to become out-dated before the next update. Thus, network performance may suffer degradation due to the out-dated control information. On the other hand, if the HELLO message exchange interval is too short, control information is always up-to-date. However, the control overhead is essentially increased. Hence, there exists a trade-off between the freshness and consistency of the control information maintained by each SU and the control overhead. Moreover, this trade-off is affected by many factors, e.g., PU traffic, SU traffic, SU node speed, and SU node locations that may also be time-varying, which makes this issue extremely challenging.

Even though a few papers have addressed the HELLO message exchange issue in traditional MANETs [43, 44, 45, 46], the methods used in traditional MANETs cannot be simply applied to mobile CR ad hoc networks because of the following two reasons. First of all, in traditional MANETs, the channel availability of every node

is uniform and fixed. The HELLO message exchange design only needs to consider changes in the node connectivity and neighborhood relationship affected by node mobility, but not the channel availability. However, in mobile CR ad hoc networks, the channel availability of each SU is non-uniform and time-varying. Therefore, in addition to the node connectivity and neighborhood relationship, any change in the channel availability of each SU also needs to be considered in the HELLO message exchange protocol design. More severely, SU node mobility may also cause a change in the channel availability since a SU may move to an area where some channels are no longer available due to the presence of PUs, which is also different from traditional MANETs.

Secondly, in traditional MANETs, since all nodes use a common control channel (CCC) for control message exchange, the duration for broadcasting a single HELLO message among neighboring nodes is always one time slot. This duration is often negligible as compared to the HELLO message exchange interval. Thus, the effect of the control message broadcast duration is often ignored. However, in mobile CR ad hoc networks, due to the non-uniform spectrum availability and the lack of a common control channel, the duration for broadcasting a single HELLO message is usually more than one time slot [42, 31, 30, 33, 34, 24]. That is, a SU may need to broadcast a HELLO message multiple times in order to ensure that the message is successfully received by all its neighbors, which further increases the control overhead. Thus, this HELLO message broadcast duration could essentially deteriorate network performance and cannot be ignored in the optimal HELLO message protocol design in mobile CR ad hoc networks.

1.4 Fighting Against the FCIE Attacks in CRAHNs

Thirdly, after the CR network is established, the security issue is also extremely important. In the last decade, most of the research efforts in CR networks focus on pure physical layer or higher layer issues (e.g., spectrum sensing techniques and

spectrum management schemes) without considering the security aspects. The security issues in CR networks have drawn the attention of the research community only in recent years [47][48]. Since CRs can intelligently adapt to their radio environment, many unique security threats are introduced in CR networks. In [47], based on the goals of the attack, three types of unique attacks in CR networks are defined: 1) dynamic spectrum access attack: an adversary mimics the signal of a primary user (PU), causing legitimate secondary users (SUs) to trigger a false positive in the spectrum sensing algorithm (e.g., the primary user emulation attack [49]); 2) belief manipulation attack: an adversary reports false information in the network, causing the learning capability of legitimate SUs to induce disadvantageous decisions (e.g., the spectrum sensing data falsification attack [50]); and 3) malicious traffic injection attack: an adversary injects malicious traffic to deteriorate the performance of CR networks (e.g., the communication jamming attack [51]).

In this research, we focus on a new security threat which belongs to the second category called the false channel information exchange (FCIE) attack in CR ad hoc networks. In a CR ad hoc network, channel availability information is essential for the realization of many networking protocols (e.g., channel rendezvous protocols [30, 52, 24] and routing protocols [53]). In these networking protocols, each node often needs to know its own channel information as well as the channel information of other nodes. If a malicious SU sends out the false channel information to its neighboring nodes, the victim SUs may make incorrect decisions about other nodes and are not able to execute these networking protocols properly. For instance, if a channel is available but claimed to be unavailable by a malicious SU, the victim SUs cannot use this channel for communications, thus it is wasted. Therefore, the network performance of the secondary network suffers significant degradation. On the other hand, if a channel is unavailable but claimed to be available, transmitting packets on this channel may cause harmful interference to PUs, which is also disadvantageous to the

legacy network.

The FCIE attack will not only significantly deteriorate network performance, but also induce great difficulties to defend against this attack. As discussed above, although the interference to PUs may be observed from failed data transmissions, the waste of available channels is extremely difficult to realize, which is more destructive to CR networks. Therefore, a mechanism is needed to identify the existence of the malicious SUs and fight against this attack. A networking authentication protocol can only guarantee the identity of an unknown node. However, it cannot distinguish the authenticity of the information in a packet. In addition, since the channel availability of SUs in CR networks is non-uniform, which is different from traditional wireless networks, no prior security schemes to detect false information in traditional wireless networks can defend against the FCIE attacks in CR networks.

1.5 Spectrum Handoff in CR Ad Hoc Networks

Finally, after the control information is exchanged among SUs, the networking protocols in CR ad hoc networks can be realized. Then, SUs are able to communicate with each other properly. However, since the spectrum availability dynamically changes with the behavior of PUs, SUs are required to adaptively adjust its own operating parameters to handle those spectrum availability changes. As discussed above, one of the most important functionalities of CR networks is spectrum mobility, which enables SUs to change the operating frequencies based on the availability of the spectrum. Spectrum mobility gives rise to a new type of handoff called spectrum handoff, which refers to the process that when the current channel used by a SU is no longer available, the SU needs to pause its on-going transmission, vacate that channel, and determine a new available channel to continue the transmission. Compared with other functionalities (spectrum sensing, spectrum management, and spectrum sharing) [4] of CR networks, spectrum mobility is less explored in the research community. However, due to the randomness of the appearance of PUs, it is

extremely difficult to achieve fast and smooth spectrum transition leading to minimum interference to legacy users and performance degradation of secondary users during a spectrum handoff. This problem becomes even more challenging in ad hoc networks where there is no centralized entity (e.g., a spectrum broker [4]) to control the spectrum mobility.

1.5.1 Proactive Spectrum Handoff Framework in CRAHNs

Based on the moment when SUs carry out spectrum handoff, there are two types of approaches to solve the spectrum handoff issue. One approach is that SUs perform spectrum switching and radio frequency (RF) front-end reconfiguration after detecting a PU [54, 7, 55, 56, 57], namely the reactive approach. Although the concept of this approach is intuitive, there is a non-negligible sensing and reconfiguration delay which causes unavoidable disruptions to both the PU and SU transmissions. Another approach is that SUs predict the future channel availability status and perform spectrum switching and RF reconfiguration before a PU occupies the channel based on observed channel usage statistics, namely the proactive approach. This approach can dramatically reduce the collisions between SUs and PUs by letting SUs vacate channels before a PU reclaims the channel. Many predictive models based on the past channel usage history are proposed for either dynamic spectrum access [58, 59, 60, 61, 62, 63, 64] or spectrum handoff [65].

However, in the prior proposals, the network coordination and rendezvous issue (i.e., before transmitting a packet between two nodes, they first find a common channel and establish a link) is either not considered[55][56][59, 60, 61, 62, 63, 64] or simplified by using a global common control channel (CCC)[54][7][57][58][65]. A SU utilizing a channel without coordinating with other SUs may lead to the failure of link establishment [5]. Therefore, network coordination has a crucial impact on the performance of SUs. Although a global CCC simplifies the network coordination among SUs [21], there are several limitations when using this approach in CR networks. First

of all, it is difficult to identify a global CCC for all the secondary users throughout the network since the spectrum availability varies with time and location. Secondly, the CCC is influenced by the primary user traffic because a PU may suddenly appear on the current control channel. For these reasons, IEEE 802.22 [66], the first standard based on the use of cognitive radio technology on the TV band between 41 and 910 MHz, does not utilize a dedicated channel for control signaling, instead dynamically choosing a channel which is not used by legacy users [67].

On the other hand, when SUs perform spectrum handoffs, a well-designed channel selection method is required to provide fairness for all SUs as well as to avoid multiple SUs to select the same channel at the same time. Even though the channel allocation issue has been well studied in traditional wireless networks (e.g., cellular networks and wireless local area networks (WLANs)), channel allocation in CR networks, especially in a spectrum handoff scenario, still lacks sufficient research. Currently, the channel selection issue in a multi-user CR network is investigated mainly using game theoretic approaches [68, 69, 70, 71], while properties of interest during spectrum handoffs, such as SU handoff delay and SU service time, are not studied. Furthermore, most of the prior work on channel allocation in spectrum handoffs [55][58] only considers a two-secondary-user scenario, where a SU greedily selects the channel which either results in the minimum service time [55] or has the highest probability of being idle [58]. However, if multiple SUs perform spectrum handoffs at the same time, these channel selection methods will cause definite collisions among SUs. Hence, the channel selection method aiming to prevent collisions among SUs in a multi-secondary-user spectrum handoff scenario is not considered in the prior work.

1.5.2 Analysis of Spectrum Handoff in CR Ad Hoc Networks

As we know, an analytical model is of great importance for performance analysis because it can provide useful insights on the operation of spectrum handoffs. However, there have been limited studies on the performance analysis of spectrum handoffs in

CR networks using analytical models. In [55] and [57], a preemptive resume priority queueing model is proposed to analyze the total service time of SU communications for proactive and reactive-decision spectrum handoffs. However, in both [55] and [57], only one pair of SUs is considered in a network, while the interference and interactions among SUs are ignored, which may greatly affect the performance of the network. Additionally, although they are not designed for the spectrum handoff scenario, some recent related works on analyzing the performance of SUs using analytical models can be found in [72] and [73]. In [72], a dynamic model for CR networks based on stochastic fluid queue theory is proposed to analyze the steady-state queue length of SUs. In [73], the stationary queue tail distribution of a single SU is analyzed using a large deviation approach. In all the above proposals, a common and severe limitation is that the authors assume that the detection of PUs is perfect (i.e., a SU transmitting pair can immediately perform channel switching if a PU is detected to appear on the current channel, thus the overlapping of SU and PU transmissions is negligible). However, since the power of a transmitted signal is much higher than the power of the received signal in wireless medium due to path loss, instantaneous collision detection is not possible for wireless communications. Thus, even if only a portion of a packet is collided with another transmission, the whole packet is wasted and need to be retransmitted. Without considering the retransmission, the performance conclusion may be inaccurate, especially in wireless communications. Unfortunately, it is not easy to simply add retransmissions in the existing models. In this research, we model the retransmissions of the collided packets in our proposed Markov model.

Furthermore, as explained above in the prior proposals, the network coordination and rendezvous issue (i.e., before transmitting a packet between two nodes, they first find a common channel and establish a link) is either not considered[55][57][59][60][72][73] or simplified by using a dedicated common control channel (CCC)[54][58][65]. Since the CCC is always available, a SU can coordinate with its receiver at any moment

when there is a transmission request. However, it is not practical to use a CCC in CR networks because it is difficult to identify a dedicated CCC for all the SUs throughout the network since the spectrum availability varies with time and location. In this research, we do not make such assumption. We model the scenario where SUs need to find an available channel for network coordination. Therefore, in this research, we consider a more practical distributed network coordination scheme in our analytical model design.

1.6 Overview of the Proposed Intelligent Spectrum Management

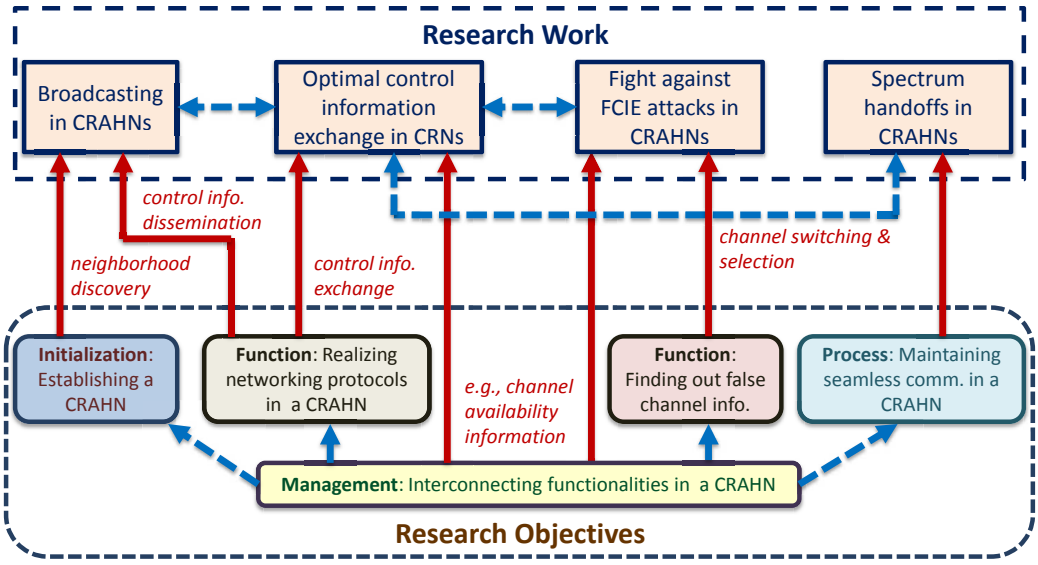

Figure 1.3: The overview of the proposed intelligent spectrum management mechanisms.

In this research, we investigate intelligent spectrum management designs in CR ad hoc networks. Figure 1.3 shows the overview of the proposed intelligent spectrum management mechanisms. We propose two broadcast protocols: 1) a QoS-based broadcast protocol under blind information and 2) a fully-distributed broadcast protocol under 2-hop location information in multi-hop CR ad hoc networks. In our design, we consider practical scenarios: 1) the network topology is not known; 2) the channel information of other SUs is not known; 3) the available channel sets of different SUs are not assumed to be the same; and 4) tight time synchronization is

not required. The performance metrics of our proposed protocol are the successful broadcast ratio (i.e., the probability that all nodes successfully receive the broadcast message) and the average broadcast delay (i.e., the average duration from the moment a broadcast starts to the moment the last node receives the broadcast message).

Secondly, a novel unified analytical model is proposed to analyze the broadcast protocols in CR ad hoc networks. In our proposed analytical model, an algorithm for calculating the successful broadcast ratio (i.e., the probability that all nodes in a network successfully receive a broadcast message) is proposed for CR ad hoc networks. The proposed algorithm is a general methodology that can be applied to any broadcast protocol proposed for multi-hop CR ad hoc networks with any topology. In addition, an algorithm for calculating the average broadcast delay (i.e., the average duration from the moment a broadcast starts to the moment the last node in the network receives the broadcast message) is proposed for CR ad hoc networks under grid topology.

Furthermore, an optimal HELLO message exchange scheme is proposed in static and mobile CR ad hoc networks. In our desinged scheme, 1) channel behavior caused by spatially distributed PUs and its impact on SU traffic is mathematically modeled for the first time; 2) the trade-off between SU throughput as well as average SU waiting time and control overhead is investigated analytically for the first time which takes into consideration the changes in the channel behavior and the impact of the HELLO message broadcast duration; 3) the impact of node mobility on the SU spectrum availability and the prompt changes in the identities of PUs is studied; and 4) two optimal HELLO message exchange protocols based on the modeled trade-off and node mobility impact are proposed for static and mobile CR ad hoc networks.

Moreover, two distributed security algorithms are proposed to fight against a particular threats named false channel information exchange (FCIE) attacks in CR ad hoc networks. We investigate the spatial correlation of the channel availability be-

tween neighboring nodes. This is because that the channel availability of neighboring nodes is correlated with the relative locations of these nodes. Using this relationship, the malicious node that sends the false channel information can be identified.

In addition, we designed a proactive spectrum handoff framework for CR ad hoc networks without the existence of a CCC. We consider more practical coordination schemes instead of using a CCC to realize channel rendezvous. We incorporate two types of channel rendezvous and coordination schemes into the spectrum handoff design and compare the performance of our proposed spectrum handoff protocol and the reactive spectrum handoff approach under different coordination schemes. We propose proactive spectrum handoff criteria and policies for SUs using a probability-based prediction method. SUs equipped with the prediction capability can proactively predict the idleness probability of the spectrum band in the near future. Thus, harmful interference between SUs and PUs can be diminished and SU throughput is increased. In addition, by considering channel rendezvous and coordination schemes, we propose a proactive spectrum handoff protocol for SUs based on our proposed handoff criteria and policies. Instead of only considering one pair of SUs in a network, we consider multiple pairs of SUs contending the spectrum band. With the aim of eliminating collisions among SUs and achieving short spectrum handoff delay, we propose a novel distributed channel selection scheme especially designed for multi-user spectrum handoff scenarios.

Finally, we also study the performance of SUs in the spectrum handoff scenario in a CR ad hoc network where multiple SUs compete for the spectrum access. A novel three dimensional Markov model to characterize the process of spectrum handoffs and analyze the performance of SUs. The interference and interactions among multiple SUs are considered in our proposed model. Since instantaneous collision detection is not feasible for wireless communications, we consider the retransmissions of the collided SU packets in spectrum handoff scenarios. We apply three different

channel selection schemes in the proposed Markov model and study their effects on the performance of SUs in spectrum handoff scenarios. We consider the spectrum sensing delay and its impact on the network performance. This feature can be easily implemented in our proposed Markov model.

CHAPTER 2: RELATED WORK

In this chapter, the related work in the proposed distributed intelligent spectrum management is introduced.

2.1 Existing Broadcast Protocols in CRNs

Currently, research on broadcasting in multi-hop CR ad hoc networks is still in its infant stage. There are only limited papers addressing the broadcasting issue in CR ad hoc networks [21, 22, 23]. However, in [21] and [22], the global network topology and the available channel information of all SUs are assumed to be known. Additionally, in [22], a common signaling channel for the whole network is employed which is also not practical. These two papers adopt impractical assumptions which make them inadequate to be used in practical scenarios. In [23], a Quality-of-Service (QoS)-based broadcast protocol under blind information is proposed. However, this scheme does not consider optimizing the network performance. Moreover, it ignores the broadcast collision issue. Other proposals aiming to locally establish a common control channel may also be considered for broadcasting [74, 75, 34, 32]. However, these proposals need a-priori channel availability information of all SUs which is usually obtained via broadcasts. In addition, although some schemes on channel hopping in CR networks can be used for finding a common channel between two nodes [30, 31, 33], they still suffer various limitations and cannot be used in broadcast scenarios. In [30] and [31], the proposed channel hopping schemes cannot guarantee rendezvous under some special circumstances. In addition, one of the proposed schemes in [30] only works when two SUs have exactly the same available channel sets. Furthermore, in [33], a jump-stay based channel hopping algorithm is proposed for guaranteed rendezvous. However, the expected rendezvous time for the asymmetric model (i.e.,

different users have different available channels) increases exponentially when the total number of channels increases. Thus, it is unsuitable for broadcast scenarios in CR ad hoc networks where channel availability is usually non-uniform and short broadcast delay is often required. Other channel hopping algorithms explained in [42] require tight time synchronization which is also not feasible before any control information is exchanged.

2.2 Existing Analytical Model for Broadcast Protocols in CRNs

Currently, no existing work on CR ad hoc networks addresses these challenges. Moreover, due to the above explained differences, the analytical methodology for broadcast protocol analysis in tradition MANETs cannot be extended to CR ad hoc networks. Specifically, the existing performance analytical papers on broadcasting in traditional multi-channel ad hoc networks cannot reflect the unique features (e.g., non-uniform channel availability and channel rendezvous schemes) in multi-hop CR ad hoc networks because: 1) a common control channel is used for broadcasting [76, 77, 78, 79, 80]; 2) only single-hop scenario is considered [76][78][81]; 3) a centralized entity is needed to schedule the broadcast [81]; and 4) multiple radios are used [82].

2.3 Background on HELLO Message Exchange

In traditional MANETs, since a CCC is used for exchanging control information, every node can broadcast HELLO messages on the CCC and any idle node can successfully receive the HELLO message on the CCC. However, in CR ad hoc networks, due to the non-uniform channel availability of SUs, a CCC may not exist [4]. Hence, SUs need to find a common available channel to broadcast the message. Different channel rendezvous schemes have been proposed for finding a common channel between two SUs [42, 31, 30, 33, 34, 24]. In these channel rendezvous schemes, SUs are required to follow well-designed channel hopping sequences so that a SU sender and receiver are guaranteed to hop on the same channel at the same time within a finite time. These channel rendezvous schemes can be used for exchanging HELLO

messages in CR ad hoc networks.

Next, we introduce the periodic HELLO message exchange scenario considered in this research and show how the main functionalities of CR networks are interconnected by the periodic HELLO message exchange. We assume that an arbitrary spectrum sensing and an arbitrary channel rendezvous scheme are used. Assume that a time slotted system is adopted. First of all, every SU follows the channel hopping sequence defined in the channel rendezvous scheme to hop through channels from one time slot to another, when it is not communicating with others. If a SU needs to perform a HELLO message update, it first conducts spectrum sensing to obtain the latest channel availability information. Then, it broadcasts a HELLO message on each channel it hops on according to the channel hopping sequence for a duration so that the neighboring SUs who may hop through channels following a different sequence can receive the control information within that duration. The durations used for spectrum sensing and HELLO message broadcast are determined by the spectrum sensing and channel rendezvous scheme used, which are usually fixed. Figure 2.1 shows the considered periodic HELLO message exchange scenario, where the interval between two rounds of HELLO message update is α. The durations of spectrum sensing and HELLO message broadcast are denoted as T_s and T_m, respectively. The total duration for one HELLO message update (denoted as T_b) is the sum of these two parts (i.e., $T_b = T_s + T_m$).

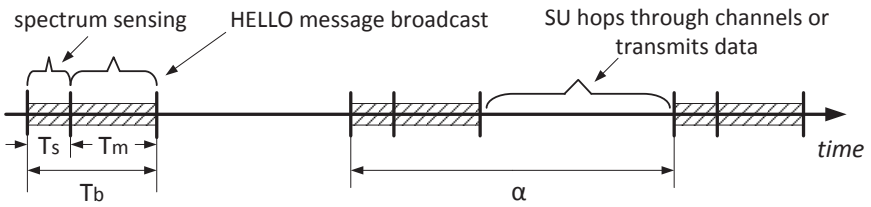

Figure 2.1: The periodic HELLO message exchange protocol.

Then, if a SU wants to transmit a data packet, it uses the channel information obtained from the previous HELLO message update and sends out a request-to-send

(RTS) packet on each available channel of the receiver using the channel rendezvous scheme. After receiving the RTS, the receiver replies with a clear-to-send (CTS) packet on the same channel if it is idle. Then, the transmitting pair can either stay on the current rendezvous channel or select a new available channel (depends on the particular spectrum sharing protocol) to start a data transmission. If a SU is currently active with a data transmission when the periodic HELLO message broadcast moment arrives, the SU continues the data transmission and does not perform the update at that moment. Moreover, if a PU packet arrives in the middle of a SU transmission. A collision occurs and the current SU transmission fails. Because the two SUs do not know the current channel availability of each other, they stay on the same channel until the next HELLO message update. Then, the two SUs switch to a new channel based on the received latest channel availability information from the update (i.e., spectrum mobility) and retransmit the collided packet after the HELLO message update.

2.4 Existing Security Schemes to Defend FCIE Attacks in CRNs

Currently, no security proposal in CR ad hoc networks can defend against the FCIE attack. In [50][83, 84, 85, 86], another attack which also belongs to the second category called the spectrum sensing data falsification (SSDF) attack is addressed. Although in both SSDF and FCIE attacks, malicious nodes report false information to other nodes, these two types of attacks are totally different on the following three aspects. First of all, the goal of SSDF attacks is to trick legitimate users to have incorrect spectrum sensing outcomes in a cooperative spectrum sensing system. However, for FCIE attacks, every SU has already obtained its own correct spectrum sensing results. The goal of FCIE attacks is to obstruct the networking protocol from being realized by broadcasting false channel information. Secondly, in SSDF attacks, sensing results are sent to a centralized entity called the fusion center to determine a correct spectrum sensing decision. However, in FCIE attacks, channel information

is sent as broadcasts to all neighboring nodes. Each node needs to determine the authenticity of the channel information by itself in a distributed fashion. Thirdly, in SSDF attacks, since all SUs sense the same area, the sensing results for legitimate SUs are often the same. Thus, malicious nodes often report the most distinct results, as compared with legitimate nodes. However, in FCIE attacks, since each SU obtains the channel information based on the sensing outcome from its proximity, different legitimate SUs often have different channel information. In addition, the false channel information sent by malicious nodes may be the same as the legitimate channel information of their neighboring nodes, which is also different from the SSDF attacks.

2.5 Existing Spectrum Handoff Protocols in CRNs

Currently, there are only limited studies addressing the spectrum handoff issue. One approach is that SUs perform spectrum switching and radio frequency (RF) front-end reconfiguration after detecting a PU [54, 7, 55, 56, 57], namely the reactive approach. Although the concept of this approach is intuitive, there is a non-negligible sensing and reconfiguration delay which causes unavoidable disruptions to both the PU and SU transmissions. Another approach is that SUs predict the future channel availability status and perform spectrum switching and RF reconfiguration before a PU occupies the channel based on observed channel usage statistics, namely the proactive approach. This approach can dramatically reduce the collisions between SUs and PUs by letting SUs vacate channels before a PU reclaims the channel. Many predictive models based on the past channel usage history are proposed for either dynamic spectrum access [58, 59, 60, 61, 62, 63, 64] or spectrum handoff [65].

In addition, a (CCC) is used for supporting the network coordination and channel related information exchange among SUs. In the prior proposals of the above two spectrum handoff approaches, the network coordination and rendezvous issue (i.e., before transmitting a packet between two nodes, they first find a common channel and establish a link) is either not considered[55][56][59, 60, 61, 62, 63, 64] or simplified

by using a global common control channel (CCC)[54][7][57][58][65]. A SU utilizing a channel without coordinating with other SUs may lead to the failure of link establishment [5].

2.6 Existing Analytical Models for Spectrum Handoff in CRNs

Related work on spectrum handoffs in CR networks falls into two categories based on the moment when SUs carry out spectrum handoffs. In the first category, SUs perform channel switching after detecting the reappearances of PUs, namely the reactive approach [54, 55, 57]. In the other category, SUs predict the future PU channel activities and perform spectrum handoffs before the disruptions with PU transmissions, namely the proactive approach [58, 59, 60, 65]. With the exception of [55] and [57], the performance analysis of all prior works on spectrum handoffs is simulation-based.

Moreover, in [55] and [57], a preemptive resume priority queueing model is proposed to analyze the total service time of SU communications for proactive and reactive-decision spectrum handoffs. However, in both [55] and [57], only one pair of SUs is considered in a network, while the interference and interactions among SUs are ignored, which may greatly affect the performance of the network. Additionally, although they are not designed for the spectrum handoff scenario, some recent related works on analyzing the performance of SUs using analytical models can be found in [72] and [73]. In [72], a dynamic model for CR networks based on stochastic fluid queue theory is proposed to analyze the steady-state queue length of SUs. In [73], the stationary queue tail distribution of a single SU is analyzed using a large deviation approach. In all the above proposals, a common and severe limitation is that the authors assume that the detection of PUs is perfect (i.e., a SU transmitting pair can immediately perform channel switching if a PU is detected to appear on the current channel, thus the overlapping of SU and PU transmissions is negligible). However, since the power of a transmitted signal is much higher than the power of the received signal in wireless medium due to path loss, instantaneous collision detection

is not possible for wireless communications. Thus, even if only a portion of a packet is collided with another transmission, the whole packet is wasted and need to be retransmitted. Without considering the retransmission, the performance conclusion may be inaccurate, especially in wireless communications. Unfortunately, it is not easy to simply add retransmissions in the existing models. In this proposal, we model the retransmissions of the collided packets in our proposed model.

Furthermore, in the prior proposals, the network coordination and rendezvous issue (i.e., before transmitting a packet between two nodes, they first find a common channel and establish a link) is either not considered[55][57][59][60][72][73] or simplified by using a dedicated common control channel (CCC)[54][58][65]. Since the CCC is always available, a SU can coordinate with its receiver at any moment when there is a transmission request. However, it is not practical to use a CCC in CR networks because it is difficult to identify a dedicated CCC for all the SUs throughout the network since the spectrum availability varies with time and location. In this proposal, we do not make such assumption. We model the scenario where SUs need to find an available channel for network coordination. Therefore, in this research, we consider a more practical distributed network coordination scheme in our analytical model design.

CHAPTER 3: DISTRIBUTED BROADCAST PROTOCOLS IN CRAHNS

In this chapter, the broadcasting issue in CR ad hoc networks is explored. Two novel distributed broadcast protocols in CRAHNs are proposed. A quality-of-service (QoS)-based broadcast protocol named QB^{2}IC is proposed in Section 3.3. In addition, a fully distributed broadcast protocol with collision avoidance named BRACER is presented in Section 3.6.

3.1 Network Model

In this research, we consider a CR ad hoc network where N SUs and K PUs co-exist in an $L \times L$ area, as shown in Figure 3.1. PUs are distributed within the area under the probability density function (pdf) $f_G(g)$. For simplicity, in this research, we consider that PUs are evenly distributed. The SUs opportunistically access M licensed channels. In Figure 3.1, the solid circle represents the transmission range of a SU with a radius of r_c. Other SUs within the transmission range are considered as the neighboring nodes of the corresponding SU. That is, only when a SU receiver is within the transmission range of a SU transmitter, the signal-to-noise ratio (SNR) at the SU receiver is considered to be acceptable for reliable communications. In addition, the dashed circle represents the sensing range of a SU with a radius of r_s. That is, if a PU is currently active within a sensing range, the corresponding SU is able to detect its presence. Since the sensing ranges of different SUs at different locations may include different PUs, their acquired available channels may be different [23][87]. In addition, because the available channels of a SU are obtained based on the sensing outcome within the sensing range, each SU is not allowed to communicate with other SUs outside its sensing range since it may mistakenly use an occupied channel by a PU, which results in interference to the PU. Therefore, in this research, we assume

that $r_c \leq r_s$. Additionally, we assume that a time-slotted system is adopted for SUs [88], where the length of a slot is long enough to transmit a broadcast packet.

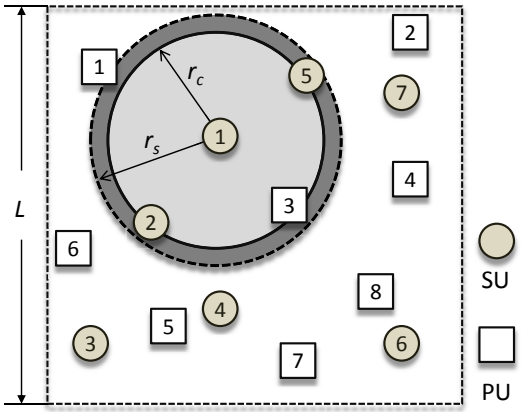

Figure 3.1: The network model of the broadcast scenario in a multi-hop CR ad hoc network.

In addition, in this research, we model the PU channel activity as an ON/OFF process, where the length of the ON period is the length of a PU packet. We assume that each PU randomly selects a channel from the spectrum band to transmit a packet. Therefore, the packets on the same channel do not necessarily belong to the same PU. This is a more practical scenario, as compared to some papers which assume that each channel is associated with a different PU. Under such practical scenario, the number of active PUs is not necessarily the number of occupied channels but depends on the total number of PUs in the network and the PU traffic intensity.

3.2 Exploring Broadcast Design in CRNs

To explore the broadcast design in CR ad hoc networks, we first investigate two straightforward broadcast schemes in multi-hop CR ad hoc networks under blind information. We observe that both broadcast schemes have drawbacks which make them unsuitable to be used in CR ad hoc networks. In the rest of the research, we use the term "sender" to indicate a SU source node or a SU who has just received a message and will rebroadcast the message. In addition, we use the term "receiver" to indicate a SU who has not received the message.

3.2.1 Random Broadcast Scheme

The first broadcast scheme is called the random broadcast scheme. Since a SU is unaware of the channel availability information of other SUs before broadcasts are executed, a straightforward action for a SU sender is to randomly select a channel from its available channel set and broadcasts a message on that channel in a time slot. In addition, as stated in Section 1, each SU sender needs to broadcast the message for multiple time slots. We denote the number of time slots that each SU sender broadcasts as S. Accordingly, for a SU receiver, without the channel availability information of the sender, it cannot constantly stay on one channel during the whole broadcast procedure since this channel may not be in the available channel set of the sender, which leads to a definite failure of the broadcast. Thus, the only fair action for the receiver is to randomly select an available channel to listen in each time slot. If the channel selected by the receiver is the same as the channel selected by the sender, the broadcast message can be successfully received. This broadcast scheme is easy to be implemented in CR ad hoc networks under blind information. However, it cannot guarantee channel rendezvous (i.e., the sender and the receiver stay on the same channel at the same time and establish a link). In other words, in each time slot, the sender tries its luck to broadcast to its neighboring nodes. Clearly, when the number of channels is large, since the probability that the sender and receiver select the same channel is low, the probability that a broadcast is successful under the random broadcast scheme is fairly low.

Figure 3.2 shows the simulation results of the random broadcast scheme under different number of channels when $N = 9$, $K = 20$, and $S = 20$. The SUs form a 3×3 grid network. We assume that the PU traffic is discrete-time, where the PU packet inter-arrival time X follows the biased-geometric distribution [89]. Additionally, other parameters are listed as follows: 1) Side length of the simulation area L=10 (unit length); 2) Radius of the sensing range r_s=2 (unit length); 3) Radius of

the transmission rage r_c=2 (unit length); 4) The normalized PU arrival rate λ_p=0.5; 5) The PU packet length L_p=10 (time slots); As mentioned in Section 1, the success rate is defined as the probability that all nodes in a network successfully receive the broadcast message and the average broadcast delay is defined as the average duration from the moment a source node starts a broadcast until the moment the last node in the network receives the broadcast message. It is shown in Figure 3.2 that the random broadcast scheme leads to very low success rate when the number of channels is large, which is not suitable to be used in multi-hop CR ad hoc networks when the number of channels is large.

3.2.2 Full Broadcast Scheme

The second broadcast scheme is called the full broadcast scheme under which each SU visits all the available channels in the spectrum. Unlike the random broadcast scheme where the channel in each time slot is randomly selected by a SU, in the full broadcast scheme, a SU sender broadcasts on all its available channels sequentially. Similarly, a SU receiver listens to its available channels sequentially. In addition, we use three different channel hopping sequences for the full broadcast scheme: 1) the channel hopping sequence under which the order for each SU to visit all the available channels is random (denoted as Full broadcast I); 2) the channel hopping sequence under which each SU visits all the available channels sequentially (denoted as Full broadcast II); and 3) the jump-stay channel hopping sequence [33] (denoted as Full broadcast III). The jump-stay channel hopping sequence can be constructed under blind information with guaranteed rendezvous. Furthermore, similar to the random broadcast scheme, each SU sender also broadcasts for a finite number of time slots, S.

Figure 3.2 shows the simulation results of the full broadcast scheme using different channel hopping sequences under different number of channels when $N = 9$, $K = 20$, and $S = 20$. Compared with the random broadcast scheme, the full broadcast

scheme using the first two channel hopping sequences also suffers a low success rate when the number of channels is large. This is because that these channel hopping sequences in the full broadcast scheme also cannot guarantee channel rendezvous. Moreover, the Full broadcast II scheme leads to an extremely low success rate when the number of channels is large, as compared to the Full broadcast I scheme. In addition, both the random broadcast scheme and the full broadcast scheme using the first two hopping sequences have a long average broadcast delay when the number of channels is large. On the other hand, the Full broadcast III scheme leads to a high success rate, as compared to other schemes. However, from Figure 3.2(b), this scheme has an extensively long average broadcast delay (almost as twice as the average broadcast delay in other scenarios). Hence, it is not suitable for broadcast scenarios where short broadcast delay is often required. Due to the low success rate in Full broadcast II and the long broadcast delay in Full broadcast III, in the rest of the research, we only use the random broadcast scheme and the Full broadcast I as the benchmarks to compare with our proposed schemes.

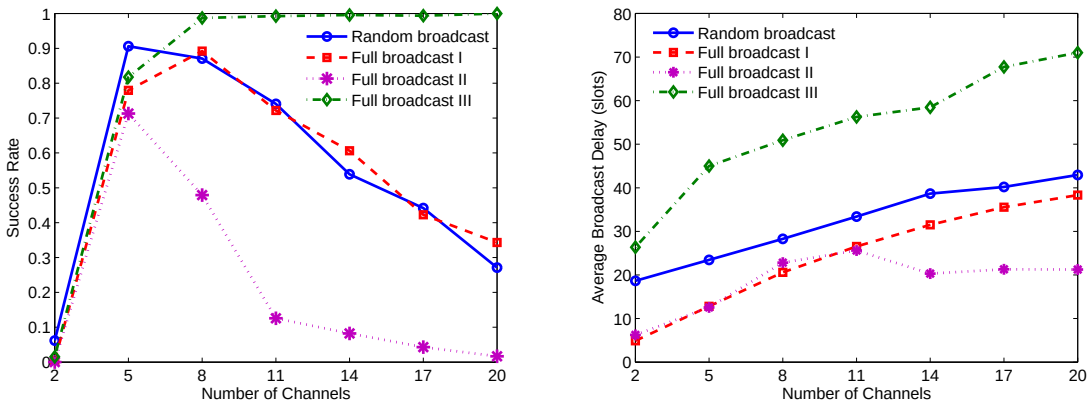

(a) Success rate.

(b) Average broadcast delay.

Figure 3.2: Success rate and average broadcast delay of the random and full broadcast schemes under different number of channels when $N = 9$, $K = 20$, and $S = 20$.

3.2.3 Remarks

From the above discussion, it is known that these straightforward broadcast schemes have limitations to be used in multi-hop CR ad hoc networks. By investi-

gating these broadcast schemes, we gain two useful insights for designing an efficient broadcast protocol in multi-hop CR ad hoc networks. First of all, from Figure 3.2, it is shown that the first three schemes suffer a very low success rate when the number of channels is large because these schemes cannot guarantee channel rendezvous. Thus, a channel hopping sequence that can guarantee channel rendezvous without the channel availability information of other SUs is required to achieve a high success rate. Secondly, all these broadcast schemes are quite costly in terms of the average broadcast delay when the number of channels is large, which is not desirable for efficient broadcasts. This is because that a SU needs to use all the available channels in the spectrum for broadcasting in these schemes. If a SU only uses a subset of its available channels for broadcasting, the broadcast delay may be reduced. However, since fewer channels are used, the success rate may also be affected. Therefore, given that the success rate is not sacrificed, properly reducing the number of channels for broadcasting can result in shorter average broadcast delay.

3.3 The Basic QB^2IC Scheme

In this section, we present the basic scheme of our proposed QB^{2}IC protocol. As mentioned in Section 3.2, the straightforward broadcast schemes are not suitable for CR ad hoc networks. Therefore, based on the insights that we gain from these schemes, the main idea of our proposed QB^{2}IC protocol is to intelligently design the channel hopping sequences for both the SU sender and the SU receiver to guarantee channel rendezvous, given that the sender and the receiver have at least one channel in common. In addition, the SU sender broadcasts on a subset of its available channels in order to reduce the average broadcast delay.

3.3.1 The Single-hop Scenario

First of all, we consider the single-hop broadcast scenario. We propose a novel channel hopping strategy for SUs to guarantee channel rendezvous. There are several existing work on single-hop channel rendezvous for CR networks [34, 30, 31, 33]. A

common feature of these prior proposals is that all SUs in a network have to follow the same mechanism to construct the channel hopping sequence for rendezvous regardless of transmitters or receivers. However, as stated in Section 1, in [34, 30, 31], the proposed channel hopping schemes cannot guarantee channel rendezvous in all scenarios under blind information. In [33], even though the proposed channel hopping sequence in the asymmetric model can guarantee channel rendezvous within $6MP(P-G)$ time slots, where P is the smallest prime number larger than M and G is the number of common channels between two SUs, $6MP(P-G)$ is usually a very large number when M is large. Therefore, this scheme may lead to very long broadcast delay when M is large. In fact, the communication pair can follow different mechanisms to construct the channel hopping sequences for channel rendezvous, which is ignored in all prior proposals. Thus, in this chapter, we use the channel hopping sequences generated by different methods for the sender and the receiver to guarantee channel rendezvous. Compared with the previous proposals in [34, 30, 31, 33], our proposed channel hopping sequences can guarantee rendezvous in all scenarios under blind information within M^2 time slots, which is more favorable in broadcast scenarios. Under our proposed basic QB^{2}IC scheme, a SU sender first randomly selects n channels from its available channel set. Then, it hops and broadcasts periodically on the selected n channels for S time slots. This channel hopping sequence with a length of S time slots is named as the broadcast sequence. The values of n and S are determined by the QoS requirements of the network. On the other hand, for each receiver, it first forms a random sequence that consists of its every available channel with a length of n time slots for each channel, namely the receiving sequence. Then, it hops and listens following the receiving sequence periodically. Denote the number of available channels of SU_i as m_i. Hence, the length of the receiving sequence of SU_i is $n \times m_i$. Figure 3.3 shows an example of the proposed QoS-based broadcast protocol. If the available channel set of the sender is $\{1, 2, 3, 6\}$, it randomly selects two channels

(e.g., $\{3, 6\}$) to broadcast for S slots (i.e., $n = 2$). Each receiver listens for two time slots on each available channel of its available channel set (e.g., $\{1, 2, 6\}$) periodically. Thus, if $S = 12$, the broadcast sequence for the sender is $\{3, 6, 3, 6, 3, 6, 3, 6, 3, 6, 3, 6\}$. In addition, the receiving sequence for the receiver is $\{1, 1, 2, 2, 6, 6, \cdots\}$. Hence, a successful broadcast is performed when both SUs hop on channel 6.

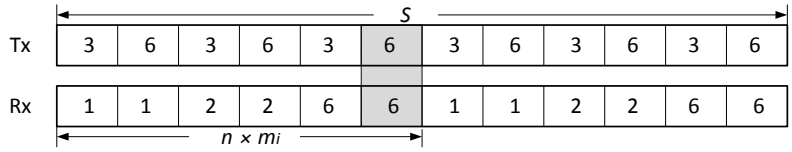

Figure 3.3: An example of the QoS-based broadcast protocol.

Based on the above rules, if the SU sender selects all its available channels and the length of the broadcast sequence S is equal to $n \times M$, the channel rendezvous is guaranteed within S time slots when the sender and each receiver have at least one channel in common. Therefore, the broadcast is ensured to be successful in the single-hop scenario. Thus, if n is sufficiently large, the probability that at least one channel selected by the sender are also in the available channel set of each receiver is high. However, on the other hand, since each SU is only equipped with one radio, it cannot broadcast on n $(n > 1)$ channels simultaneously. Hence, it takes a long time to finish broadcasting on all n channels when n is large.

From the above analysis, there exists a trade-off between the success rate and the average broadcast delay for different values of n and S. Figure 3.4 shows the simulation and analytical results of the success rate and the average broadcast delay for a single-hop broadcast scenario when $K = 40$ under various values of n and S. The PU traffic and other parameters are the same to generate Figure 3.2. It is illustrated that higher success rate often indicates longer average broadcast delay. Therefore, if the QoS requirements (i.e., the minimum required success rate and the maximum allowed average broadcast delay) are given, proper n and S can be selected.

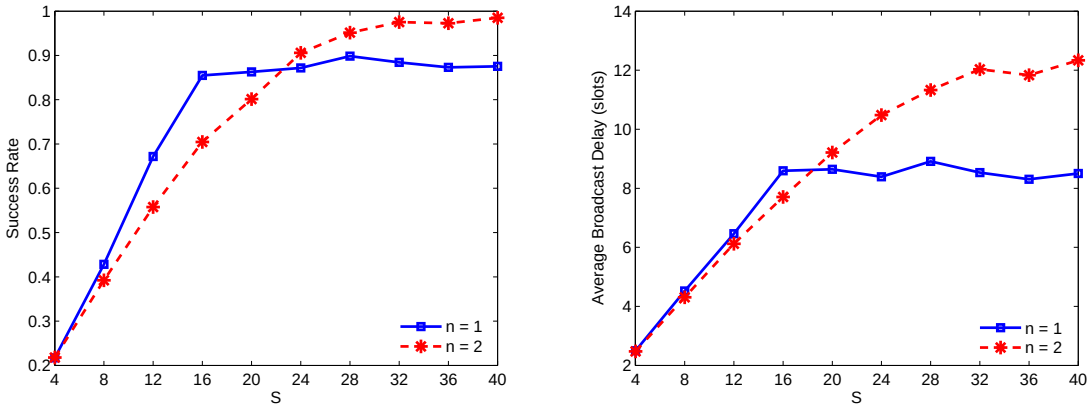

(a) Success rate. (b) Average broadcast delay.

Figure 3.4: The trade-off between the success rate and average broadcast delay under different n and S.

3.3.2 The Multi-hop Scenario

Next, we investigate the basic scheme of the proposed protocol in the multi-hop broadcast scenario. We consider two 4-SU networks as shown in Figure 3.5. The first topology of the 4-SU network is a single-hop scenario where SU_1 is the source node. The second topology is a multi-hop scenario evolved from the first topology when SU_1 moves away from SU_4. Since we want to consider the broadcast collision issue, the multi-hop scenario is studied in such a grid topology instead of a simple chain topology, as shown in Figure 3.5. Without loss of generality, we assume that SU_1 is the source node and other nodes are by default receivers. Each receiver first follows the proposed receiving sequence to hop through and listen on the channels. When a receiver successfully receives the broadcast message, it becomes a sender who needs to rebroadcast the message. Therefore, it follows the rules of the senders and generates the proposed broadcast sequence to rebroadcast.

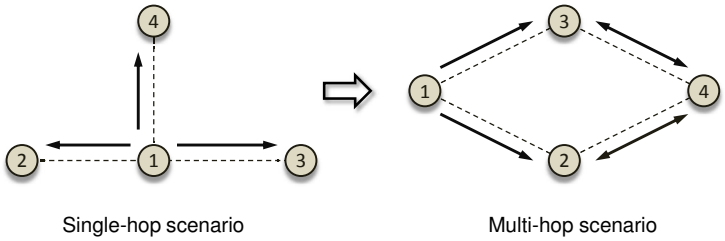

Figure 3.5: Two different topologies of two 4-SU networks.

Our proposed QB^{2}IC protocol has special advantages when applied to multi-hop scenarios in CR networks, as compared to traditional ad hoc networks. In traditional ad hoc networks, if a node (e.g., SU_4) receives multiple copies of a message from its parent nodes (e.g., SU_2 and SU_3) simultaneously, a broadcast collision occurs and all copies of the message are discarded. Unfortunately, in traditional ad hoc networks, such broadcast collision is unavoidable in multi-hop scenarios if the parent nodes broadcast at the same time. However, under our proposed QB^{2}IC protocol, since the receiver can only listen to one channel at a time, as long as the parent nodes do not select the same channel to broadcast, such broadcast collision can be avoided. In fact, when the number of channels is large and different SUs obtain different available channels, the probability that two parent nodes select the same channel at the same time is fairly low.

In addition, under our proposed QB^{2}IC protocol, the success rate of the broadcast for the whole network can be improved in the multi-hop scenario. This is because that a SU may not only receive the broadcast message from its parent node, but also receive the message from its child node (e.g., SU_2 can receive the message from SU_4 if SU_4 receives the message from the path $SU_1 \rightarrow SU_3 \rightarrow SU_4$). This is usually different from the broadcast schemes in traditional MANETs where nodes receive broadcast messages from their parent nodes. More importantly, if the channels used for broadcast in different paths are different, the probability that one of the channels is in the available channel set of the receiver is increased, as compared to the scenario where a SU only receives the message from its parent nodes. Thus, by utilizing the diversity of users and channels, the success rate of the whole network can be increased. Figure 3.6 shows the performance comparison between the single-hop scenario and the multi-hop scenario shown in Figure 3.5 when $n = 1$. It is illustrated that the improvement of the success rate under the multi-hop scenario is up to 30%, while the multi-hop scenario only costs up to 20% additional average broadcast delay.

Therefore, under our proposed QB^{2}IC protocol, the success rate is benefited in the multi-hop scenario due to the diversity of users and channels.

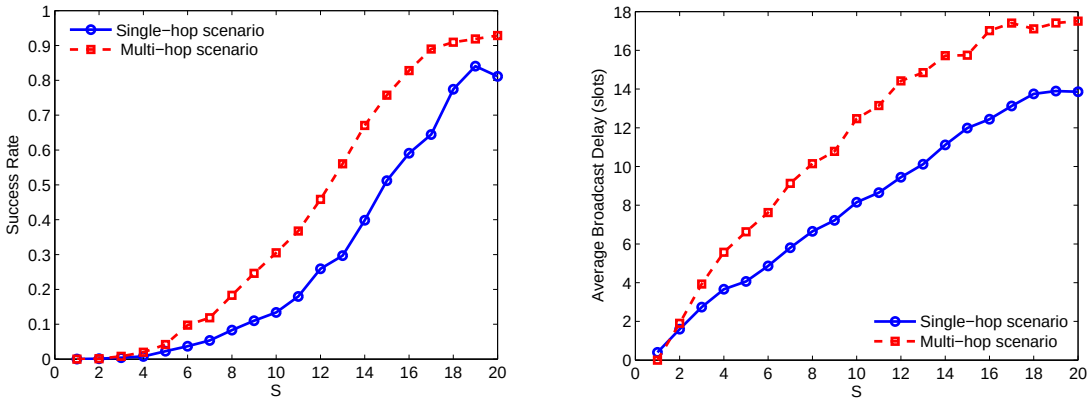

(a) Success rate.

(b) Average broadcast delay.

Figure 3.6: Comparison between the single-hop and the multi-hop scenarios.

3.4 The Enhanced QB^2IC Scheme

In this section, we first conduct an analysis on the channel availability of different SUs. Then, based on the results of this analysis, an enhanced QB^{2}IC scheme for multi-hop CR ad hoc networks is presented.

3.4.1 Analysis of the Channel Availability

Based on the considered network model, the available channels of a SU are determined by the active PUs within its sensing range. Thus, first of all, we derive the average number of available channels of a SU. The size of the simulation area and the sensing range is denoted as A_L and A_S, respectively. Since PUs are evenly distributed in the considered simulation area, the probability that p PUs are in a sensing range is

$$\Pr(p) = \binom{K}{p} \left(\frac{A_S}{A_L}\right)^p \left(\frac{A_L - A_S}{A_L}\right)^{K-p}, \tag{3.1}$$

where $\binom{K}{p}$ represents the total combinations of K choosing p. In addition, we denote the probability that a PU is active as ρ. Therefore, given that there are p PUs in a

sensing range, the probability that there are b PUs active is

$$\Pr(b|p) = \binom{p}{b}\rho^b(1-\rho)^{p-b}. \tag{3.2}$$

Furthermore, given that there are p PUs and b active PUs within a sensing range, the probability that there are c available channels is denoted as $\Pr(c|p,b)$. Since the number of available channels is only related to the number of active PUs, c is independent of p. In addition, since an active PU randomly selects a channel from M channels in the spectrum, $\Pr(c|p,b)$ is equivalent to the probability that there are exactly c empty boxes given that b distinguishable balls are randomly put into a total of M distinguishable boxes and a box can have more than one ball (because we do not limit a channel to only one PU). Thus, $\Pr(c|p,b)$ can be expressed as:

$$\Pr(c|p,b) = \frac{\binom{M}{c}(M-c)!S(b,M-c)}{M^b}, c \in [\max(0,M-b), M], \tag{3.3}$$

where $S(b,M-c)$ is the Stirling number of the second kind. In addition, $S(b,M-c)$ is defined as

$$S(b,M-c) = \frac{1}{(M-c)!}\sum_{i=0}^{M-c}(-1)^i\binom{M-c}{i}(M-c-i)^b. \tag{3.4}$$

Thus, the probability that there are c available channels and there are p PUs and b active PUs in the sensing range of a SU is the product of (3.1), (3.2), and (3.3). Then, the average number of available channels of a SU, $E[c]$, is written as

$$E[c] = \sum_{p=0}^{K}\sum_{b=0}^{p}\sum_{c=\max(0,M-b)}^{M}\frac{c\binom{M}{c}(M-c)!S(b,M-c)}{M^b}\binom{p}{b}\rho^b(1-\rho)^{p-b}\binom{K}{p}\left(\frac{A_S}{A_L}\right)^p\left(\frac{A_L-A_S}{A_L}\right)^{K-p}. \tag{3.5}$$

In addition, another important parameter is the average number of common channels between two neighboring SUs. Figure 3.7 illustrates an example of two neighboring SUs whose sensing ranges overlap, where d is the distance between the two SUs.

Assume that SU_i and SU_j can hear each other. As shown in Figure 3.7, the sensing ranges of the two SUs are divided into three areas. A_3 (the dark area) represents the area of the overlapping part, while A_1 (the white area) and A_2 (the gray area) represent the areas of the sensing ranges of SU_i and SU_j without A_3, respectively.

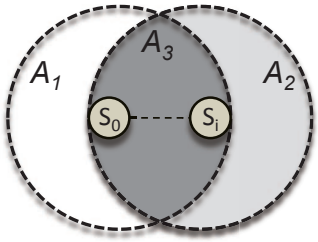

Figure 3.7: Two neighboring SUs whose sensing ranges overlap.

Define $A^* = A_1 + A_2 + A_3$. Therefore, based on basic geometry, A^* can be obtained as follows:

$$A^* = (2\pi - 2\alpha)r_s^2 + d\sqrt{r_s^2 - \left(\frac{d}{2}\right)^2}, \tag{3.6}$$

where $\alpha = \cos^{-1}\frac{d}{2r_s}$. Thus, the channels that are used by the active PUs within A^* are those that cannot be used by either SU_i or SU_j. In other words, the common channels between two neighboring SUs are those that are not used by the active PUs within A^*. Thus, similar to the derivation process for $E[c]$, the average number of common channels between two neighboring SUs, $E[u]$, is obtained from

$$E[u] = \sum_{y=0}^{K}\sum_{z=0}^{y}\sum_{u=\max(0,M-z)}^{M} \frac{u\binom{M}{u}(M-u)!S(z,M-u)}{M^z}\binom{y}{z}\rho^z(1-\rho)^{y-z}\binom{K}{y}\left(\frac{A^*}{A_L}\right)^y\left(\frac{A_L-A^*}{A_L}\right)^{K-y}, \tag{3.7}$$

where y and z are the number of PUs and active PUs within A^*, respectively.

Then, we define the ratio of the average number of common channels between two neighboring SUs to the average number of available channels of a SU as

$$P_c = \frac{E[u]}{E[c]}, \tag{3.8}$$

P_c measures the similarity of the available channel sets between two neighboring

SUs. If $P_c = 1$, this means that the available channels between two neighboring SUs are exactly the same. On the other hand, if $P_c = 0$, this means that the available channels between two neighboring SUs are completely different. Figure 3.8 shows the simulation and analytical results of P_c when $r_c = r_s$ and both SUs are at the border of each other's sensing range. Since the sensed available channels of two SUs might be the most distinct when they are apart the most, Figure 3.8 shows the lower bound of P_c. Figure 3.8 indicates that the simulation and analytical results coincide and also implies that even though the available channels of different SUs are different, the similarity of available channels between neighboring SUs is high ($> 85\%$).

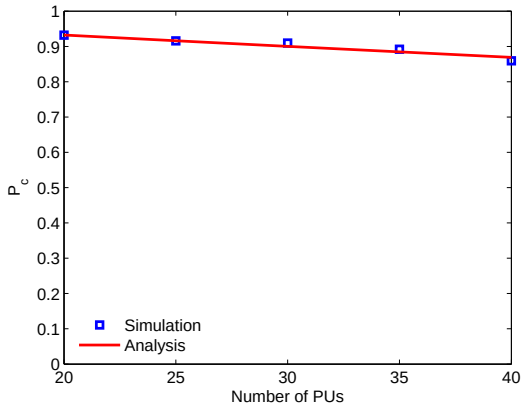

Figure 3.8: The ratio of the average number of common channels between two neighboring SUs to the average number of available channels of one SU when $\rho = 0.9$.

3.4.2 The Enhanced QB^2IC Scheme

The above analysis of the channel availability indicates that neighboring SUs have very similar available channel sets. Thus, inspired by this observation, we propose an enhanced QB^{2}IC scheme to further improve the performance.

The main idea of our enhanced scheme is that each SU selects the first θ channels from its available channel set based on the indexes of the channels to form a new available channel set. Based on the downsized available channel set, each SU follows the basic scheme to broadcast. Since the available channel sets of neighboring SUs are similar, the downsized available channel sets of neighboring SUs are also similar.

In this way, if the threshold θ is properly selected, the success rate does not degrade significantly. However, since the number of the channels that each receiver needs to listen is reduced, the average broadcast delay can be greatly reduced.

However, there again exists a trade-off between the success rate and the average broadcast delay when selecting the threshold θ. As shown in Figure 3.9, when θ increases, the success rate increases but the average broadcast delay also increases. Thus, if the QoS requirements are given, a proper θ can be selected.

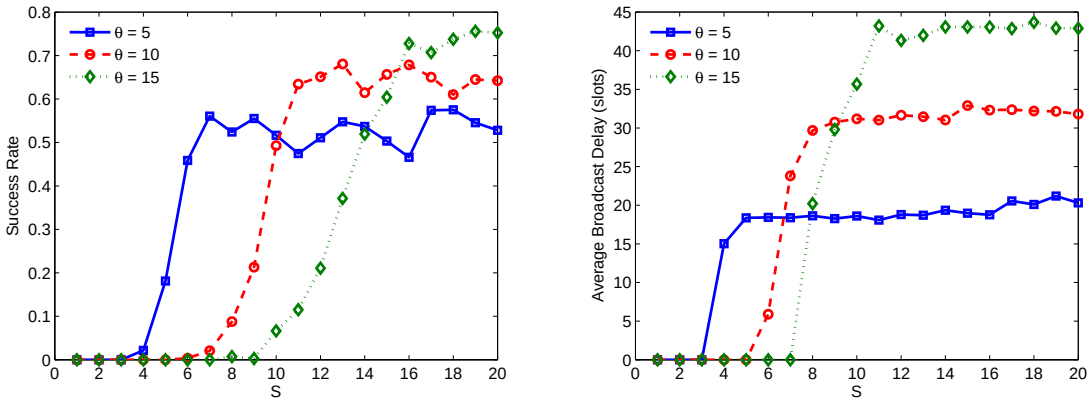

(a) Success rate. (b) Average broadcast delay.

Figure 3.9: Success rate and average broadcast delay of the proposed enhanced QB^{2}IC scheme under various θ.

3.5 Performance Evaluation

In this section, we evaluate the performance of the proposed QB^{2}IC protocol. Since there is no existing comparable broadcast scheme under blind information for multi-hop CR ad hoc networks, we compare our proposed broadcast schemes with the random broadcast scheme and the full broadcast scheme with the first channel hopping sequence introduced in Section 3.2. As mentioned in Section 3.2, we also assume that the PU traffic is discrete-time, where the PU packet inter-arrival time X follows the biased-geometric distribution whose probability mass function (pmf) is given by [90]:

$$\Pr(X=x) = \begin{cases} 0 & x < l \\ \lambda_p(1-\lambda_p)^{(x-l)} & x \geq l, \end{cases} \tag{3.9}$$

where x is the number of time slots between packet arrivals, $l \geq 0$ represents the minimum number of time slots between two adjacent packets, and λ_p is the probability that a PU packet arrives during one time slot (i.e., λ_p is the normalized arrival rate of PU packets). Thus, the probability that a PU is active can be written as $\rho = \frac{L_p}{L_p + \frac{1-\lambda_p}{\lambda_p}}$, where L_p is the fixed PU packet length. It is noted that the PU traffic model is used to obtain simulation results. In fact, our proposed QB^{2}IC broadcast protocol does not rely on specific PU traffic models. In addition, denote σ as the probability that a transmission is successful. That is, if $\sigma = 1$, it means that there is no transmission error and a transmission is always successful. Moreover, the default parameters used to obtain the simulation results are listed in Table 3.1. For the topology of the CR ad hoc network, we assume that SUs form a 4×4 grid network with the distance between two adjacent SUs equal to r_c.

Table 3.1: Simulation Parameters

Number of SUs N	16
Number of PUs K	40
Number of channels M	20
Side length of the simulation area L	10 (unit length)
Radius of the sensing range r_s	2 (unit length)
Radius of the transmission rage r_c	2 (unit length)
Number of selected channels n	1
The normalized PU arrival rate λ_p	0.5
The PU packet length L_p	10 (time slots)
The probability of a successful transmission σ	1

Figure 3.10 depicts the performance results of the two proposed QB^{2}IC schemes (for the enhanced scheme, $\theta = 10$), the random broadcast scheme, and the full broadcast scheme under different S when $K = 40$, $M = 20$, $n = 1$, and $\sigma = 1$. It is shown that when S is large (e.g., $S = 19$), the basic scheme outperforms the other three broadcast schemes in terms of higher success rate. However, the enhanced scheme can greatly reduce the average broadcast delay while obtaining satisfactory success rate. Both the proposed QB^{2}IC schemes outperform the random broadcast scheme and the full broadcast scheme in terms of higher success rate and shorter average

broadcast delay.

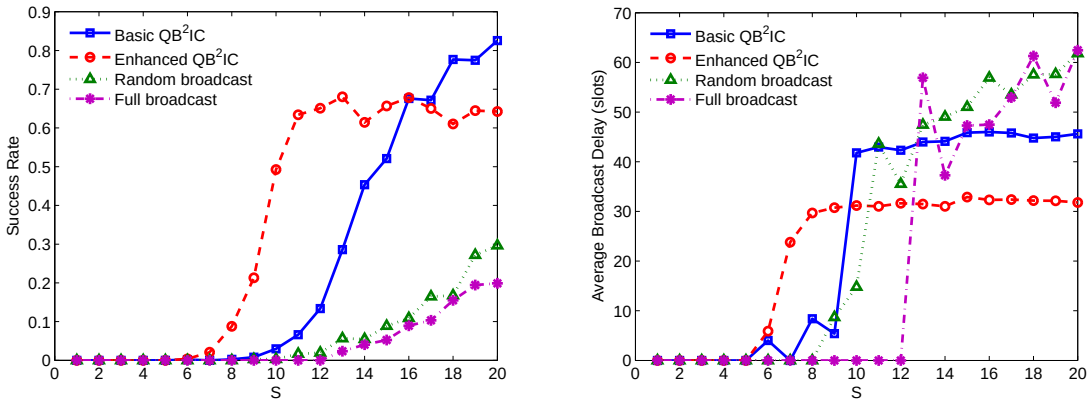

(a) Success rate. (b) Average broadcast delay.

Figure 3.10: Success rate and average broadcast delay of the proposed QB^{2}IC schemes with the random and full broadcast schemes under various S.

3.5.1 The Impact of the Number of SUs and PUs

Figure 3.11 and 3.12 show the impact of the number SUs and the number of PUs on the network performance, respectively, where the secondary network is a grid network when $S = 20$. On the other hand, Figure 3.13 depicts the impact of the number of SUs on the network performance where the secondary network is not a grid network. In Figure 3.11, SUs form a 2×2 network for $N = 4$ and a 3×3 network for $N = 9$. It is shown that the average broadcast delay increases as the number of SUs in the network increases. This is because that the increase of the number of hops leads to a longer broadcast delay. However, the success rate of the basic QB^{2}IC scheme does not decrease significantly when the number of SUs increases. This is because that the multi-hop scenario benefits the success rate due to the diversity of channels. On the other hand, as shown in Figure 3.12, the success rate decreases when the number of PUs increases. This is because that the number of common channels between neighboring nodes decreases when the total number of PUs increases, which leads to a lower success rate.

We also investigate the impact of the number of SUs on the network performance

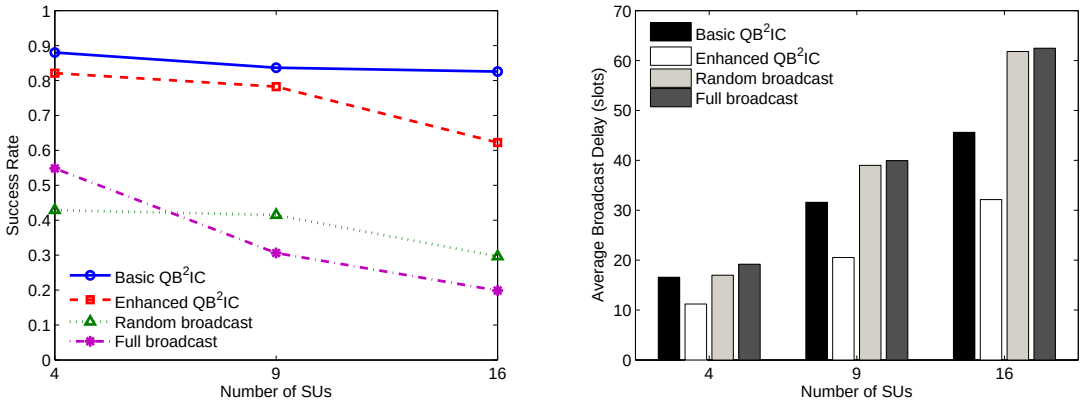

(a) Success rate. (b) Average broadcast delay.

Figure 3.11: The impact of the number of SUs on the network performance where the secondary network is a grid network.

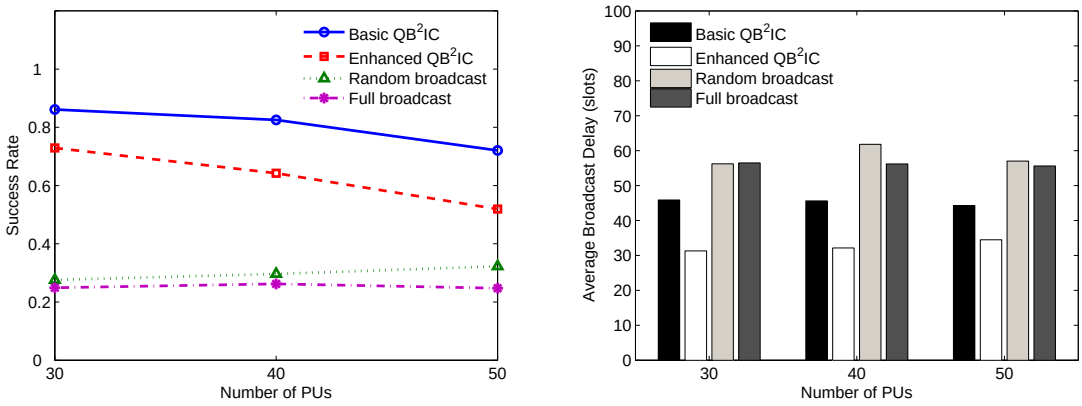

(a) Success rate. (b) Average broadcast delay.

Figure 3.12: The impact of the number of PUs on the network performance.

where the secondary network is not a grid network. Figure 3.13 shows the results of the basic broadcast scheme where the SUs are randomly distributed in the simulation area. In Figure 3.13(a), it is shown that when the number of SUs increases, the success rate of the whole network also increases. This is because that if the number of SUs within the same area is large, the diversity of senders and channels increases. Thus, the number of potential senders of a SU increases. Therefore, in our proposed QB^{2}IC protocol, the probability that one of the channels used by these senders is in the available channel set of the receiver is increased. Hence, the probability that all nodes in the network can successfully receive the broadcast message also increases.

Due to the same reason, in Figure 3.13(b), it is shown that the average broadcast delay does not increase significantly when the number of SUs increases. That is, when the number of SUs increases by 10 times, the average broadcast delay only increases by 40% for the basic scheme and 51% for the enhanced scheme. To sum up, it is shown that our proposed basic and enhanced broadcast schemes are scalable when the CR ad hoc network size increases.

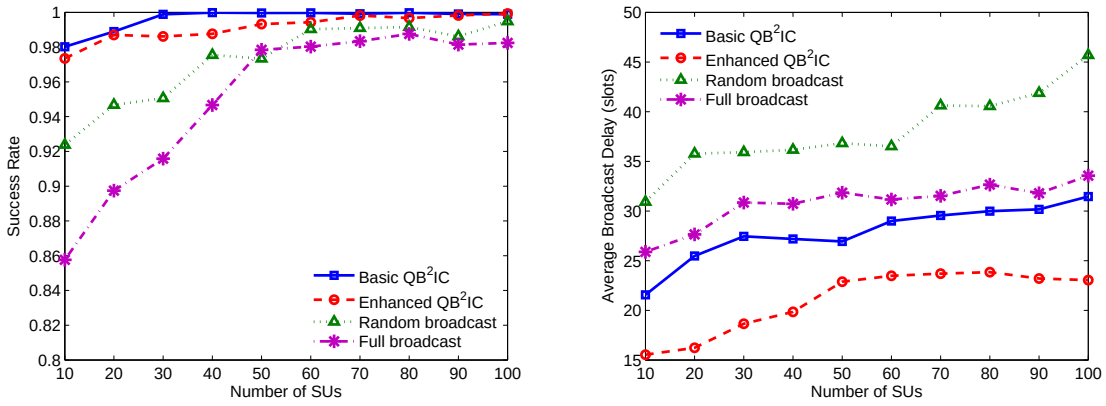

(a) Success rate.

(b) Average broadcast delay.

Figure 3.13: The impact of the number of SUs on the network performance where the secondary network is *not* a grid network.

3.5.2 The Impact of the Number of Channels

Figure 3.14 shows the impact of the number of channels on the network performance when $K = 30$ and $N = 9$. For the length of the broadcasting sequence, we set $S = 2M$. In addition, for the enhanced scheme, we let $\theta = M/2$. As stated in Section 3.3, the number of channels leads to a trade-off in terms of the success rate and broadcast delay. On one hand, a large M ensures that the probability that two parent nodes select the same channel at the same time is low. Therefore, as shown in Figure 3.14(a), expect the full broadcast scheme, the success rate of the other three broadcast schemes increases as the number of channels increases. In addition, both our proposed basic and enhanced schemes have very similar and high success rates (i.e., ¿0.95). However, the random and full broadcast schemes result in relatively low success rates. On the other hand, a large M also leads to a long broadcast delay.

Hence, as shown in Figure 3.14(b), the average broadcast delay of all four schemes increases as the number of channels increases. Moreover, our proposed enhanced scheme outperforms other the three broadcast schemes in terms of shorter average broadcast delay.

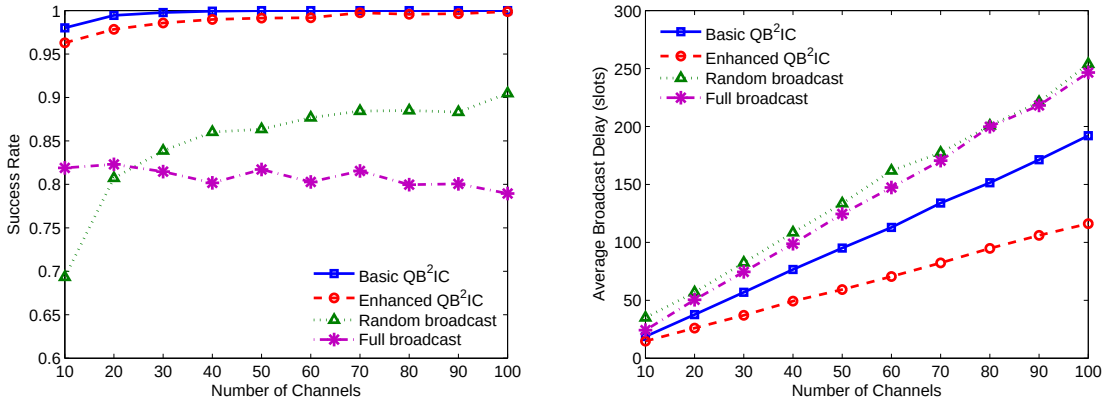

(a) Success rate.

(b) Average broadcast delay.

Figure 3.14: The impact of the number of channels.

3.5.3 The Impact of the Channel Availability Variation

In this section, we study the impact of the channel availability variation on the network performance. Note that during a broadcast process, the channel availability of the sender and receiver may change due to either PU activity (i.e., a new PU may claim one of the available channels during a broadcast) and PU mobility (i.e., a new active PU may move into the sensing range of a SU). This channel availability change may also affect the network performance. Therefore, the robustness of the proposed broadcast scheme against the channel availability variation needs to be investigated. Figure 3.15 depicts the impact of the channel availability change due to PU activity on the basic broadcast scheme when $n = 2$, $S = 40$ and $M = 20$. We let the PU packet arrival rate change from 5pkt/s to 50pkt/s and the PU packet length is 50 slots. This means that the probability that a PU is active, ρ, varies from 0.35 to 0.85. It is shown that the impact of the PU activity on the network performance is quite limited. When PUs are very densely deployed (i.e., 40 PUs within a 10×10 area) and PU traffic is very heavy (i.e., $\rho = 0.85$), the decrease of the success rate is only

up to 5% and the increase of the average broadcast delay is only up to 9%.

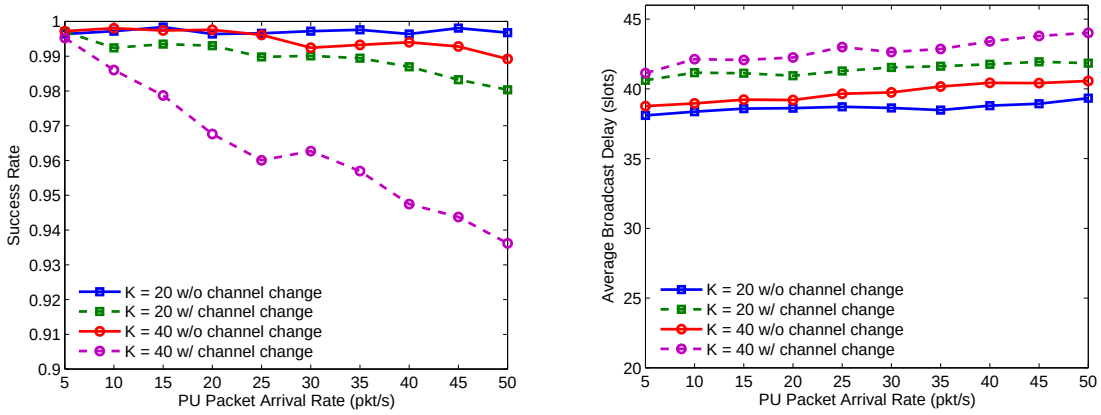

(a) Success rate. (b) Average broadcast delay.

Figure 3.15: The impact of the channel availability change due to PU activity.

In addition, Figure 3.15 depicts the impact of the channel availability change due to PU mobility. We use the Random Waypoint Mobility Model to characterize the movement pattern for PUs [91]. Under this model, a PU begins by staying in a location for a certain period of time (e.g., a pause time which is uniformly distributed between $[0, 4s]$). Once the pause period expires, the PU randomly selects a speed that is uniformly distributed between $[0, v_{max}]$ and moves for a random time that is uniformly distributed between $[0, 4s]$. Upon its arrival, the PU pauses for a random time period before starting the movement again. Figure 3.16 depicts the impact of the channel availability change due to PU mobility on the network performance. Similar to the impact of PU activity on the network performance, it is shown that the impact of the PU mobility is also quite trivial. When PUs are very densely deployed (i.e., 40 PUs within a 10×10 area) and PUs move very fast (i.e., the maximum PU speed is 40m/s), the decrease of the success rate is only up to 1% and the increase of the average broadcast delay is only up to 2%.

3.5.4 The Impact of Transmission Errors

In this section, we investigate the impact of transmission errors on the network performance. It is known that various factors (e.g., transmission contention, channel

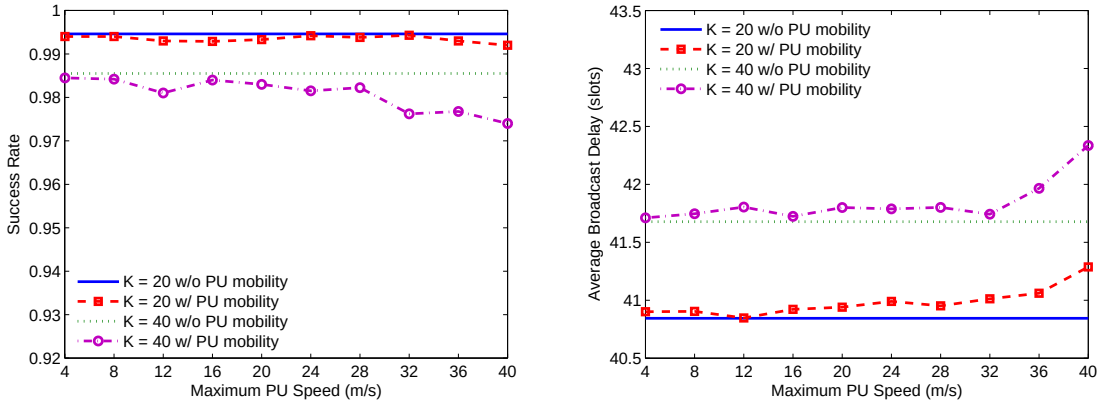

(a) Success rate.

(b) Average broadcast delay.

Figure 3.16: The impact of the channel availability change due to PU mobility.

quality, etc.) can lead to transmission errors. These transmission errors may cause failed broadcasts. However, as stated in Section 1, due to the ACK implosion problem, ACK messages are not feasible to be used to prevent failed broadcasts in CR ad hoc networks. Even though ACKs are not applied to solve the transmission error problem, our proposed QB^{2}IC protocol can still be used in a radio environment where transmission errors exist. By increasing the number of channels selected by the sender (i.e., n) or increasing the number of times that the sender broadcasts the message (i.e., S), the probability that a sender and a receiver have a channel rendezvous increases. Therefore, our proposed QB^{2}IC protocol can still achieve satisfactory QoS requirements. Figure 3.17 shows the simulation results of the basic scheme of the proposed QB^{2}IC protocol when $N = 4$ under various n, S, and σ, where SUs form a 2×2 grid network. It is shown that by increasing n or S, our proposed QB^{2}IC protocol can still achieve satisfactory performance.

3.6 The Proposed BRACER Protocol

In this section, we introduce the proposed broadcast protocol for multi-hop CR ad hoc networks, BRACER. There are three components of the proposed BRACER protocol: 1) the construction of the broadcasting sequences; 2) the distributed broadcast scheduling scheme; and 3) the broadcast collision avoidance scheme. We assume

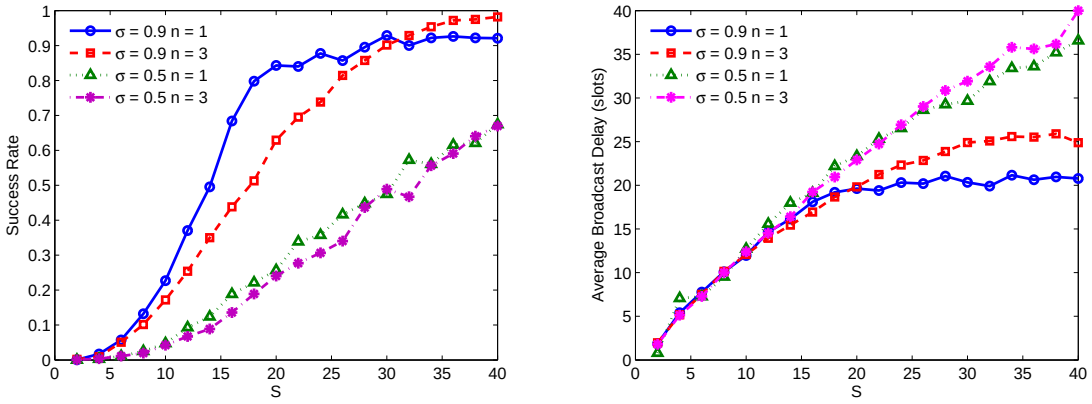

(a) Success rate.

(b) Average broadcast delay.

Figure 3.17: Success rate and average broadcast delay of the basic scheme of the proposed QB^{2}IC protocol when $N = 4$ under various n, S, and σ.

that a time-slotted system is adopted for SUs, where the length of a time slot is long enough to transmit a broadcast packet [88]. We also assume that each SU knows the locations of its all 2-hop neighbors. We claim that this is a more valid assumption than the knowledge of global network topology. We provide a detailed discussion on this issue in Section 3.8. In the rest of the chapter, we use the term "sender" to indicate a SU who has just received a message and will rebroadcast the message. In addition, we use the term "receiver" to indicate a SU who has not received the message. The notations used in our protocol design are listed in Table 3.2.

Table 3.2: Notations used in the Protocol

$N(v)$	The set of the neighboring nodes of node v
$N(N(v))$	The set of the neighbors of the neighboring nodes of node v
$d(v,u)$	The Euclidean distance between node v and u
r_c	The radius of the transmission range of each node
$\lvert \cdot \rvert$	The number of elements in a set
L_v	The downsized available channel set of node v
$w(v)$	The size of the downsized available channel set of node v
C	The set of the initial w of intermediate nodes
BS_v	The broadcasting sequence for a sender v
RS_v	The broadcasting sequence for a receiver v
DS_v	The default sequence of a sender v
st_v	The starting time slot of a sender v
rt_v	The time slot that a receiver v receives the message
R_v	The random number assigned to a receiver v by its sender

3.6.1 Construction of the Broadcasting Sequences

The broadcasting sequences are the sequences of channels by which a sender and its receivers hop for successful broadcasts. First of all, we consider the single-hop broadcast scenario. Due to the non-uniform channel availability in CR ad hoc networks, a SU sender may have to use multiple channels for broadcasting in order to let all its neighboring nodes receive the broadcast message. Accordingly, the neighboring nodes may also have to listen to multiple channels in order to receive the broadcast message. Hence, the first issue to design a broadcast protocol is which channels should be used for broadcasting. One possible method is to broadcast on all the available channels of the SU sender. However, this method is quite costly in terms of the broadcast delay when the number of available channels is large. Therefore, we propose to select a subset of available channels from the original available channel set of each SU. First, the available channels of each SU are ranked based on the channel indexes. Then, each SU selects the first w channels from the ranked channel list and forms a downsized available channel set. The value of w needs to be carefully designed to ensure that at least one common channel exists between the downsized available channel sets of the SU sender and each of its neighboring nodes. The detailed derivation process to obtain a proper w is given in Section 3.7. Based on the derivation process, each SU can calculate the value of w of its own and its 1-hop neighbors before a broadcast starts.

On the other hand, the second issue is the sequences of the channels by which a sender and its receivers hop for successful broadcasts. In this chapter, we design different broadcasting sequences for a SU sender and its receivers to guarantee a successful broadcast in the single-hop scenario as long as they have at least one common channel. The sender hops and broadcasts a message on each channel in a time slot following its own sequence. On the other hand, the receiver hops and listens on each channel following its own sequence. The pseudo-codes for constructing the

broadcasting sequences are shown in Algorithm 1 and 2.

Algorithm 1: Construction of the broadcasting sequence BS_v for a SU sender v.

Input: $w(v), L_v$.

Output: BS_v.

randomize the order of elements in L_v;

$BS_v \leftarrow \varnothing$;

$i \leftarrow 1$

while $i \leq w(v)^2$ do

$BS_v(i) \leftarrow L_v((i \mod w(v)) + 1)$;

$i \leftarrow i + 1$;

Return BS_v;

Algorithm 2: Construction of the broadcasting sequence RS_v for a SU receiver v.

Input: $w(v), L_v$.

Output: RS_v.

randomize the order of elements in L_v;

$RS_v \leftarrow \varnothing$;

$i \leftarrow 1$

while $i \leq w(v)$ do

$j \leftarrow 1$;

while $j \leq w(v)$ do $RS_v((i-1)w(v) + j) \leftarrow L_v(i)$;

$j \leftarrow j + 1$;

$i \leftarrow i + 1$ Return BS_v;

From Algorithm 1 and 2, for a SU sender, it hops periodically on the w available channels for w periods (i.e., w^2 time slots). For each receiver, it stays on one of the w available channels for w time slots. Then, it repeats for every channel in the w avail-

able channels. Figure 3.18 gives an example to illustrate the construction of the broadcasting sequences for SU senders and receivers. In Figure 3.18, the downsized available channel set of a sender and a receiver is $\{1, 2\}$ and $\{2, 3, 4\}$, respectively. Based on Algorithm 1, the broadcasting sequence of the sender is $\{2, 1, 2, 1\}$. Similarly, based on Algorithm 2, the broadcasting sequence of the receiver is $\{4, 4, 4, 3, 3, 3, 2, 2, 2\}$. Since a sender usually does not know the length of the broadcasting sequence of the receiver, it broadcasts the message following its broadcasting sequence for $\lfloor \frac{M^2}{w^2} \rfloor + 1$ cycles, where M is the total number of channels. In this way, the total length of time slots that the sender broadcasts is bound to be longer than one cycle of the receiver's broadcasting sequence. As shown in Figure 3.18, the shaded part represents a successful broadcast.

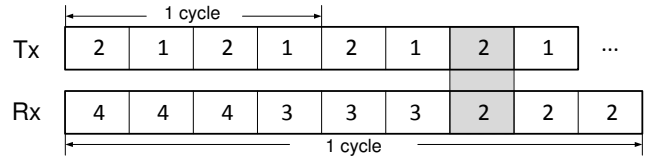

Figure 3.18: An example of the broadcasting sequences.

Since every SU calculates the initial value of w based on its local information and the derivation process in Section 3.7, different SUs may obtain different values of w. We further denote w_s and w_r as the w used by the sender and the receiver to construct their broadcasting sequences, respectively. Note that w_s and w_r may not necessarily be the same as the initial w calculated by each SU. They also depend on the initial w of its neighboring nodes. The following theorem gives an upper-bound on the single-hop broadcast delay.

Theorem 1: If $w_s \leq w_r$, the single-hop broadcast is a guaranteed success within w_r^2 time slots as long as the sender and the receiver have at least one common channel between their downsized available channel sets.

Proof. Based on Algorithm 1, a SU sender broadcasts on all the channels in its down-

sized available channel set in w_s consecutive time slots. Based on Algorithm 2, a SU receiver listens to every channel in its downsized available channel set for w_r consecutive time slots. If $w_s \leq w_r$, during the w_r consecutive time slots for which the SU receiver stays on the same channel, every channel of the SU sender must appear at least once. Thus, as long as the SU sender and the receiver have at least one common channel, there must exists a time slot that the sender and the receiver hop on the same channel during one cycle of the broadcasting sequence of the receiver (i.e., w_r^2). Since we let the total length of time slots that the sender broadcasts be longer than one cycle of the receiver's broadcasting sequence, the broadcast is guaranteed to be successful. □

Then, how to determine w_s and w_r? From Theorem 1, $w_s \leq w_r$ is a sufficient condition of a single-hop successful broadcast. Therefore, in order to satisfy this condition, a proper w_r needs to be selected by any SU who has not received the broadcast message to ensure the reception of the broadcast message sent from any potential neighbor. Since w_r depends on w_s and a SU receiver usually does not know which neighboring node is sending until it receives the broadcast message, it selects the largest initial w of all its 1-hop neighbors as its w_r. That is, for a SU receiver v, $w_r(v) = \max\{w(u)|u \in N(v)\}$. On the other hand, the sender uses its calculated initial w as w_s to broadcast. Therefore, the w_s selected by the actual sender is bound to be smaller than or equal to this w_r. Thus, according to Theorem 1, the single-hop broadcast is a guaranteed success as long as the sender and its receiver have at least one common channel between their downsized available channel sets.

To illustrate the above discussed operation, we consider a multi-hop scenario shown in Figure 3.19. The initial w calculated by each SU before the broadcast starts based on its local information are shown. Every node also calculates the initial w of its 1-hop neighbors. Without loss of generality, node A is assumed to be the source node. Based on Theorem 1, the values of w_r employed by each receiver can

be obtained. For instance, since node B knows the initial w of its neighbors (i.e., $w(A)$=3, $w(D)$=4, and $w(F)$=4), it selects the largest initial w as its own w_r (i.e., $w_r(B)=4$). Similarly, we have $w_r(C)=4, w_r(D)=3, w_r(E)=4$, and $w_r(F)=5$. Then, all nodes except node A use their w_r to construct the broadcasting sequences based on Algorithm 2. On the other hand, since each sender uses its calculated initial w as w_s, we have $w_s(A)=3$, $w_s(B)=3$, $w_s(C)=5$, $w_s(D)=4$, $w_s(E)=2$, and $w_s(F)=4$. Then, if a node needs to broadcast a message, it uses its w_s to construct the broadcasting sequence based on Algorithm 1.

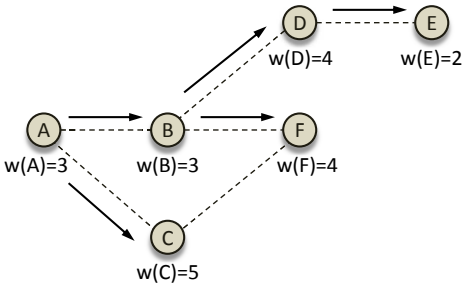

Figure 3.19: A multi-hop broadcast scenario.

3.6.2 The Distributed Broadcast Scheduling Scheme

Next, we consider the broadcast scheduling issue in the multi-hop broadcast scenario. The goal of the proposed distributed broadcast scheduling scheme is to intelligently select SU nodes for rebroadcasting in order to achieve the shortest broadcast delay.

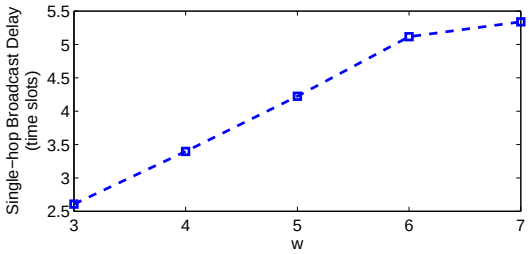

Figure 3.20: The single-hop broadcast delay when w_s=w_r=w.

First, from the simulation results shown in Figure 3.20, we can observe that the single-hop broadcast delay increases when w increases. Therefore, in a multi-hop

broadcast scenario, if there are multiple intermediate nodes with the same child node, the intermediate node with the smallest w is selected to rebroadcast. If there are more than one intermediate node with the smallest w, all these nodes should rebroadcast and a broadcast collision avoidance scheme (which is explained in detail in Section 3.6.3) is executed before they rebroadcast the message. The pseudo-code of the proposed scheduling scheme is shown in Algorithm 3, where node v has just received the broadcast message from node q and needs to decide whether to rebroadcast. Node q includes the calculated initial w of its 1-hop neighbors in the broadcast message. Algorithm 1 indicates that each SU should know the locations of its 1-hop neighbors (in order to obtain $N(v)$) and its 2-hop neighbors (in order to obtain $N(q)$ and $d(u,k)$). Once a node receives the message, it executes Algorithm 1 to decide whether it should rebroadcast or not. If it needs to rebroadcast, it uses its calculated initial w as w_s to construct the broadcasting sequence based on Algorithm 3. Thus, as illustrated in Figure 3.19, the message deliveries are shown by the arrows.

Algorithm 3: The pseudo-code of the broadcast scheduling scheme for a SU sender v.

Input: $q, N(v), N(N(v)), \{w(u)|u \in N(q)\}$.

Output: Decision of rebroadcasting.

$C \leftarrow \{w(v)\}$;

if $\{k|k \in (N(v) - N(v) \cap N(q))\} \neq \varnothing$ then

    foreach k do

        if $\{u|u \in N(q), d(u,k) \leq r_c, u \neq v\} \neq \varnothing$ do

        foreach u do

            $C \leftarrow \{C, w(u)\}$;

        if $w(v) = \min C$ and $|\{e|e = \min C\}| = 1$ then

            return TRUE;

        else if $w(v) = \min C$ and $|\{e|e = \min C\}| > 1$ then

            run Algorithm 4;

```
            return TRUE;
        else
            return FALSE;
        return TRUE;
else
    return FALSE;
```

From the above design, it is noted that each SU (either sending or receiving) follows the same rules and no centralized entity or prior information about the sender is required. Thus, the proposed broadcast scheduling scheme is fully distributed. In addition, since the node with the smallest w is selected for rebroadcasting, the broadcast delay is the shortest. Moreover, because only a subset of intermediate nodes are selected to rebroadcast, the number of intermediate nodes that need to forward the message is reduced. Thus, the probability that multiple senders broadcasting to the same receiver simultaneously can be reduced. Hence, the proposed broadcast scheduling scheme also contributes to the broadcast collision avoidance.

3.6.3 The Broadcast Collision Avoidance Scheme

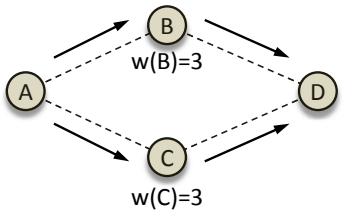

Figure 3.21: The broadcast scenario where a broadcast collision may occur.

From Algorithm 1, if there are multiple intermediate nodes with the same child node, only the intermediate node with the smallest w should rebroadcast. However, if more than one intermediate node with the same smallest w, all these intermediate nodes should rebroadcast and a broadcast collision may occur if these nodes deliver the messages on the same channel at the same time. For instance, in the example

shown in Figure 3.21 where node A is the source node, node B and C have the same w, which may lead to a broadcast collision when they rebroadcast simultaneously.

Most broadcast collision avoidance methods in traditional ad hoc networks assign different time slots to different intermediate nodes to avoid simultaneous transmissions. However, these methods cannot be applied to CR ad hoc networks because the exact time for the intermediate nodes to receive the broadcast message is random. As a result, to assign different time slots for different intermediate nodes is very challenging. In addition, since the intermediate nodes use multiple channels for broadcasting, the channel on which the broadcast collision occurs is also unknown. To the best of our knowledge, no existing collision avoidance scheme can address these challenges in CR ad hoc networks.

In this research, we propose a broadcast collision avoidance scheme for CR ad hoc networks. The main idea is to prohibit intermediate nodes from rebroadcasting on the same channel at the same time. Our proposed broadcast collision avoidance scheme works in a scenario where the intermediate nodes have the same parent node, as shown in Figure 3.21. The procedure of the proposed broadcast collision avoidance scheme is summarized as follows:

Step 1 Generating a Default Sequenc: When a source node (e.g., node A in Figure 3.21) broadcasts the message, it includes its own original available channel set in the message. Hence, if an intermediate node receives the message, it obtains the original available channel information of its parent node. Then, the intermediate node uses the first w available channels of its parent node to generate a default sequence, where w is its own calculated initial w (which may not be the same as the initial w of its parent node). If a channel in the default sequence is not available for this intermediate node, a void channel is assigned to replace the corresponding channel. For instance, if node B and C both obtain $w=3$ and the original available channels of node A, B, and C are $\{1, 2, 3, 4, 5\}$, $\{2, 3, 4, 5\}$, and $\{1, 3, 4, 6\}$, respectively, node B and C only

use the first three available channels of node A to generate their default sequences. Therefore, the default sequence of node B is $\{0, 2, 3\}$ and the default sequence of node C is $\{1, 0, 3\}$, where 0 means a void channel. A node does not send anything on a void channel.

Step 2 Circular Shifting the Default Sequence with a Random Number: Apart from the available channel set, the source node also includes a distinctive integer for each intermediate node v randomly selected from $[1, w(v)]$. If there are more than $w(v)$ intermediate nodes, the parent node randomly selects $w(v)$ of them and assigns a random integer. Only those intermediate nodes that acquire the random integer will rebroadcast the packet. Then, each intermediate node generates a new sequence from its default sequence using circular shift and the random integer. If we denote the default sequence as DS and the random integer as R, the intermediate node performs circular shift on the DS for R times (there is no difference of right-shift or left-shift). For instance, if node B and C get 3 and 1 as their random integers, respectively, the new sequences they generate from left-handed circular shift are $\{0, 2, 3\}$ and $\{0, 3, 1\}$, respectively.

Step 3 Forming the Broadcasting Sequence: Denote the starting time slot of the source node's broadcasting sequence as st and the time slot when an intermediate node receives the broadcast message as rt. The source node includes its st in the broadcast message. Then, the intermediate node performs circular shift on the new sequence generated from Step 2 for another $(rt-st+1)$ times. It repeats that sequence for $w(v)$ times to form a cycle of its broadcasting sequence.

The pseudo-code of the broadcast collision avoidance scheme is shown in Algorithm 4, where q is the source node and Circshift() is the function of circular shift. To further elaborate the scheme, Figure 3.22 shows an example of the proposed broadcast collision avoidance scheme. Without loss of generality, the starting time slot of the source node is 1. When node B and C do not receive the broadcast message, they hop

through the channels based on the broadcasting sequences generated from Algorithm 2. Then, node B and C receive the broadcast message at time slot 4 and 1, respectively. Based on Algorithm 4 and if the random integers for node B and C are 3 and 1, respectively, node B forms the broadcasting sequence as $\{2, 3, 0, 2, 3, 0, 2, 3, 0\}$ and node C forms the broadcasting sequence as $\{3, 1, 0, 3, 1, 0, 3, 1, 0\}$. Then, they start rebroadcasting from time slot 5 and 2 using the broadcasting sequences, respectively. The underlined channels are those a node hops on if it starts from time slot 1.

Algorithm 4: The pseudo-code of the broadcast collision avoidance scheme for SU v.

Input: $q, L_q, L_v, st_q, rt_v, R_v, w(v)$.

Output: BS'_v.

$BS'_v \leftarrow \varnothing$;

$i \leftarrow 1$;

$l \leftarrow 1$;

while $i \leq w(v)$ do

    $j \leftarrow 1$;

    while $j \leq w(v)$ do

        if $L_v(i) = L_q(j)$ then

            $DS_v(j) \leftarrow L_q(j)$;

$T_v \leftarrow$ Circshift(DS_v, R_v);

while $l \leq w(v)^2$ do

$BS'_v(l) \leftarrow T_v(l+(rt_v - st_q)+1 \mod w(v))$;

$l \leftarrow l + 1$;

Return BS'_v;

Therefore, by constructing the broadcasting sequences from the same channel set (the channel set of the common parent node, node A) but circular shifting different times for different nodes, the intermediate nodes are guaranteed not to send on the

same channel at the same time. Thus, broadcast collisions can be avoided. A trade-off of the proposed broadcast collision avoidance scheme is that less available channels are used for broadcasting because some void channels may be assigned. However, the benefit (e.g., the increase of the successful broadcast ratio) gained from eliminating broadcast collisions is greater than the loss of a very few number of channels. Hence, the only issue left is the derivation of the initial w, which is introduced in Section 3.7.

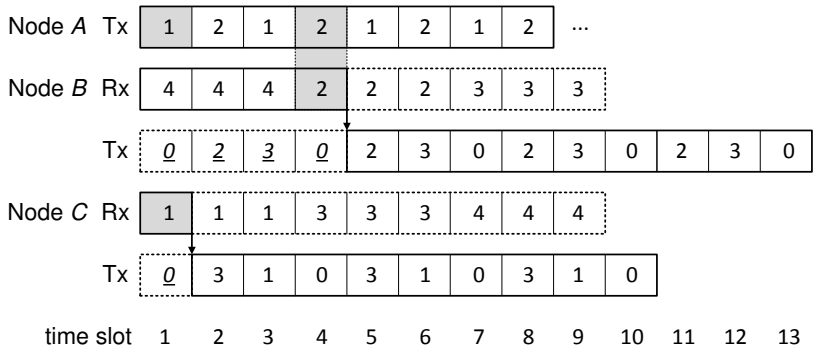

Figure 3.22: An example of the proposed broadcast collision avoidance scheme.

3.6.4 Protocol Flow Chart

In this section, we summarize the procedure of the proposed BRACER protocol. Figure 3.23 illustrates the flow chart of the proposed broadcast protocol. As shown in Figure 3.23, before a broadcast starts, every SU node first calculates its own initial w and the initial w of its 1-hop neighboring nodes using the 2-hop location information and the derivation process given in Section 3.7. If this node is the source node, it uses its own initial w as its w_s and constructs the broadcasting sequence based on Algorithm 1. Then, it hops and broadcasts a message on each channel during one time slot following its sequence. On the other hand, if this node is not the source node, it is by default a receiver. Then, it uses the maximum w of its 1-hop neighboring nodes as its w_r and constructs the broadcasting sequence based on Algorithm 2. It hops and listens on each channel during one time slot following its sequence. If the node receives the broadcast message from a sender, it runs the broadcast scheduling scheme

based on Algorithm 3 to determine whether it needs to rebroadcast this message. If it needs to rebroadcast and there is only one smallest w, it uses its own w as w_s and runs Algorithm 1 to rebroadcast. If it needs to rebroadcast and there are more than one smallest w, it runs the broadcast collision avoidance scheme based on Algorithm 4 to rebroadcast the message.

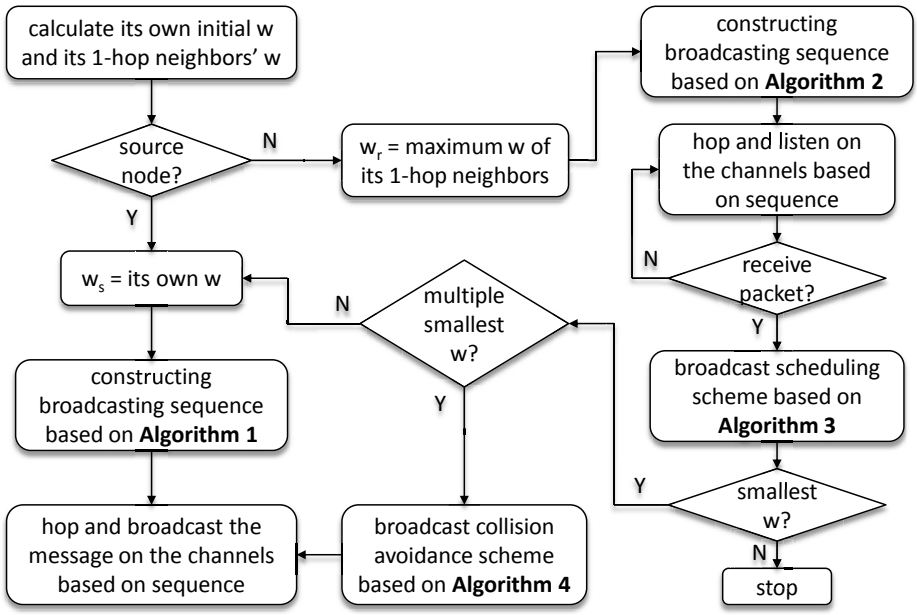

Figure 3.23: The flow chart of the proposed BRACER protocol.

3.7 The Derivation of the Value of w

In this section, we first introduce a network model we consider. Then, based on this model, we present the derivation process of the size of the downsized available channel set w.

3.7.1 The Network Model

In this chapter, we consider a CR ad hoc network where N SUs and K primary users (PUs) co-exist in an $\alpha \times \alpha$ area. PUs and SUs are distributed based on the model in Chapter 3.1. In addition, apart from the broadcast collision, other factors may also contribute to the packet error (e.g., channel quality, modulation schemes, and coding rate). However, in this chapter, we only consider broadcast collisions as the reason for the packet error. We claim that this is a valid assumption in most broadcast

scenarios [10, 11, 12, 13, 14, 15, 16, 18, 19, 21, 22]. In addition, we consider that since PUs at different locations can claim any channels for communications, the packets on the same channel do not necessarily belong to the same PU. This is a more practical scenario, as compared to some papers which assume that each channel is associated with a different PU. Under such a practical scenario, only those PUs that are within the sensing range of a SU and are active during the broadcast process contribute to the unavailable channels of the SU [23].

3.7.2 The Derivation of the Value of w

The value of w is essential to ensure a successful single-hop broadcast. Denote the probability of a successful single-hop broadcast as $P_{succ}(w)$, where $P_{succ}(w)$ is a function of w. Our goal is to obtain an appropriate w that satisfies the condition: $P_{succ}(w) \geq 1-\epsilon$, where ϵ is a small pre-defined value. From Theorem 1, the condition that at least one common channel exists between the downsized available channel sets of a SU pair is a necessary condition for a successful single-hop broadcast. Therefore, if we denote the source SU of a single-hop broadcast as S_0 and the neighbors of S_0 as $\{S_1, S_2, \cdots, S_H\}$, where H is the number of neighbors, $P_{succ}(w)$ is equal to the probability that there is at least one common channel between S_0 and each of its neighbors in their downsized available channel sets.

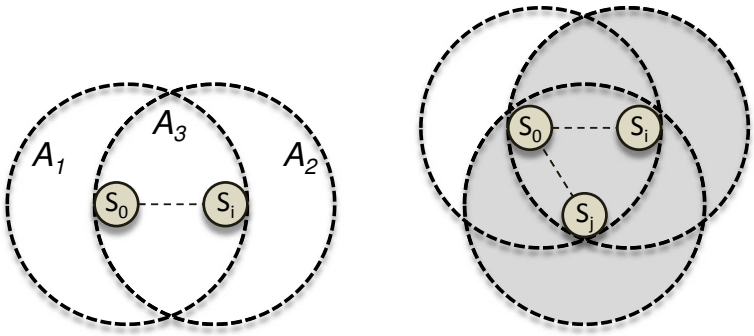

(a) The single-pair scenario. (b) The multi-pair scenario.

Figure 3.24: The single-hop broadcast scenario.

3.7.2.1 The single-pair scenario

We first calculate the probability that there is at least one common channel between the downsized available channel sets of S_0 and one of its neighbors S_i. The relative locations of the two SUs and their sensing ranges are shown in Figure 3.24(a). As illustrated in Figure 3.24(a), sensing ranges are divided into three areas: A_1, A_2, and A_3. Note that PUs in different areas have different impact on the channel availability of the two SUs. For instance, if a PU is active within A_3, the channel used by this PU is unavailable for both SUs. However, if a PU is active within A_1, the channel used by this PU is only unavailable for S_0. Thus, we first calculate the probability that a channel is available within each area, $P_k, k \in [1, 2, 3]$. The size of the total network area is denoted as A_L (i.e., $A_L = \alpha^2$). Since the locations of PUs are evenly distributed, the probability that p PUs are within A_k is

$$\Pr(p) = \binom{K}{p} \left(\frac{A_k}{A_L}\right)^p \left(\frac{A_L - A_k}{A_L}\right)^{K-p}, \tag{3.10}$$

where $\binom{K}{p}$ represents the total combinations of K choosing p. In addition, we define the probability that a PU is active, ρ, as:

$$\rho = \frac{E[\text{ON duration}]}{E[\text{ON duration}] + E[\text{OFF duration}]}, \tag{3.11}$$

where $E[\cdot]$ represents the expectation of the random variable. Therefore, given that there are p PUs within A_k, the probability that there are b PUs active is

$$\Pr(b|p) = \binom{p}{b} \rho^b (1-\rho)^{p-b}. \tag{3.12}$$

Furthermore, given that there are p PUs and b active PUs within A_k, the probability that there are c available channels is denoted as $\Pr(c|p, b)$. Since the number of available channels is only related to the number of active PUs, c is independent of p.

In addition, since an active PU randomly selects a channel from M channels in the band, $\Pr(c|p,b)$ is equivalent to the probability that there are exactly c empty boxes given that b balls are randomly put into a total of M boxes and a box can have more than one ball (because we do not limit a channel to only one PU). Thus, $\Pr(c|p,b)$ can be expressed as:

$$\Pr(c|p,b) = \frac{\binom{M}{c}\binom{b-1}{b-M+c}}{\binom{b+M-1}{b}}, c \in [\max(0, M-b), M]. \tag{3.13}$$

Hence, the probability that there are c available channels and there are p PUs and b active PUs within A_k is the product of (3.10), (3.12), and (3.13). Then, the probability that a channel is available within A_k is obtained from (3.14).

$$P_k = \frac{1}{M}\sum_{p=0}^{K}\sum_{b=0}^{p}\sum_{c=\max(0,M-b)}^{M}\frac{c\binom{M}{c}\binom{b-1}{b-M+c}}{\binom{b+M-1}{b}}\binom{p}{b}\rho^b(1-\rho)^{p-b}\binom{K}{p}\left(\frac{A_k}{A_L}\right)^p\left(\frac{A_L-A_k}{A_L}\right)^{K-p}. \tag{3.14}$$

Next, we consider the relationship between the downsized available channel sets of the two SUs. In our derivation, we only consider the scenario where the sender and its receiver have the same w (i.e., w_s=w_r). If $w_r > w_s$, the channels after the first w_s channels do not affect the number of common channels. Thus, the derivation process is the same. Figure 3.25 shows an example of the channel availability status of two SUs when $w(S_0) = 3$, where a shaded square indicates an idle channel and a white square indicates a busy channel. A square with a cross means that a channel can be either idle or busy. Since each SU only selects the first w available channels to form a downsized available channel set, the availability status of the channels after the first w available channels is not specified. Then, without loss of generality, we denote t and h as the index of the last available channel in the downsized available channel sets of S_0 and S_i, respectively. We first assume that $t \leq h$. Hence, from channel 1 to t, there are four possible scenarios of every channel in terms of its availability for the

two SUs. They are: 1) the channel is available for both SUs (denoted as $C1$); 2) the channel is unavailable for both SUs (denoted as $C2$); 3) the channel is only available for S_0 (denoted as $C3$); and 4) the channel is only available for S_i (denoted as $C4$). In addition, from channel $t+1$ to h (if $t < h$), there are two possible scenarios: 1) the channel is available for S_i but it can be any status for S_0 (denoted as $C5$) and 2) the channel is unavailable for S_i but it can be any status for S_0 (denoted as $C6$). Based on Figure 3.24(a), the probabilities of the above six scenarios can be obtained: 1) $P_{C1} = P_1P_2P_3$; 2) $P_{C2} = (1-P_3) + (1-P_1)(1-P_2)P_3$; 3) $P_{C3} = P_1P_3(1-P_2)$; 4) $P_{C4} = (1-P_1)P_2P_3$; 5) $P_{C5} = P_{C1} + P_{C4}$; and 6) $P_{C6} = P_{C2} + P_{C3}$.

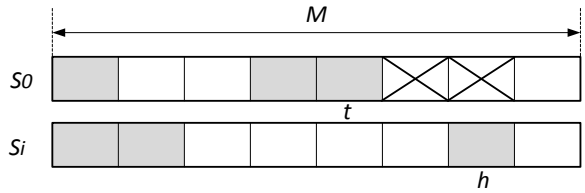

Figure 3.25: An example of the channel availability status when $w(S_0) = 3$.

Denote $Z(0,i)$ as the number of common channels between S_0 and S_i in their downsized available channel sets. In order to obtain $\Pr(Z(0,i) = z)$, we need to consider all the combinations of the channel status for every channel from channel 1 to h. There are two possible cases: 1) $t = h$ and 2) $t < h$. For the first case, channel h is a common channel between the two SUs. In addition, from channel 1 to channel $h-1$, there must be $z-1$ channels in scenario $C1$; $h-2w+z$ channels in $C2$, and $w-z$ channels in $C3$ and $C4$, respectively. Since $t = h$, no channel is in scenario $C5$ or $C6$. Thus, the probability that there are $z (z > 0)$ common channels in the first case is

$$P'(h) = \binom{h-1}{z-1}\binom{h-z}{w-z}\binom{h-w}{w-z} P_{C1}^{z} P_{C2}^{h-2w+z} P_{C3}^{w-z} P_{C4}^{w-z}. \tag{6}$$

For the second case, since $t < h$, the common available channels can only be between channel 1 to t. We denote the number of available channels for S_i from channel 1 to t as x. Thus, from channel 1 to t, similar to the first case, there are z channels in $C1$;

$t-w-x+z$ channels in $C2$; $w-z$ channels in $C3$; and $x-z$ channels in $C4$. In addition, from channel $t+1$ to h, there are $w-x$ channels in $C5$ and $h-t-w+x$ channels in $C6$. Therefore, the probability that there are totally z common channels is obtained from (7). If we switch S_0 and S_i in Figure 3.25, we can obtain the probability for the dual case. Hence, the probability that there are z common channels in the second case is expressed in (3.7).

$$P_1''(h) = P_{C1}^{z} P_{C3}^{w-z} \sum_{t=w}^{h-1} \sum_{x=\max(0,w+t-h)}^{t-w} \binom{t-1}{w-1} \binom{w}{z} \binom{t-w}{x-z} \binom{h-t-1}{w-x-1} P_{C4}^{x-z} P_{C2}^{(t-w-x+z)} (P_{C1}+P_{C4})^{(w-x)} (P_{C2}+P_{C3})^{(h-t-w+x)}. \tag{3.6}$$

$$\begin{aligned} P''(h) &= P_{C1}^{z} P_{C3}^{w-z} \sum_{t=w}^{h-1} \sum_{x=\max(0,w+t-h)}^{t-w} \binom{t-1}{w-1} \binom{w}{z} \binom{t-w}{x-z} \binom{h-t-1}{w-x-1} P_{C4}^{x-z} P_{C2}^{(t-w-x+z)} \\ &\quad (P_{C1}+P_{C4})^{(w-x)} (P_{C2}+P_{C3})^{(h-t-w+x)} + P_{C1}^{z} P_{C4}^{w-z} \sum_{t=w}^{h-1} \sum_{x=\max(0,w+t-h)}^{t-w} \binom{t-1}{w-1} \\ &\quad \binom{w}{z} \binom{t-w}{x-z} \binom{h-t-1}{w-x-1} P_{C3}^{x-z} P_{C2}^{(t-w-x+z)} (P_{C1}+P_{C3})^{(w-x)} (P_{C2}+P_{C4})^{(h-t-w+x)}. \end{aligned} \tag{3.7}$$

Therefore, the probability that there are z common channels for the first w available channels for each SU is

$$\Pr(Z(0,i)=z) = \sum_{h=2w-z}^{M} P'(h) + P''(h). \tag{3.8}$$

Thus, the probability of a successful single-hop broadcast from S_0 to S_i is

$$P_{succ}(w) = 1 - \Pr(Z(0,i)=0). \tag{3.9}$$

Figure 3.26 shows the analytical and simulation results of $P_{succ}(w)$ in the single-pair scenario under various w and different M. To obtain these results, the number of PUs $K = 40$ and the probability that a PU is active $\rho = 0.9$. In addition, the side length of the network area $\alpha = 10$ (unit length) and two neighboring SUs are at the

border of each other's sensing range where $r_s = 2$ (unit length). As shown in Figure 3.26, the simulation results match extremely well with the analytical results.

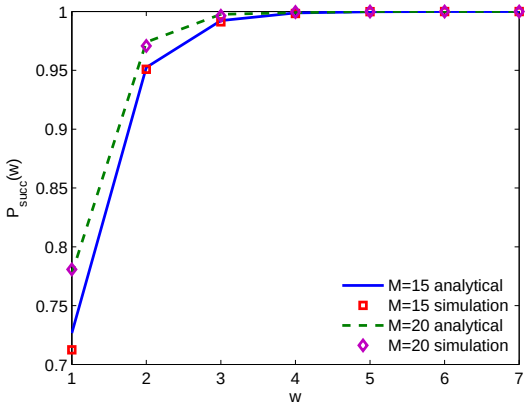

Figure 3.26: Analytical and simulation results of $P_{succ}(w)$ in the single-pair scenario under various w and different M.

3.7.2.2 The multi-pair scenario

we extend the above results to a multi-pair scenario, as shown in Figure 3.24(b) where S_i and S_j are two neighbors of S_0. Based on the knowledge of combination mathematics, the probability of a successful broadcast in the multi-pair scenario shown in Figure 3.24(b) is

$$\begin{aligned} P_{succ}(w) = 1 - \Pr(Z(0,i)=0) - \Pr(Z(0,j)=0) \\ + \Pr(Z(0,i,j)=0), \end{aligned} \tag{3.10}$$

where $\Pr(z(0,i,j) = 0)$ is the probability that both S_i and S_j do not have any common channel in the downsized available channel sets with S_0. Since the other two terms in (3.10) (i.e., $\Pr(Z(0,i) = 0)$ and $\Pr(Z(0,j) = 0)$) can be obtained from (3.8), we only need to calculate $\Pr(Z(0,i,j) = 0)$.

To calculate $\Pr(Z(0,i,j)=0)$, we use the same idea from the single-pair scenario. That is, we consider S_i and S_j together as one new neighboring node. The sensing range of the new neighboring node is the union of the sensing ranges of the two original nodes (i.e., the shaded area in Figure 3.24(b)). Therefore, we can obtain

new P_1, P_2, and P_3 for the multi-pair scenario based on the new size of the sensing range. Moreover, the probabilities of every scenario of the channel status can also be obtained accordingly. Therefore, by using (6)-(3.8), we can calculate $\Pr(Z(0,i,j) = 0)$. Then, given the locations of the H neighbors, each SU can get the probability of a successful single-hop broadcast by performing the same procedure iteratively for H times. Finally, by letting $P_{succ}(w) \geq 1 - \epsilon$, a proper w can be acquired for S_0.

3.8 Discussion on the Proposed BRACER Protocol

It is noted that our proposed BRACER protocol is particularly designed for broadcast scenarios in multi-hop CR ad hoc networks without a common control channel. There are two implementation issues that are essential to the performance of our proposed distributed broadcast protocol: 1) the 2-hop location information; and 2) the time synchronization. In this section, we provide a further discussion on these two issues.

3.8.1 2-hop Location Information

It is known that in our proposed BRACER protocol, every SU node needs the location information of its 2-hop neighboring nodes in order to calculate the size of the downsized available channel sets of its 1-hop neighboring nodes. Even though the localization issue for CR ad hoc networks is out of the scope of this paper, we hereby introduce several solutions to obtain the 2-hop location information in detail. Generally speaking, the location information for a traditional ad hoc network can be obtained either from external positioning techniques (e.g., Global Positioning System (GPS) [92]) or from some localization algorithms without external positioning techniques [93, 94, 95]. Hence, GPS is an option to obtain the location information of the 2-hop neighboring nodes in CR ad hoc networks. However, GPS requires additional hardware and consumes extra energy, which may not be efficient in CR ad hoc networks where cost and power constraints are often needed.

On the other hand, a number of localization algorithms that do not rely on GPS

for CR ad hoc networks have been proposed [96, 97, 98, 99]. In these works, the legacy localization algorithms proposed for traditional ad hoc networks, such as time-of-arrival (TOA)-based, angle-of-arrival (AOA)-based, and received-signal-strength (RSS)-based methods are improved and adopted in CR ad hoc networks. These localization algorithms often require the assistance from certain special nodes with known location information (named reference nodes). However, all these algorithms ignore the control message exchange issue between the reference nodes and the regular nodes in CR ad hoc networks. The control message exchange issue is either not considered or simplified by using a common control channel. It is known that transmitting messages on a global common channel without any additional control information is not feasible in CR ad hoc networks. Therefore, in order to receive the control message containing the location information from the reference nodes, a communication mechanism that does not rely on any other control information (i.e., under blind information) between the reference nodes and the regular nodes is needed. As mentioned before, in [23], a QoS-based broadcast protocol under blind information is proposed. We can use this scheme as the communication scheme between the reference nodes and the regular nodes to obtain the 2-hop location information. Since the broadcast protocol proposed in [23] can only support QoS provisioning, the successful broadcast ratio and average broadcast delay of this scheme for the whole network are not optimized. Therefore, this scheme is suitable to be used in the early stage of a broadcast procedure. After every node in the network acquires the 2-hop location information, the proposed BRACER protocol can be executed.

3.8.2 Time Synchronization

It is known that an advantage of our proposed BRACER protocol is that it does not require tight time synchronization. This special advantage is essential since tight time synchronization is extremely difficult to achieve in a real ad hoc network system. In this chapter, we define tight time synchronization as the scenario where time slots

of different nodes are precisely aligned. This means that the proposed BRACER protocol can guarantee the successful reception of a whole broadcast message even if the time slots of the sender and the receiver have an offset. Denote the length of the offset as δ. Without the loss of generality, δ is less than a time slot. Based on Theorem 1, in order to guarantee a successful single-hop broadcast, w_s must be smaller than or equal to w_r. Thus, we consider the time synchronization issue under the following two scenarios.

3.8.2.1 Scenario I

w_s is strictly smaller than w_r. If $w_s < w_r$ and the sender and the receiver have at least one common channel between their downsized available channel sets, we have the following theorem:

Theorem 2: If $w_s < w_r$, the single-hop broadcast is a guaranteed success within w_r^2 time slots even if the time slots of the sender and the receiver have an offset.

Proof. Similar to the proof of Theorem 1, if $w_s < w_r$, during the w_r consecutive time slots for which the receiver stays on the same channel, every channel of the sender must appear at least once. More importantly, since δ is less than a time slot, at least a whole time slot of the common channel between the sender and the receiver must be completely covered by the w_r consecutive time slots of the common channel. That is, the receiver can hear a whole time slot of the common channel when the sender broadcasts the message. Thus, a successful single-hop broadcast is guaranteed. □

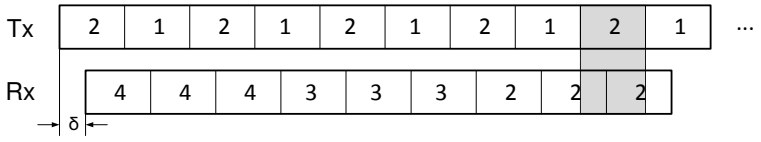

Figure 3.27: An example of Scenario I when time slots are unsynchronized.

Figure 3.27 shows an example of Scenario 1 where $w_s < w_r$. We assume that the time slots of the sender are ahead of the receiver with an offset of δ. As illustrated in Figure 3.27, on the 9-th slot of the sender's broadcasting sequence, the sender and

the receiver are on the same channel (i.e., channel 2). In addition, this time slot is completely covered by the 3 consecutive time slots when the receiver is on channel 2. Hence, the broadcast message can be successfully received by the receiver.

3.8.2.2 Scenario II

w_s is equal to w_r. If $w_s = w_r$, there are two sub-cases: 1) *Case 1*: a time slot of the common channel is completely covered by the w_r consecutive time slots of the receiver on the same channel; and 2) *Case 2*: a time slot of the common channel is partially covered by the w_r consecutive time slots of the receiver on the same channel. Figure 3.28 shows an example of Case 1 in Scenario II. Similar to Scenario I, the broadcast message can still be successfully received even if an offset exists.

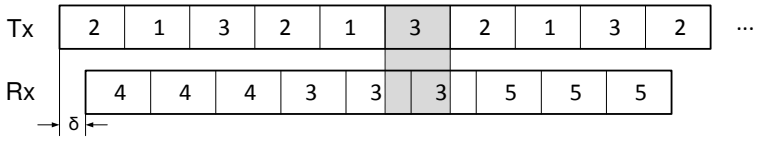

Figure 3.28: An example of Case 1 in Scenario II when time slots are unsynchronized.

On the other hand, Figure 3.29 shows an example of Case 2 in Scenario II. This case occurs when the time slot of the common channel of the sender is partially covered by the first and the last time slot of the w_r consecutive time slots of the receiver. From the communication theory, it is known that if a node only receives a part of a packet, it cannot decode this packet correctly and will drop it at the physical (PHY) layer. Thus, even if the sender and the receiver have a common channel, the receiver cannot successfully receive the broadcast message within w_r^2 time slots in Case 2.

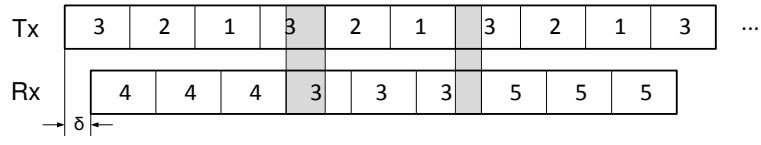

Figure 3.29: An example of Case 2 in Scenario II when time slots are unsynchronized.

We provide two simple modifications of our proposed BRACER protocol for this case. The first way is that the receiver always shift the whole cycle of the broadcasting

sequence one slot forward or one slot backward after it hops for one cycle (i.e., w_r^2 time slots) and has not received the broadcast message. At the same time, the total length of time slots that the sender broadcasts needs to be longer than three cycles of the receiver's broadcasting sequence. That is, the sender broadcasts the message following its broadcasting sequence for $\lfloor \frac{3 \times M^2}{w_s^2} \rfloor + 1$ cycles. In this way, Case 2 becomes Case 1. Then, even if the receiver may not receive the message within one cycle, it can still successfully receive the message in the following cycle, as shown in Figure 3.30.

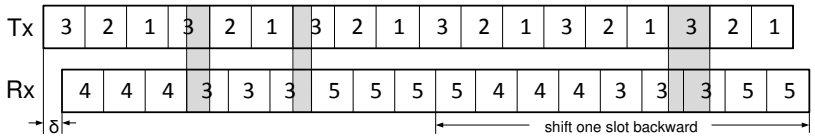

Figure 3.30: An example of the first way of modification for Case 2 in Scenario II when time slots are unsynchronized.

On the other hand, the second way is that the receiver v selects $w_r(v)$ to be $\max\{w(u)|u \in N(v)\} + 1$, where $N(v)$ is the set of the neighboring nodes of the receiver v. Therefore, the w_r of the receiver is always larger than the w_s used by the sender. In this way, Case 2 becomes Scenario I. Based on Theroem 2, the successful broadcast is guaranteed within w_r^2 time slots, as shown in Figure 3.31. To sum up, from the above analysis, it is known that our proposed BRACER protocol can be used in an environment where tight time synchronization is not required.

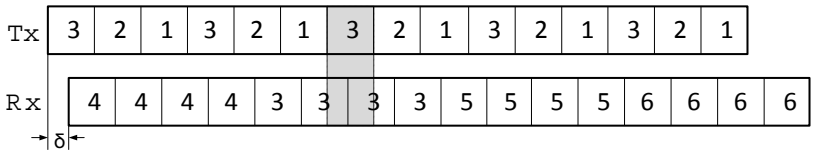

Figure 3.31: An example of the second way of modification for Case 2 in Scenario II when time slots are unsynchronized.

3.9 Performance Evaluation

In this section, we evaluate the performance of the proposed broadcast protocol. We consider two types of PU traffic models in the simulation [89]. The first

PU traffic model is discrete-time, where the PU packet inter-arrival time follows the biased-geometric distribution [90]. The second PU traffic model is continuous-time, where the PU packet inter-arrival time follows the Pareto distribution [90]. We assume that the probability that a PU is active is fixed (i.e., $\rho = 0.9$). In addition, the side length of the network area $\alpha = 10$ (unit length). We assume that the radius of the sensing range and the transmission range are the same (i.e., $r_s = r_c = 2$ (unit length)). In this chapter, we mainly investigate the following two performance metrics: 1) successful broadcast ratio: the probability that all nodes in a network successfully receive the broadcast message and 2) average broadcast delay: the average duration from the moment a broadcast starts to the moment the last node receives the broadcast message. In addition, we compare our proposed broadcast protocol with five other schemes: 1) Random+Flooding: each SU randomly selects a channel to hop and uses flooding (i.e., a SU is obligated to rebroadcast once receiving the message); 2) Sequence+Flooding (1/3 of our design): each SU downsizes its available channel set and constructs broadcasting sequences based on our scheme and uses flooding; 3) Sequence+Schedule (2/3 of our design): each SU constructs broadcasting sequences based on our scheme and uses our broadcast scheduling scheme; 4) Basic QoS Scheme: each SU uses the basic scheme of the QoS-based broadcast protocol to broadcast [23]; and 5) JS+Flooding: each SU uses the jump-stay scheme [33] to construct the broadcasting sequences and uses flooding.

3.9.1 Successful Broadcast Ratio

Since the single-hop successful broadcast ratio depends on w which is related to a pre-defined value ϵ, we define $\epsilon = 0.001$. In fact, ϵ can be an arbitrary small value. Thus, based on Section 3.7, each SU calculates a proper w before the broadcast starts in our scheme, the Sequence+Flooding scheme, and the Sequence+Schedule scheme. Table 3.3 and 3.4 show the simulation results of the successful broadcast ratio under different number of SUs and PUs, where the value in the upper cell is for

the discrete-time PU traffic and the lower cell is for the continous-time PU traffic. In Table 3.3, $M = 20$ and $K = 40$. In Table 3.4, $M = 20$ and $N = 20$. As shown in Table 3.3 and 3.4, the successful broadcast ratio is higher than 99% under our proposed broadcast protocol in all scenarios. In addition, the proposed broadcast protocol outperforms other schemes in terms of higher successful broadcast ratio. Since the jump-stay scheme requires that the i-th available channel in the available channel set is also channel i, it cannot utilize the technique in our scheme to downsize the original available channel set. In addition, the jump-stay scheme can guarantee rendezvous within $6MP(P-G)$, where P is the smallest prime number larger than M and G is the number of common channels between two SUs. Thus, in order to ensure a successful broadcast, each SU broadcasts the message for $6MP(P-G)$ slots. However, $6MP(P-G)$ is usually a very large number when M is large. Hence, to better illustrate the trade-off between the successful broadcast ratio and broadcast delay, we compare our scheme with JS+Flooding in Section 3.9.2.

Table 3.3: Successful broadcast ratio under different number of SUs

	N=5	N=10	N=15	N=20	N=25
Random+Flooding	0.8801	0.8180	0.8100	0.8726	0.8821
	0.8630	0.9148	0.9075	0.8698	0.8708
Sequence+Flooding	0.9849	0.9839	0.9828	0.9823	0.9863
	0.9762	0.9769	0.9777	0.9773	0.9719
Sequence+Schedule	0.9859	0.9864	0.9823	0.9857	0.9855
	0.9812	0.9845	0.9849	0.9876	0.9861
Basic QoS Scheme	0.8915	0.9022	0.8543	0.9314	0.9317
	0.8739	0.8386	0.8952	0.8498	0.8624
Proposed Scheme	0.9991	0.9973	0.9969	0.9982	0.9909
	0.9994	0.9959	0.9954	0.9967	0.9951

3.9.2 Average Broadcast Delay

Table 3.5 and 3.6 show the simulation results of the average broadcast delay under different number of SUs and PUs. Similarly to the successful broadcast ratio, in Table 3.5, $M = 20$ and $K = 40$. In Table 3.6, $M = 20$ and $N = 20$. As shown in Table 3.5 and 3.6, the proposed broadcast protocol outperforms other schemes in

Table 3.4: Successful broadcast ratio under different number of PUs

	K=20	K=30	K=40	K=50	K=60
Random+Flooding	0.8189	0.8326	0.8842	0.9208	0.8907
	0.7980	0.8738	0.9191	0.9139	0.8849
Sequence+Flooding	0.9866	0.9863	0.9823	0.9819	0.9871
	0.9742	0.9765	0.9773	0.9711	0.9797
Sequence+Schedule	0.9868	0.9872	0.9857	0.9881	0.9872
	0.9874	0.9885	0.9876	0.9833	0.9850
Basic QoS Scheme	0.9502	0.9167	0.9314	0.8222	0.7884
	0.8950	0.8921	0.8498	0.8792	0.8463
Proposed Scheme	0.9978	0.9976	0.9982	0.9951	0.9921
	0.9946	0.9941	0.9967	0.9977	0.9969

terms of shorter average broadcast delay. Furthermore, Figure 3.32 and 3.33 show the average broadcast delay under different number of channels when $N = 10$ and $K = 40$. As explained in Section 3.9.1, besides our proposed scheme, we also compare with JS+Flooding and our scheme without downsizing the available channel set (i.e., w=M). It is shown that even though the successful broadcast ratio is similar, the broadcast delay under JS+Flooding is much longer than our proposed scheme.

Table 3.5: Average broadcast delay under different number of SUs

Delay (unit: slots)	N=5	N=10	N=15	N=20	N=25
Random+Flooding	19.781	26.483	28.003	29.252	31.203
	20.981	23.765	27.686	33.153	32.883
Sequence+Flooding	8.458	11.168	12.744	14.243	15.909
	7.712	11.799	12.903	14.534	17.257
Sequence+Schedule	7.811	10.995	13.324	13.896	15.823
	7.155	11.457	13.553	14.551	15.078
Basic QoS Scheme	15.576	19.642	26.447	22.745	24.599
	16.093	23.164	21.698	26.834	32.078
Proposed Scheme	7.066	10.532	12.259	13.353	15.198
	6.545	11.097	12.786	13.639	14.801

To sum up, our proposed broadcast protocol outperforms Random+Flooding in terms of higher successful broadcast ratio and shorter broadcast delay. It also outperforms JS+Flooding in terms of shorter broadcast delay. In addition, even with the trade-off in our proposed broadcast collision avoidance scheme as explained in

Table 3.6: Average broadcast delay under different number of PUs

Delay (unit: slots)	K=20	K=30	K=40	K=50	K=60
Random+Flooding	29.189	31.459	25.737	25.361	24.243
	34.547	30.629	27.617	28.424	26.399
Sequence+Flooding	13.918	14.886	14.243	14.649	14.259
	14.413	13.958	14.534	14.867	14.389
Sequence+Schedule	12.747	14.206	13.896	14.361	14.014
	13.652	14.086	14.551	14.521	14.237
Basic QoS Scheme	25.148	25.187	22.745	27.182	28.533
	29.111	24.931	26.834	24.639	24.907
Proposed Scheme	12.322	13.555	13.352	14.279	13.597
	13.249	13.401	13.639	13.335	13.471

Section 3.6.3 and limited overhead, our proposed scheme and the schemes that use a part of our design (e.g., Sequence+Flooding) can still achieve better performance results than Random+Flooding for both metrics and JS+Flooding for the broadcast delay.

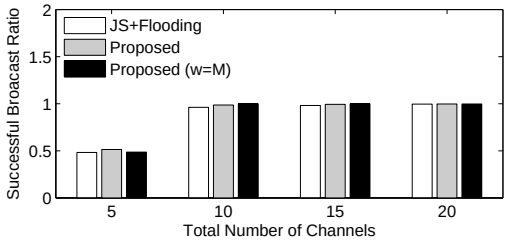

Figure 3.32: Successful broadcast ratio under different number of channels.

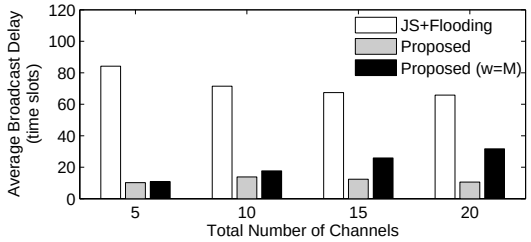

Figure 3.33: Average broadcast delay under different number of channels.

3.9.3 The Impact of Unsynchronized Time Slots

From the discussion in Section 3.8.2, it is known that our proposed BRACER protocol has an advantage that tight time synchronization is not required. Accordingly, we provide two modifications of our proposed protocol when time slots are unsyn-

chronized. In this section, we evaluate the impact of the unsynchronized time slots on the performance of the proposed BRACER protocol.

Figure 3.34 and 3.35 show the single-hop successful broadcast ratio and the average broadcast delay under different scenarios. In the first modification, we let $w_s = w_r = w$, whereas in the second modification, we let $w_s = w$ and $w_r = w+1$. It is shown that unsynchronized scenarios usually lead to lower successful broadcast ratio and longer average broadcast delay than the synchronized scenario. However, with the modifications of our proposed protocol, the low successful broadcast ratio can be significantly improved. From the figures, we may see that the second modification outperforms the first modification in terms of higher successful broadcast ratio. However, it also results in longer average broadcast delay than the first modification. Furthermore, when $w > 5$, the performance of the two modifications is very close to the unsynchronized scenario without modification. This is because that when w is large enough, more than one common channels exist between the sender and the receiver. Thus, there is at least one time slot on the common channel that is completely covered by the w_r consecutive time slots. Hence, the receiver can successfully receive the message without any modification.

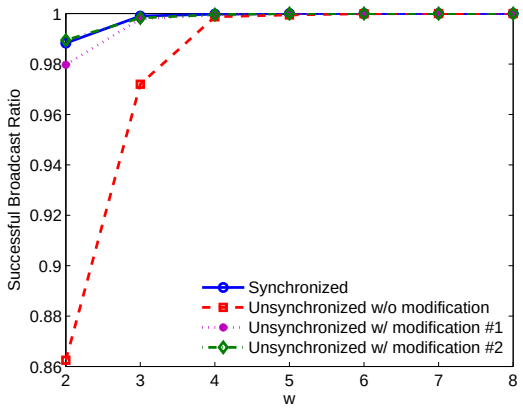

Figure 3.34: The impact of unsynchronized time slots on the single-hop successful broadcast ratio.

Figure 3.36 and 3.37 show the multi-hop successful broadcast ratio and average broadcast delay under different scenarios. It is illustrated in Figure 3.36 that when

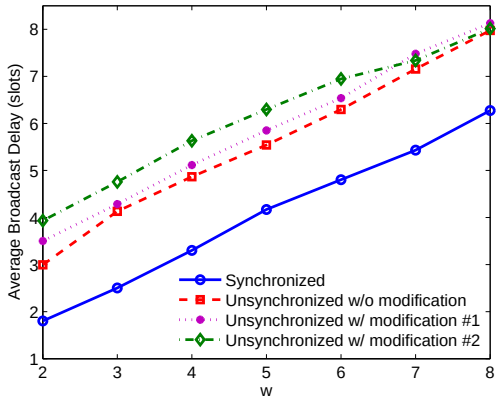

Figure 3.35: The impact of unsynchronized time slots on the single-hop average broadcast delay.

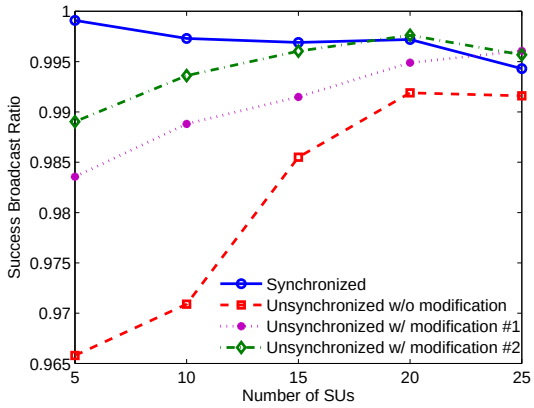

Figure 3.36: The impact of unsynchronized time slots on the multi-hop successful broadcast ratio.

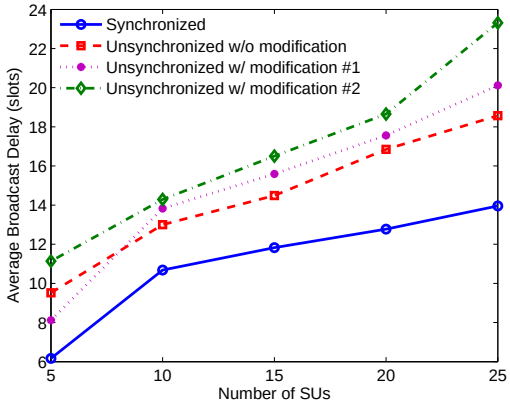

Figure 3.37: The impact of unsynchronized time slots on the multi-hop average broadcast delay.

the number of SUs is small (e.g., $N < 20$), the synchronized scenario outperforms all the unsynchronized scenarios in terms of higher successful broadcast ratio. This is because when N is small, each SU usually selects small w for broadcasting. Thus, from Figure 3.34, the successful broadcast ratio of the unsynchronized scenarios is lower than the synchronized scenario. However, when N is large (e.g., $N > 20$), the unsynchronized scenarios with both modifications outperform the synchronized scenario in terms of higher successful broadcast ratio. This is because when N is large, a receiver often has more than one senders. These senders broadcast the message on different channels to the receiver. Thus, the impact of unsynchronized time slots is diminished. Additionally, both modifications increase the probability that a receiver receives the broadcast message by either extending the broadcasting sequence or increasing the downsized available channel set. Therefore, the successful broadcast ratio of the unsynchronized scenarios with modifications is higher than that of the synchronized scenario. From Figure 3.36 and 3.37, the modifications can achieve up to 4% improvement on the successful broadcast ratio but cost up to 5% longer average broadcast delay as compared to the scenario without modification. The first modification even achieves shorter average broadcast delay when $N = 5$. Therefore, it is worthy to use the modifications when time slots are unsynchronized.

3.9.4 Broadcast Collision Analysis

In this section, we evaluate the performance of broadcast collisions for our proposed BRACER protocol. Since broadcast collisions usually lead to the waste of network resources, they should be efficiently avoided to save network resources. In this chapter, we use the average number of broadcast collisions in a broadcast procedure per SU node as the performance metric.

Figure 3.38 shows the average number of broadcast collisions under different numbers of channels. It is illustrated that the Proposed Scheme outperforms the Sequence+Flooding and Sequence+Schedule schemes in terms of fewer broadcast col-

lisions on average. This means that the broadcast collision avoidance scheme in the Proposed Scheme can effectively avoid broadcast collisions. In addition, the Proposed Scheme also incurs fewer broadcast collisions than the Random+Flooding scheme when $M \leq 20$. That is, the Random+Flooding scheme performs better than the Proposed Scheme only when M is very large. This is because that in the Random+Flooding scheme, each sender randomly selects an available channel in the band to broadcast. If the number of channels is large, the probability that two senders select the same channel is fairly low. However, when M is small, the Random+Flooding scheme leads to the highest number of broadcast collisions among the four schemes (e.g., M=5). Even though the Random+Flooding scheme causes the fewest broadcast collisions when M is large, the successful broadcast ratio and average broadcast delay of the Random+Flooding scheme are not acceptable, as shown in Table 3.3∼3.6. Additionally, the Sequence+Schedule scheme performs better than the Sequence+Flooding scheme, as shown in Figure 3.38. This means that our proposed distributed broadcast scheduling scheme also contributes to the collision avoidance.

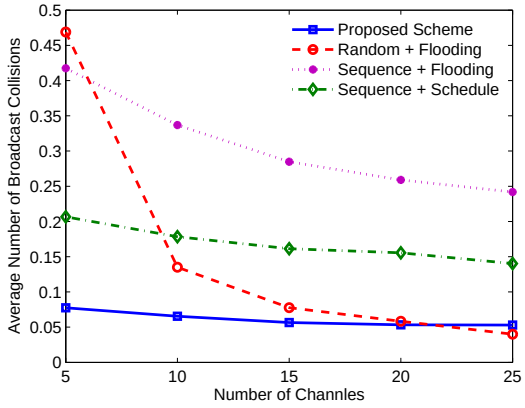

Figure 3.38: Average number of broadcast collisions under different numbers of channels when $N = 10$.

3.9.5 Overhead Analysis

Overhead is an important metric to evaluate the efficiency of a broadcast protocol. To evaluate the impact of overhead, we use normalized overhead as the performance metric [100, 101, 102]. Normalized overhead is defined as the ratio of the total broad-

cast packets (in bits) propagated by every node in the network to the total broadcast packets (in bits) received by the receivers [100, 101, 102].

We denote the length of the original broadcast packet as L_b. Extra information needs to be added in the original broadcast packet in order to realize the proposed BRACER protocol. The extra information in a broadcast packet mainly consists of three parts. First of all, as mentioned in Section 3.6.2, the sender should include the calculated initial w of its 1-hop neighbors in the broadcast message. Secondly, as described in Section 3.6.3, the sender should include its own channel availability information and the starting time slot of its broadcasting sequence in the message. Thirdly, the sender should include random integers for the intermediate nodes who need to rebroadcast to the same node. Thus, if we define the length of the initial w, the starting time slot, and the random integer as 8 bits, the length of the total extra information in a broadcast packet in bits for a node is

$$\Theta = 8N_a + M + 8 + 8N_b, \tag{3.11}$$

where N_a is the number of the 1-hop neighbors of the node and N_b is the number of the intermediate nodes who need to rebroadcast to the same node. Therefore, the total length of a broadcast packet of the proposed BRACER protocol is $L_b + \Theta$.

Figure 3.39 shows the normalized overhead under different lengths of the original broadcast packet. We set the range of the original broadcast packet length as $[50, 500]$ bits. Since broadcast packets are control packets which are often very short, they mainly fall in this range. In addition, we compare our proposed scheme with the Sequence+Flooding and Sequence+Schedule schemes. The Random+Flooding scheme does not require the 2-hop location information, so we exclude it for fair comparison. The length of the extra information in a broadcast packet for the Sequence+Flooding and Sequence+Schedule schemes are Θ=0 and Θ=$8N_a$, respectively. Thus, the Proposed Scheme has the longest broadcast packets among the three schemes. Even

though the Proposed Scheme has the longest extra information in a packet, it outperforms the other two schemes in terms of lower normalized overhead, as shown in Figure 3.39.

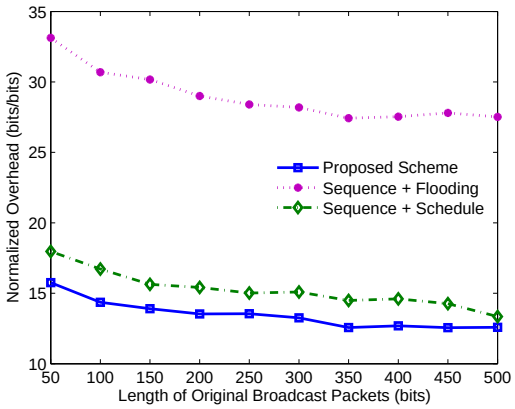

Figure 3.39: Normalized overhead under different lengths of the original broadcast packet.

Figure 3.40 shows the normalized overhead under different numbers of SUs. We use the AODV route request (RREQ) packet as a typical original broadcast packet (i.e., $L_b = 192$ bits) [35]. From Figure 3.40, it is shown that the proposed BRACER broadcast protocol outperforms the other two schemes in terms of lower normalized overhead under various numbers of SUs. More importantly, when the number of SUs increases by 400%, the normalized overhead of the Proposed Scheme only increases by 115%. Thus, the scalability of the proposed BRACER protocol is satisfactory.

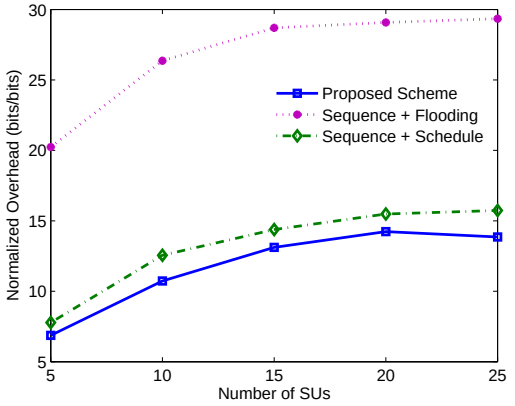

Figure 3.40: Normalized overhead under different numbers of SUs when $L_b = 192$ bits.

CHAPTER 4: ANALYTICAL MODEL FOR BROADCASTS IN CRAHNS

In CR ad hoc networks, control information exchange among nodes, such as channel availability and routing information, is often sent out as network-wide broadcasts (i.e., messages that are sent to all other nodes in a network) [5]. Such control information exchange is crucial for the realization of most networking protocols. In addition, some exigent data packets such as emergency messages and alarm signals are also delivered as network-wide broadcasts [9]. Therefore, broadcast is an essential operation in CR ad hoc networks.

As stated in Chapter 1, due to the randomness of the single-hop successful broadcast ratio and broadcast delay, the broadcast performance of a multi-hop CR ad hoc network is extremely challenging to analyze. Therefore, in this chapter, we study the performance analysis of broadcast protocols for multi-hop CR ad hoc networks. A novel unified analytical model is proposed to analyze the broadcast protocols in CR ad hoc networks with any topology. Specifically, in this chapter, we propose to decompose an intricate network into several simple networks which are tractable for analysis. We also propose systematic methodologies for such decomposition. The main contributions of this chapter are given as follows:

1) An algorithm for calculating the successful broadcast ratio (i.e., the probability that all nodes in a network successfully receive a broadcast message) is proposed for CR ad hoc networks. The proposed algorithm is a general methodology that can be applied to any broadcast protocol proposed for multi-hop CR ad hoc networks with any topology. 2) An algorithm for calculating the average broadcast delay (i.e., the average duration from the moment a broadcast starts to the moment the last node in the network receives the broadcast message) is proposed for CR ad hoc networks

under grid topology. 3) The derivation methods of the single-hop performance metrics, successful broadcast ratio, average broadcast delay, and broadcast collision rate (i.e., the probability that a single-hop broadcast fails due to broadcast collisions), for three different broadcast protocols in CR ad hoc networks under practical scenarios (e.g., no dedicated common control channel exists and the channel information of any other SUs is not known) are proposed. 4) A hardware system is developed to implement different broadcast protocols in multi-hop CR ad hoc networks and validate our proposed unified analytical model. To the best of our knowledge, this is the first analytical work on the performance analysis of broadcast protocols for multi-hop CR ad hoc networks.

4.1 Calculating the Successful Broadcast Ratio

In this section, we present the proposed algorithm for calculating the successful broadcast ratio of a broadcast protocol in multi-hop CR ad hoc networks. We first introduce a unique challenge of calculating the successful broadcast ratio. Then, the details of the proposed algorithm are presented. In addition, an example is given to show the process of the proposed algorithm. For simplicity, we assume that the wireless channels are error-free (i.e., the white noise of the channels is ignored). However, the probability that a broadcast fails due to the channel noise can be easily added in our analysis, if necessary. In the rest of the chapter, we use the term "sender" to indicate a SU who has just received a broadcast message and will rebroadcast the message. In addition, we use the term "receiver" to indicate a SU who has not received the broadcast message yet.

4.1.1 The Unique Challenge

Let $G(V, E)$ denote the topology of a CR ad hoc network, where V is the set of all SU nodes in the network and E is the set of all links in the network. The problem of calculating the successful broadcast ratio is described as: given a CR ad hoc network $G(V, E)$, from the source node v_s, every other node follows a certain rule

to rebroadcast (e.g., simple flooding or the broadcast scheduling algorithm used in the distributed broadcast scheme in [24]), what is the successful broadcast ratio of $G(V, E)$?

The single-hop successful broadcast ratio may not always be one in CR ad hoc networks due to various reasons. Therefore, a SU may not be able to receive the broadcast message from its direct parent node. However, during the broadcast procedure, it may receive the message from other nodes via different paths in the network. This is different from the broadcast schemes in traditional MANETs, where nodes usually receive broadcast messages from their parent nodes. This feature imposes a special challenge of calculating the successful broadcast ratio for the whole CR ad hoc network. That is, there exist multiple message propagation scenarios for all the nodes to successfully receive the message. The overall successful broadcast ratio is the sum of the successful broadcast ratio of all these propagation scenarios. However, it is extremely challenging to calculate the successful broadcast ratio for every message propagation scenario when the network topology is complicated.

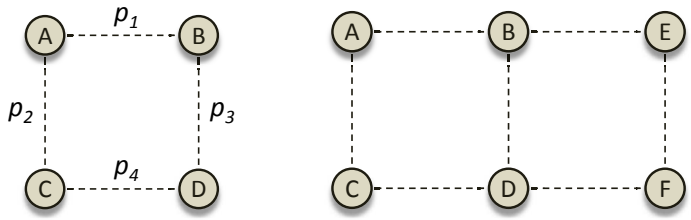

(a) A 2×2 grid network.

(b) A 2×3 grid network.

Figure 4.1: An example for showing the unique challenge when calculating the successful broadcast ratio.

To further illustrate this challenge, we consider a simple 2×2 grid network shown in Figure 4.1(a), where node A is the source node. There are four links in the network, where the successful broadcast ratio over each link is given. The single-hop successful broadcast ratio depends on the specific broadcast protocol used. The method to obtain the single-hop successful broadcast ratio may be different for different protocols. We will explain the methods for calculating the single-hop successful broadcast ratio

for various protocols in Section 4.3. If simple flooding is used to propagate the message, there are totally seven different scenarios for all nodes to successfully receive the message. They are: 1) $A \to B \to D \to C$; 2) $A \to B \to D$ and $A \to C$; 3) $A \to B$ and $A \to C \to D$; 4) $A \to C \to D \to B$; 5) $A \to B \to D$, $A \to C \to D$ and B, C do not have a collision at D; 6) $A \to C \to D \to B$, $A \to B$ and A, D do not have a collision at B; and 7) $A \to B \to D \to C$, $A \to C$ and A, D do not have a collision at C. Accordingly, since the broadcast events to different SU nodes are independent, the successful broadcast ratio for these seven scenarios is: $p_1(1-p_2)p_3p_4$, $p_1p_2p_3(1-p_4)$, $p_1p_2(1-p_3)p_4$, $(1-p_1)p_2p_3p_4$, $p_1p_2p_3p_4-p_{q1}$, $p_1p_2p_3p_4-p_{q2}$, and $p_1p_2p_3p_4-p_{q2}$, where p_{q1} is the probability that B and C fail to broadcast to D due to broadcast collisions and p_{q2} is the probability that A and D fail to broadcast due to broadcast collisions. The probability that two nodes have a collision also depends on the specific broadcast protocol used. Therefore, the overall successful broadcast ratio is the sum of the successful broadcast ratio of these seven scenarios, that is,

$$\begin{aligned} P_{succ} = {} & p_1(1-p_2)p_3p_4 + p_1p_2p_3(1-p_4) + p_1p_2(1-p_3)p_4 + \\ & (1-p_1)p_2p_3p_4 + (p_1p_2p_3p_4 - p_{q1}) + 2(p_1p_2p_3p_4 - p_{q2}). \end{aligned} \tag{4.1}$$

Then, we increase the dimension of the grid network to 2×3, as shown in Figure 4.1(b). If simple flooding is used, the total number of message propagation scenarios is 40. The overall successful broadcast ratio is the sum of the successful broadcast ratio of all these 40 message propagation scenarios. Note that although only 2 additional nodes and 3 additional links are added, the total number of propagation scenarios increases significantly. Moreover, if the grid network size is 2×4, the total number of message propagation scenarios is 252. If we further increase the dimension of the grid network to 3×3, it is almost impossible to obtain the successful broadcast ratio of every possible message propagation scenario. Therefore, when the number of nodes and links increases in a CR ad hoc network, the total number of message

propagation scenarios increases exponentially. It is extremely challenging to identify every possible message propagation scenario and calculate the successful broadcast ratio for each scenario in a complicated network.

4.1.2 The Proposed Algorithm

We develop an iterative algorithm to address the above challenge. The main idea of the proposed algorithm is to decompose a complicated network into a few simpler networks so that the successful broadcast ratio of these simpler networks is straightforward to obtain and the complexity of the original network can be reduced. Then, the successful broadcast ratio of the overall network can be acquired. The notations used in the proposed algorithm are listed in Table 4.1. The pseudo-codes of the proposed algorithm for calculating the successful broadcast ratio is shown in Algorithm 1.

Table 4.1: Notations used in the Proposed Algorithm 1

$E(v)$	The set of all the links that connect to node v
$e(v,u)$	The link that connects node v and u
$P(v,u)$	The successful broadcast ratio from node v to u
$P(G(V,E))$	The successful broadcast ratio of the network $G(V,E)$
$P_q(v,u,k)$	The probability that node v and u fail to broadcast to node k due to broadcast collisions
$\lvert\cdot\rvert$	The number of elements in a set

Algorithm 1: The proposed algorithm for calculating the successful broadcast ratio.

Input: The topology of the network $G(V,E)$, the source node v_s.

Output: $P(G(V,E))$.

if $|V| > 2$ then

  if $|E(v_s)| > 1$ do

    $E_1 \leftarrow E$; $V_1 \leftarrow V$;

    $E_2 \leftarrow E$; $V_2 \leftarrow V$;

    Randomly select $e(v_s, v_i) \in E(v_s)$;

    foreach $v_k, e(v_i, v_k) \in E(v_i)$ do

$E_1 \leftarrow E_1 + e(v_s, v_k)$;

if $e(v_s, v_k) \in E(v_s)$ then

$P(v_s, v_k) \leftarrow 1-(1-P(v_i, v_k))(1-P(v_s, v_k))-P_q(v_s, v_i, v_k)$;

else

$P(v_s, v_k) \leftarrow P(v_i, v_k)$;

$E_1 \leftarrow E_1 - E(v_i)$; $V_1 \leftarrow V_1 - v_i$; $E_2 \leftarrow E_2 - e(v_s, v_i)$;

$P(G(V, E)) \leftarrow P(v_s, v_i)P(G_1(V_1, E_1)) + (1-P(v_s, v_i))P(G_2(V_2, E_2))$;

return $P(G(V, E))$;

else if $|E(v_s)| = 1$ then

$E_1 \leftarrow E$; $V_1 \leftarrow V$;

select $e(v_s, v_i) \in E(v_s)$

foreach $v_k, e(v_i, v_k) \in E(v_i)$ do

$E_1 \leftarrow E_1 + e(v_s, v_k)$; $P(v_s, v_k) \leftarrow P(v_i, v_k)$;

$E_1 \leftarrow E_1 - E(v_i)$; $V_1 \leftarrow V_1 - v_i$

$P(G(V, E)) \leftarrow P(v_s, v_i)P(G_1(V_1, E_1))$;

return $P(G(V, E))$;

else if $|V| = 2$ then select $e(v_s, v_i) \in E(v_s)$;

$P(v_s, v_i)$;

Under the proposed algorithm, at each iteration round, a link that connects to the source node is randomly selected. Based on whether the broadcast over this link is successful or not, the network is decomposed into two simpler networks. If the broadcast over this link is successful, all links that connect to the other node of the selected link will connect to the source node. If the broadcast over this link fails, this link is simply removed from the network. The successful broadcast ratio over each remaining link is updated accordingly after each iteration. The process terminates when only two nodes are left in the remaining networks.

4.1.3 An Illustrative Example

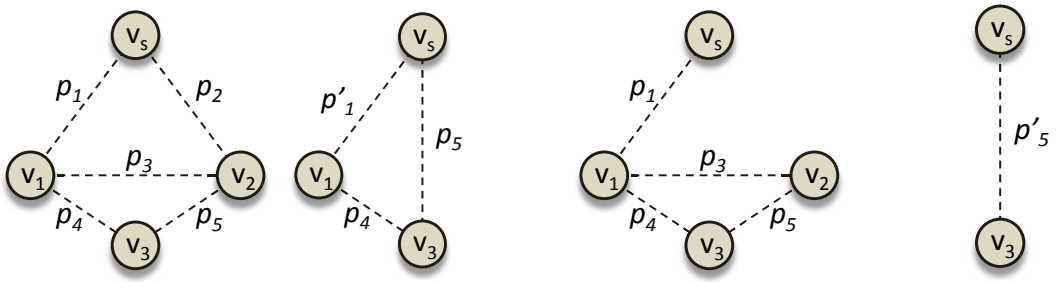

(a) The original network.

(b) Link $e(v_s, v_2)$ is successful.

(c) Link $e(v_s, v_2)$ is failed.

(d) Link $e(v_s, v_1)$ is successful after 4.2(b).

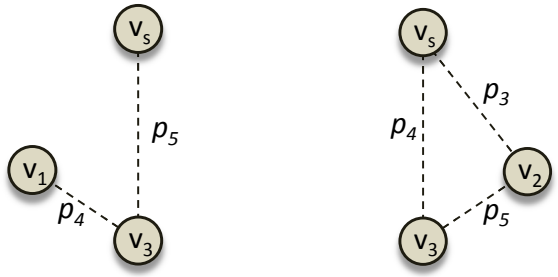

(e) Link $e(v_s, v_1)$ is failed after 4.2(b).

(f) Link $e(v_s, v_1)$ is successful after 4.2(c).

Figure 4.2: The process of the proposed Algorithm 1 for a 4-node CR ad hoc network.

We use an example to illustrate the process of the proposed Algorithm 1. As shown in Figure 4.2(a), the original CR ad hoc network consists of 4 nodes and 5 links. Based on Algorithm 1, since the source node v_s has two links, we randomly select one of these two links (e.g., link $e(v_s, v_2)$). In the first iteration, if the broadcast over the link $e(v_s, v_2)$ is successful, all nodes that are originally connected to v_2 are connected to the source node, as shown in Figure 4.2(b). In addition, the successful broadcast ratios of the new links are updated. That is, $P(v_s, v_3) = P(v_2, v_3) = p_5$ and $p_1' = 1-(1-p_1)(1-p_3)-P_q(v_s, v_2, v_1)$ because the message propagation scenarios in the original network for v_1 to successfully receive the message directly from v_s or v_2 are: 1) $v_s \to v_1$ only; 2) $v_s \to v_2 \to v_1$ only; and 3) $v_s \to v_1, v_s \to v_2 \to v_1$ and v_s, v_2 do not have a collision at v_1. The probability $(1-p_1)(1-p_3)$ in calculating p_1' is the probability that both v_s and v_2 fail to broadcast to v_1. In addition, the probability that node v_s and v_2 fail to broadcast to node v_1 due to broadcast collisions

$P_q(v_s, v_2, v_1)$ will be calculated in Section 4.3. On the other hand, if the broadcast over the link $e(v_s, v_2)$ fails, this link is simply removed from the network, as shown in Figure 4.2(c). The successful broadcast ratio of the original network can be obtained from the successful broadcast ratio of the two simpler networks, as shown in Figure 4.2(b) and 4.2(c). In the second iteration, these two simpler networks can be further decomposed following the same procedure. For the network shown in Figure 4.2(b), assume that we select the link $e(v_s, v_1)$. Similar to the process of the first iteration, this network is further decomposed into two networks, as shown in Figure 4.2(d) and 4.2(e), where $p_5' = 1-(1-p_4)(1-p_5)-P_q(v_s, v_1, v_3)$. Then, the successful broadcast ratio of the network shown in Figure 4.2(b) can be obtained from the successful broadcast ratio of these two new networks shown in Figure 4.2(d) and 4.2(e). For the network shown in Figure 4.2(c), since the source node has only one link, this link must be successful for other nodes to receive the message. Thus, this network is reduced to the network shown in Figure 4.2(f) and the successful broadcast ratio of this network can be obtained from the successful ratio of the network shown in Figure 4.2(f). Therefore, if we repeat this process, the complexity of the networks from the second iteration can be further reduced. Finally, the original network can be decomposed into several single-hop networks. Then, the procedure of the proposed Algorithm 1 terminates. Therefore, the successful broadcast ratio of the original network can be expressed as

$$\begin{aligned} P_{succ} = {} & p_2\{[1-(1-p_1)(1-p_3)-P_q(v_s, v_2, v_1)][1-(1-p_4) \\ & (1-p_5)-P_q(v_s,v_1,v_3)]+[(1-p_1)(1-p_3)+P_q(v_s,v_2,v_1)]p_4p_5\} \\ & +(1-p_2)p_1\{p_3[1-(1-p_4)(1-p_5)-P_q(v_s,v_2,v_3)]+(1-p_3)p_4p_5\}. \end{aligned} \tag{4.2}$$

4.2 Calculating the Average Broadcast Delay

In this section, we introduce the proposed algorithm for calculating the average broadcast delay of a broadcast protocol. Similar to the previous section, we first

present the unique challenge of calculating the average broadcast delay for a CR ad hoc network. Then, the detailed algorithm is given. Furthermore, an example is shown to illustrate the process of the proposed algorithm.

4.2.1 The Unique Challenge

Since the single-hop broadcast delay depends on various factors, such as the channel availability of the communication pair and specific broadcast protocol, the single-hop broadcast delay is random. Figure 4.3 illustrates the randomness of the single-hop broadcast delay in CR ad hoc networks. In Figure 4.3, node A is the sender and broadcasts the message on each available channel sequentially. In addition, node B is the receiver and constantly listens on the channel shown in the bold font. Since node B does not have any information about the sender before a broadcast starts, the channel it stays on is randomly selected. It is shown that, even though the channel availability of node B is the same in the two scenarios shown in Figure 4.3(a) and 4.3(b), the single-hop broadcast delay is quite different (i.e., it takes 1 time slot for a successful broadcast in Figure 4.3(a), while it takes 5 time slots for a successful broadcast in Figure 4.3(b)). Hence, due to this randomness, to obtain the single-hop broadcast delay in CR ad hoc networks is challenging. Moreover, if the number of senders and receivers is larger than one, it is even more difficult.

(a) B is on channel 1. (b) B is on channel 5.

Figure 4.3: An example for showing the randomness of the single-hop broadcast delay in CR ad hoc networks.

4.2.2 The Proposed Algorithm

Since to obtain the closed form expression of the average broadcast delay for arbitrary network topology is extremely complicated, in this chapter, we focus on the grid topology. However, the proposed methodology can be applied to any network topology. We define the level of SUs as h if they are h hops to the source node

(denoted as $L = h$). Figure 4.4 shows an example of an 8-node CR ad hoc network with the levels of SUs where A is the source node. Then, the original network is decomposed into H_m levels, where H_m is the distance from the source node to the furthest node in the network. To make the derivation process tractable, we first make two assumptions. First of all, we assume that the broadcast message is propagated from the source node to the furthest node sequentially based on the relative distance to the source node. This means that, we assume that the nodes who are closer to the source node receive the message sooner than the nodes who are farther away from the source node. Based on this assumption, we categorize the SUs based on their relative distances to the source node. We further justify this assumption using simulation. We apply the broadcast protocol proposed in [23] to the network shown in Figure 4.4. Figure 4.5 shows the simulation results of the average delay for different nodes to receive the broadcast message in the network shown in Figure 4.4. It is shown that nodes at a higher level (e.g., nodes D and E at the second level) receive the broadcast message later than the nodes at a lower level on average (e.g., nodes B and C at the first level), which justifies our first assumption. The second assumption is that only the nodes that are at the highest level or have a path leading to the furthest node (excluding the source node) contribute to the overall average broadcast delay. Other nodes will be removed from the network for calculating the average broadcast delay. This assumption is straightforward since those nodes are independent of the message propagation path to the nodes at the highest level. For instance, in Figure 4.4, nodes G and H do not contribute to the message propagation to node F. Thus, they can be removed when calculating the average broadcast delay of the network.

The main idea of the proposed algorithm is that the overall average broadcast delay is the sum of the average broadcast delay at each level. At each level, it is a simple network whose average broadcast delay can be obtained. That is, $\Gamma = \sum_i^{H_m} D_i$, where Γ is the overall average broadcast delay and D_i is the average broadcast delay

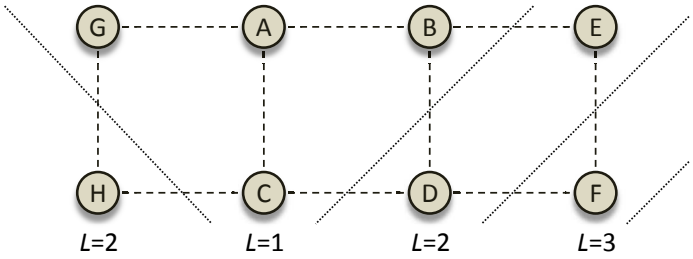

Figure 4.4: An example of a 8-node CR ad hoc network with the levels of SUs.

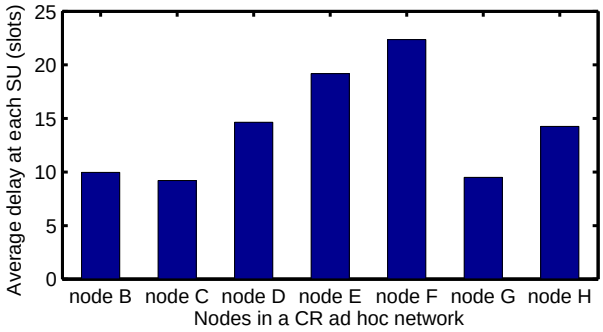

Figure 4.5: The average delay for different nodes to receive the broadcast message in the network shown in Figure 4.4.

of the nodes at level i.

Then, we calculate the average broadcast delay at level i, D_i. Based on the number of parent nodes, there exist only two scenarios of the single-hop broadcast in a grid topology network. The first scenario is that a SU only has one parent node (denoted as Scenario I, as shown in Figure 4.6(a)), while the second scenario is that a SU has two parent nodes (denoted as Scenario II, as shown in Figure 4.6(b)). We further prove that the maximum number of parent nodes for a node in grid topology networks is two. The proof is: if there are more than two parent nodes (say, three), these three nodes should be at the same level. However, for any node that is the parent node of any two of those parent nodes (exactly 1-hop away), it needs more than two hops to reach the third parent node. That is, these three nodes cannot be at the same level. Therefore, only the two single-hop broadcast scenarios shown in Figure 4.6 exist. We assume that for the nodes at the same level, there are α Scenario I and β Scenario II.

(a) Scenario I. (b) Scenario II.

Figure 4.6: Two single-hop broadcast scenarios in a grid topology network.

If the current level, level i, is not the highest level, the average broadcast delay at level i is the mean of the single-hop average broadcast delay of the nodes at level i. That is, $D_i = (\alpha\tau_1 + \beta\tau_2)/(\alpha+\beta)$, where τ_1 and τ_2 are the single-hop average broadcast delay of Scenario I and II, respectively. Denote the probabilities that the single-hop broadcast is successful at time slot k as $P_I(k)$ and $P_{II}(k)$ for Scenario I and II, respectively. $P_I(k)$ and $P_{II}(k)$ can be obtained based on a specific broadcast protocol, which is explained in Section 4.3. Given a successful broadcast, we first obtain the conditional probability that the single-hop broadcast is successful at time slot k for the two scenarios:

$$P_1(k) = \frac{P_I(k)}{\sum_j P_I(j)},$$
$$P_2(k) = \frac{P_{II}(k)}{\sum_j P_{II}(j)}. \tag{4.3}$$

Therefore, we have $\tau_1 = \sum_{k=1}^{T_m} kP_1(k)$ and $\tau_2 = \sum_{k=1}^{T_m} kP_2(k)$, where T_m is the maximum length of time slots the sender uses for broadcasting.

If the current level is the highest level, the calculation method for D_i is different. Since the probability that the broadcast is successful at time slot k is different in the two broadcast scenarios, we need to consider two cases: the last SU node at level i successfully receives the broadcast message is under Scenario I or Scenario II. Therefore, we first assume that the last SU node successfully receives the broadcast message at time slot d is under Scenario I and no other SU receives the message at time slot d under Scenario II. Thus, we have the probability that the single-hop

broadcast delay is d at level i as

$$P'(D_i=d)=\binom{\alpha}{1}P_1(d)\left[\sum_{k=1}^{d}P_1(k)\right]^{\alpha-1}\left[\sum_{k=1}^{d-1}P_2(k)\right]^{\beta}. \tag{4.4}$$

Next, we assume that the last SU node successfully receives the broadcast message at time slot d under Scenario II and no other SU node receives the message at time slot d under Scenario I. Thus, we obtain

$$P''(D_i=d)=\binom{\beta}{1}P_2(d)\left[\sum_{k=1}^{d-1}P_1(k)\right]^{\alpha}\left[\sum_{k=1}^{d}P_2(k)\right]^{\beta-1}. \tag{4.5}$$

Last, we assume that under both scenarios, at least one node receives the broadcast message at time slot d. Hence, we have

$$P'''(D_i=d)=\binom{\alpha}{1}\binom{\beta}{1}P_1(d)P_2(d)\left[\sum_{k=1}^{d-1}P_1(k)\right]^{\alpha-1}\left[\sum_{k=1}^{d-1}P_2(k)\right]^{\beta-1}. \tag{4.6}$$

Therefore, the probability that the single-hop broadcast delay is d at level i can be written as

$$\Pr(D_i=d)=P'(D_i=d)+P''(D_i=d)+P'''(D_i=d). \tag{4.7}$$

Then, the average broadcast delay at level i is

$$D_i=\sum_{d=1}^{T_m}d\Pr(D_i=d). \tag{4.8}$$

4.2.3 An Illustrative Example

We use the example shown in Figure 4.4 to illustrate the proposed algorithm for calculating the average broadcast delay. From Figure 4.4, there are three levels of nodes in the network. As explained above, according to our second assumption, we first remove nodes G and H for the consideration of average broadcast delay. Then, at the first level, since both nodes B and C are under Scenario I, for D_1, we have

$$D_1 = \tau_1 = \sum_{k=1}^{T_m} \frac{kP_I(k)}{\sum_j P_I(j)}. \tag{4.9}$$

That is, the average broadcast delay at level 1 is the same as the single-hop broadcast delay under Scenario I. At the second level, nodes D and E are under different scenarios. Therefore, we have

$$D_2 = \frac{\tau_1 + \tau_2}{2} = \frac{1}{2}\left[\sum_{k=1}^{T_m} \frac{kP_I(k)}{\sum_j P_I(j)} + \sum_{k=1}^{T_m} \frac{kP_{II}(k)}{\sum_j P_{II}(j)}\right]. \tag{4.10}$$

Finally, for D_3, since this is the highest level, D_3 can be obtained using (4.8), where $\alpha = 0$ and $\beta = 1$. That is,

$$D_3 = \sum_{d=1}^{T_m} d\frac{P_{II}(d)}{\sum_j P_{II}(j)}. \tag{4.11}$$

By summing up the average broadcast delay of these three levels, the overall average broadcast delay for the network shown in Figure 4.4 can be written as $\Gamma = \sum_{i=1}^{3} D_i$.

4.3 Broadcasting in CR Ad Hoc Networks

In this section, we first introduce several existing broadcast designs, i.e., the random scheme and the schemes proposed in [23][24], for CR ad hoc networks under practical scenarios. Since the broadcast schemes proposed in [21] and [22] are based on impractical assumptions (i.e., a dedicated common control channel for the whole network is employed and the available channel information of all SUs are assumed to be known), we exclude these proposals in this research. In addition, we propose the derivation methods to calculate the single-hop broadcast performance metrics (i.e., successful broadcast ratio, average broadcast delay, and broadcast collision rate) for each protocol.

4.3.1 Random Broadcast Scheme

The first broadcast scheme is called the random broadcast scheme. Since a SU is unaware of the channel availability information of other SUs before broadcasts are executed, a straightforward action for a SU sender is to randomly select a channel

from its available channel set and broadcasts a message on that channel in a time slot. If the channel selected by the receiver is the same as the channel selected by the sender, the broadcast message can be successfully received. Figure 4.7 illustrates the procedure of the random broadcast scheme, where the shaded part represents a successful broadcast.

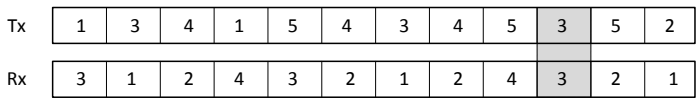

Figure 4.7: An example of the random broadcast scheme.

4.3.1.1 Single-hop Successful Broadcast Ratio for the Random Broadcast Scheme

We first calculate the single-hop successful broadcast ratio for the random broadcast scheme. Without loss of generality, in the rest of the chapter, the sender and the receiver of the single-hop link is denoted as A and B. We further denote the numbers of available channels for the single-hop communication pair as N_A and N_B, respectively. The number of common channels between A and B is Z_{AB}. Therefore, the probability that the single-hop broadcast is successful in a time slot is

$$p_r = \binom{Z_{AB}}{1} \frac{1}{N_A} \frac{1}{N_B} = \frac{Z_{AB}}{N_A N_B}. \tag{4.12}$$

Therefore, if the length of the time slots that the sender uses for broadcasting is S_r, the single-hop successful broadcast ratio for the random broadcast scheme is

$$P_{rand} = 1 - \left(1 - \frac{Z_{AB}}{N_A N_B}\right)^{S_r}. \tag{4.13}$$

4.3.1.2 Single-hop Average Broadcast Delay for the Random Broadcast Scheme

Next, we calculate the single-hop average broadcast delay for the random broadcast scheme. In this chapter, since we focus on grid topology for the broadcast delay, we only need to consider the two single-hop broadcast scenarios shown in Figure

4.6. For Scenario I, since the sender and the receiver randomly select a channel in a time slot, the probability that the single-hop broadcast is successful at time slot k is $P_I(k) = (1-p_r)^{k-1}p_r$, where p_r is given in (4.12). For scenario II, since there are two senders, we denote the other sender as C and the number of available channels of C is N_C. In addition, the number of common channels between B and C is Z_{BC}. Thus, similar to (4.12), the probability that the single-hop broadcast is successful between C and B in a time slot is $p_m = \frac{Z_{BC}}{N_B N_C}$. Hence, the probability that the single-hop broadcast is successful under Scenario II in a time slot is $p_{r2} = [1-(1-p_r)(1-p_m)]-p_{q1}$, where p_{q1} is the probability that nodes A and C have a broadcast collision at node B in a time slot. The derivation of p_{q1} is given in Section 4.3.1.3. Hence, the probability that the single-hop broadcast is successful at time slot k can be expressed as

$$P_{II}(k) = (1-p_{r2})^{k-1}p_{r2}. \tag{4.14}$$

Then, based on (4.3), given the single-hop broadcast is successful, the conditional probability that the receiver successfully receives the broadcast message at time slot k for both scenarios under the random broadcast scheme, $P_1(k)$ and $P_2(k)$, can be obtained.

$$P_I(k) = \begin{cases} \sum_{y=y^*}^{y^{**}} \frac{\binom{Z_{AB}}{y}\binom{N_A-Z_{AB}}{n-y}}{\binom{N_A}{n}} \frac{\binom{N_B-\lfloor\frac{k-1}{n}\rfloor-1}{y-1}}{n\binom{N_B}{y}}, & \text{if } k \le n(N_B-y) \\ \sum_{y=y^*}^{y^{**}} \frac{\binom{Z_{AB}}{y}\binom{N_A-Z_{AB}}{n-y}}{\binom{N_A}{n}} \frac{1}{n\binom{N_B}{y}}, & \text{if } n(N_B-y) < k \le n(N_B-y+1) \\ 0, & \text{if } k > n(N_B-y+1). \end{cases} \tag{4.15}$$

$$P_{II}(k) = \begin{cases} \sum_{y=y^*}^{y^{**}} \sum_{x=x^*}^{x^{**}} \sum_{q=0}^{q^*} \frac{\binom{Z_{AB}}{y}\binom{N_A-Z_{AB}}{n-y}}{\binom{N_A}{n}} \frac{\binom{N_B-\lfloor\frac{k-1}{n}\rfloor-1}{2y-2q-1}}{n\binom{N_B}{2y-2q}} \Pr(x)\Pr(q), & \text{if } k \le n(N_B-2y+2q) \\ \sum_{y=y^*}^{y^{**}} \sum_{x=x^*}^{x^{**}} \sum_{q=0}^{q^*} \frac{\binom{Z_{AB}}{y}\binom{N_A-Z_{AB}}{n-y}}{\binom{N_A}{n}} \frac{1}{n\binom{N_B}{2y-2q}} \Pr(x)\Pr(q), & \\ \text{if } n(N_B-2y+2q) < k \le n(N_B-2y+2q+1) & \\ 0, & \text{if } k > n(N_B-2y+2q+1). \end{cases} \tag{4.16}$$

4.3.1.3 Single-hop Broadcast Collision Rate for the Random Broadcast Scheme

Next, we calculate the single-hop broadcast collision rate for the random broadcast scheme. We first derive the probability that nodes A and C have a broadcast collision at node B in a time slot, p_{q1}. p_{q1} is equivalent to the probability that all the three nodes select the same channel. Denote the number of common channels among the three nodes as Z_{ABC}. Thus, we have

$$p_{q1} = \frac{Z_{ABC}}{N_A N_B N_C}. \tag{4.17}$$

Since the length of the time slots that the sender uses for broadcasting is S_r, the probability that a single-hop broadcast fails due to broadcast collisions for the random broadcast scheme can be written as

$$P_q(A, C, B) = \sum_{l=1}^{S_r} \binom{S_r}{l} p_{q1}^{l} \left[(1-p_r)(1-p_m)\right]^{S_r - l}, \tag{4.18}$$

where l is the number of time slots when nodes A and C have a broadcast collision at node B.

4.3.2 QoS-based Broadcast Scheme

The second scheme is called the QoS-based broadcast scheme [23][103]. The main idea of the QoS-based broadcast scheme is to let the sender broadcast on a subset of its available channels in order to reduce the broadcast delay. In addition, the channel hopping sequences of both the sender and the receiver are designed for guaranteed rendezvous, given that the sender and the receiver have at least one channel in common in their hopping sequences. Figure 4.8 shows an example of the QoS-based broadcast scheme. For each sender, it randomly selects n channels from its available channel set. Then, it hops and broadcasts periodically on the selected n channels for S time slots. The values of n and S are determined by the QoS requirements of the network (i.e., the successful broadcast ratio and the average broadcast delay). On

the other hand, for each receiver, it first forms a random sequence that consists of its every available channel with a length of n time slots for each channel. Then, it hops and listens following this sequence periodically.

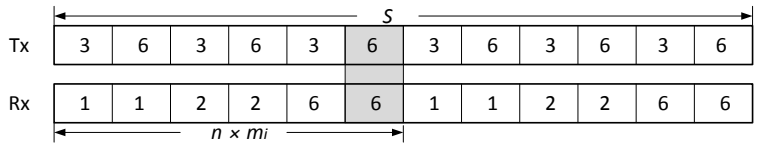

Figure 4.8: An example of the QoS-based broadcast scheme.

4.3.2.1 Single-hop Successful Broadcast Ratio for the QoS-based Broadcast Scheme

We continue to use the notations for calculating the single-hop performance metrics in the random broadcast scheme for the QoS-based broadcast scheme. Denote the number of channels in the n channels selected by node A which are also in the available channel set of node B as y. We assume that the length of time slots that the sender uses for broadcasting, S, is a multiple of n. Thus, the single-hop successful broadcast ratio for the QoS-based broadcast protocol is

$$P_{qos} = \sum_{y=y^*}^{y^{**}} H(y), \tag{4.19}$$

where $y^* = \max(1, n+Z_{AB}-N_A)$, $y^{**} = \min(n, Z_{AB})$, and $H(y)$ is written as

$$H(y) = \begin{cases} \frac{\binom{Z_{AB}}{y}\binom{N_A-Z_{AB}}{n-y}}{\binom{N_A}{n}} \frac{\binom{N_B}{y}-\binom{N_B-\frac{S}{n}}{y}}{\binom{N_B}{y}}, & \text{if } y < N_B - \frac{S}{n} \\ \frac{\binom{Z_{AB}}{y}\binom{N_A-Z_{AB}}{n-y}}{\binom{N_A}{n}}, & \text{if } y \geq N_B - \frac{S}{n}, \end{cases} \tag{4.20}$$

where $\frac{\binom{Z_{AB}}{y}\binom{N_A-Z_{AB}}{n-y}}{\binom{N_A}{n}}$ is the probability that there are y common channels between the sender and the receiver in the selected n channels by the sender. (4.20) indicates that when S is large enough (the case when $y \geq N_B - \frac{S}{n}$), the single-hop successful broadcast ratio is independent of S.

4.3.2.2 Single-hop Average Broadcast Delay for the QoS-based Broadcast Scheme

Secondly, we calculate the single-hop average broadcast delay for the QoS-based broadcast scheme. Similar to the random broadcast scheme, we first calculate the probability that the single-hop broadcast is successful at time slot k. Based on the broadcast protocol shown in Figure 4.8, one cycle of the broadcasting sequence of the receiver consists of N_B sections, where each section includes the same channel repeated for n times. If the channel in a section is the first appearing common available channel of nodes A and B, the single-hop broadcast is successful within that section. Denote the sections of one cycle of the broadcasting sequence of the receiver as $[f_1, f_2, \cdots, f_{N_B}]$. We calculate the probability that for a particular y, the channel in f_i is the first appearing common available channel, $\Pr(f_i), i \in [1, N_B{-}y{+}1]$. This probability is equal to the probability that the first ball is in the i-th box if y balls are randomly put in N_B boxes. Therefore, $\Pr(f_i) = \frac{\binom{N_B-i}{y-1}}{\binom{N_B}{y}}$. Since time slot k is in the $(\lfloor \frac{k-1}{n} \rfloor + 1)$-th section, the probability that the single-hop broadcast is successful in $f_{\lfloor \frac{k-1}{n} \rfloor+1}$ is $\frac{\binom{N_B-\lfloor \frac{k-1}{n} \rfloor-1}{y-1}}{\binom{N_B}{y}}$. On the other hand, given that the first appearing common available channel is in $f_{\lfloor \frac{k-1}{n} \rfloor+1}$, since the channels in the broadcasting sequence of the sender is evenly distributed, the conditional probability that the broadcast is successful in time slot k is $\frac{1}{n}$. Therefore, for Scenario I, the probability that the single-hop broadcast is successful at time slot k is expressed in (4.15).

For Scenario II, for simplicity, we assume that both the two senders have the same number of common available channels with the receiver (i.e., $Z_{AB} = Z_{BC}$). In addition, the numbers of channels that are also available for the receiver in the

---

$$P_{II}(k) = \begin{cases} \sum_{z_1=1}^{w}\sum_{z_2=1}^{w}\sum_{x=0}^{z^*}\sum_{q=0}^{q^*} \frac{\binom{w-\lfloor \frac{k-1}{w} \rfloor-1}{z_1+z_2-2q-1}}{w\binom{w}{z_1+z_2-2q}} \Pr(z_1)\Pr(z_2)G(x)U(q), & \text{if } k \le w(w-z_1+z_2+2q) \\ \sum_{z_1=1}^{w}\sum_{z_2=1}^{w}\sum_{x=0}^{z^*}\sum_{q=0}^{q^*} \frac{1}{w\binom{w}{z_1+z_2-2q}} \Pr(z_1)\Pr(z_2)G(x)U(q), & \\ \text{if } w(w-z_1+z_2+2q) < k \le w(w-z_1+z_2+2q+1) & \\ 0, & \text{if } k > w(w-z_1+z_2+2q+1). \end{cases} \tag{4.21}$$

selected n channels by the two senders are the same (denoted as y). Denote the number of channels in the available channel sets of the two senders that are also available for all three nodes as x. Therefore, the probability that there are x channels that are available for all three nodes in their selected available channel sets is $\Pr(x) = \left(\frac{Z_{ABC}}{Z_{AB}}\right)^x \left(1 - \frac{Z_{ABC}}{Z_{AB}}\right)^{y-x}$, where Z_{ABC} is the number of channels that are available for all three nodes. Therefore, the probability that the single-hop broadcast is successful at time slot k under Scenario II is written in (4.16), where $\Pr(q)$ is the probability that there are q channels out of x channels appearing in the same time slots. In addition, $x^* = \max(0, y - Z_{AB} + Z_{ABC})$, $x^{**} = \min(y, Z_{ABC})$, and $q^* = \min(x, y-1)$. Thus, $\Pr(q)$ is written as

$$\Pr(q) = \begin{cases} \frac{\binom{x}{q}[(n-q)! - \sum_{j=1}^{x-q}(-1)^{(j+1)}\binom{x-q}{j}(n-q-j)!]}{n!}, & \text{if } 0 \leq q < x \\ \frac{(n-q)!}{n!}, & \text{if } q = x. \end{cases} \tag{4.21}$$

Then, based on (4.3), given the single-hop broadcast is successful, the conditional probability that the receiver successfully receives the broadcast message at time slot k for both scenarios under the QoS-based broadcast scheme, $P_1(k)$ and $P_2(k)$, can be obtained.

4.3.2.3 Single-hop Broadcast Collision Rate for the QoS-based Broadcast Scheme

Then, we calculate the single-hop broadcast collision rate for the QoS-based broadcast scheme. The probability that two senders have a broadcast collision is equivalent to the probability that all the common channels selected by the two senders appear in the same time slots. Therefore, using (4.22), the probability that a single-hop broadcast fails due to broadcast collisions for the QoS-based broadcast scheme is

$$P_q(A, C, B) = \sum_{y=y*}^{y^{**}} \frac{\binom{Z_{AB}}{y}\binom{N_A - Z_{AB}}{n-y}\binom{Z_{ABC}}{y}}{\binom{N_A}{n}\binom{Z_{AB}}{y}^2} \frac{(n-y)!}{n!}. \tag{4.22}$$

4.3.3 Distributed Broadcast Scheme

The third broadcast scheme considered in this chapter is called the distributed broadcast scheme [24][104]. In this scheme, all SU nodes in the network intelligently select a subset of available channels from the original available channel set for broadcasting. The size of the downsized available channel set is denoted as w. The value of w needs to be carefully designed to ensure that at least one common channel exists between the downsized available channel sets of the SU sender and each of its neighboring nodes. Figure 4.9 gives an example of the broadcasting sequences of the distributed broadcast scheme. For a SU sender, it hops periodically on the w available channels for w cycles (one cycle consists of w^2 time slots). For each receiver, it stays on one of the w available channels for w time slots. Then, it repeats for every channel in the w available channels.

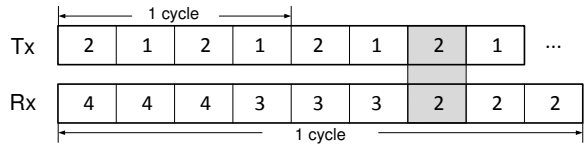

Figure 4.9: An example of the broadcasting sequences of the distributed broadcast scheme.

4.3.3.1 Single-hop Successful Broadcast Ratio for the Distributed Broadcast Scheme

Similar to the previous schemes, we first calculate the single-hop successful broadcast ratio for the distributed broadcast scheme. As discussed above, the size of the downsized available channel set, w, has significant impact on the performance of the distributed broadcast scheme. If w is given, the single-hop successful broadcast ratio is equivalent to the probability that the sender and the receiver have at least one channel in common in their downsized available channel sets. That is, $P_{dist} = 1 - \Pr(Z(0,i) = 0)$, where $\Pr(Z(0,i) = 0)$ is the probability that the sender and the receiver do not have any common channel in their downsized available channel sets. The derivation process of $\Pr(Z(0,i) = 0)$ is the same as the method proposed in

[24].

4.3.3.2 Single-hop Average Broadcast Delay for the Distributed Broadcast Scheme

Then, we calculate the single-hop average broadcast delay for the distributed broadcast scheme. For simplicity, we assume that the w obtained by the receiver is the same as the w of the sender. In addition, we denote the number of common channels between the sender and the receiver as z. We calculate the probability that the single-hop broadcast is successful at time slot k under Scenario I. Based on the broadcast protocol proposed in [24], the broadcasting sequence of a receiver consists of w sections where each section includes the same channel repeated for w times. Similar to the QoS-based broadcast scheme, the probability that for a particular z, the channel in $t_{\lfloor \frac{k-1}{w} \rfloor+1}$ is the first appearing common available channel in the downsized available channel set of the sender is expressed as $\Pr(t_{\lfloor \frac{k-1}{w} \rfloor+1}) = \frac{\binom{w-\lfloor \frac{k-1}{w} \rfloor-1}{z-1}}{\binom{w}{z}}$.

In addition, given that the first appearing common available channel is in $(\lfloor \frac{k-1}{w} \rfloor + 1)$-th section, the conditional probability that the broadcast is successful in time slot k is $\frac{1}{w}$. Therefore, for Scenario I, the probability that the single-hop broadcast is successful at time slot k is expressed as

$$P_I(k)=\begin{cases} \sum_{z=1}^{w} \frac{\binom{w-\lfloor \frac{k-1}{w} \rfloor-1}{z-1}}{w\binom{w}{z}} \Pr(z), & \text{if } k \le w(w-z) \\ \sum_{z=1}^{w} \frac{1}{w\binom{w}{z}} \Pr(z), & \text{if } w(w-z) < k \le w(w-z+1) \\ 0, & \text{if } k > w(w-z+1), \end{cases} \tag{4.23}$$

where $\Pr(z)$ is the probability that there are z common channels in the downsized available channel sets between the sender and the receiver. The derivation process of $\Pr(z)$ is given in [24].

Then, for Scenario II, denote the numbers of common available channels that the two senders have with the receiver in the downsized available channel sets as z_1 and z_2, respectively. In addition, denote the number of channels in the downsized available

channel sets of the two senders that are available for all three nodes as x. Since the available channels are evenly distributed in the spectrum band, the probability that there are x channels that are available for all three nodes in their downsized available channel sets is $G(x) = \binom{z^*}{x} P_A^x (1-P_A)^{z^*-x}$, where P_A is the probability that a channel is available for all three nodes and $z^* = \min(z_1, z_2)$. In addition, P_A can be obtained from [24]. Therefore, similar to the QoS-based broadcast scheme, the probability that the single-hop broadcast is successful at time slot k under Scenario II is expressed in (4.21), where $U(q)$ is the probability that there are q channels out of x channels appearing at the same time slots. In addition, $q^* = \min(x, z^* - 1)$. Using (4.22), $U(q)$ can be written as

$$U(q) = \begin{cases} \frac{\binom{x}{q}[(w-q)! - \sum_{j=1}^{x-q}(-1)^{(j+1)}\binom{x-q}{j}(w-q-j)!]}{w!}, & \text{if } 0 \leq q < x \\ \frac{(w-q)!}{w!}, & \text{if } q = x. \end{cases} \tag{25}$$

Then, based on (4.3), given the single-hop broadcast is successful, the conditional probability that the receiver successfully receives the broadcast message at time slot k for both scenarios under the distributed broadcast scheme, $P_1(k)$ and $P_2(k)$, can be obtained.

4.3.3.3 Single-hop Broadcast Collision Rate for the Distributed Broadcast Scheme

Finally, we calculate the single-hop broadcast collision rate for the distributed broadcast scheme. Note that in [24], a broadcast collision avoidance scheme is proposed. If this scheme is used, broadcast collisions can be avoided. However, it involves significant changes to the broadcasting sequences of the senders shown in Figure 4.9. To make the analysis tractable, in this chapter, we do not consider the broadcast collision avoidance scheme. Therefore, similar to the QoS-based broadcast scheme, the probability that a single-hop broadcast fails due to broadcast collisions for the distributed broadcast scheme is

$$P_q(A, C, B) = \sum_{z=1}^{w} \frac{(w-z)!}{w!} P_A^z \Pr(z). \tag{4.26}$$

4.4 Performance Evaluation

In this section, we validate our proposed unified analytical model using both hardware implementation and simulation in order to prove its correctness.

4.4.1 Validating Analysis using Hardware Implementation

The considered broadcast schemes have been implemented in embedded wireless radios. Each radio contains a Qualcomm Atheros IEEE 802.11 a/b/g chipset, and MADWIFI is used as the medium access control (MAC) driver. The three broadcast schemes are implemented as sub-functions of the MAC driver.

4.4.1.1 Time Slot and Synchronization

To support synchronized transmission of broadcast messages in different time slots, we first need to implement timing events that are synchronized among all communication nodes [105]. In order to minimize the impact by the software in the driver, a hardware register called software beacon alert (SWBA) is utilized to generate timing events. To support different timing events, the value in the SWBA register must be set into the time interval between the current timing event and the next expected timing event. Based on this mechanism, the time-line of each communication node is split into consecutive time slots each consisting of two portions: channel switching (CSS) and packet transmission/reception (PTR), as shown in Figure 4.10.

To synchronize time slots among all nodes, we adopt two mechanisms of IEEE 802.11 [106]: target beacon transmission time (TBTT) and timing synchronization function (TSF). Within each beacon interval, the first time slot must be aligned with TBTT, as shown in Figure 4.10. Through TSF, the time in the TSF register of different nodes is synchronized. Since TBTT is determined based on the timing value of the TSF register, the time slots of different nodes are synchronized accordingly.

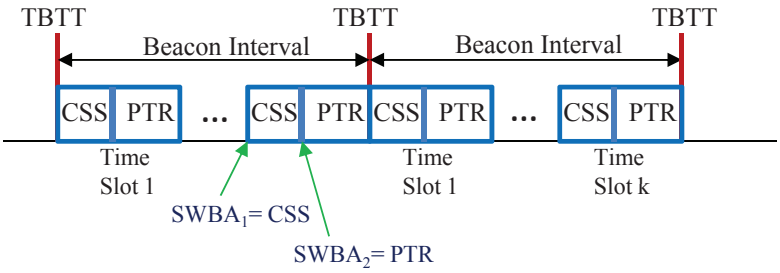

Figure 4.10: Synchronized time slots for IEEE 802.11 chipsets.

4.4.1.2 Packet Transmission/Reception and Channel Selection

In a source node, a broadcast message is generated in the PTR portion of a time slot and is then sent in a selected channel. This process repeats for S time slots. Other nodes in the network attempt to receive the broadcast message from its neighboring nodes and then rebroadcast it. Due to slot-by-slot operation, when a broadcast message is received, it is rebroadcast in the next time slot in the selected channel. This process is also repeated for S time slots. Since the same message may be received for multiple times, a sequence number is added into each broadcast message to avoid redundant broadcast messages. It should be noted that the channel selection for packet transmission and reception follows the rules set by the specific broadcast schemes developed in this chapter. The channel set in each node reflects the activities of primary nodes and is determined according to off-line simulations.

4.4.1.3 Performance Measurement

Two performance metrics are used in our implementation: the successful broadcast ratio and the average broadcast delay. The former metric measures the probability that a broadcast message can be successfully received by all nodes in a network, and the latter one records the average delivery time from the source node to the last node. In order to get stable performance results, we repeat the experiments for N measurements as shown in Figure 4.12. Within t_e seconds, one round of experiment is conducted. t_e is selected large enough so that all non-source nodes finish the process of receiving/rebroadcasting messages within the same period. In our experiments, we set t_e to be 3 seconds for a multi-hop CR ad hoc network under Topology 1 as shown

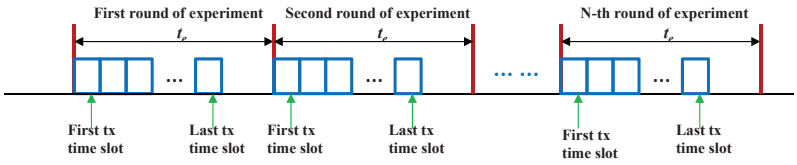

Figure 4.12: Repeating experiments.

in Figure 4.13(a).

Figure 4.14 shows comparisons between analytical results and experimental measurements for the random and QoS-based broadcast schemes. The comparisons for the distributed broadcast scheme are depicted in Figure 4.15, where two cases are considered: 1) Case 1: all nodes have the same w (i.e., $w(A) = w(B) = w(C) = w(D) = 5$) and 2) Case 2: some nodes have different w (i.e., $w(A) = w(B) = w(D) = 5$ and $w(C) = 4$). As we can see from Figs. 4.14 and 4.15, the implementation results fit the analytical results fairly well.

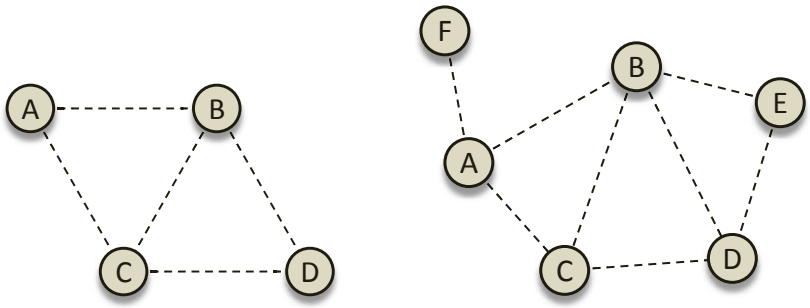

(a) Topology 1. (b) Topology 2.

Figure 4.13: Topology 1 and 2 considered in the performance evaluation.

4.4.2 Validating Analysis using Simulation

Due to the constraint on the total number of channels for hardware testing, we also use simulations to validate our proposed analytical model when the number of channels varies from 10 to 40. The side length of the simulation area L_s=10 (unit length). PUs are evenly distributed within this area. The total number of PUs is denoted as $K = 40$. The total number of channels is denoted as M. Furthermore, each SU has a circular transmission range with a radius of r_c. The SUs within the transmission range are considered as the neighboring nodes of the corresponding SU.

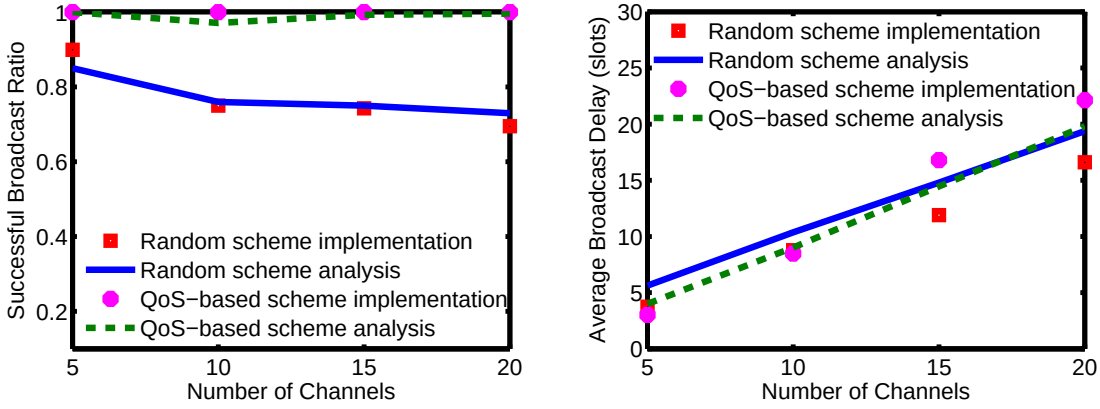

(a) Successful broadcast ratio. (b) Average broadcast delay.

Figure 4.14: Analytical and implementation results using the random and QoS-based broadcast schemes under Topology 1.

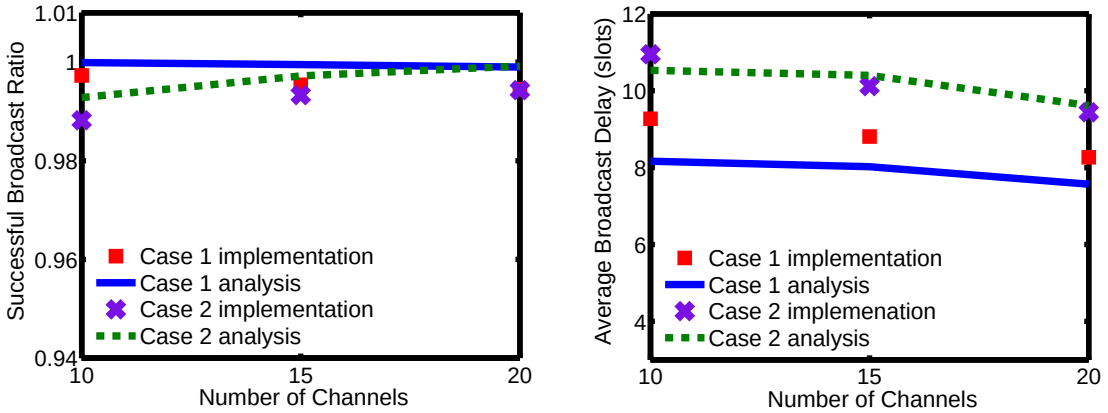

(a) Successful broadcast ratio. (b) Average broadcast delay.

Figure 4.15: Analytical and implementation results using the distributed broadcast scheme under Topology 1.

In addition, each SU also has a circular sensing range with a radius of r_s. That is, if a PU is currently active within the sensing range of a SU, the corresponding SU is able to detect its appearance. Moreover, we consider the PU traffic model used in [89], where the PU packet inter-arrival time follows the biased-geometric distribution [90][107]. In fact, our proposed algorithms do not rely on specific PU traffic models. We assume that the probability that a PU is active is fixed (i.e., $\rho = 0.9$). Each PU randomly selects a channel from the spectrum band to transmit one packet. Since the available channels for each SU depends on the sensing outcome in its sensing range, we use the values from the simulation as the input for the proposed analytical model (e.g., the number of common available channels between nodes A and B, Z_{AB}). In addition, we assume that the SU channel availability is stable during a broadcast duration.

4.4.2.1 Single-hop Performance

We first investigate the single-hop performance of each broadcast protocol considered in this chapter, because this performance is the foundation of the multi-hop performance evaluation. We study the two single-hop broadcast scenarios shown in Figure 4.6. In our study, the nodes are at the border of each other's sensing range. Figure 4.16(a) to 4.16(c) show the analytical and simulation results of the single-hop successful broadcast ratio using the three considered broadcast schemes under Scenario I and II. For the random broadcast scheme, S_r is set to be the same as the

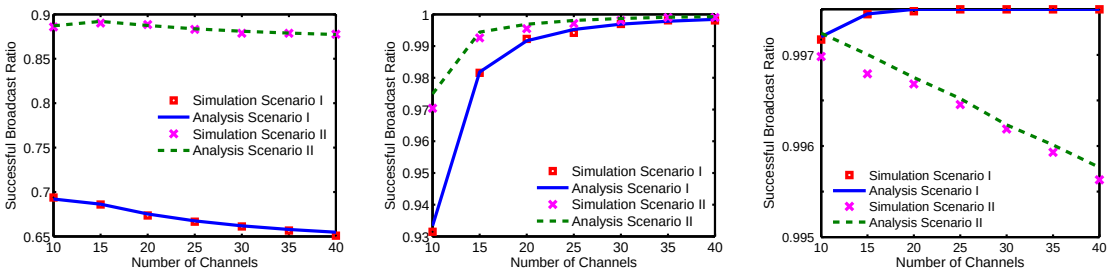

(a) Random broadcast scheme. (b) QoS-based broadcast scheme. (c) Distributed broadcast scheme.

Figure 4.16: Analytical and simulation results of the single-hop successful broadcast ratio using the three broadcast schemes under Scenario I and II.

number of channels, M. For the QoS-based broadcast scheme, $n = 2$ and $S = 2M$. In addition, for the distributed scheme, $w = 5$. It is shown that the simulation and analytical results match very well with the maximum difference of 0.4%, 0.5%, and 0.7% for the three schemes, respectively. The figure indicates that the distributed broadcast scheme can achieve the highest single-hop successful broadcast ratio.

In addition, Figure 4.17(a) to 4.17(c) illustrate the analytical and simulation re-

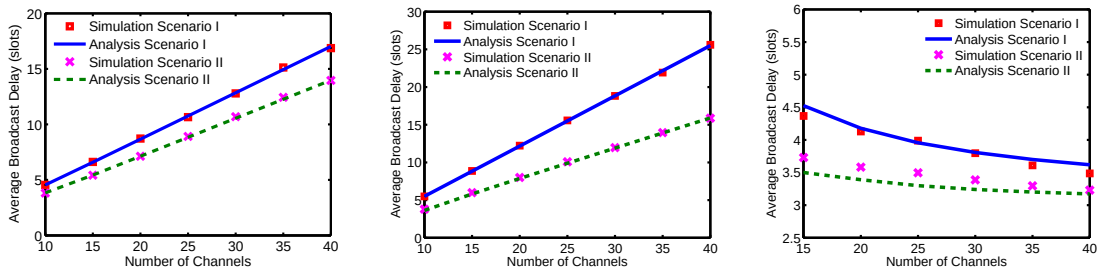

(a) Random broadcast scheme. (b) QoS-based broadcast scheme. (c) Distributed broadcast scheme.

Figure 4.17: Analytical and simulation results of the single-hop average broadcast delay using the three broadcast schemes under Scenario I and II.

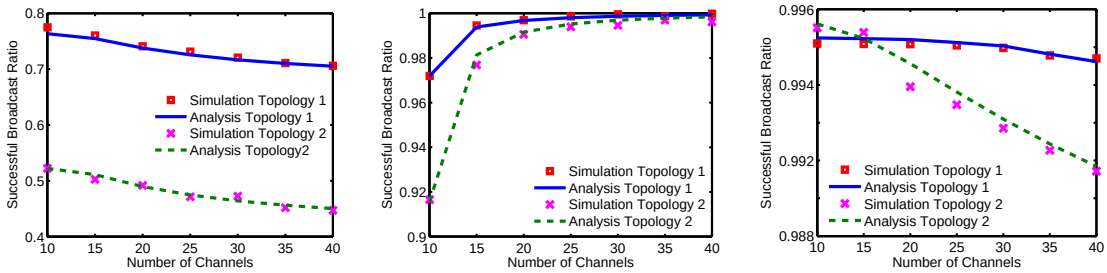

(a) Random broadcast scheme. (b) QoS-based broadcast scheme. (c) Distributed broadcast scheme.

Figure 4.18: Analytical and simulation results of the successful broadcast ratio using the three broadcast schemes under Topology 1 and 2.

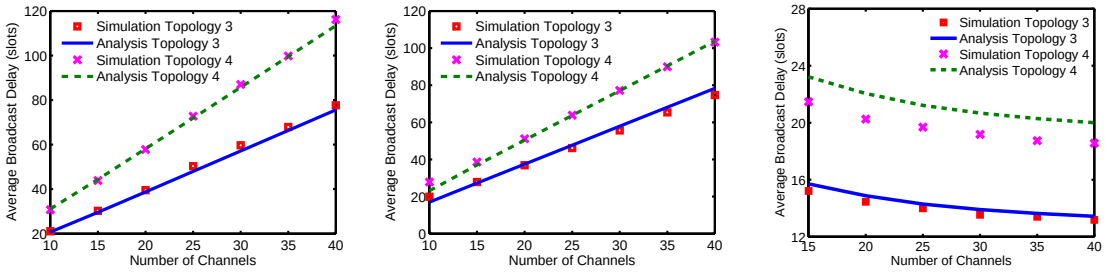

(a) Random broadcast scheme. (b) QoS-based broadcast scheme. (c) Distributed broadcast scheme.

Figure 4.19: Analytical and simulation results of the average broadcast delay using the three broadcast schemes under Topology 3 and 4.

sults of the single-hop average broadcast delay using the three considered broadcast schemes under Scenario I and II. It is also shown that the simulation and analytical results match very well with the maximum difference of 1.4%, 3.7%, and 5.5% for the three schemes, respectively. The distributed broadcast scheme results in the lowest single-hop average broadcast delay among the three schemes.

4.4.2.2 Successful Broadcast Ratio of Multi-hop CR ad hoc Networks

Next, we investigate the multi-hop performance. For the successful broadcast ratio, we study the two topologies shown in Figure 4.13(a) and 4.13(b). The coordinates of nodes in Topology 1 are $A(4,4), B(6,4), C(5,2.28)$, and $D(7,2.28)$. On the other hand, note that Topology 2 is a 6-node network under arbitrary topology. Moreover, the coordinates of nodes in Topology 2 are $A(4,4), B(5.8,4.8), C(5,3), D(6.6,3)$, $E(7,4.5)$, and $F(3,5)$. The parameters of each broadcast scheme are set to be the same as in the single-hop performance evaluation. In all topologies considered in the performance evaluation, node A is the source node. Figure 4.18(a) to 4.18(c) show the analytical and simulation results of the broadcast ratio using the three considered broadcast schemes under Topology 1 and 2. It is shown that the simulation results fit the analytical results well with the maximum difference of 2.1%, 4.6%, and 0.4% for the three schemes, respectively. The distributed broadcast scheme still has the best performance of successful broadcast ratio among the three schemes.

4.4.2.3 Average Broadcast Delay of Multi-hop CR ad hoc Networks

For the average broadcast delay, we investigate two grid topology networks: 1) a 3×3 grid network (denoted as Topology 3); and 2) a 4×4 grid network (denoted as Topology 4). Figure 4.19(a) to 4.19(c) depict the analytical and simulation results of the average broadcast delay using the three considered broadcast schemes under Topology 3 and 4. It is shown that the simulation and analytical results coincide with each other well with the maximum difference of 4.9%, 9.4%, and 6.5% for the three schemes, respectively. Again, the distributed broadcast scheme has a much lower

average broadcast delay, as compared to the other two schemes.

4.4.3 System Parameter Design using the Proposed Analytical Model

The system parameters of the proposed broadcast protocols in [21, 22, 23, 24] are not designed to achieve the optimal performance due to the lack of analytical analysis. In this chapter, we investigate the system parameter design of the random broadcast scheme using the proposed analytical model. In the random broadcast scheme, the length of time slots that the sender uses for broadcasting, S_r, is crucial to the performance of the broadcasting. Note that there exists a trade-off when determining S_r. If S_r is large, the successful broadcast ratio is high. However, the average broadcast delay is also long. On the other hand, if S_r is small, the average broadcast delay is short. However, the successful broadcast ratio is low. Hence, to design an optimal S_r is essential to the performance of the random broadcast scheme. We use an example to illustrate the process of the system parameter design. Consider a CR ad hoc network under Topology 1 shown in Figure 4.13(a). We assume that the single-hop successful broadcast ratio over each link is the same, which can be obtained from (4.13) (denoted as p). Thus, using the proposed algorithm for calculating the successful broadcast ratio, the successful broadcast ratio for the random broadcast scheme under Topology 1 is

$$\begin{aligned} P_{succ}=&p[1-(1-p)^2-P_q]^2+p^3\{1-[1-(1-p)^2-P_q]\} \\ &+(1-p)p^2[1-(1-p)^2-P_q]+(1-p)^2p^3, \end{aligned} \tag{4.27}$$

where P_q is given in (4.18). It is known that P_{succ} is a function of S_r.

On the other hand, we calculate the average broadcast delay under Topology 1, where node A is the source node. Since there are two levels in the network, we need to obtain the average broadcast delay of each level. Thus, using the proposed algorithm

for calculating the average broadcast delay, we have

$$\Gamma = \sum_{d=1}^{S_r} dP_1(d) + \sum_{d=1}^{S_r} dP_2(d), \tag{4.28}$$

where $P_1(d)$ and $P_2(d)$ can be obtained from Section 4.3.1.2 and (4.3). Note that Γ is also a function of S_r. Define the objective function of a broadcast protocol, Θ, as the rate between the successful broadcast ratio and the average broadcast delay. Therefore, we have $\Theta = \frac{P_{succ}}{\Gamma}$. Thus, the optimization problem of the protocol design becomes finding the optimal S_r that maximizes the objective function, Θ. Then, using certain numerical method, the optimal S_r can be obtained. Figure 4.20 shows the numerical results of the objective function under various S_r. It is shown that a proper S_r exists to achieve the optimal performance of a broadcast protocol. For instance, when $M = 10$, the optimal S_r is 11. The corresponding successful broadcast ratio is 81.25% and the average broadcast delay is 8.85 time slots.

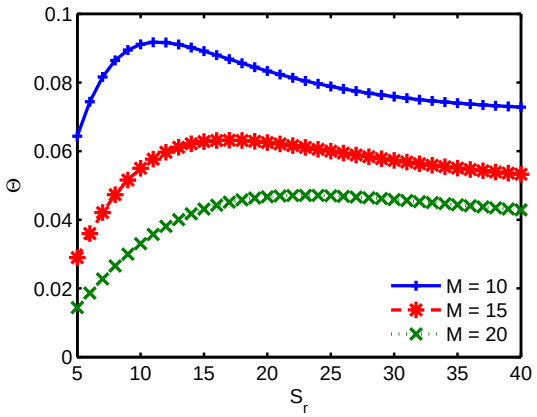

Figure 4.20: The numerical results of the objective function under various S_r.

CHAPTER 5: OPTIMAL HELLO EXCHANGE SCHEME IN CRAHNS

In this chapter, we study the optimal HELLO message exchange protocol in mobile CR ad hoc networks. The proposed HELLO message exchange protocol can achieve the optimal network performance in terms of SU throughput, average SU waiting time, and control overhead. It is not only important, but also necessary to link many essential functionalities in CR networks (i.e., spectrum sensing, spectrum sharing, and spectrum mobility) to form an operative framework. Moreover, the proposed HELLO message exchange protocol is independent of the particular spectrum sensing, channel rendezvous, and networking protocols adopted. More specifically, the main contributions of this research are:

1) The channel behavior caused by spatially distributed PUs and its impact on SU traffic is mathematically modeled for the first time.

2) The trade-off between SU throughput as well as average SU waiting time and control overhead is investigated analytically for the first time which takes into consideration the changes in the channel behavior and the impact of the HELLO message broadcast duration.

3) The impact of node mobility on the SU spectrum availability and the prompt changes in the identities of PUs is studied.

4) Two optimal HELLO message exchange protocols based on the modeled trade-off and node mobility impact are proposed for static and mobile CR ad hoc networks.

To the best of our knowledge, this is the first work that investigates the optimal HELLO message exchange protocol design for both static and mobile CR ad hoc networks.

5.1 Network Model

In this chapter, we consider a CR ad hoc network where N SUs and K PUs coexist in an $l \times l$ area. PUs are evenly distributed within the area. SUs opportunistically access M licensed channels. Each SU has a circular transmission range with a radius of r_c. The SUs within the transmission range are considered as the neighboring nodes of the corresponding SU. Each SU also has a circular sensing range with a radius of r_s. If a PU is currently active within the sensing range of a SU, the corresponding SU is able to detect its appearance. Since different SUs have different local sensing ranges which include different PUs, their acquired available channels may be different.

In addition, we assume that the PU and SU traffic follows the M/D/1 model. Denote the average PU and SU packet arrival rates as λ_p and λ_s, respectively, and the average PU and SU packet lengths in terms of time as L_p and L_s, respectively. Assume that each PU randomly selects a channel from the spectrum band to transmit one packet which consists of multiple time slots. Moreover, because PUs at different locations can claim any channels for communications, the packets on the same channel do not necessarily belong to the same PU. Thus, the PU channel behavior usually does not follow the same traffic behavior as a single PU. This is a more practical scenario, as compared to some papers which assume that each channel is associated with a different PU. Under such a practical scenario, only those PUs that are within the sensing range of a SU and are active contribute to the unavailable channels of the SU.

5.2 The Optimal HELLO Exchange Protocol for Static CRAHNs

In this section, we first consider the HELLO message exchange protocol for static CR ad hoc networks. The problem is formulated by investigating the trade-off between SU throughput as well as average SU waiting time and control overhead under different scenarios. Then, SU throughput and average waiting time are analytically studied. Finally, based on the analysis, the optimal HELLO message exchange inter-

val, α^*, is obtained.

5.2.1 Problem Formulation

To formulate the optimal HELLO message exchange problem, we first define two scenarios. Denote the average SU service time as $\overline{X_s}$. If $\lambda_s\overline{X_s}<1$, we define that the SU traffic is unsaturated (or, stable). That is, any SU packet generated and waiting in the queue can be served eventually given an infinite queue length. Hence, SU throughput is equal to the average SU arrival rate. On the other hand, if $\lambda_s\overline{X_s}\geq 1$, we define that the SU traffic is saturated (or, unstable). Since there is always a SU packet transmission request following the previously finished transmission, SU throughput is $S=\frac{1}{\overline{X_s}}$. Therefore, SU throughput is expressed as

$$S=\begin{cases}\lambda_s & \text{if} \quad \lambda_s\overline{X_s}<1\\ \frac{1}{\overline{X_s}} & \text{if} \quad \lambda_s\overline{X_s}\geq 1.\end{cases} \tag{5.1}$$

Thus, we formulate two objective utility functions under the above two different scenarios that capture the trade-off in determining the optimal HELLO message exchange interval. For the saturated scenario, the objective utility function is defined as

$$U_1(\alpha)=S(\alpha)-\frac{1}{\alpha t_s}, \tag{5.2}$$

where t_s is the length of a time slot. In addition, the unit of the HELLO message exchange interval α is time slot. The second term of the objective function is the average number of HELLO messages sent by a SU. Hence, our goal is to obtain the optimal α^* that maximizes $U_1(\alpha)$. Moreover, since the objective function may not maintain its concavity under all PU and SU traffic scenarios, we add another quality-of-service (QoS) condition that the SU throughput should not be less than a threshold. That is, $S(\alpha)\geq\eta$, where η is a threshold. Thus, we have $\alpha^*=\arg\max U_1(\alpha), w.r.t.\ S(\alpha)\geq\eta$.

For the unsaturated scenario, since SU throughput is always the same (from (5.1)), we use the SU average waiting time as the metric. Denote the SU average waiting

time as $\overline{W_s}(\alpha)$. Thus, the objective utility function is defined as

$$U_2(\alpha) = \frac{1}{\overline{W_s}(\alpha)t_s} - \frac{1}{\alpha t_s}. \tag{5.3}$$

The unit of $\overline{W_s}(\alpha)$ is time slot. Similar to SU throughput, $\overline{W_s}(\alpha)$ should be less than a threshold τ (i.e., $\overline{W_s}(\alpha) \leq \tau$).

Therefore, based on the objective functions and the QoS conditions, the optimal HELLO message exchange interval, α^*, can be obtained. Before that, we need to first derive the SU throughput $S(\alpha)$ and average SU waiting time $W_s(\alpha)$. However, how to mathematically model the channel behavior caused by spatially distributed PUs and the impact of the periodic HELLO message update on SU traffic is still very challenging. We propose analytical models to address this challenge in Section 5.2.2∼5.2.4.

5.2.2 The Derivation of SU Throughput

From (5.1), the average SU service time $\overline{X_s}$ is crucial for evaluating the SU throughput of CR ad hoc networks. In addition, since there also exist PU transmissions on the channels, SUs are not able to fully utilize the channels. Therefore, the average SU service time is usually longer than the average SU packet length in terms of time. That is, $\overline{X_s} \geq L_s$. Next, we derive $\overline{X_s}$ considering the PU traffic on the channels.

Since SUs and PUs co-exist on the spectrum band, $\overline{X_s}$ is affected by various factors (e.g., SU packet length, PU traffic, number of PUs, and number of channels). We first consider the scenario where the HELLO message exchange is not implemented. As mentioned earlier, since a PU packet may arrive in the middle of a SU transmission, the SU packet may need to be transmitted several times before it is successful. Figure 5.1 shows an example of the scenario where the SU packet is retransmitted once. From Figure 5.1, at t_1, a new SU packet is transmitted on channel i. Before the transmission is finished, a PU packet arrives on channel i at t_2 and the channel

becomes busy. Thus, a collision occurs and the current SU transmission fails. Then, since we allow PUs to spatially reuse the channel, at t_3, another PU packet arrives on channel i from a different PU at a different location. Both PUs are within the sensing ranges of the two SUs, so the channel is busy and cannot be used until all PU transmissions end. Thus, at t_4, all PU transmissions end and channel i becomes idle again. The previously collided SU packet is retransmitted. Finally, at t_5, the SU packet is successfully transmitted.

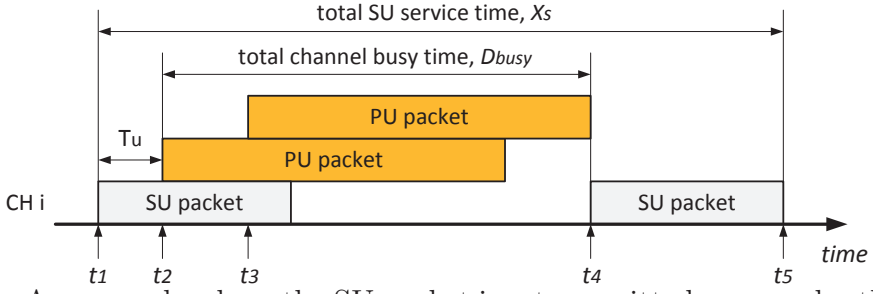

Figure 5.1: An example where the SU packet is retransmitted once under the scenario *without* the periodic HELLO message exchange.

Therefore, from Figure 5.1, the total SU service time is the duration from t_1 to t_5. Denote the duration from t_1 to t_2 and the total channel busy time (i.e., the duration from t_2 to t_4) as T_u and D_{busy}, respectively. Thus, when the SU packet is retransmitted once, the average SU service time is

$$\overline{X_{s,1}} = \overline{T_u} + \overline{D_{busy}} + L_s. \tag{5.4}$$

Given that a PU packet arrives during a SU transmission, the probability that the PU packet arrives at an arbitrary time slot is the same. Thus, we have $\overline{T_u} = \frac{L_s}{2}$. In addition, the derivation of the average channel busy duration, $\overline{D_{busy}}$, is given in Section 5.2.4. Hence, the average SU service time when the SU packet is retransmitted once is obtained. Since a SU packet may be retransmitted several times, using a similar method, we can obtain the average SU service time when a SU packet is retransmitted $h, h \in \{0, 1, 2, \cdots\}$ times, $\overline{X_{s,h}}$. Therefore, we have

$$\overline{X_{s,h}} = \left(\frac{L_s}{2} + \overline{D_{busy}}\right) h + L_s, \quad h = 0, 1, 2, \cdots . \tag{5.5}$$

Then, we calculate the probability that a SU packet is retransmitted h times, $P_{s,h}$. Denote the probability that a PU packet does not arrive in the middle of a SU packet transmission as P_0. Therefore, we have $P_{s,h} = (1 - P_0)^h P_0$. Since P_0 is equal to the probability that the channel is idle for L_s consecutive time slots, we obtain $P_0 = (1 - p_{01})^{L_s}$, where p_{01} is the probability that the current time slot is busy given that the previous time slot is idle. The derivation of p_{01} is also given in Section 5.2.4. Hence, the average SU service time is

$$\overline{X_s} = \sum_{h=0}^{\infty} \overline{X_{s,h}} \cdot P_{s,h}. \tag{5.6}$$

Next, we consider the scenario where the periodic HELLO message exchange is implemented. Figure 5.2 shows an example where the SU packet is retransmitted once under the periodic HELLO message exchange scenario. In Figure 5.2, the dark rectangles represent HELLO message updates. Even though the dark rectangles are shown on channel i in the figure, it does not mean that the HELLO message updates are on channel i. They only represent the periods of time which are used for the updates. From Section 5.1, it is known that the HELLO message update is related to the adopted channel rendezvous scheme and usually involves multiple channels. Different from the scenario without HELLO message exchange, under this scenario, the SU does not have to wait until the current channel becomes idle again and then retransmits the unsuccessful packet. Instead, after the current SU packet is collided, if the two SUs perform the HELLO message exchange before t_4 (e.g., at t'), based on the newly obtained channel availability of each other, they can switch to a new idle channel (e.g., channel j in Figure 5.2) and start the packet retransmission. Thus, the total SU service time can be reduced. Moreover, in Figure 5.2, the channel switching delay is ignored, but it can be easily added in the total SU service time if necessary.

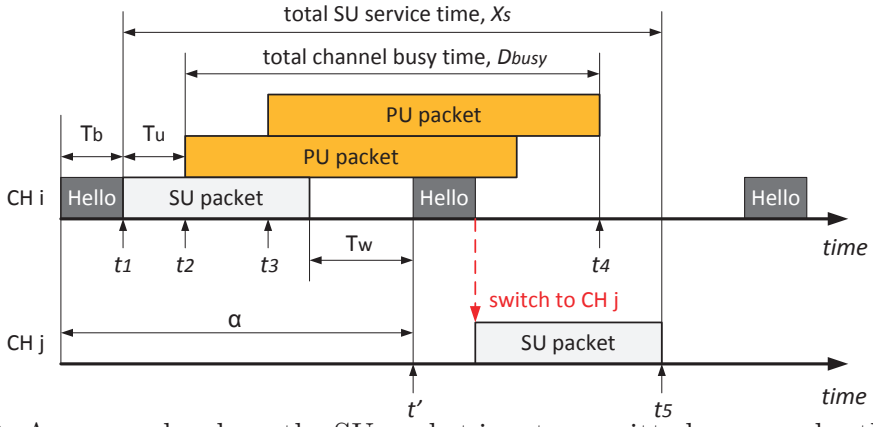

Figure 5.2: An example where the SU packet is retransmitted once under the scenario *with* the periodic HELLO message exchange.

Denote the duration from the moment the current collided packet is finished to the moment of the next upcoming HELLO message update as T_w. Thus, similar to the scenario without the HELLO message exchange, given that a HELLO message update is performed before the channel busy duration ends, the average SU service time when the SU packet is retransmitted once is

$$\overline{X'_{s,1}} = L_s + \overline{T_w} + T_b + L_s. \tag{5.7}$$

There are two cases when calculating $\overline{T_w}$. If $\overline{D_{busy}} + \overline{T_u} - L_s < \alpha$, then given that a HELLO message update is performed before the channel busy duration ends, the probability that the HELLO message update arrives at an arbitrary time slot is the same. Therefore, $\overline{T_w} = \frac{\overline{D_{busy}}+\overline{T_u}-L_s}{2}$. On the other hand, if $\overline{D_{busy}} + \overline{T_u} - L_s \geq \alpha$, a HELLO message update is guaranteed to arrive before the channel busy duration ends. Thus, $\overline{T_w} = \frac{\alpha}{2}$.

In addition, there exists a probability that the HELLO message update is not performed before the channel busy duration ends. The average SU service time under this scenario is equivalent to the scenario without the HELLO message exchange. Thus, we have $\overline{X''_{s,1}} = \overline{T_u} + \overline{D_{busy}} + L_s$. Denote the probability that the HELLO message update is performed before the channel busy duration ends as P_m. Hence,

the average SU service time when the SU packet is retransmitted once is

$$\overline{X_{s,1}} = P_m \overline{X'_{s,1}} + (1 - P_m)\overline{X''_{s,1}}. \tag{5.8}$$

Since the HELLO update is performed periodically with the interval α and the PU packet arrives randomly on a channel, we obtain

$$P_m = \begin{cases} \frac{\overline{D_{busy}} + \overline{T_u} - L_s}{\alpha} & \text{if } \overline{D_{busy}} + \overline{T_u} - L_s < \alpha \\ 1 & \text{if } \overline{D_{busy}} + \overline{T_u} - L_s \geq \alpha. \end{cases} \tag{5.9}$$

Then, we calculate the average SU service time when the SU packet is retransmitted h times. Given that a SU packet is retransmitted h times, the number of times that the HELLO message update is performed before the channel busy duration ends is denoted as z. Therefore, the average SU service time when a SU packet is retransmitted h times is

$$\begin{aligned} \overline{X_{s,h}} = \sum_{z=0}^{h} \binom{h}{z} P_m^z (1 - P_m)^{h-z} [z(L_s + \overline{T_w} + T_b) + \\ (h - z)(\overline{T_u} + \overline{D_{busy}}) + L_s], \qquad h = 0, 1, 2, \cdots . \end{aligned} \tag{5.10}$$

Using (5.1) and (5.6), the SU throughput can be obtained. Figure 5.3 shows the analytical and simulation results of SU throughput with periodic HELLO message exchange under saturated and unsaturated scenarios. It is shown that the simulation validates the analysis very well.

5.2.3 The Derivation of the Average SU Waiting Time

Next, we derive the average SU waiting time. Using the Pollaczek-Khinchine formula for the M/G/1 system [108], the average SU waiting time is given by

$$\overline{W_s} = \frac{\lambda_s \overline{X_s^2}}{2(1 - \lambda_s \overline{X_s})}, \tag{5.11}$$

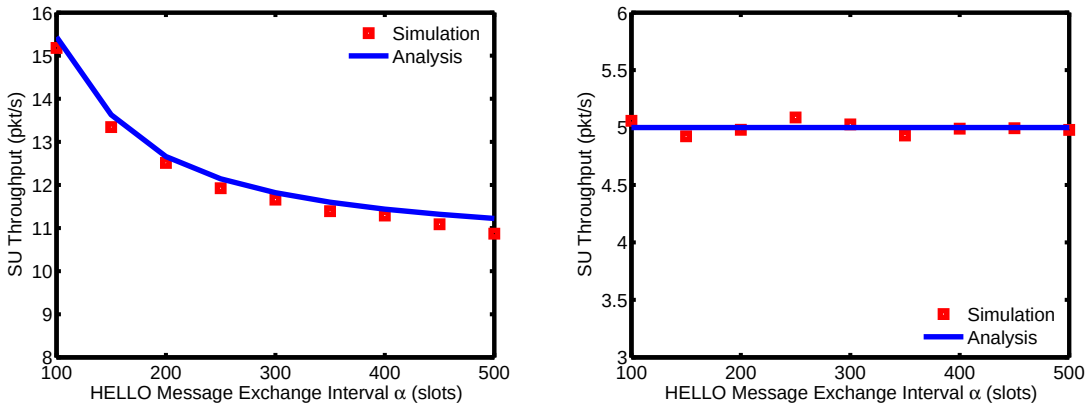

(a) The saturated scenario with λ_s=20 pkt/s. (b) The unsaturated scenario with λ_s=5 pkt/s.

Figure 5.3: The analytical and simulation results of SU throughput with periodic HELLO message exchange under saturated and unsaturated scenarios.

where $\overline{X_s^2}=\sigma^2+(\overline{X_s})^2$. In addition, the variance σ^2 is expressed as

$$\sigma^2 = \sum_{h=0}^{\infty}(X_{s,h} - \overline{X_s})^2 \cdot P_{s,h}. \tag{5.12}$$

Hence, the average SU waiting time is obtained. Therefore, the only two unknown parameters are $\overline{D_{busy}}$ and p_{01}. The derivation process of these two parameters is given in the next section.

5.2.4 The Derivation of the Average Channel Busy Duration

In this section, the derivation process of the average channel busy duration, $\overline{D_{busy}}$, is introduced. We use "0" and "1" to represent that the channel is idle and busy, respectively. Denote $H(t)$ as the status of the channel at time slot t. In addition, $Q(t)$ is the number of consecutive idle slots until time slot t from the last busy time slot. Figure 5.4 shows three examples of the idle periods on a channel when $Q(t) = 1, 2, 3$.

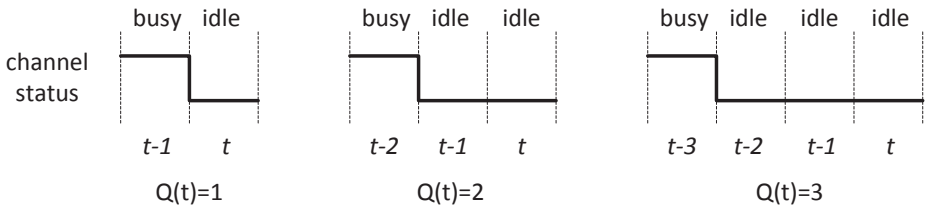

Figure 5.4: Three examples of the different idle period lengths on a channel.

Based on the channel status of two consecutive time slots, we define the following four conditional probabilities: 1) $p_{00} = \Pr(H(t)=0|H(t-1)=0)$; 2) $p_{01} = \Pr(H(t)=1|H(t-1)=0)$; 3) $p_{10} = \Pr(H(t)=0|H(t-1)=1)$; and 4) $p_{11} = \Pr(H(t)=1|H(t-1)=1)$. Therefore, from Figure 5.4, the probability that there are k consecutive idle time slots can be expressed as $\Pr(Q(t)=k) = \Pr(H(t)=0, H(t-1)=0, \cdots, H(t-k)=1)$. Then, since the PU arrival process is memoryless, using the Bayes' theorem and the Markov property, we have

$$\begin{aligned}
&\Pr(Q(t)=k) \\
=&\Pr(H(t)=0|H(t-1)=0,\cdots,H(t-k)=1)\cdot \\
&\Pr(H(t-1)=0|H(t-2)=0,\cdots,H(t-k)=1)\cdots \\
&\Pr(H(t-k+1)=0|H(t-k)=1)\cdot\Pr(H(t-k)=1) \\
=&\Pr(H(t)=0|H(t-1)=0)\cdot\Pr(H(t-1)=0|H(t-2)=0)\cdots \\
&\Pr(H(t-k+1)=0|(H(t-k)=1)\cdot\Pr(H(t-k)=1) \\
=&\underbrace{p_{00}\cdots p_{00}}_{k-1}p_{10}\Pr(H(t-k)=1) \\
=&p_{00}^{k-1}p_{10}\Pr(H(t-k)=1) \\
=&p_{00}^{k-1}p_{10}P_{busy},
\end{aligned} \tag{5.13}$$

where $P_{busy} = \Pr(H(t)=1)$ is the probability that the channel is busy in a time slot. Note that (5.13) is the absolute probability that there are k consecutive idle slots. Thus, given that the channel is idle, the conditional probability is

$$P_k = \frac{\Pr(Q(t)=k)}{\sum_k \Pr(Q(t)=k)} = \frac{p_{00}^{k-1}p_{10}P_{busy}}{P_{idle}}, \tag{5.14}$$

where $P_{idle} = \Pr(H(t)=0)$ is the probability that the channel is idle in a time slot. Denote $\overline{D_{idle}}$ as the average idle duration on a channel. Thus, $\overline{D_{idle}} = \sum_k^\infty kP_k$.

Next, we calculate p_{00}. The probability that p PUs are within the sensing ranges

of the two SUs, A^*, is $\Pr(p) = \binom{K}{p}\left(\frac{A^*}{A_L}\right)^p\left(\frac{A_L-A^*}{A_L}\right)^{K-p}$, where $A_L = l^2$ is the total network area under consideration. In addition, the area of the sensing ranges of the two SUs is $A^*=2(\pi-\theta)r_s^2+d_{12}\sqrt{r_s^2-(\frac{d_{12}}{2})^2}$, where d_{12} is the distance between the two SUs and $\theta = \cos^{-1}\frac{d_{12}}{2r_s}$. Given that there are p PUs within the sensing ranges of the two SUs, the probability that there are u PUs inactive is $\Pr(u|p) = \binom{p}{u}\rho^{p-u}(1-\rho)^u$, where ρ is the probability that a PU is active. Since a PU is a $M/D/1$ system, we have $\rho = L_p/[L_p+(1-\lambda_p)/\lambda_p]$. Then, given that there are u PUs inactive and $(p-u)$ PUs active, the probability that there are m active PUs who finish the transmissions in the previous slot is

$$\Pr(m|u,p) = \binom{p-u}{m}\left(\frac{1}{L_p}\right)^m\left(1-\frac{1}{L_p}\right)^{p-u-m}. \tag{5.15}$$

Then, given that there are u PUs inactive and m active PUs who finish the transmissions in the previous slot, the probability that there are q PUs who start transmissions in the current slot is

$$\Pr(q|u,m) = \binom{u+m}{q}\lambda_p^q\left(1-\lambda_p\right)^{u+m-q}. \tag{5.16}$$

Finally, given that there are q PUs who start transmissions in the current slot, the probability that the current slot is idle is equal to the probability that all these q PUs do not select this channel. Thus, we have $P_s = \left(\frac{M-1}{M}\right)^q$. Therefore, the conditional probability p_{00} is expressed as

$$p_{00} = \sum_{p=0}^{K}\sum_{u=0}^{p}\sum_{m=0}^{p-u}\sum_{q=0}^{u+m} P_s \Pr(q|u,m)\Pr(m|u,p)\Pr(u|p)\Pr(p). \tag{5.17}$$

Since the sum of the conditional probabilities p_{01} and p_{00} is one, we have $p_{01} = 1-p_{00}$. Using a similar method, p_{10} and p_{11} can also be obtained.

To calculate P_{idle} and P_{busy}, we use the method proposed in [24]. Given that there are p PUs within A^*, the probability that there are b PUs active is $\Pr(b|p)=$

$\binom{p}{b}\rho^b(1-\rho)^{p-b}$. Furthermore, given that there are p PUs and b active PUs within A_k, the probability that there are c available channels is

$$\Pr(c|p,b)=\frac{\binom{M}{c}(M-c)!\Theta(b,M-c)}{M^b}, c\in[\max(0,M-b),M], \tag{5.18}$$

where $\Theta(b,M-c)$ is the Stirling number of the second kind. Therefore, the probability that a time slot is idle is

$$P_{idle}=\sum_{p=0}^{K}\sum_{b=0}^{p}\sum_{c=\max(0,M-b)}^{M}\frac{c}{M}\Pr(c|p,b)\Pr(b|p)\Pr(p). \tag{5.19}$$

Then, $P_{busy}=1-P_{idle}$. Hence, the average channel busy duration is

$$\overline{D_{busy}}=\frac{P_{busy}\overline{D_{idle}}}{P_{idle}}. \tag{5.20}$$

5.3 The Optimal HELLO Exchange Protocol for Mobile CRAHNs

In this section, we first propose an adaptive optimal HELLO message exchange protocol for mobile CR ad hoc networks. In this chapter, we assume that only SUs are mobile and PUs are static [109][110]. Then, the impact of the change in the identities of PUs within the sensing ranges on the HELLO message exchange design is analyzed. Based on the analysis, a supplementary HELLO message update scheme is proposed to further enhance the network performance.

5.3.1 The Adaptive Optimal HELLO Exchange in Mobile CRAHNs

Node mobility plays an essential role in the networking protocol design for CR networks. Currently, there are only a few papers addressing the impact of node mobility on the spectrum access in mobile CR ad hoc networks [109]. However, in [109], both the time interval that a SU moves inside a PU interference range and the time duration that a SU is located within a PU interference range follow the exponential distribution. In addition, in [109], the PU spatial reuse of the channel is

not considered. The PU channel process is modeled as an exponential distribution. These assumptions are over-simplified and unrealistic. In this chapter, we do not make such assumptions. In fact, one of the advantages of the proposed optimal HELLO message exchange protocol is that it does not rely on any mobility model. By using the most updated control information (e.g., SU location), SUs can calculate the changes in the channel availability caused by node mobility and adaptively adjust the optimal exchange interval for the next HELLO message update.

We propose an adaptive optimal HELLO message exchange protocol for mobile CR ad hoc networks that is based on the analytical models proposed in Section 5.2 but incorporates the impact of node mobility. From Section 5.2, in order to obtain the optimal HELLO message exchange interval, two important factors are PU traffic intensity (i.e., λ_p and L_p) and the number of PUs within the sensing ranges of the two SUs (i.e., p). If we assume that the PU traffic intensity does not change, the optimal HELLO message exchange interval only depends on p. Furthermore, from the derivation in Section 5.2.4, p depends on the area of the sensing ranges of the two SUs, which also relies on the relative distance between the two SUs, d_{12}. Hence, if d_{12} changes, the corresponding optimal HELLO message exchange interval also changes and can be calculated if d_{12} is known. Therefore, under our design, during each HELLO message update, in addition to the channel availability information, the two SUs also exchange their current location information (e.g., location coordinates from a certain positioning technique). Then, the two SUs obtain a new optimal HELLO message exchange interval based on the new location information. The beauty of this design is that the impact of node mobility on the optimal exchange interval is easily considered and can be practically implemented.

5.3.2 The Supplementary HELLO Message Update Scheme

Besides the change in the number of PUs within the sensing ranges, the change in the identities of PUs within the sensing ranges also has an effect on the network

performance. That is, due to SU movement, the change in the identities of PUs may cause prompt changes on the channel behavior. We name the prompt changes in the identities of PUs the "short-term" effect. Hence, we analyze the impact of this "short-term" effect on the HELLO message exchange design. Based on the analysis, a supplementary HELLO message update scheme for the proposed adaptive optimal HELLO message exchange protocol is proposed.

The "short-term" effect of SU mobility has two scenarios: 1) new PUs arrive within the sensing ranges of the two SUs; and 2) old PUs leave the sensing ranges. Since only the first scenario may have a negative effect on the SU performance, we study this scenario. First of all, we derive the probability distribution of the inter-arrival time of new PUs. That is, the cumulative distribution function (CDF) of the inter-arrival time of new PUs is defined as

$$F_{T_a}(t) = \Pr(T_a \leq t), \tag{5.21}$$

where T_a is the inter-arrival time of new PUs. Figure 5.5 shows a moving scenario after t seconds. Denote the speed of the moving SU as v. Thus, from location A to B, the distance that the SU moves is vt. The shaded part is the new area that the sensing range of the moving SU sweeps during the movement. Denote the shaded area as A_d. Thus, the probability $\Pr(T_a \leq t)$ is equal to the probability that there exists at least one new PU within A_d.

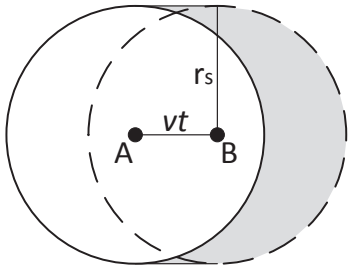

Figure 5.5: The SU moving scenario from A to B after t seconds.

Denote the probability that there are y PUs within an area A as $P_A(y)$. Thus, we have

$$\begin{aligned}\Pr(T_a \le t) &= \Pr(\text{at least one PU is located within } A_d) \\ &= \sum_{y=1}^{\infty} P_{A_d}(y).\end{aligned} \tag{5.22}$$

If PUs are uniformly distributed within the network area, $P_{A_d}(y) = \binom{K}{y}\left(\frac{A_d}{A_L}\right)^y\left(1-\frac{A_d}{A_L}\right)^{K-y}$. In addition, from Figure 5.5, we have $A_d = 2r_s vt$. Therefore, the CDF of the inter-arrival time is

$$\begin{aligned}F_{T_a}(t) &= \sum_{y=1}^{\infty}\binom{K}{y}\left(\frac{A_d}{A_L}\right)^y\left(1-\frac{A_d}{A_L}\right)^{K-y} \\ &= 1-\left(1-\frac{2r_s v}{A_L}t\right)^K.\end{aligned} \tag{5.23}$$

Figure 5.6 shows the simulation and analytical results of the CDF of the inter-arrival time of new PUs under different SU speeds. It is shown that the simulation and analytical results match perfectly.

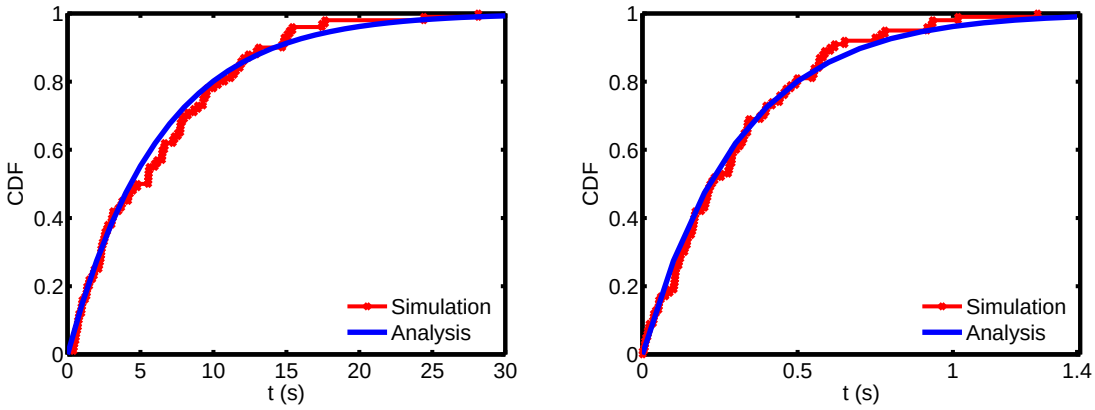

(a) The SU speed is 0.5 m/s. (b) The SU speed is 10 m/s.

Figure 5.6: The simulation and analytical results of the CDF of the inter-arrival time of new PUs, T_a.

Then, by differentiating (5.23), the probability density function (pdf) of the inter-arrival time of new PUs is

$$f_{T_a}(t) = -K\left(-\frac{2r_s v}{A_L}\right)\left(1-\frac{2r_s v}{A_L}t\right)^{K-1}. \tag{5.24}$$

Therefore, the expected inter-arrival time of new PUs is

$$
\begin{aligned}
E[T_a] &= \int_0^{\frac{A_L}{2r_s v}} t f_{T_a}(t) \mathrm{d}t \\
&= \int_0^{\frac{A_L}{2r_s v}} t \left[-K \left(-\frac{2r_s v}{A_L} \right) \left(1 - \frac{2r_s v}{A_L} t \right)^{K-1} \right] \mathrm{d}t \\
&= \frac{A_L}{(K+1)2r_s v}. \qquad (5.25)
\end{aligned}
$$

From the above analysis, it is known that on average every $E[T_a]$ seconds, a new PU arrives in the SU sensing range. This new PU may be active and use one of the channels, which leads to prompt changes on the channel behavior. In addition, when $v \to \infty$, $E[T_a] \to 0$. This means that the faster the SU moves, the more frequent new PUs arrive. Hence, the "short-term" effect of SU mobility is more significant. Thus, in addition to the adaptive optimal HELLO message exchange protocol, we propose that the two SUs also perform a HELLO message update every $E[T_a]$ seconds to cope with the "short-term" effect. We name it the supplementary HELLO message exchange scheme. If we denote the HELLO message update interval for the supplementary scheme as β, we have $\beta = E[T_a]$. Figure 5.7 illustrates the update moments in the adaptive optimal HELLO message exchange protocol and the supplementary update scheme. After each update, SUs adjust the next optimal α based on the updated relative locations. In addition, SUs also perform a HELLO message update every β seconds if the SU speed does not change.

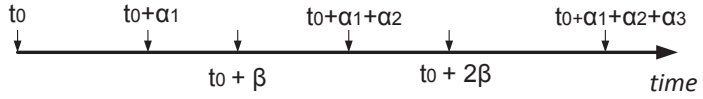

Figure 5.7: The proposed adaptive optimal HELLO message exchange protocol and the supplementary update scheme for mobile CR ad hoc networks.

5.4 Performance Evaluation

In this section, we evaluate the performance of the proposed HELLO message exchange protocol. We use the common frequency hopping scheme as the channel rendezvous scheme [42]. Under this scheme, since all SUs follow the same channel hopping sequence, they always hop on the same channel at the same time. One round

of channel hopping can guarantee the reception of the HELLO message. Therefore, the HELLO message broadcast duration is $T_m = M$. Assume that the spectrum sensing time for each channel is 1ms. Thus, the HELLO message update duration T_b is determined. In addition, the side length of the network area $l = 100$m. We assume that the radii of the sensing range and the transmission range are the same (i.e., $r_s = r_c = 20$m). Other simulation parameters are given in Table 5.1.

Table 5.1: Simulation Parameters

Number of PUs K	40
Number of channels M	5
Time slot length t_s	2 ms
SU packet length L_s	20 slots
PU packet arrival rate λ_p	5 pkt/s
PU packet length L_p	100 slots

5.4.1 Static CR Ad Hoc Networks

5.4.1.1 The Trade-off under Different Scenarios

We first evaluate the performance in static CR ad hoc networks. Figure 5.8(a) and 5.8(b) illustrate the trade-off between SU throughput as well as average SU waiting time and control overhead in the saturated and unsaturated scenario, respectively. Since both the network revenue (i.e., SU throughput and average SU waiting time) and the network cost (i.e., control overhead) are monotonic functions of the HELLO message exchange interval, any α leads to a Pareto-optimal solution [111]. However, by considering the proposed objective utility functions and the QoS conditions, a single optimal HELLO message exchange interval can be obtained. Network designers can adjust the objective utility functions and the QoS conditions to obtain a different optimal HELLO message exchange interval based on different requirements.

5.4.1.2 The Impact of the HELLO Message Exchange Duration

Figure 5.9 shows the impact of the HELLO message exchange duration T_b on the network performance under saturated and unsaturated scenarios. It is shown that

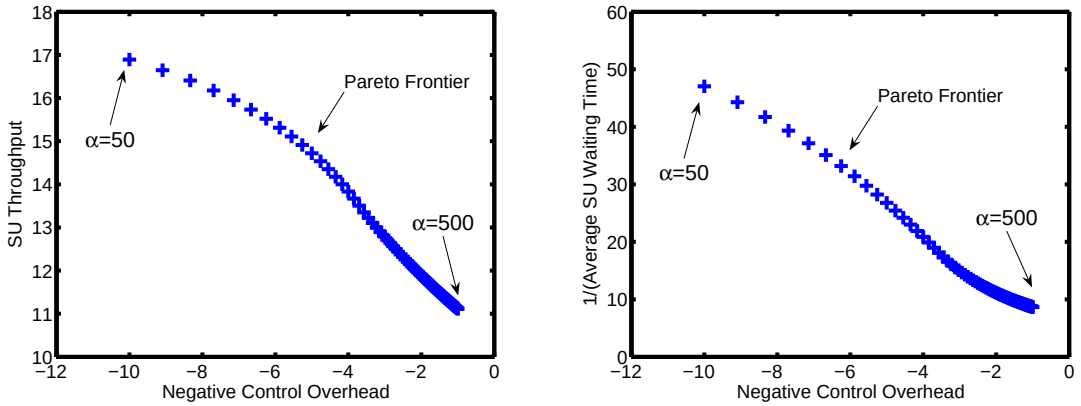

(a) The trade-off under the saturated scenario with λ_s=20 pkt/s.

(b) The trade-off under the unsaturated scenario with λ_s=5 pkt/s.

Figure 5.8: The trade-off between SU throughput/average SU waiting time and control overhead under saturated and unsaturated scenarios.

when T_b increases, network performance suffers degradation (i.e., SU throughput decreases and average SU waiting time increases). Thus, the HELLO message exchange duration has a significant impact on network performance and cannot be ignored in networking protocol designs in CR networks.

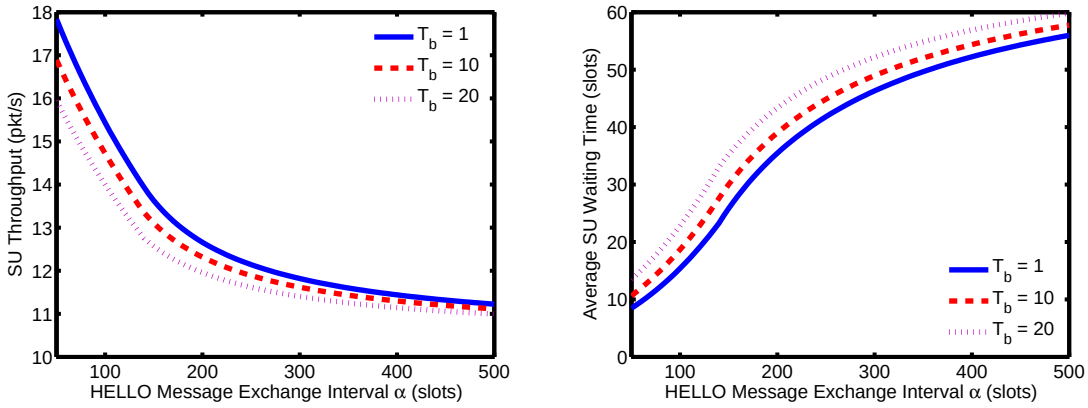

(a) SU throughput under the saturated scenario.

(b) Average SU waiting time under the unsaturated scenario.

Figure 5.9: The impact of the HELLO message update duration T_b on network performance.

5.4.1.3 Performance Comparison with the Change-Triggered Scheme

We compare our proposed HELLO message exchange protocol with the change-triggered HELLO message exchange scheme: a SU performs a HELLO message update whenever a change in the channel availability is detected. We consider 4 SUs (two pairs) located in the same neighborhood. Figure 5.10 shows the performance

comparison between these two schemes when $T_b = 10$ slots and $\lambda_s = 20$pkt/s. Since SUs can always obtain the latest channel availability information under the change-triggered scheme, SU throughput is higher than the proposed scheme (up to 12% higher from Figure 5.10(a)). However, the change-triggered scheme causes very high control overhead (up to 87% higher from Figure 5.10(b)) because SUs need to perform the HELLO message update with a high frequency, which often leads to a waste of channel resources. Therefore, considering this trade-off, the proposed optimal HELLO message exchange protocol outperforms the change-triggered scheme in terms of higher utilities, as shown in Figure 5.10(c).

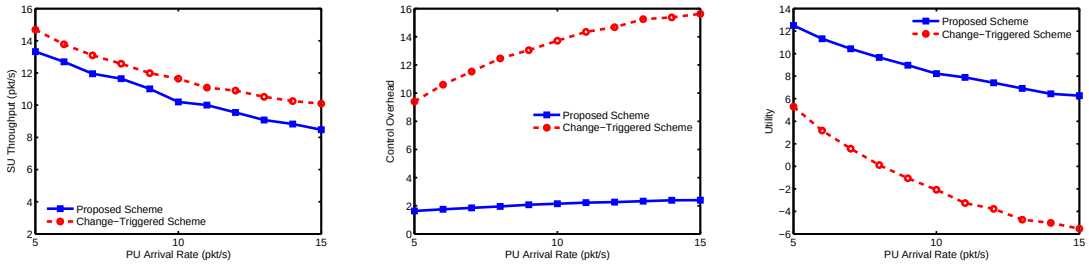

(a) SU throughput. (b) Control overhead. (c) Utility.

Figure 5.10: Performance comparison between the proposed optimal HELLO message exchange and the change-triggered scheme in static CR ad hoc networks.

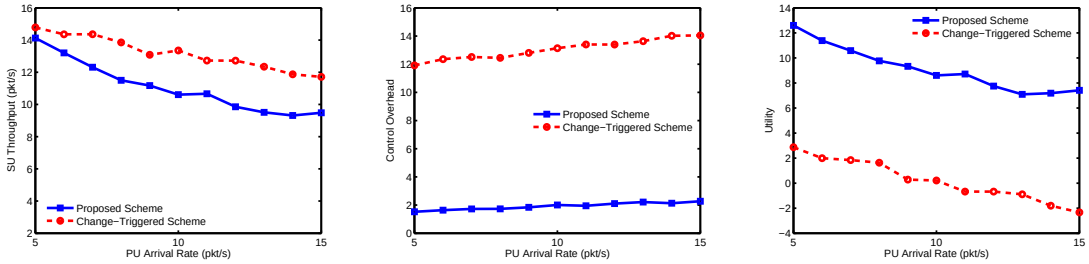

(a) SU throughput. (b) Control overhead. (c) Utility.

Figure 5.11: Performance comparison between the proposed optimal HELLO message exchange and the change-triggered scheme in mobile CR ad hoc networks.

5.4.2 Mobile CR Ad Hoc Networks

Next, we evaluate the performance of the proposed optimal HELLO message exchange protocol in mobile CR ad hoc networks. We consider the Random Way-point as the mobility model [112]. Two SUs are originally located at random locations

within the transmission ranges of each other. The mobile SU randomly selects a speed from $[0, v_{max}]$ and a direction. The maximum SU speed, v_{max}, is set to be 10m/s. Figure 5.11 shows the performance comparison between the proposed optimal HELLO message exchange scheme and the change-triggered scheme in mobile CR ad hoc networks. Similar to the static scenario, the SU throughput under the change-triggered scheme is higher than the proposed protocol (up to 22%), but the change-triggered scheme results in much higher control overhead (up to 85%). Thus, the proposed optimal HELLO message exchange protocol outperforms the change-triggered scheme in terms of higher utilities.

Figure 5.12 shows the impact of the maximum SU speed on network performance. It is shown that SU throughput without the supplementary scheme suffers greater degradation when the maximum SU speed increases, as compared to the scenario with the supplementary scheme. This is because that there is no mechanism to cope with the "short-term" effect. In addition, even with the supplementary scheme, the proposed adaptive scheme does not generate too much excessive control overhead.

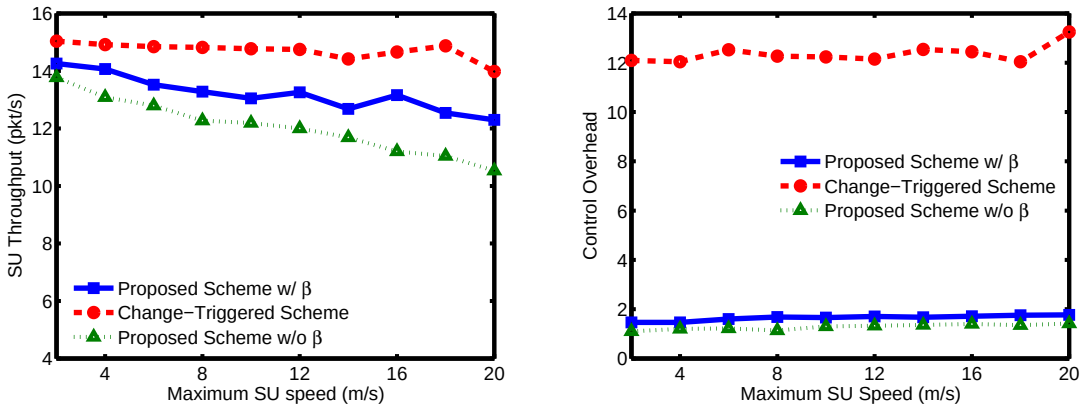

(a) SU throughput. (b) Control overhead.

Figure 5.12: The impact of the maximum SU speed on network performance.

CHAPTER 6: SECURITY SCHEMES FOR FCIE ATTACKS IN CRAHNS

In this chapter, we propose a distributed algorithm to fight against the FCIE attacks in CR ad hoc networks. We investigate the spatial correlation of the channel availability between neighboring nodes. This is because that the channel availability of neighboring nodes is correlated with the relative locations of these nodes. Using this relationship, the malicious node that sends the false channel information can be identified. To the best of our knowledge, this is the first work that defines and addresses the FCIE attacks in CR ad hoc networks.

6.1 The Spatial Correlation of the Channel Availability

In this section, we first introduce a network model we consider. Then, based on this model, we investigate the spatial correlation of the channel availability between two neighboring nodes.

6.1.1 The Network Model

In this chapter, we consider a CR ad hoc network where N SUs and K PUs coexist in an $L \times L$ area, as shown in Figure 6.1. PUs are distributed within the area under the probability density function (pdf) $f_X(x)$. For simplicity, in this chapter, we consider that PUs are evenly distributed. The SUs opportunistically access M licensed channels. In Figure 6.1, the solid circle represents the transmission range of a SU with a radius of r_c. Other SUs within the transmission range are considered as the neighboring nodes of the corresponding SU. In addition, the dashed circle represents the sensing range of a SU with a radius of r_s. If a PU is currently active within a sensing range, the corresponding SU is able to detect its appearance. Since the sensing ranges of different SUs at different locations may include different PUs,

their acquired available channels may be different. In addition, because the available channels of a SU are obtained based on the sensing outcome within the sensing range, each SU is not allowed to communicate with other SUs outside its sensing range since it may mistakenly use an occupied channel by a PU, which results in interference to the PU. Therefore, in this chapter, we assume that $r_c \leq r_s$.

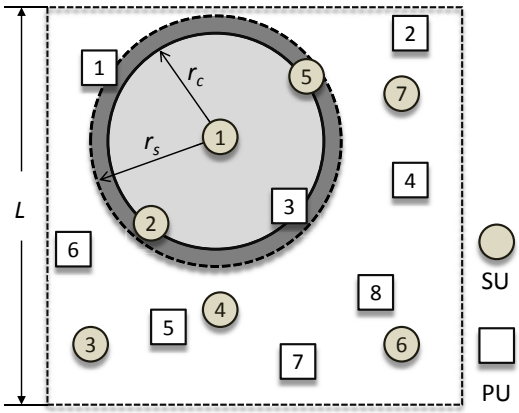

Figure 6.1: The network model of a CR ad hoc network.

In addition, in this chapter, we model the PU channel activity as an ON/OFF process, where the length of the ON period is the length of a PU packet [89]. We assume that each PU randomly selects a channel from the spectrum band to transmit a packet. Therefore, the packets on the same channel do not necessarily belong to the same PU. This is a more practical scenario, as compared to some papers which assume that each channel is associated with a different PU. Under such a practical scenario, the number of active PUs is not necessarily the number of occupied channels but depends on the total number of PUs in the network and the PU traffic intensity.

6.1.2 The Spatial Correlation of the Channel Availability

Next, we analyze the spatial correlation of the channel availability between two neighboring SUs. We assume that the channel availability information for both SUs is true. Figure 6.2 shows the relative locations of two neighboring SUs whose sensing ranges overlap, where d_{12} is the distance between SU_1 and SU_2.

We denote $\mathbf{Q}_1$ and $\mathbf{Q}_2$ as the channel information for SU_1 and SU_2, respectively.

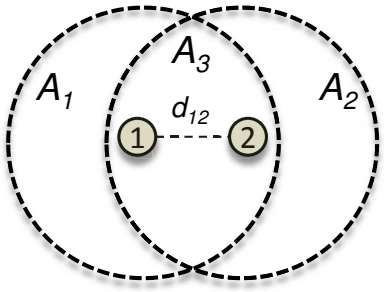

Figure 6.2: Two neighboring SUs whose sensing ranges overlap.

In addition, we define $\mathbf{Q}_i = [q_i^1, q_i^2, \cdots, q_i^M]$, where q_i^j is a binary number indicating the availability of channel j for SU_i (i.e., we use 1 to indicate that the channel is available and 0 to indicate that the channel is unavailable). Given $\mathbf{Q}_1$ and $\mathbf{Q}_2$, the relationship of the channel availabilities between the two SUs can be expressed as $\{\mathbf{Q}_1, \mathbf{Q}_2\} = [(q_1^1, q_2^1), (q_1^2, q_2^2), \cdots, (q_1^M, q_2^M)]$. Therefore, based on the availability of each channel, there are four possible scenarios in $\{\mathbf{Q}_1, \mathbf{Q}_2\}$. They are: 1) the channel is available for both SUs ($q_1^j = q_2^j = 1$); 2) the channel is only available for SU_1 ($q_1^j = 1, q_2^j = 0$); 3) the channel is only available for SU_2 ($q_1^j = 0, q_2^j = 1$); and 4) the channel is unavailable for both SUs ($q_1^j = q_2^j = 0$). We denote the numbers of channels in these four scenarios as $\mathbf{V} = [v_1, v_2, v_3, v_4]$.

We calculate the probability distribution of $v_k, k \in [1, 2, 3, 4]$. We first calculate the probability distribution of v_1. As illustrated in Figure 6.2, sensing ranges are divided into three areas: A_1, A_2, and A_3. Note that PUs in different areas contribute to different channel availability for the two SUs. For instance, if a PU is active within A_3, the channel used by this PU is unavailable for both SUs. However, if a PU is active within A_1, the channel used by this PU is only unavailable for SU_1. Therefore, the probability distribution of v_k is affected by the numbers of active PUs within these three areas. Since v_1 is the number of channels that are available for both SUs, the channels of v_1 cannot be used by any active PU within the union area of the sensing ranges. Define $A^* = A_1 + A_2 + A_3$. Therefore, based on basic geometry, the union area

of the sensing ranges A^* can be obtained as follows:

$$A^* = 2(\pi - \alpha)r_s^2 + d_{12}\sqrt{r_s^2 - \left(\frac{d_{12}}{2}\right)^2}, \tag{6.1}$$

where $\alpha = \cos^{-1}\frac{d_{12}}{2r_s}$. Thus, we need to calculate the number of channels that are not used by any active PU within A^*. The size of the total network area is denoted as A_L (i.e., $A_L = L^2$). Since the locations of PUs are evenly distributed, the probability that p PUs are within A^* is

$$\Pr(p) = \binom{K}{p}\left(\frac{A^*}{A_L}\right)^p\left(\frac{A_L - A^*}{A_L}\right)^{K-p}, \tag{6.2}$$

where $\binom{K}{p}$ represents the total combinations of K choosing p. In addition, we define the probability that a PU is active, ρ, as:

$$\rho = \frac{E[\text{ON duration}]}{E[\text{ON duration}] + E[\text{OFF duration}]}, \tag{6.3}$$

where $E[\cdot]$ represents the expectation of the random variable. Therefore, given that there are p PUs within A^*, the probability that there are b PUs active is

$$\Pr(b|p) = \binom{p}{b}\rho^b(1-\rho)^{p-b}. \tag{6.4}$$

Furthermore, given that there are p PUs and b active PUs within A^*, the probability that there are c channels available for both SUs is denoted as $\Pr(c|p,b)$. Since the number of available channels is only related to the number of active PUs, c is independent of p. In addition, since an active PU randomly selects a channel from M channels in the band, $\Pr(c|p,b)$ is equivalent to the probability that there are exactly c empty boxes given that b distinguishable balls are randomly put into a total of M distinguishable boxes and a box can have more than one ball (because we do not limit

$$\Pr(v_2{=}c){=}\sum_{p=0}^{K}\sum_{b=0}^{p}\sum_{z_s=0}^{b}\sum_{z_1=0}^{z_s}\sum_{u=\min(1,b-z_s)}^{\min(M,b-z_s)}\sum_{w=\min(M-u,M)}^{\max(M-u-z_1,0)}\frac{1}{M^b}\binom{M}{u}\binom{M-u}{w}\binom{w}{c}u!S(z_s{-}z_1,u)$$
$$\sum_{l=l^*}^{u}\binom{u}{l}(M{-}w{-}l)!S(z_1,M{-}u{-}w{-}l)\sum_{k=k^*}^{M-w}\binom{M-u}{k}(M{-}w{+}c{-}k)!S(b{-}z_s,M{-}w{+}c{-}k)$$
$$P_a(z_1,z_s,A_1,A_s)P_a(z_s,b,A_s,A^*)\Pr(b|p)\Pr(p). \tag{6.5}$$

$$\Pr(v_4{=}c){=}\sum_{p=0}^{K}\sum_{b=0}^{p}\sum_{z_s=0}^{b}\sum_{z_1=0}^{z_s}\sum_{u=\min(1,b-z_s)}^{\min(M,b-z_s)}\sum_{w=\min(M-u,M)}^{\max(M-u-z_1,0)}\frac{1}{M^b}\binom{M}{u}\binom{M-u}{w}\binom{w}{c}u!S(z_s{-}z_1,u)$$
$$\sum_{l=l^*}^{u}\binom{u}{l}(M{-}w{-}l)!S(z_1,M{-}u{-}w{-}l)\sum_{k=k^{**}}^{u+w}\binom{u+w}{k}(u{+}w{+}c{-}k)!S(b{-}z_s,u{+}w{+}c{-}k)$$
$$P_a(z_1,z_s,A_1,A_s)P_a(z_s,b,A_s,A^*)\Pr(b|p)\Pr(p). \tag{6.6}$$

---

a channel to only one PU). Thus, $\Pr(c|p,b)$ can be expressed as:

$$\Pr(c|p,b){=}\frac{\binom{M}{c}(M{-}c)!S(b,M{-}c)}{M^b}, c{\in}[\max(0,M{-}b),M], \tag{6.5}$$

where $S(b,M-c)$ is the Stirling number of the second kind. In addition, $S(b,M-c)$ is defined as

$$S(b,M{-}c)=\frac{1}{(M{-}c)!}\sum_{i=0}^{M-c}(-1)^i\binom{M-c}{i}(M{-}c{-}i)^b. \tag{6.6}$$

Hence, the joint probability that there are c available channels and there are p PUs and b active PUs within A^* is the product of (6.2), (6.4), and (5). Thus, the probability mass function (pmf) of v_1 is expressed as

$$\Pr(v_1=c)=\sum_{p=0}^{K}\sum_{b=0}^{p}\Pr(c|p,b)\Pr(b|p)\Pr(p). \tag{6.7}$$

Next, we calculate the probability distribution of v_2. Denote the number of active PUs within a sensing range A_s as z_s. Gven that there are b active PUs within A^*, the probability that there are z_s active PUs within A_s is written as

$$P_a(z_s, b, A_s, A^*) = \binom{b}{z_s} \left(\frac{A_s}{A^*}\right)^{z_s} \left(\frac{A^* - A_s}{A^*}\right)^{b-z_s}. \quad (6.8)$$

In addition, denote the number of active PUs within A_1 as z_1. We can obtain the probability that there are z_1 active PUs within A_1 given z_s active PUs within A_s by $P_a(z_1, z_s, A_1, A_s)$. Thus, the active PUs within A_2 and A_3 can be obtained by $z_2 = b - z_s$ and $z_3 = z_s - z_1$, respectively. We further denote the number of channels used by z_3 as u. Similar to (5), the total number of possible cases is $\binom{M}{u} u! S(z_s - z_1, u)$. Since A_3 is the overlapping area of the two sensing ranges, these u channels used by z_3 PUs cannot be used by either SU_1 or SU_2. Then, denote the number of available channels for SU_1 as w. Given z_1 PUs active within A_1, the total possible cases are $\binom{M-u}{w} \sum_{l=l^*}^{u} \binom{u}{l} (M-w-l)! S(z_1, M-u-w-l)$, where $l^* = \max(0, M-w-z_1)$. Next, given z_2 active PUs within A_2, the total possible cases are $\binom{w}{c} \sum_{k=k^*}^{M-w} \binom{M-u}{k} (M-w+c-k)! S(b-z_s, M-w+c-k)$, where $k^* = \max(0, M+c-w-z_2)$. Therefore, the pmf of v_2 is obtained from (6.5). Since SU_1 and SU_2 are symmetric, the pmf of v_3 can be easily obtained from (6.5) by switching z_1 and z_2.

Using the same derivation method, the pmf of v_4 is obtained from (6.6), where $k^{**} = \max(0, u+w+c-z_2)$. From (6.7) to (6.6), the expectations of v_k, $E[v_k]$, can be derived. Figure 6.3 shows the analytical and simulation results of the expectations of $v_k, k \in [1, 2, 4]$ under different ratios between d_{12} and r_s. It is illustrated that the expectations of v_k changes linearly with the relative distance between the two neighboring nodes. Therefore, it is known that the channel availability between two neighboring nodes is highly related to the relative locations of the two nodes. By using this relationship, the abnormal channel availability caused by the FCIE attack can be detected.

6.2 The Proposed Algorithm to Fight Against FCIE Attacks

In this section, the proposed algorithm to fight against the FCIE attacks is presented. We assume that a malicious node cannot change its channel information

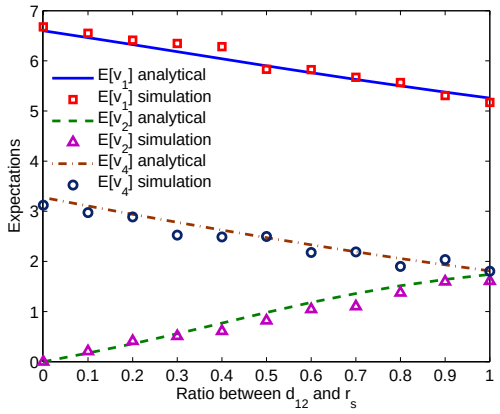

Figure 6.3: The expectations of $v_k, k \in [1, 2, 4]$ under different relative distances between two nodes.

after receiving the legitimate channel information from its neighboring nodes. This assumption can be justified using certain verification protocols. Without loss of generality, for the rest of the chapter, we denote SU_1 as the legitimate node who needs to determine whether a neighboring node is malicious or not. In addition, we denote SU_2 as the node whose integrity is unknown and may report false channel information to SU_1.

6.2.1 The Basic Approach

We first introduce the basic approach in which SU_1 only uses its own channel information to determine whether SU_2 is malicious or not. Since the malicious node does not have the channel information of the legitimate node, it only randomly selects a few channels from the band to deceive the legitimate nodes. Therefore, given the relative locations of the legitimate node and the malicious node, the channel availability between these two nodes should be different from the channel availability relationship between two legitimate nodes. The main idea of the proposed security algorithm is to decide how deflected the channel availability relationship between a legitimate node and a malicious node is, as compared with the authentic channel availability.

Figure 6.4 shows the variance of the sum of v_1 and v_4 under different relative distances between two neighboring nodes. It is observed that when two nodes are

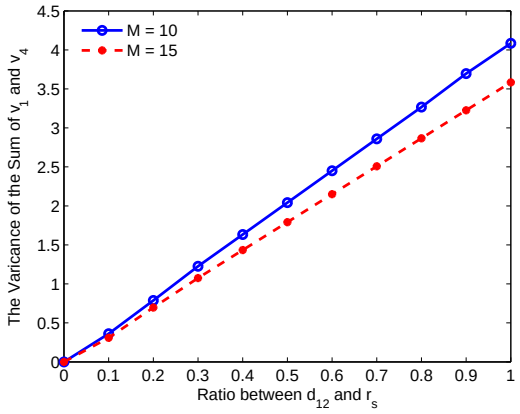

Figure 6.4: The variance of the sum of v_1 and v_4.

close to each other, the variance of the sum of v_1 and v_4 is very small. This means that the sum of v_1 and v_4 is almost invariant when two nodes are close. However, since a malicious node randomly selects channels to deceive, the combined channel availability scenarios can only change either between $(q_1^j=1, q_2^j=1)$ and $(q_1^j=1, q_2^j=0)$, or $(q_1^j=0, q_2^j=1)$ and $(q_1^j=0, q_2^j=0)$. Changes between other channel availability scenarios are not allowed. Thus, as long as the numbers of changes in the above two cases are not exactly the same, either change in the above two cases leads to the change of the sum of v_1 and v_4. Therefore, we can use this information to identify the malicious node.

We assume that the four scenarios of the channel availability between two nodes observed by SU_1 is $\hat{\mathbf{V}} = [\hat{v}_1, \hat{v}_2, \hat{v}_3, \hat{v}_4]$. Given the distance between these two nodes and the probability distribution of v_1 and v_4, the joint probability distribution function can be obtained. Moreover, the expectation and variance of the sum of v_1 and v_4 is denoted as $E[v_1 + v_4]$ and $Var(v_1 + v_4)$. In addition, the Euclidean distance between $\hat{v}_1 + \hat{v}_4$ and $E[v_1 + v_4]$ is defined as

$$\|(\hat{v}_1 + \hat{v}_4) - E[v_1 + v_4]\| = \sqrt{\{(\hat{v}_1 + \hat{v}_4) - E[v_1 + v_4]\}^2}. \tag{6.11}$$

Then, the proposed scheme is formed as a hypothesis test problem given in the fol-

lowing inequality, where H_1 means that SU_2 is a malicious node, H_0 means that SU_2 is a legitimate node, and γ is the threshold to decide whether SU_2 is malicious or not. We further define γ as $\beta\sqrt{Var(v_1 + v_4)}$, where β is a scaling coefficient.

$$\|(\hat{v}_1 + \hat{v}_4) - E[v_1 + v_4]\| \underset{H_0}{\overset{H_1}{\gtrless}} \gamma. \tag{6.12}$$

Therefore, using (6.12), we can determine the legitimacy of SU_2.

6.2.2 The Improved Approach with the Assistance of an Honest Node

Next, we introduce an improved approach with the assistance of another node who is known to be honest. As shown in Figure 6.5, SU_3 is a legitimate node who is a neighboring node of both SU_1 and SU_2. From Figure 3.24(b), it is illustrated that the shaded area is a part of the sensing range of SU_3 which overlaps with the sensing range of SU_2. However, since this area is not covered by the sensing range of SU_1, SU_3 can give SU_1 the channel information on this area. By properly utilizing the channel information of SU_3, the probability of successfully identifying SU_2 can be further improved.

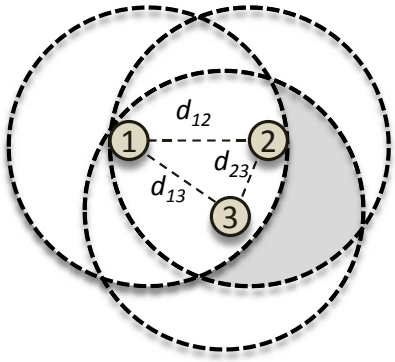

Figure 6.5: Two neighboring SUs whose sensing ranges overlap.

Denote the shaded area shown in Figure 3.24(b) as A_d. Since A_d is also covered by the sensing range of SU_2, the channel information of SU_3 can be used by the improved approach. However, another part of the sensing range of SU_3, denoted as A_f, is not covered by the sensing ranges of either SU_1 or SU_2. Since A_f incurs extra

channel information which cannot be used to improve the credibility of the proposed approach, the channel information of SU_3 is used only when $A_d > A_f$. Then, if SU_3 is used in the improved approach, we consider SU_1 and SU_3 as a combined node whose sensing range is the union of the sensing ranges of these two nodes. The new combined node is denoted as SU_1'. Similar to Section 6.1.2, we further denote the numbers of channel availability between SU_1' and SU_2 in the four scenarios as $\mathbf{V}' = [v_1', v_2', v_3', v_4']$. Then, we need to obtain the probability distribution of these four random variables.

We use the same method in Section 6.1.2 to obtain the probability distribution of $v_k', k \in [1, 2, 3, 4]$. Based on the locations of SU_1' and SU_2, the three new areas A_1', A_2', and A_3' can be obtained. Then, based on (6.7), (6.5) and (6.6), the probability distribution of $v_k', k \in [1, 2, 3, 4]$ is obtained. In addition, the expectation and variance of the sum of v_1' and v_4', $E[v_1' + v_4']$ and $Var(v_1' + v_4')$ can also be acquired.

Denote the vector of channel availability in the four scenarios observed by SU_1' as $\hat{\mathbf{V}}' = [\hat{v}_1', \hat{v}_2', \hat{v}_3', \hat{v}_4']$. Therefore, similar to the basic approach, the detection of a malicious node is formulated as a hypothesis testing problem in

$$\|(\hat{v}_1' + \hat{v}_4') - E[v_1' + v_4']\| \underset{H_0}{\overset{H_1}{\gtrless}} \gamma'. \tag{6.13}$$

where $\|(\hat{v}_1' + \hat{v}_4') - E[v_1' + v_4']\| = \sqrt{\{(\hat{v}_1' + \hat{v}_4') - E[v_1' + v_4']\}^2}$ and $\gamma' = \beta\sqrt{Var(v_1' + v_4')}$.

In addition, if the distance between SU_3 and SU_2 is shorter than the distance between SU_1 and SU_2 (i.e., $d_{23} < d_{12}$), SU_3 has a larger area in its sensing range that overlaps with SU_2 than SU_1. Therefore, SU_1 can directly utilize the channel information of SU_3 as in the basic approach to further improve the probability of identifying the integrity of SU_2.

6.3 Performance Evaluation

In this section, we evaluate the performance of the proposed algorithm to defend against the FCIE attack. The parameters used to obtain the simulation results are

listed in Table 6.1. Malicious nodes are randomly selected from the SU nodes. The major performance metrics considered in this chapter are the detection rate (i.e., the probability that a malicious node is identified) and false alarm rate (i.e., the probability that a legitimate node is incorrectly determined as a malicious node).

Table 6.1: Simulation Parameters

Number of SUs N	10
Number of PUs K	20
Number of channels M	10
Side length of the simulation area L	4 (unit length)
Radius of the sensing range r_s	1 (unit length)
Radius of the transmission rage r_c	1 (unit length)
The probability that a PU is active ρ	0.9
The scaling coefficient β	1

Figure 6.6 shows the detection rate under different numbers of false channels manipulated by the malicious node when the total number of channels M changes. Generally, since additional channel information is used, the improved approach outperforms the basic approach in terms of higher detection rate. In addition, it is shown that, if M is fixed, the detection rate increases when the number of false channels increases. This is because that the channel availability between the two nodes is more deflected if there are more false channels. In addition, the detection rate increases when M increases if the number of false channels is fixed. This is because that when M is large, the randomness of the channel availability decreases. Thus, the creditability of the proposed algorithm improves.

Figure 6.7 shows the false alarm rate of the proposed algorithm under different numbers of channels. It is shown that the false alarm rate increases when the number of channels increases. This is because that, when M is large, the variance of the sum of $v_1 + v_4$ decreases, as shown in Figure 6.4. Then, the threshold of the hypothesis testing problem is low. Thus, the proposed algorithm is more sensitive to the change of the channel availability when M is large, which may incur false detection. However, by increasing the scaling coefficient β, the threshold of the hypothesis testing problem

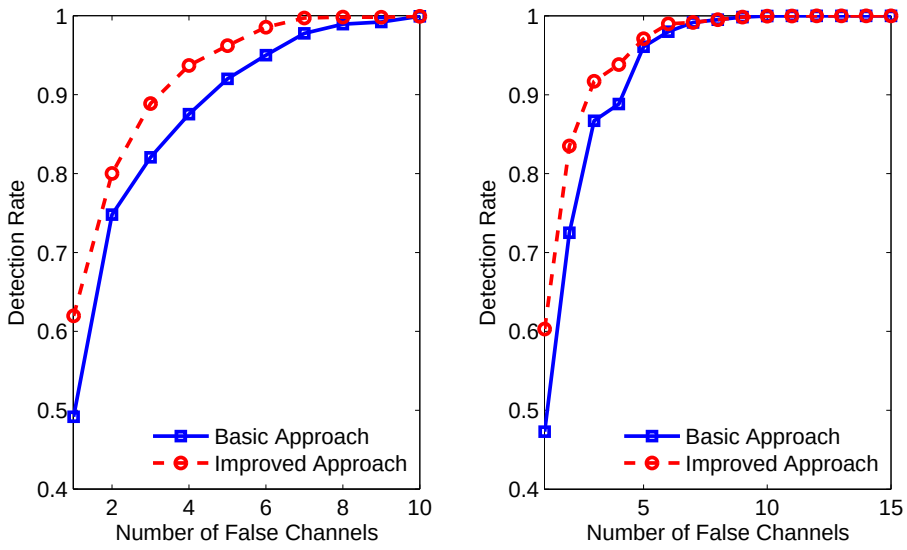

(a) Detection rate when $M = 10$. (b) Detection rate when $M = 15$.

Figure 6.6: Detection rate under different numbers of false channels manipulated by the malicious node.

increases. Hence, the false alarm rate reduces significantly when β is large.

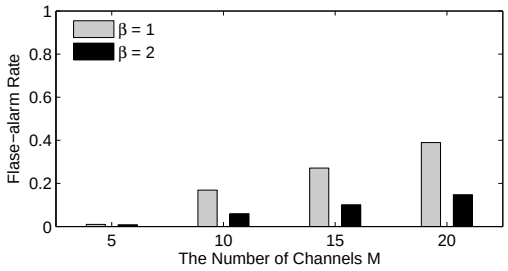

Figure 6.7: The false alarm rate under different numbers of channels.

Figure 6.8 depicts the impact of the scaling coefficient β to the network performance. The threshold of the hypothesis testing problem is affected by this scaling coefficient. From Figure 6.8, it is shown that the difference between the detection rate and the false alarm rate first increases and then decreases when β increases. This is because that there exists a trade-off when the threshold changes. That is, when the threshold is low, the detection rate is high. However, the false alarm rate is also relatively high. On the other hand, when the threshold is high, both the detection rate and the false alarm rate are relatively low. Therefore, by evaluating the differ-

ence between the detection rate and the false alarm rate, an optimal threshold can be obtained.

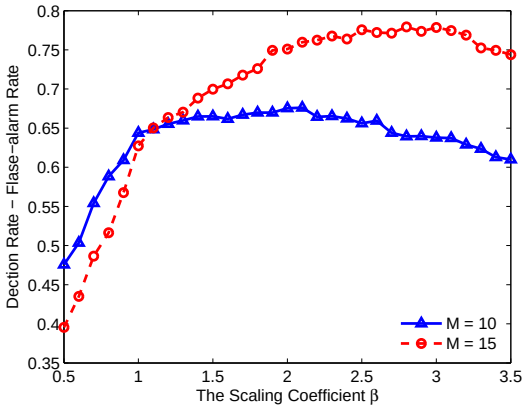

Figure 6.8: The impact of the scaling coefficient β with different M.

CHAPTER 7: SPECTRUM HANDOFF PROTOCOLS IN CRAHNS

In this chapter, a proactive spectrum handoff framework is presented. In the proposed proactive spectrum handoff framework, SUs predict the future channel availability status and perform spectrum switching and RF reconfiguration before a PU occupies the channel based on observed channel usage statistics. In addition, a distributed channel selection scheme is proposed in the multi-user scenario to avoid collisions when multiple pairs of SUs perform spectrum handoffs simultaneously.

7.1 Network Coordination and Assumptions

In this section, we first describe the decentralized network coordination schemes we consider in this research. Based on the number of users making link agreements simultaneously, we define two types of network coordination schemes called single rendezvous coordination scheme (i.e., only one pair of SUs can exchange control information and establish a link at one time) and multiple rendezvous coordination scheme (i.e., multiple pairs of SUs can use different channels to exchange control information and establish multiple links at the same time). Then, the network assumptions made in this chapter are introduced.

7.1.1 Single Rendezvous Coordination Scheme

Throughout this section, we consider a network scenario where N SUs form a CR ad hoc network and opportunistically access M orthogonal licensed channels. For the single rendezvous coordination scheme, we use Common Hopping as the channel coordination scheme [42]. Figure 7.1 illustrates the operations of Common Hopping, under which the channels are time-slotted and SUs communicate with each other in a synchronous manner. This is similar to the frequency hopping technique used in

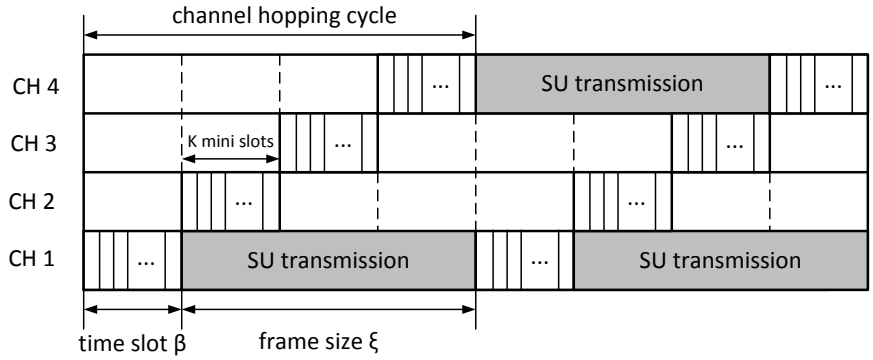

Figure 7.1: An example of the single rendezvous coordination scheme.

Bluetooth [113]. When no packet needs to be transmitted, all the SU devices hop through channels using the same hopping sequence (e.g., the hopping pattern cycles through channels $1, 2, \cdots, M$). The length of a time slot (i.e., the dwelling time on each channel during hopping) is denoted as β. In order to cooperate with the channel selection algorithm proposed in Chapter 7.3, a time slot is further divided into N mini slots, as shown in Figure 7.1. If a SU wants to initiate a transmission, it first generates a pseudo-random sequence of length N (which is explained in detail in Chapter 7.3) and sends a request-to-send (RTS) packet in the corresponding mini slot based on the sequence, if no other RTS is heard before this mini slot. Then, after the SU transmitter successfully receives a clear-to-send (CTS) packet from the receiver, they pause the channel hopping and remain on the same channel for data transmissions, while other non-transmitting SUs continue hopping. After the data being successfully transmitted, the SU pair rejoins the channel hopping.

7.1.2 Multiple Rendezvous Coordination Scheme

Unlike in the single rendezvous coordination scheme that only one pair of SUs can make an agreement in one time slot, in the multiple rendezvous coordination scheme, multiple SU pairs can make agreements simultaneously on different channels. A typical example of this type of coordination schemes is McMAC [114]. Figure 7.2 depicts the operations of McMAC. Instead of using the same channel hopping

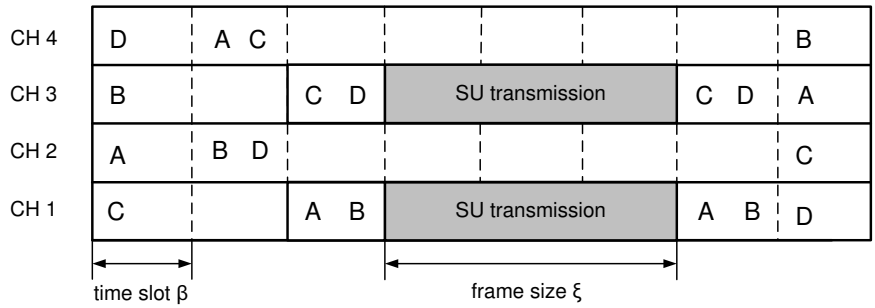

Figure 7.2: An example of the multiple rendezvous coordination scheme.

sequence for all SUs, in McMAC, each SU generates a distinct pseudo-random hopping sequence (in Figire 7.2, the channel hopping sequence for user A is 2-4-1-3, and for user B is 3-2-1-4, etc.). When a SU is idle, it follows its default hopping sequence to hop through the channels. Similar to the single rendezvous coordination scheme, each time slot is also divided into N mini slots (they are not shown in Figure 7.2). If a SU intends to send data to a receiver, it temporarily tunes to the current channel of the receiver (i.e., in Figure 7.2, SUs AB and CD are two transmitting pairs that intend to initiate new transmissions at the same time). Then, it generates a pseudo-random sequence and sends a RTS packet in its corresponding mini slot, if no other RTS is heard before this mini slot. If the receiver replies with a CTS, both the transmitter and the receiver stop channel hopping and start a data transmission on the same channel. When they finish the data transmission, they resume to their default channel hopping sequences. Similar to [114], in this chapter, we consider the scenario where SUs are aware of each other's channel hopping sequences.

In this chapter, we assume that stringent time synchronization among SUs for channel hopping can be achieved without the need to exchange control messages on a CCC in both cases. We consider a synchronization scheme similar to the one used in [114] that every SU includes a time stamp in every packet it sends. Then, a SU transmitter obtains the clock information of the intended SU receiver by listening to the corresponding channel and estimates the rate of clock drift to realize time

synchronization. Various schemes have been proposed to calculate the rate of clock drift for synchronization [115]. The design of efficient synchronization mechanisms without a CCC to realize single rendezvous and multiple rendezvous coordination schemes is out of the scope of this research.

In both types of coordination schemes, we assume that any SU data packet is transmitted at the beginning of a time slot and ends at the end of a time slot. This implies that the length of a SU data packet, δ, is a multiple of the time slot. This assumption is commonly used in time-slotted systems [116][117][118]. We further define that a SU data packet is segmented into frames and each frame contains c time slots. The length of a frame is denoted as ξ, so $\xi = c\beta$. As shown in Figure 7.1, at the end of a frame, the two SUs can either rejoin the channel hopping when a data transmission ends, or start another data transmission by exchanging RTS/CTS packets.

In this research, we model each licensed channel as an ON-OFF process [60][119]. As shown in Figure 7.3, each rectangle represents a PU data packet being transmitted on a channel (i.e., the ON period) and the other blank areas represent the idle periods (i.e., the OFF period). The length of a rectangle indicates the packet length of a PU data packet. Therefore, a SU can only utilize a channel when no PU transmits at the same time. In Figure 7.3, t_0 represents the finishing moment of the last sensed PU packet. Thus, for the i-th channel at any future time t ($t > t_0$), the status of the channel is denoted as $N_i(t)$ which is a binary random variable with values 0 and 1 representing the idle and the busy state, respectively.

Due to the fact that the power of a transmitted signal is much higher than the power of the received signal in wireless medium, instantaneous collision detection is not possible for wireless nodes. Thus, we assume that if a SU frame collides with a PU packet, the wasted frame can only be retransmitted at the end of the frame. In addition, in our proposed spectrum handoff protocol, we assume that each SU is

equipped with two radios. One is used for data and control message transmission, namely the transmitting radio. The other is applied to scan all the channels in the band and to obtain the channel occupancy information, namely the scanning radio. The scanning radio has two major functions for the proposed protocol: 1) observe the channel usage and store the channel statistics in the memory for future channel availability prediction and 2) confirm that the newly selected channel is idle for SU transmissions.

7.2 Proposed Proactive Spectrum Handoff Protocol

In this section, we first propose the spectrum handoff criteria and policies that a CR transmitting pair is required to follow. Then, the details of the proposed spectrum handoff protocol are presented.

7.2.1 Proposed Spectrum Handoff Criteria and Policies

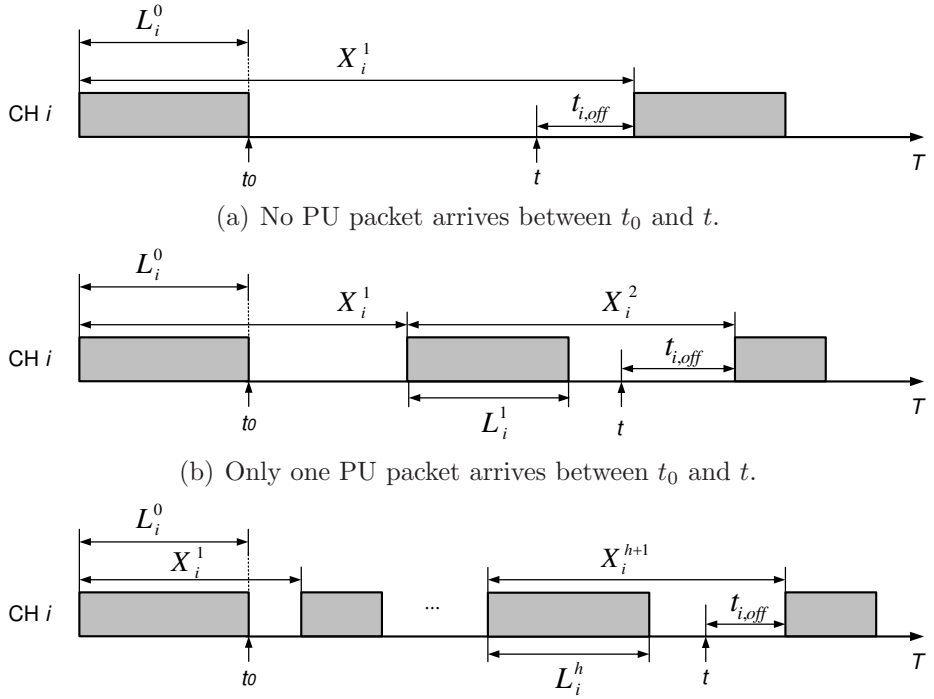

(a) No PU packet arrives between t_0 and t.

(b) Only one PU packet arrives between t_0 and t.

(c) h PU packets arrive between t_0 and t.

Figure 7.3: The PU activity on channel i.

By utilizing the sensed channel usage statistics, a SU can make predictions of

the channel availability before the current transmission frame ends. Based on the prediction, the SU decides whether to stay in the present channel, or switch to a new channel, or stop the on-going transmission. We propose two criteria for determining whether a spectrum handoff should occur: 1) the predicted probability that the current and a candidate channel (i.e., a channel that can be selected for continuing the current data transmission) is busy or idle and 2) the expected length of the channel idle period. Based on these criteria, we design spectrum handoff policies.

Figure 7.3 shows the PU traffic activity on channel i, where X_i^k and T_i^k represent the inter-arrival time and arrival time of the k-th packet, respectively. As shown in Figure 7.3(a), the probability that channel i is idle given that no PU packet arrives between t_0 and t is given by

$$\Pr(N_i(t) = 0) = \Pr(X_i^1 > t + L_i^0), \tag{7.1}$$

where L_i^k denotes the length of the k-th PU data packet on channel i. As shown in Figure 7.3(b), the probability that channel i is idle given that only one PU packet arrives between t_0 and t is given by

$$\Pr(N_i(t)=0)=\Pr(X_i^1+L_i^1<t+L_i^0)\Pr(X_i^1+X_i^2>t+L_i^0). \tag{7.2}$$

Similarly, in Figure 7.3(c), the probability that channel i is idle given that h ($h \in [1, U]$) PU packets arrive, where U is the maximum number of PU packets that could arrive between t_0 and t, is

$$\Pr(N_i(t)=0)=\Pr(\sum_{k=1}^{h}X_i^k+L_i^h<t+L_i^0)\Pr(\sum_{k=1}^{h+1}X_i^k>t+L_i^0). \tag{7.3}$$

Therefore, the probability that channel i is idle at time t can be obtained by (7.4),

which is shown in the next page.

$$\Pr(N_i(t)=0)=\Pr(X_i^1>t+L_i^0)+\sum_{h=1}^{U}\left[\Pr(\sum_{k=1}^{h}X_i^k+L_i^h<t+L_i^0)\Pr(\sum_{k=1}^{h+1}X_i^k>t+L_i^0))\right] \tag{7.4}$$

$$\Pr(t_{i,off}>\eta|N_i(t)=0)=\frac{\Pr(X_i^1>t+L_i^0+\eta)+\sum_{h=1}^{U}\left[\Pr(\sum_{k=1}^{h}X_i^k+L_i^h<t+L_i^0)\Pr(\sum_{k=1}^{h+1}X_i^k>t+L_i^0+\eta))\right]}{\Pr(X_i^1>t+L_i^0)+\sum_{h=1}^{U}\left[\Pr(\sum_{k=1}^{h}X_i^k+L_i^h<t+L_i^0)\Pr(\sum_{k=1}^{h+1}X_i^k>t+L_i^0))\right]} \tag{7.5}$$

Let t_{off} represent the duration from t to the beginning of the next PU packet, as shown in Figure 7.3. Following the same derivation, for channel i, the probability that the duration of idleness is longer than η given that the channel is idle at t is obtained by (7.5), where η is the length of a frame plus a time slot (i.e., $\eta = \xi + \beta$).

Thus, if the PU traffic model is known and the channel statistics (e.g., PU packet arrival rate, PU packet length) are obtained from the scanning radio, the predicted probabilities can be calculated. Hence, based on the above prediction, the policy that a SU should switch to a new channel is:

$$\Pr(N_i(t)=0)<\tau_L, \tag{7.6}$$

where τ_L is the probability threshold below which a channel is considered to be busy and the SU needs to carry out a spectrum handoff, that is, the current channel is no longer considered to be idle at the end of the frame transmission. In addition, the policies that a channel j becomes a candidate channel at time t are:

$$\begin{cases} \Pr(N_j(t)=0)\geq\tau_H \\ \Pr(t_{j,off}>\eta|N_i(t)=0)\geq\theta, \end{cases} \tag{7.7}$$

where τ_H is the probability threshold for a channel to be considered idle at the end of the current frame and θ is the probability threshold for a channel to be considered idle for the next frame transmission. The second criterion in (7.7) means that, in order

to support at least one SU frame, the probability that the duration of the idleness of channel j to be longer than a frame size must be higher than or equal to θ.

According to Figure 7.3 and (7.13), we calculate the spectrum handoff criteria proposed in Chapter 7.2. We denote the finishing moment of the last PU packet as 0 and the future time as slot n. Hence, the probability that channel i is idle given that no PU arrival occurs between slot 1 and n is given by

$$P_0 = 1 - \sum_{i=1}^{n} x(1-x)^{(i-1)}, \tag{7.8}$$

where x is the normalized arrival rate. As shown in Figure 7.3(b), the probability that channel i is idle given that only one PU packet arrives between slot 1 and n is

$$P_1 = \sum_{m=1}^{n-L} \left[1 - \sum_{i=1}^{n-m-L+1} x(1-x)^{(i-1)} \right] x(1-x)^{(m-1)}, \tag{7.9}$$

where m is the time slot at which a PU transmission starts and L is the length of a PU packet. Similarly, in Figure 7.3(c), the probability that channel i is idle given that h PU packets arrive between slot 1 and n is

$$P_h = \sum_{m_h=h}^{n-hL} \left[1 - \sum_{i=1}^{n-m_h-hL+1} x(1-x)^{(i-1)} \right] x^h (1-x)^{(m_h-h)}. \tag{7.10}$$

Therefore, the total probability that channel i is idle at slot n is obtained as follows:

$$\Pr(N_i(n) = 0) = \sum_{i=0}^{U} P_i. \tag{7.11}$$

Secondly, due to the memoryless property of geometric distribution, the probability that the duration of the idleness is longer than η slots on channel i is given by

$$P(t_{off} > \eta | N_i(n) = 0) = 1 - \sum_{i=1}^{\eta} x(1-x)^{(i-1)}. \tag{7.12}$$

7.2.2 Proposed Spectrum Handoff Protocol Details

The proposed spectrum handoff protocol is based on the above proposed spectrum handoff policies. It consists of two parts. The first part, namely Protocol 1, describes how a SU pair initiates a new transmission. Regardless of the coordination schemes used during channel hopping, if a data packet arrives at a SU, the SU predicts the availability of the next hopping channel (in the single rendezvous coordination scheme case) or the hopping channel of the receiver (in the multiple rendezvous coordination scheme case) at the beginning of the next slot. Based on the prediction results, if the channel satisfies the policies in (7.7) for data transmissions, the channel is considered available. Then, the SU transmitter generates a pseudo-random sequence and sends a RTS packet on the same hopping channel during the corresponding mini slot for this SU in the next time slot, if no other RTS is heard before this mini slot. Upon receiving the RTS packet, the intended SU receiver replies a CTS packet in the same mini slot. Then, if the CTS packet is successfully received by the SU transmitter, the two SUs pause the channel hopping and start the data transmission on the same channel in the next time slot. Note that if more than one pair of SUs contend the same hopping channel for new data transmissions, only the SU pair who exchange the RTS/CTS packets first claims the channel, as described in Appendix A. Hence, no RTS collision will occur. The following is the pseudo code of the protocol for initiating a new transmission, where DAT is the flag for data transmission requests, DSF is the data sending flag, t is the beginning of the next slot, and k is the next hopping channel in the single rendezvous coordination scheme or the hopping channel for the receiver in the multiple rendezvous coordination scheme.

Algorithm 1: Proposed algorithm to initiate a new transmission. Register initiation: DAT:=0, DSF:=0;

if a new data packet needs to be transmitted

DAT := 1;

end if

if DAT=1

predicting $\Pr(N_k(t) = 0)$, $\Pr(t_{off} > \eta | N_k(t) = 0)$;

end if

if $\Pr(N_k(t) = 0) \geq \tau_H$ AND $\Pr(t_{off} > \eta | N_k(t) = 0) \geq \theta$

generating a pseudo-random sequence;

else wait for the next time slot;

end if

if no RTS is heard before the corresponding mini slot

sending RTS;

else wait for the next time slot;

end if

upon receiving CTS then

DSF := 1;

if DSF=1

DSF := 0;

transmitting a data frame;

DAT := 0 when transmission ends;

end if

The second part, namely Protocol 2, is on the proactive spectrum handoff during a SU transmission. Figure 7.4 illustrates the operations of Protocol 2. The goal of our proposed protocol is to determine whether the SU transmitting pair needs to carry out a spectrum handoff and then switch to a new channel by the time a frame transmission ends. Using the proposed protocol, the SU transmitting pair can avoid disruptions with PUs when PUs appear. The following is the pseudo code of the protocol for the proactive spectrum handoff, where CSW is the channel switching

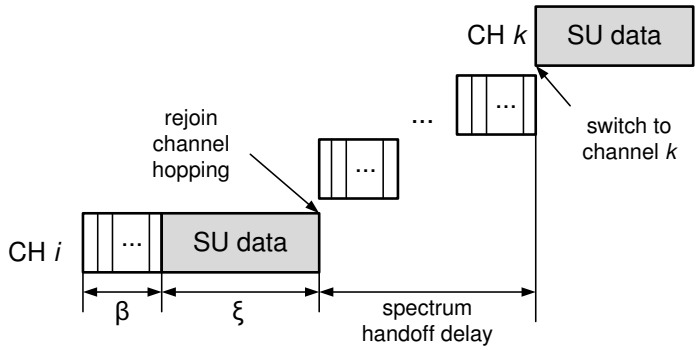

Figure 7.4: Proposed proactive spectrum handoff protocol.

flag, NUC and LSC are the number and the list of the candidate channels for data transmissions, respectively, and channel i is the current channel. As similar in Protocol 1, DAT is the flag for data transmission requests and DSF is the data-sending flag.

Algorithm 2: Proposed proactive spectrum handoff protocol Register initiation: CSW:=0, DSF:=0, NUC:=0, LSC:=$\emptyset$;

for $j := 0, j \leq M$ do

predicting $\Pr(N_j(t) = 0)$, $\Pr(t_{off} > \eta | N_k(t) = 0)$;

end for

if $\Pr(N_i(t) = 0) < \tau_L$ AND DAT=1

CSW := 1;

end if

if CSW=1

for $k := 0, k \leq M$ do

if $\Pr(N_k(t) = 0) \geq \tau_H$ AND $\Pr(t_{off} > \eta | N_k(t) = 0) \geq \theta$

NUC := NUC+1;

LSC(NUC) := k;

end if

end for

end if

if LSC=$\emptyset$

wait for the next time slot;

elseif LSC $\neq \emptyset$

generating a pseudo-random sequence;

broadcast channel availability information;

end if

upon receiving channel availability information then

switching to the selected channel;

starting the scanning radio;

if channel is busy

wait for the next time slot;

else DSF := 1 CSW:=0;

end if

if DSF=1

DSF := 0;

transmitting a data frame;

DAT := 0 when transmission ends;

end if

Based on the sensed channel usage information, a SU transmitter checks the spectrum handoff policy in (7.6) for the current channel by predicting the channel availability at the end of the frame. If the policy is not satisfied, this means that the current channel is still available for the next frame transmission. Then, the SU transmitting pair does not perform a spectrum handoff and keeps staying on the same channel. However, if the policy is satisfied, the channel-switching (CSW) flag is set, that is, the current channel is considered to be busy during the next frame time and the SUs need to perform a spectrum handoff by the end of the frame to avoid harmful interference to a PU who may use the current channel. After the CSW is set, the two

SUs rejoin the channel hopping in the next time slot after the previous frame.

In the proposed distributed channel selection algorithm (which is explained in detail in Chapter 7.3), the SUs that need to perform spectrum handoffs at the same time are required to update the predicted channel availability information with each other on the same channel. Note that in the single rendezvous coordination scheme, all SUs that do not transmit data follow the same hopping sequence. Therefore, when the CSW flag is set, the SUs that need to perform spectrum handoffs pause the current transmissions and resume the channel hopping with the same sequence, so they will hop to the same channel. However, in the multiple rendezvous coordination scheme, each SU follows a default hopping sequence which may not be the same as other's hopping sequences. In order to be able to exchange channel availability information among SUs on the same channel, in our proposed protocol, SUs are required to follow the same hopping sequence only when performing spectrum handoffs.

On the other hand, the SU transmitter checks the criteria in (7.7) for available handoff candidate channels in the band. If no channel is available, then the on-going transmission stops immediately at the end of the frame. The two SUs hop to the next channel for one more time slot and check the channel availability based on the criteria in (7.7) at the beginning of the next time slot for both the single rendezvous and the multiple rendezvous coordination schemes. However, if the set of the handoff candidate channels is not empty, the SU transmitter triggers a distributed channel selection algorithm (which is explained in detail in Chapter IV) in the next time slot. Using the proposed channel selection algorithm, both the SU transmitter and receiver can compute the target channel if it is available. Then, both SU nodes switch to the target channel and start the data transmission for the next frame.

Note that there is a possibility that the prediction is not correct and a PU is on the channel which the SUs switch to. Hence, at the beginning of the frame, the SU transmitting pair restarts the scanning radio to confirm that the selected channel

is idle. If the channel is sensed busy, the two SUs immediately rejoin the channel hopping and wait for the next time slot for spectrum handoffs.

7.3 Distributed Channel Selection Algorithm

In this section, we present the details of our proposed distributed channel selection algorithm. We define the spectrum handoff delay as the duration from the moment a SU starts to perform a spectrum handoff to the moment it resumes the data transmission, as shown in Figure 7.4.

7.3.1 Procedure of the Proposed Channel Selection Algorithm

As explained in Chapter 1, the channel selection issue should be handled with caution to avoid collisions among SUs. On one hand, preventing SU collisions is more important in the spectrum handoff scenario than in general channel allocation scenarios [71] due to the fact that collisions among SUs lead to data transmission failures, thus they may result in long spectrum handoff delay, which has deteriorating effect on delay-sensitive network applications. Additionally, the channel selection algorithm also should be executed fast in order to achieve short handoff delay. Furthermore, since no centralized network entity exists in CR ad hoc networks to manage the spectrum allocation, the channel selection algorithm should be applied in a distributed manner to prevent SU collisions.

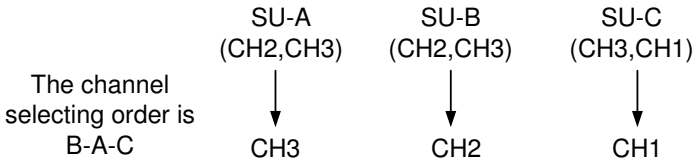

Figure 7.5: An example of the proposed channel selection scheme.

Our goal is to design a channel selection scheme for the spectrum handoff scenario in CR ad hoc networks that can eliminate collisions among SUs in a distributed fashion. Figure 7.5 describes an example of the proposed channel selection scheme, where three SUs, A, B, and C, perform spectrum handoffs at the same time. In the

parenthesis, the candidate channels are ordered based on the criterion for channel selection (e.g., the probability that a channel is idle). The proposed channel selection procedure is summarized as follows:

Step 1 Pseudo-random Sequence Generation: At each time slot, a pseudo-random channel selecting sequence with a length of N is generated locally that all SU transmitters who need to initiate new transmissions and who are involved in spectrum handoffs should follow. In Figure 7.5, the channel selecting sequence for all SUs is *B-A-C*. Since the sequence is generated with the same seed (e.g., the time stamp), every SU generates the same channel selecting sequence at the same time slot. However, the selecting sequences are different at different time slots.

Step 2 Channel Information Update: For both the single rendezvous coordination scheme and the multiple rendezvous coordination scheme, all SUs follow the same sequence to hop through the channels during a spectrum handoff. When a SU needs to perform a spectrum handoff at the beginning of a time slot, it broadcasts the sensed channel availability information to neighboring SU nodes on the current hopping channel only in the corresponding mini slot based on the selecting sequence generated in Step 1. In addition, for the SU transmitter who needs to initiate a new transmission, it sends a RTS in the corresponding mini slot. Thus, the channel information messages and RTS packets do not collide with each other. Since every SU may have different neighbors and may not receive the channel information from all SUs involved in the spectrum handoffs, each SU is required to broadcast its own channel information with its previously received channel information from other SUs. Therefore, a SU can obtain the channel availability information predicted by the SUs who need to perform spectrum handoffs and whose orders of broadcast are earlier than this SU.

Step 3 Channel Selection: Every SU pair who needs to perform a spectrum handoff computes the target handoff channel for its spectrum handoff based on the selecting sequence and the criterion for channel selection. The pseudo code of the algorithm

for computing the target channel is presented in Algorithm 3, where C_i denotes the target handoff channel for SU_i. In the example shown in Figure 7.5, based on the selecting sequence, SU-B selects the first channel (i.e., channel 2) in its available channel list. Other SUs know that SU-B will select channel 2 based on the channel selecting sequence and the obtained channel availability information from SU-B, so they delete channel 2 in their available channel lists. Then, SU-A selects channel 3, and so on so forth. Therefore, for each SU, the proposed channel selection algorithm terminates until an available channel is selected or all available channels are depleted. If the target channel exists, then the SU pair selects it to resume its data transmission; otherwise, the SU pair waits for the next time slot to perform the spectrum handoff. Since the selecting sequence and the channel availability information of each SU are known to every SU who perform spectrum handoffs at the same time, the target channel for each SU (i.e., $C_k, k \in [1, N]$) is also known. Thus, the collision among SUs can be avoided.

Algorithm 3: Proposed distributed channel selection algorithm Input: Selecting sequence s, the list of candidate channels $l_n, n \in [1, N]$.

Output: target channel C_k.

for $i := 1, i \leq N$ do

if $s(i) \neq k$ then

if $l_{s(i)}$ is received directly from SU $s(i)$ then

if $l_{s(i)} = \emptyset$ then

$C_{s(i)} := NULL$;

else if $l_{s(i)} \neq \emptyset$ then

$C_{s(i)} := \arg\max_{j \in l_{s(i)}}(\Pr(N_j(t) = 0))$;

end if

end if

for $m := i + 1, m \leq N$ do

if $C_{s(i)} \in l_{s(m)}$ then

$l_{s(m)} := l_{s(m)} - C_{s(i)}$;

end if

end for

else if $s(i) = k$ then

if $l_k = \emptyset$ then

return $C_k := NULL$; break;

else if $l_k \neq \emptyset$ then

return $C_k := \arg\max_{j \in l_k}(\Pr(N_j(t) = 0))$; break;

end if

end if

end for

7.3.2 Fairness of the Proposed Channel Selection Algorithm

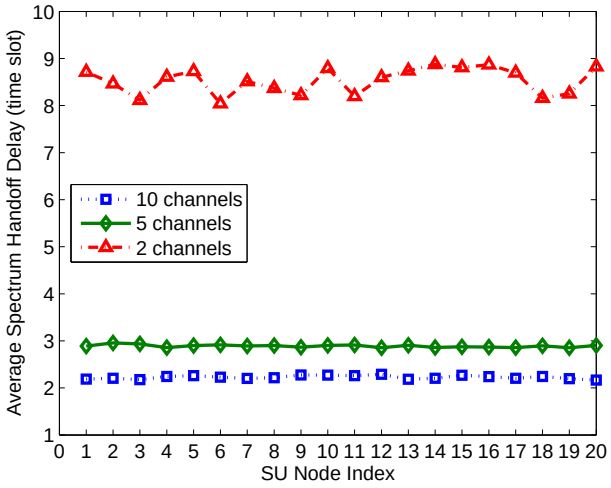

Figure 7.6: Fairness of the proposed channel selection scheme.

The above procedure shows that our proposed channel selection scheme can avoid collisions among SUs during spectrum handoffs and it is a fully distributed algorithm. In addition, from the above discussion, we observe that an important feature of the proposed distributed channel selection scheme is fairness. Unlike the previous

definition of fairness as equal channel capacity for every user [71], in this research, we define fairness as equal average handoff delay for every SU. This is because that, from the network performance point of view, handoff delay is the most important metric to evaluate a spectrum handoff protocol. Thus, letting every SU have equal average handoff delay is fair.

7.3.3 Scalability of the Proposed Channel Selection Algorithm

For CR ad hoc networks where nodes membership may change over time, an important issue is the scalability of the proposed channel selection algorithm when the network size increases. Even though the number of SUs in a network may vary, as illustrated in Algorithm 3, only those SUs who are involved in the spectrum handoff process at the same time will activate the algorithm, which may not be a large number. In addition, from the number of broadcasted messages during the second step of the proposed channel selection scheme, our proposed channel selection algorithm will not result in excessive overhead when the network size increases.

Since the number of channel information message updates affects the spectrum handoff delay (i.e., more channel information messages updated results in longer spectrum handoff delay), Figure 7.7 shows the simulation result of the average spectrum handoff delay under different network sizes. It is shown that when the network size changes from 10 SU pairs to 40 SU pairs (i.e., the network size increases 300%), the spectrum handoff delay only increases 14.5%, 16%, and 105% for the cases when the number of channels is 10, 5, and 2, respectively.

7.4 Performance Evaluation

In this section, we evaluate the performance of the proposed proactive spectrum handoff protocol and the proposed distributed channel selection scheme in various network scenarios.

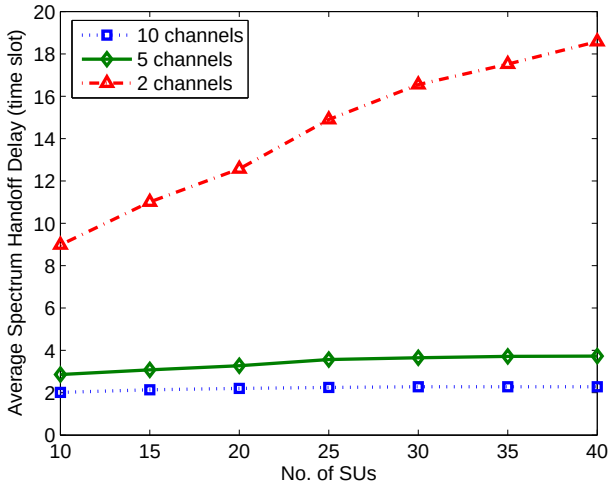

Figure 7.7: Scalability of the proposed channel selection scheme.

7.4.1 Simulation Setup

The parameters used to obtain the simulation results are listed in Table 7.1. The channel parameters are chosen based on the IEEE 802.11 frequency hopping spread spectrum (FHSS) system [120]. The lengths of SU packets and PU packets are fixed in the simulation. We adopt two types of PU traffic models in the simulation. The first PU traffic model is a time slotted system, where the inter-arrival time X follows the biased-geometric distribution whose probability mass function (pmf) is given by [90]:

$$\Pr(X=d) = \begin{cases} 0 & d < l \\ \lambda_n(1-\lambda_n)^{(d-l)} & d \geq l, \end{cases} \tag{7.13}$$

where d is the number of time slots between packet arrivals, $l \geq 0$ represents the minimum number of time slots between two adjacent packets, and λ_n is the probability that a packet arrives during one time slot (i.e., λ_n is the normalized arrival rate of data packets, that is, $\lambda_n = \lambda_p \beta$, where λ_p is the PU packet arrival rate in terms of packets/second). Based on this model, if we set l as the packet length, then a new packet will not be generated until the previous packet finishes its transmission.

The second PU traffic model we consider is Pareto traffic, where the cumulative

distribution function (CDF) of the inter-arrival time X is given by [90]:

$$F_X(x) = \begin{cases} 1 - \left(\frac{a}{x}\right)^b & x \geq a \\ 0 & x < a, \end{cases} \tag{7.14}$$

where $a = L_{min}$, $b = \frac{1}{1-\lambda_p a}$, and L_{min} is the minimum PU packet length sensed by SUs [90]. The distinctive differences between Pareto traffic and biased-geometric traffic are that the PU packet inter-arrival time of Pareto traffic is heavy-tailed and it does not possess the memoryless property. Therefore, the derivations of the spectrum handoff criteria under biased-geometric and Pareto PU traffic are different and given in Appendix C and D, respectively.

Table 7.1: Simulation Parameters

Channel bit rate	2Mbps
Time slot	2ms
Mini slot	0.264ms
RTS	288 bits
CTS	240 bits
Length of a SU packet	12×10^5 bits
Length of a PU packet	2×10^5 bits
Simulation time	40s

7.4.2 Spectrum Handoff Criteria for Biased-Geometric Traffic

According to Figure 7.3 and (7.13), we calculate the spectrum handoff criteria. We denote the finishing moment of the last PU packet as n_0 and the future time as slot n. Hence, the probability that channel i is idle and no PU arrival occurs between slot n_0+1 and n is given by

$$P_0 = 1 - \sum_{i=1}^{n-n_0} \lambda_n (1-\lambda_n)^{(i-1)}, \tag{7.15}$$

where λ_n is the normalized arrival rate. As shown in Figure 7.3(b), the probability that channel i is idle and only one PU packet arrives between slot n_0+1 and n is

$$P_1 = \sum_{m=1}^{n-n_0-L} \left[1 - \sum_{i=1}^{n-n_0-m-L+1} \lambda_n (1-\lambda_n)^{(i-1)} \right] \lambda_n (1-\lambda_n)^{(m-1)}, \tag{7.16}$$

where m is the time slot at which a PU transmission starts and L is the length of a PU packet. Similarly, in Figure 7.3(c), the probability that channel i is idle and h PU packets arrive between slot n_0+1 and n is

$$P_h = \sum_{m_h=h}^{n-n_0-hL} \left[1 - \sum_{i=1}^{n-n_0-m_h-hL+1} \lambda_n (1-\lambda_n)^{(i-1)} \right] \lambda_n^h (1-\lambda_n)^{(m_h-h)}. \tag{7.17}$$

Therefore, the total probability that channel i is idle at slot n is obtained as follows:

$$\Pr(N_i(n) = 0) = \sum_{i=0}^{U} P_i. \tag{7.18}$$

Secondly, due to the memoryless property of the geometric distribution, the probability that the duration of the idleness is longer than η slots on channel i is given by

$$\Pr(t_{i,off} > \eta | N_i(n) = 0) = 1 - \sum_{i=1}^{\eta} \lambda_n (1-\lambda_n)^{(i-1)}. \tag{7.19}$$

7.4.3 Spectrum Handoff Criteria for Pareto Traffic

We follow the exact derivation procedure to calculate the spectrum handoff criteria of Pareto traffic. It is noted in (7.4) and (7.5) that the key is to obtain the expression of the distribution of the sum of W Pareto random variables (i.e., $V = \sum_{i=1}^{W} X_i$). In [121], the authors proved that, when $a = 1$, $0 < b < 2$ and $b \neq 1$, the CDF of V is given by

$$\Pr(\sum_{i=1}^{W} X_i > x) = \frac{-1}{\pi} \sum_{j=1}^{W} \binom{W}{j} (-\Gamma(1-b))^j \sin(\pi b j) \sum_{m=0}^{\infty} \frac{C_{W-j,m} \Gamma(m+bj)}{x^{(m+bj)}}, \tag{7.20}$$

where $\Gamma(\cdot)$ is the Gamma function and $C_{W-j,m}$ is the m-th coefficient in the series expansion of the $(W-j)$-th power of the confluent hyper-geometric function.

Therefore, the probability that channel i is idle and the probability that the duration of the idleness is longer than a frame size can be obtained by (7.4) and (7.5) if a is normalized to one and b is carefully selected.

7.4.4 The Proposed Proactive Spectrum Handoff Scheme

We first compare the proposed proactive spectrum handoff scheme with the reactive spectrum handoff approach. In the reactive spectrum handoff approach, a SU transmits a packet without predicting the availability of the current channel at the moment when a frame ends (i.e., using the policy in (7.6)). That is, a SU does not change the current channel by the end of a frame if the previous frame is successfully received. A spectrum handoff occurs only if the on-going transmission actually collides with a PU transmission and the collided SU frame needs to be retransmitted. We choose the average SU throughput (i.e., the successfully transmitted data per unit time) and collision rate (i.e., the number of collisions between SUs and PUs per SU packet transmitted) as the performance metrics.

In order to conduct a fair comparison, we assume that channel prediction is a capability of SUs (i.e., SUs can select candidate channels based on the policy in (7.7) in both schemes). Therefore, the only difference between the proposed proactive spectrum handoff scheme and the reactive spectrum handoff scheme is the mechanism to trigger the spectrum handoffs. In addition, in order to solely investigate the performance of the two spectrum handoff schemes, we adopt a general random channel selection scheme (i.e., a SU randomly selects a channel from its candidate channels) in both schemes.

Figure 7.8 and Figure 7.9 illustrate the performance results of the two spectrum handoff schemes under different PU traffic models, when the network coordination scheme is the single rendezvous coordination scheme, where there are 10 SU pairs

and 10 channels in the network. For biased-geometric PU traffic, the prediction thresholds are set to be $\tau_L = \tau_H = 0.6$ and $\theta = 0.8$. As shown in Figure 7.8(a), under biased-geometric PU traffic, when both SU traffic and PU traffic are light (e.g., λ_s=20 packets/second and λ_p=0.5 packets/second), the SU throughput is similar in both schemes. This is because when the traffic is light, collisions between SUs and PUs are much fewer than the case when the traffic is heavy. SUs have less probability of retransmitting a packet in both cases, thus the performance difference between the proactive spectrum handoff scheme and the reactive spectrum handoff scheme is not very obvious. However, when the SU and PU traffic are heavy (e.g., λ_s=100 packets/second and λ_p=10 packets/second), the proactive spectrum handoff scheme outperforms the reactive scheme in terms of 30% higher throughput. From Figure 7.8(b), it is shown that the collision rate using the proposed proactive scheme is always lower than using the reactive scheme.

For Pareto PU traffic, the prediction thresholds are set to be $\tau_L = \tau_H = \theta = 0.5$. To investigate the impact of Pareto PU traffic to the network performance, we use the Hurst index to indicate the burstiness of the traffic. The Hurst index H corresponding to the Pareto distribution [90] is defined as:

$$H = \frac{3 - b}{2}. \tag{7.21}$$

We set the PU packet arrival rate λ_p to be fixed at 10 packets/second. Thus, H is a function of L_{min}. As shown in Figure 7.9, the proposed proactive spectrum handoff scheme outperforms the reactive spectrum handoff scheme in terms of higher throughput and lower collision rate. In addition, even when $H \rightarrow 1$ and the primary traffic exhibits high burstiness (i.e., PU packets tend to arrive intensely in a short period of time while in some other periods of time, the PU arrival rate is fairly low), the proposed proactive scheme still performs better than the reactive scheme.

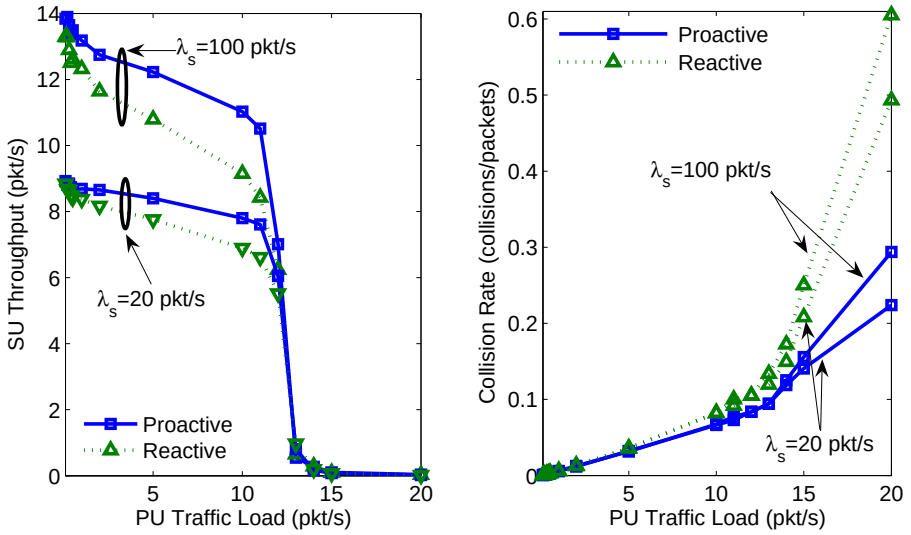

(a) Average SU throughput. (b) Collision rate.

Figure 7.8: Network performance results under biased-geometric PU traffic.

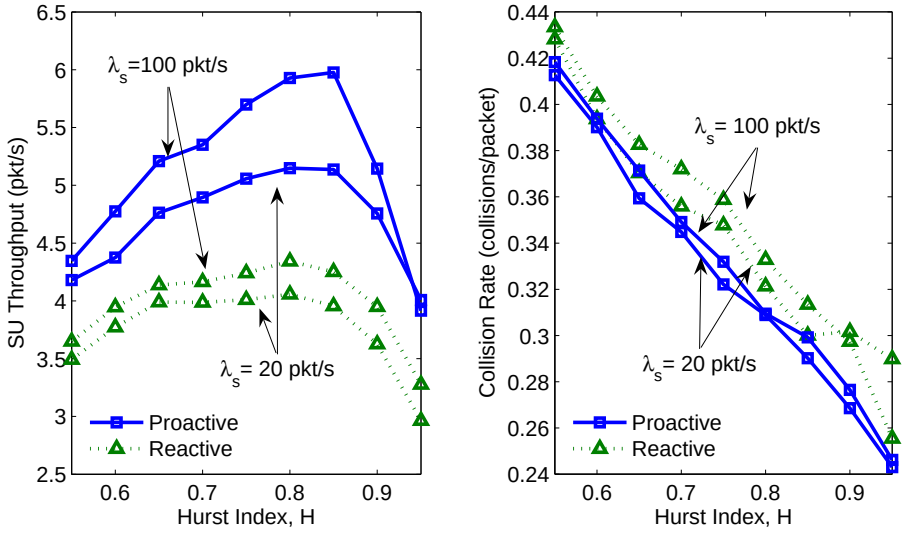

(a) Average SU throughput. (b) Collision rate.

Figure 7.9: Network performance results under Pareto PU traffic.

The Effect of Practical Scanning Radios: Now, we consider more practical scanning radios. We assume that only one channel can be sensed at a time and the duration of spectrum sensing per channel is not negligible and is denoted as t_s. Thus, it takes a scanning radio $M \times t_s$ time to sense the whole band. Since this practical scanning radio cannot provide the most updated channel information of all channels,

the sensing results (e.g., PU arrival rate and PU packet length) of some channels may be outdated, especially when the behavior of PU traffic varies significantly between the last sensing of a channel and the prediction moment. These outdated sensing results may lead to inaccurate prediction of the channel status $N_i(t)$ and channel idleness duration $t_{i,off}$.

Figure 7.10 shows the simulation results of the proposed proactive spectrum handoff scheme and the reactive spectrum handoff scheme under ideal sensing (i.e., all channels can be sensed simultaneously) and practical sensing when $t_s = 0.1$ second. We apply a periodic PU traffic model (i.e., the PU traffic changes between 10 packets/second and 30 packet/second every 10 seconds, i.e., every 0.5×10^4 time slots). It is observed that even though the practical sensing radio is applied, the proposed proactive scheme still outperforms the reactive scheme in terms of higher throughput and lower collision rate. Note that the accumulated throughput using the reactive scheme under practical sensing without channel prediction is higher than using the proposed proactive scheme by approximately 18%. This is because when practical sensing is applied, the channel prediction results might not be accurate. Thus, the number of available channels based on this inaccurate prediction is less than the actual number of available channels in the band. Hence, the reactive scheme without prediction yields higher throughput. However, from Figure 7.10(b), we can see that the collision rate using the reactive scheme without prediction is much higher than using the proposed proactive scheme by approximately 120%. Considering this trade-off, the reactive scheme is not applicable.

The Effect of Network Coordination Schemes: In order to conduct a comprehensive comparison, besides the single rendezvous coordination and multiple rendezvous coordination schemes considered in the chapter, we also investigate the following two scenarios: 1) the network coordination is implemented with a CCC (i.e., SUs send control messages through an out-of-band CCC to establish links), and 2) no network

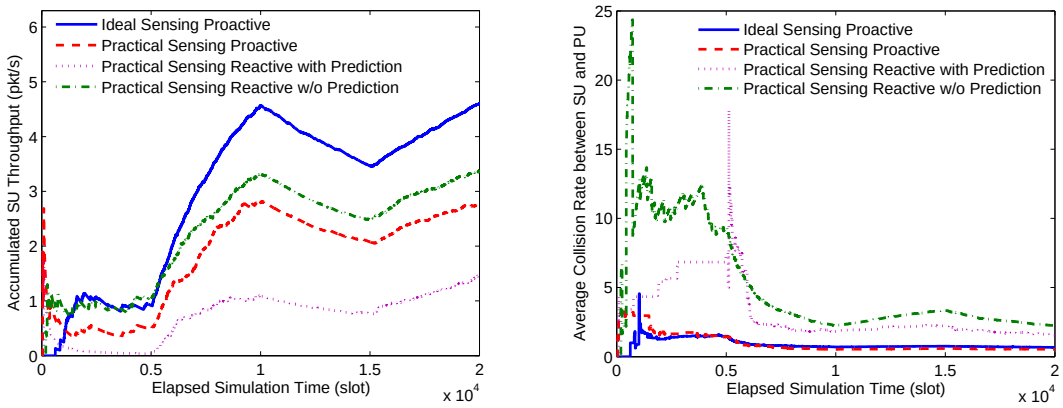

(a) Accumulated SU throughput.

(b) Average collision rate.

Figure 7.10: Simulation results under ideal and practical scanning.

coordination scheme is used (i.e., a SU transmitter randomly selects a channel to send out a RTS without informing the receiver the channel information). To study how long a link between two nodes can be established, we introduce a new performance metric: rendezvous time. Rendezvous time is defined as the duration from the moment a data transmission request is generated at a SU transmitter to the moment a link for that data transmission request is established.

Figure 7.11 shows the simulation results of the networks using different network coordination schemes with varying SU traffic load under the proposed proactive spectrum handoff scheme and the general random channel selection scheme. The PU traffic load is fixed at 10 packets/second. There are totally 10 SU pairs and 10 channels in the network. Figure 7.11(a) shows that the SU throughput without network coordination is the lowest among the four networks. This is because that without coordination, a SU transmitter randomly selects a channel to send out a RTS regardless of the current channel of the receiver. There is a high possibility that the intended receiver is not on the same channel through which the transmitter sends data. Thus, if a CTS is not received by the SU transmitter, it needs to randomly select a channel and send a RTS again until a CTS is received, which leads to low throughput. For the other three cases, the throughput with CCC is always the highest because the

control channel is always available, while in the single and multiple rendezvous coordination schemes, the channels to which SUs hop may not be available due to the existence of PUs. Thus, the rendezvous time is longer (shown in Figure 7.11(b)) than the rendezvous time with CCC, which results in lower throughput. Therefore, from Figure 7.11, we observe that network coordination is crucial to the performance of a CR network. Additionally, the performance of the multiple rendezvous coordination scheme is close to the performance of the network using CCC.

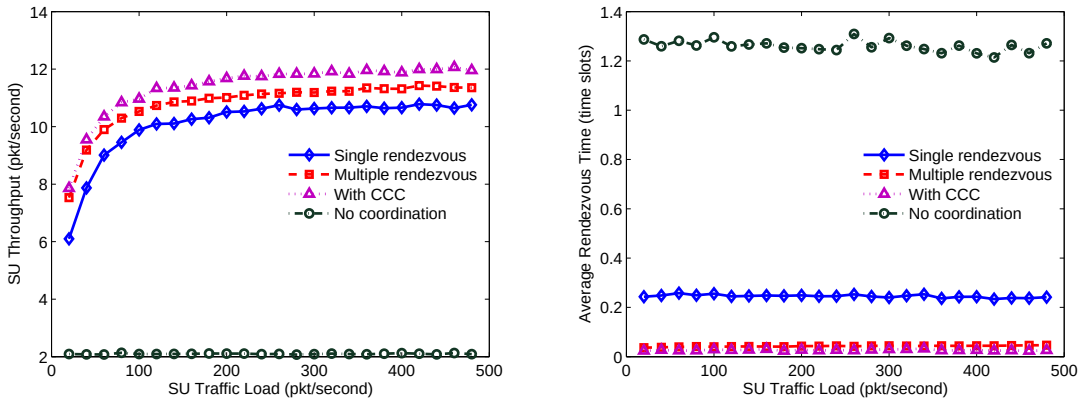

(a) SU throughput. (b) Average rendezvous time.

Figure 7.11: Simulation results of the networks under different network coordination schemes.

The Effect of Prediction Thresholds: Figure 7.12 shows the performance results under varying prediction thresholds, τ_H, τ_L, and θ. It is observed that there exists a trade-off in selecting the prediction thresholds. From Figure 7.12(a) and 7.12(c), when the thresholds are small, the probability that the conditions in (7.7) are satisfied is high. Thus, the number of available channels for spectrum handoff is large and the throughput is high. However, the confidence level of the prediction is low. Therefore, the collision rate is high, shown in Figure 7.12(b) and 7.12(d). On the other hand, when the thresholds are large, the number of available channels becomes fairly small. Hence, the SU throughput is low. Therefore, based on certain design requirements, proper prediction thresholds should be selected.

The Effect of Spectrum Sensing Errors: Figure 7.13 shows the effect of spectrum

sensing errors on the performance of different spectrum handoff schemes using the single rendezvous coordination scheme. We use a coefficient χ to indicate the level of imperfect spectrum sensing, where $\chi \in [0, 1]$ represents the probability that the result of spectrum sensing is wrong (the spectrum sensing errors include both miss detection and false alarm [122]). When $\chi = 0$, it means that the spectrum sensing is perfect and there is no error, whereas when $\chi = 1$, it means that the spectrum sensing is completely incorrect. It is shown in Figure 7.13 that the SU performance becomes worse as χ increases. However, when χ is small, the proposed proactive spectrum handoff scheme still outperforms the reactive spectrum handoff scheme in terms of higher throughput and lower collision rate.

7.4.5 The Proposed Distributed Channel Selection Scheme

To investigate the performance of the proposed distributed channel selection scheme, we compare it with the following three different channel selection methods under the proposed proactive spectrum handoff scenario using the single rendezvous coordination scheme:

1) Random channel selection: A SU randomly chooses a channel from its predicted available channels. 2) Greedy channel selection: In this method, only one pair of SUs is considered in the network. The SUs can obtain all the channel usage information and predict the service time on each channel. Thus, when a spectrum handoff occurs, a SU selects a pre-determined channel that leads to the minimum service time [55]. 3) Local bargaining: In this method, SUs form a local group to achieve a collision-free channel assignment. To make an agreement among SUs, a four-way handshake is needed between neighbors (i.e., request, acknowledgment, action, and acknowledgment). Since one of the SUs is the initiating node which serves as a group header, the total number of control messages exchanged is $2N_{LB}$, where N_{LB} is the number of SUs need to perform spectrum handoffs [71]. Since for channel selection schemes, reducing the number of collisions among SUs is the primary goal, we consider the

SU throughput, average SU service time (i.e., the duration from the moment a SU starts a data transmission to the moment it finishes the data transmission), number of collisions among SUs, and average spectrum handoff delay as the performance metrics.

One-pair-SU Scenario: Figure 7.14(a) and Figure 7.14(b) show the SU throughput and the average service time of different channel selection schemes in a one-pair-SU scenario, respectively. Because only one pair of SUs exists in the network, there is no collision among SUs. Thus, in this scenario, the greedy channel selection scheme performs the best among all the schemes. This is because that the handoff target channel a SU transmitter selects is pre-determined based on channel observation history. Hence, no signaling message is needed between the SU transmitting pair. While in other schemes, the SU transmitter needs to inform the receiver about the newly selected channel. Thus, the throughput is lower and the average service time is longer than the greedy scheme. However, among the three schemes other than the greedy scheme, our proposed channel selection scheme has the best performance in terms of higher throughput and shorter total service time.

Multiple-pair-SU Scenario: Figure 7.15(a) and Figure 7.15(b) show the SU throughput and the average service time of different channel selection schemes in a 10-pair-SU scenario, respectively. In the greedy channel selection method, all pairs of SUs always select the same pre-determined channel for spectrum handoffs. Therefore, the greedy method always leads to collisions among SUs. The throughput of SUs using the greedy method is almost zero. Because the proposed channel selection scheme can totally eliminate collisions among SUs, the throughput is higher and the average service time is shorter than the other channel selection schemes. In addition, as shown in Figure 7.15(a), when the PU traffic load is larger than 12 packets/second, the SU throughput under the greedy channel selection method is zero due to constant collisions among SUs. Thus, the average service time is infinite under the same

circumstance. Hence, the result of SU service time is only shown until when the PU traffic load is 12 packets/second in Figure 7.15(b).

Figure 7.16(a) and Figure 7.16(b) show the performance under different number of SUs, when there are 10 channels and the SU and PU traffic load is 500 packets/second and 10 packets/second, respectively. In Figure 7.16(a), we only show the performance of the local bargaining method, random channel selection, and the proposed channel selection. We exclude the greedy method because the greedy method constantly achieves zero throughput. Thus, its average service time is meaningless. As shown in the Figure 7.16(a), the proposed channel selection scheme constantly achieves the highest throughput. This is because that the random channel selection scheme cannot eliminate collisions among SUs during spectrum handoffs. Additionally, in the local bargaining method, all SUs involved need to broadcast signaling messages twice in order to obtain a collision-free channel assignment, which leads to longer spectrum handoff delay and lower throughput. Additionally, as shown in Figure 7.16(b), the greedy method and the random channel selection method cause more collisions among SUs, while the local bargaining method and the proposed channel selection method can eliminate collisions. On the other hand, the local bargaining method causes much longer average spectrum handoff delay than the proposed channel selection scheme, as shown in Figure 7.16(c). Therefore, the proposed channel selection scheme is the most suitable one for spectrum handoff scenarios.

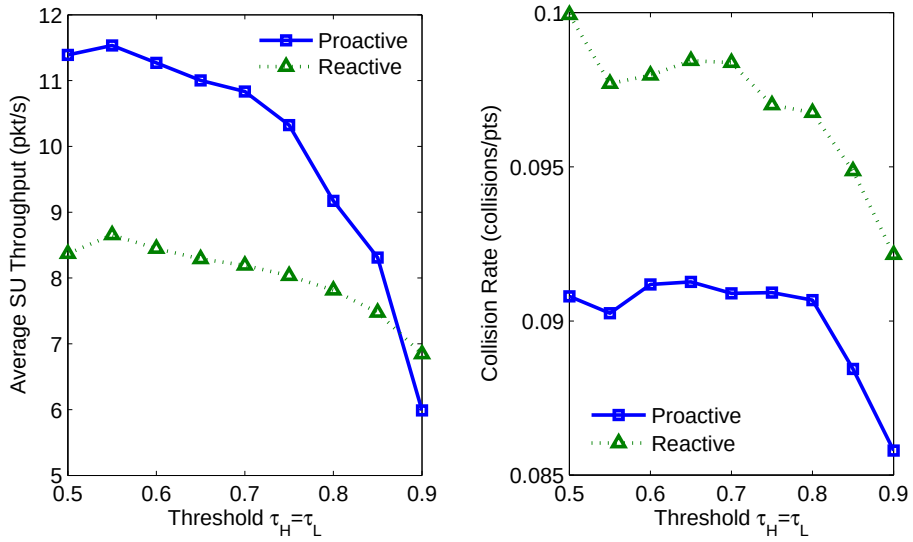

(a) Average SU throughput. (b) Collision Rate.

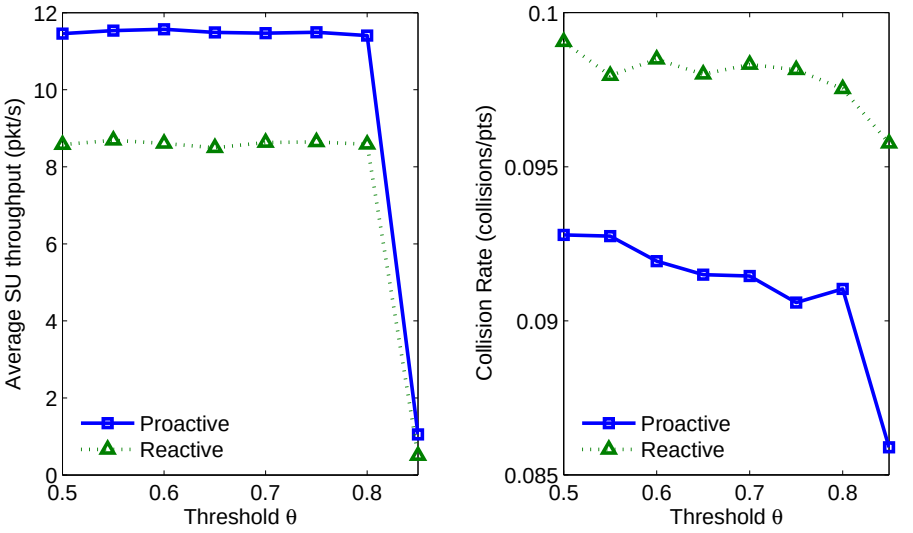

(c) Average SU throughput. (d) Collision Rate.

Figure 7.12: Performance results under varying thresholds.

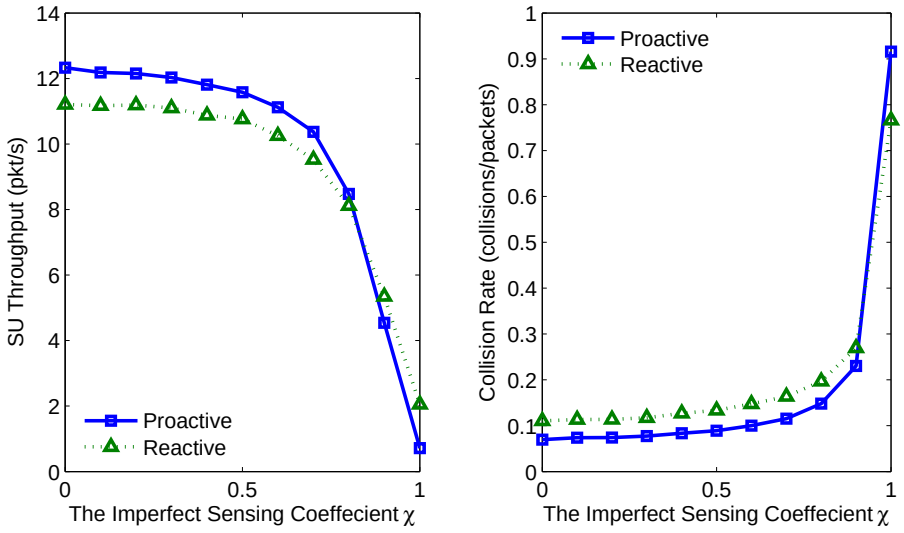

(a) SU throughput. (b) Collision rate.

Figure 7.13: Performance comparison under imperfect spectrum sensing.

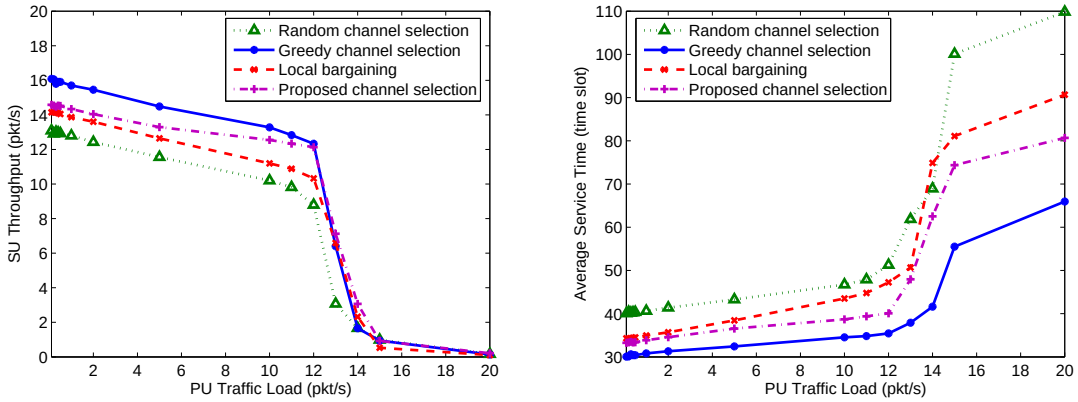

(a) SU throughput. (b) SU average service time.

Figure 7.14: Performance of the channel selection schemes in a one-pair-SU scenario.

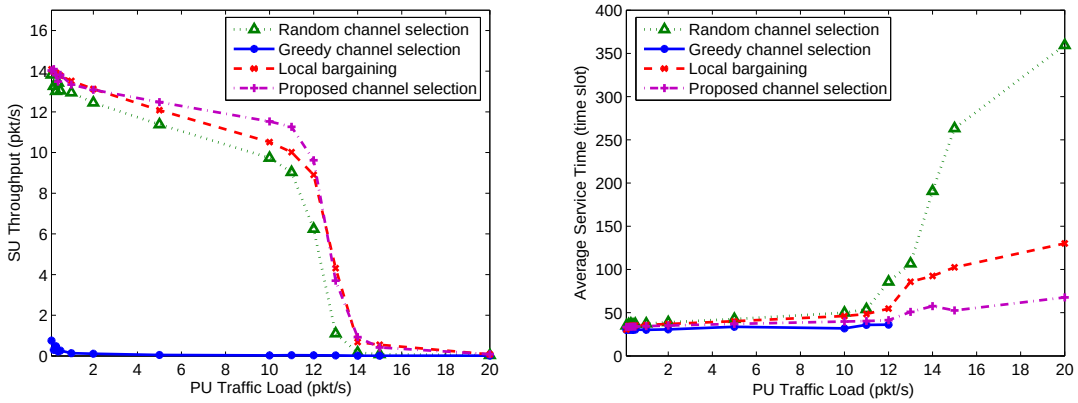

(a) SU throughput. (b) SU average service time.

Figure 7.15: Performance of the channel selection schemes in a 10-pair-SU scenario.

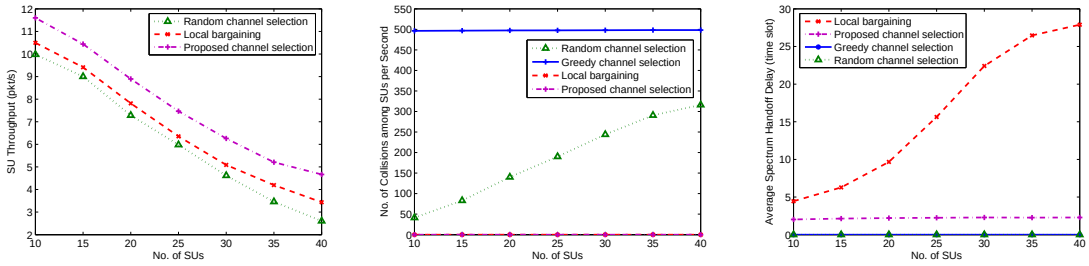

(a) SU throughput.

(b) Number of collisions among SUs per second.

(c) Average spectrum handoff delay.

Figure 7.16: Performance of the channel selection schemes in a multiple-pair-SU scenario under varying number of SUs.

CHAPTER 8: ANALYSIS ON SPECTRUM HANDOFFS IN CRAHNS

In this chapter, we propose an analytical model to analyze the spectrum handoffs in CRAHNs. We assume that any SU data packet is transmitted at the beginning of a time slot and ends at the end of a time slot. This implies that the length of a SU packet is a multiple of a time slot. This assumption is commonly used in time-slotted systems [123][117][124]. We further define that a SU packet is segmented into frames and each frame contains c time slots. At the end of a frame, the two SUs can either rejoin the channel hopping when a data transmission ends, or start another frame by exchanging RTS/CTS packets on the same channel. Therefore, if a SU packet collides with a PU packet, only the collided frame will be retransmitted while the successfully received frames will not be retransmitted. Thus, the probability of successfully transmitting a whole packet is improved.

8.1 Spectrum Handoff Process

Figure 8.1 shows an example of a spectrum handoff process considered in this chapter in a three-channel scenario. Before a data transmission starts, SUs hop through the channels following the same frequency-hopping sequence. Once a successful RTS/CTS handshake between a SU transmitter and its receiver takes place, the two SUs pause the channel hopping and start the data transmission. If a PU packet transmission starts in the middle of a SU transmission, the transmitter cannot instantaneously detect the collision. Thus, the SU transmitting pair will know the successful transmission or collided transmission till the end of the frame (e.g., the transmitter does not receive the acknowledgment (ACK) from the receiver). Then, the two SUs resume the channel hopping for coordination until they find another idle channel for the retransmission of the previously unsuccessful frame. On the other

hand, if a SU frame does not collide with a PU packet, the SU transmitter continues to transmit the next frame on the same channel until all frames have been successfully transmitted.

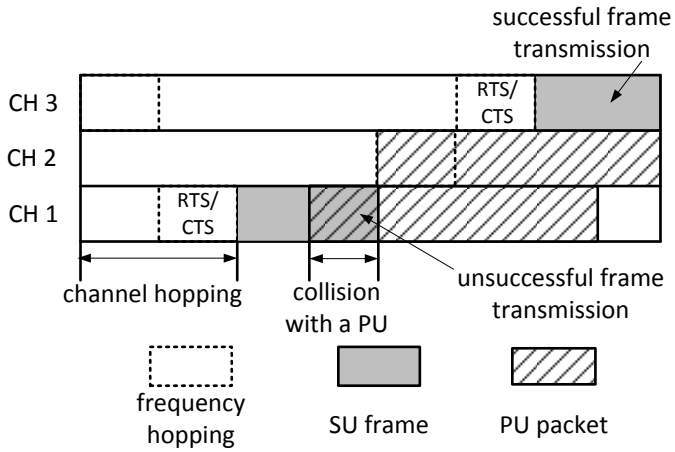

Figure 8.1: An example of the spectrum handoff process.

8.2 The Proposed Three Dimensional Discrete-time Markov Model

In this section, we develop a Markov model to analyze the performance of the spectrum handoff process. For simplicity, we assume the same number of neighbors per SU, which permits us to focus on any SU to analyze the performance. We ignore the propagation delay or any processing time in our analysis. We also assume that the destination of any data packet from a SU transmitter is always available, that is, the probability that the selected SU receiver is not busy is one.

8.2.1 The Proposed Markov Model

Based on the time slotted channels, any action of a SU can only be taken at the beginning of a time slot. In addition, the status of a SU in the current time slot only relies on its immediate past time slot. Such discrete-time characteristics allow us to model the status of a SU using Markov chain analysis. From Figure 8.1, the status of a SU in a time slot can only be one of the following: 1. Idle: no packet arrives at a SU. 2. Transmitting: the transmission of a SU does not collide with PU packets in a time slot, i.e., successful transmission. 3. Collided: the transmission of a SU collides

with PU packets in a time slot, i.e., unsuccessful transmission. 4. Backlogged: a SU has a packet to transmit in the buffer but fails to access a channel. Note that there are two cases that a SU can be in the Backlogged status. In the first case, when a SU pair initiates a new transmission, if multiple SU pairs select the same channel for transmissions, a collision among SUs occurs and no SU pair can access the channel. Thus, the packet is backlogged. Similarly, in the second case, when a SU pair performs a spectrum handoff, if multiple SU pairs select the same channel, a collision among SUs occurs and the frame in each SU is also backlogged.

As mentioned in Chapter 1, we consider the scenario that when a collision between a SU and PU happens, the overlapping of a SU frame and a PU packet is not negligible. Thus, the number of time slots that a SU frame collides with a PU packet is an important parameter to the performance of SUs. Based on the above analysis, the state of the proposed Markov model at time slot t is defined by a vector $(N_t(t), N_c(t), N_f(t))$, where $N_t(t), N_c(t),$ and $N_f(t)$ denote the number of time slots including the current slot that are successfully transmitted in the current frame, the number of time slots including the current slot that are collided with a PU packet in the current frame, and the number of frames that have been successfully transmitted plus the current frame that is in the middle of a transmission at time slot t, respectively. Therefore, $N_t(t)+N_c(t) \leq c$. Figure 8.2 shows the state transition diagram of our proposed three dimensional Markov chain. There are totally $(h+1)$ tiers in the state transition diagram. For each tier, it is a two dimensional Markov chain with a fixed $N_f(t)$. Table 8.1 summarizes the notations used in our Markov model.

Table 8.1: Notations Used in the Markov Analysis

Symbol	Definition
p	Probability that a PU packet arrives in a time slot
s	Probability that a SU packet arrives in a time slot
h	Number of frames in a SU packet
c	Number of time slots in a frame
q	Probability of a collision among SUs
u	Probability that at least one channel is idle

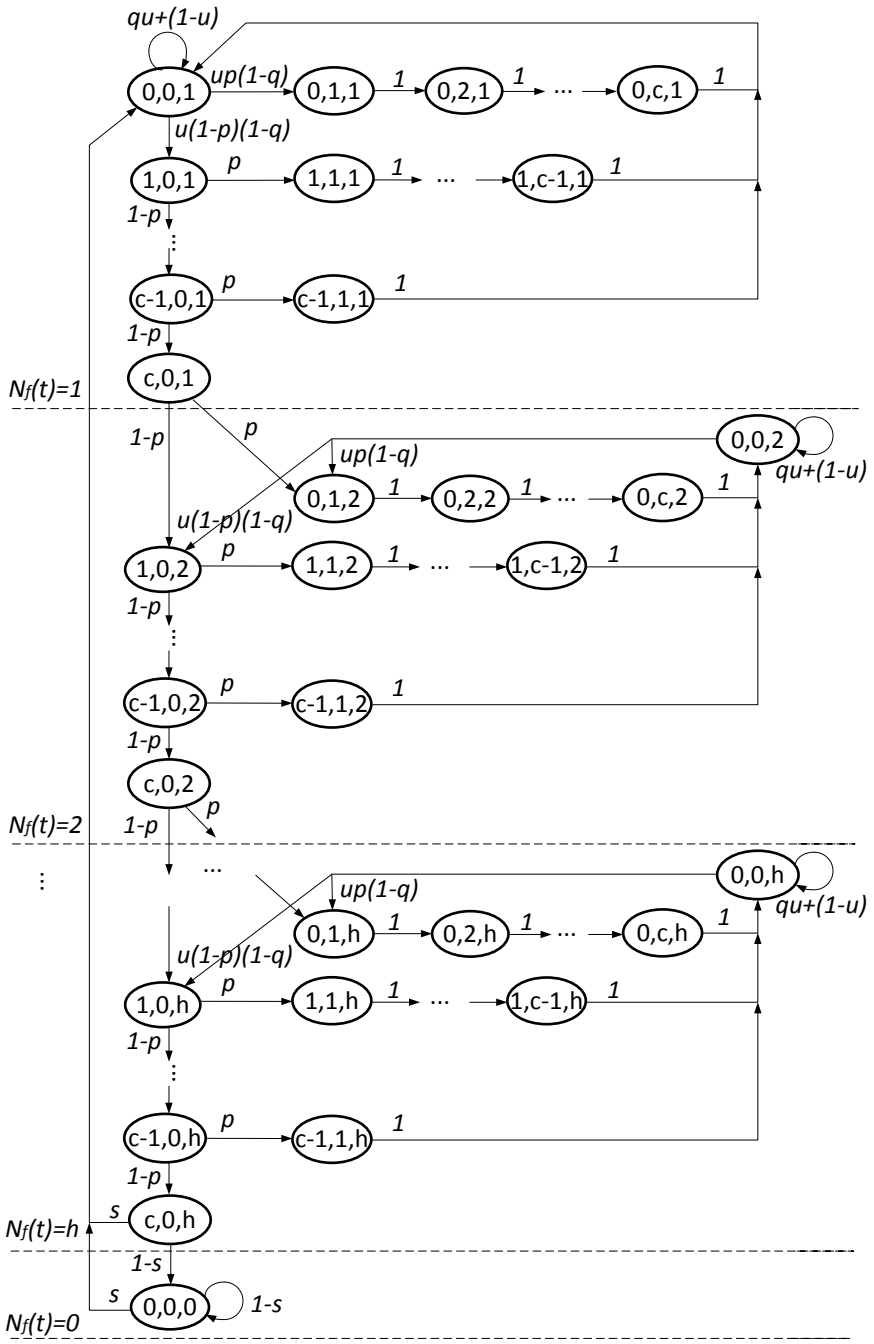

Figure 8.2: The transition diagram of the proposed Markov model.

From Figure 8.2, it is observed that the proposed Markov model accurately capture the status of a SU in a time slot. The state $(N_t(t)=0, N_c(t)=0, N_f(t)=0)$ in Figure 8.2 represents that a SU is in the $Idle$ status. Similarly, the states $(N_t(t) \in [1, c], N_c(t) = 0, N_f(t) \in [1, h])$ represent the $Transmitting$ status, i.e., no collision. The states

($N_t(t) \in [0, c-1], N_c(t) \in [1, c], N_f(t) \in [1, h]$) represent the *Collided* status. At last, the states ($N_t(t)$=0, $N_c(t)$=0, $N_f(t) \in [1, h]$) represent the *Backlogged* status, where ($N_t(t)$=0, $N_c(t)$=0, $N_f(t)$=1) is the Backlogged status during a new transmission. As shown in Figure 8.2, the feature of the common frequency-hopping sequence scheme is captured in our model that a SU can only start a new transmission when there is a channel available. In the following discussion, we use the terms "states" in our proposed Markov model and the "status" of a SU in a time slot interchangeably. We also use the notations ($N_t(t+1)$=i, $N_c(t+1)$=j, $N_f(t+1)$=k) and (i, j, k) to represent a state interchangeably.

8.2.2 Derivation of Steady-State Probabilities

To obtain the steady-state probabilities of the states in the three dimensional Markov chain shown in Figure 8.2, we first get the one-step state transition probability. We denote the one-step state transition probability from time slot t to $t+1$ as $P(i_1, j_1, k_1|i_0, j_0, k_0)$=$P(N_t(t+1)$=$i_1, N_c(t+1)$=$j_1, N_f(t+1)$=$k_1|N_t(t)$=$i_0, N_c(t)$=$j_0, N_f(t) = k_0)$. Thus, the non-zero one-step state transition probabilities for any

$0<i_0<c, 0<j_0<c,$ and $0<k_0<h$ are given as follows:

$$\begin{cases} P(0,0,k_0|0,0,k_0) = qu + (1-u) \\ P(1,0,k_0|0,0,k_0) = u(1-p)(1-q) \\ P(0,1,k_0|0,0,k_0) = up(1-q) \\ P(i_0,j_0+1,k_0|i_0,j_0,k_0) = 1 \\ P(i_0,1,k_0|i_0,0,k_0) = p \\ P(i_0+1,0,k_0|i_0,0,k_0) = 1-p \\ P(1,0,k_0+1|c,0,k_0) = 1-p \\ P(0,1,k_0+1|c,0,k_0) = p \\ P(0,0,0|c,0,h) = 1-s \\ P(0,0,1|c,0,h) = s \\ P(0,0,0|0,0,0) = 1-s \\ P(0,0,1|0,0,0) = s \end{cases} \tag{8.1}$$

Let $P_{(i,j,k)}=\lim_{t\to\infty} P(N_t(t)=i, N_c(t)=j, N_f(t)=k), i \in [0,c], j \in [0,c], k \in [0,h]$ be the steady-state probability of the Markov chain. We first study a simple case where no PU exists in the CR network. Then, we consider the scenario where SUs coexist with PUs.

1) No PU Exists in a Network: In this case, since the probability that a PU packet arrives in a time slot is equal to zero (i.e., $p=0$), all channels are always available for SUs (i.e., u=1) and a SU does not need to perform spectrum handoffs during a data transmission. Thus, a SU cannot be in the Collided state. In addition, a SU can only be in the Backlogged state when it initiates a new transmission (i.e., the Backlogged states are reduced to $(N_t(t)=0, N_c(t)=0, N_f(t)=1)$. Thus, the steady-state probabilities of the Transmitting and Idle state can be represented in terms of the

steady-state probability of the Backlogged state $P_{(0,0,1)}$. Hence, from Figure 8.2,

$$P_{(i,0,k)} = (1-q)P_{(0,0,1)}, \text{ for } 1 \leq i \leq c, 1 \leq k \leq h, \tag{8.2}$$

$$P_{(0,0,0)} = \frac{(1-s)(1-q)}{s} P_{(0,0,1)}. \tag{8.3}$$

Since $\sum_i \sum_j \sum_k P_{(i,j,k)}$=1, we can calculate the steady-state probability of every state in the Markov chain. Note that the probability of a collision among SUs, q, depends on the channel selection scheme. The derivation of q is given in Chapter 7.3.

2) SUs Coexist with PUs in a Network: If the probability that a PU packet arrives in a time slot is not equal to zero (i.e., $p \neq 0$), collisions between SUs and PUs may occur when a SU transmits a frame. Thus, the steady-state probabilities of the Collided states are not zero. Similar to the no-PU case, we represent the steady-state probabilities in terms of $P_{(0,0,1)}$. First of all, for the first tier in Figure 8.2, we can obtain the steady-state probabilities of all the Transmitting states in terms of $P_{(0,0,1)}$, that is,

$$P_{(i,0,1)} = u(1-q)(1-p)^i P_{(0,0,1)}, \text{ for } 1 \leq i \leq c. \tag{8.4}$$

Then, for the Collided states with $i = 0$,

$$P_{(0,j,1)} = up(1-q)P_{(0,0,1)}, \text{ for } 1 \leq j \leq c. \tag{8.5}$$

For the Collided states with $i > 0$,

$$P_{(i,j,1)} = u(1-q)p(1-p)^i P_{(0,0,1)}, \text{ for } 1 \leq i \leq c-1, 1 \leq j \leq c. \tag{8.6}$$

For the k-th ($k > 1$) tier, we first derive $P_{(1,0,k)}$ and $P_{(0,1,k)}$:

$$P_{(1,0,k)} = (1-p)P_{(c,0,k-1)} + u(1-p)(1-q)P_{(0,0,k)}, \tag{8.7}$$

$$P_{(0,1,k)} = pP_{(c,0,k-1)} + up(1-q)P_{(0,0,k)}. \tag{8.8}$$

Then, the steady-state probabilities of the Transmitting states when $i > 1$ can be represented as

$$P_{(i,0,k)} = (1-p)^{i-1}P_{(1,0,k)}, \text{ for } 1 < i \leq c. \tag{8.9}$$

Similar to the derivation method for the first tier, for the Collided states with $i = 0$,

$$P_{(0,j,k)} = P_{(0,1,k)}, \text{ for } 1 \leq j \leq c. \tag{8.10}$$

For the Collided states with $i > 0$,

$$P_{(i,j,k)} = p(1-p)^{i-1}P_{(1,0,k)}, \text{ for } 1 \leq i \leq c-1, 1 \leq j \leq c. \tag{8.11}$$

Then, for the *Backlogged* state in the k-th tier,

$$\sum_{i=0}^{c-1} P_{(i,c-i,k)} = u(1-q)P_{(0,0,k)}. \tag{8.12}$$

Combining (8.7) through (8.12), we obtain the following equations using basic mathematical manipulations:

$$P_{(1,0,k)} = \frac{1}{(1-p)^{c-1}}P_{(c,0,k-1)}, \tag{8.13}$$

$$P_{(0,1,k)} = \frac{p}{(1-p)^{c}}P_{(c,0,k-1)}, \tag{8.14}$$

$$P_{(0,0,k)} = \frac{1-(1-p)^{c}}{u(1-q)(1-p)^{c}}P_{(c,0,k-1)}. \tag{8.15}$$

Then, from (8.9),

$$P_{(c,0,k-1)} = (1-p)^{c-1}P_{(1,0,k-1)}. \tag{8.16}$$

Combining (8.13) and (8.16), we find the following relationship:

$$P_{(c,0,k)} = P_{(c,0,k-1)}. \tag{8.17}$$

Thus,

$$P_{(c,0,k)} = u(1-q)(1-p)^c P_{(0,0,1)}. \tag{8.18}$$

(8.18) indicates the steady-state probabilities of the states in the k-th tier are independent of k. Now, we have all the steady-state probabilities of the states in all tiers except the state $(0,0,0)$. At last, for the $Idle$ state,

$$P_{(0,0,0)} = \frac{1-s}{s} u(1-q)(1-p)^c P_{(0,0,1)}. \tag{8.19}$$

Similarly, since $\sum_i \sum_j \sum_k P_{(i,j,k)} = 1$, we can get the steady-state probability of every state in the Markov chain. If we denote Θ as the normalized throughput of SU transmissions, Θ is the summation of the steady-state probabilities of all the $Transmitting$ states in our proposed Markov model. That is,

$$\Theta = \sum_{k=1}^{h} \sum_{i=1}^{c} P_{(i,0,k)}. \tag{8.20}$$

8.2.3 The Probability that at Least One Channel is Idle

In the above derivations, u and q are unknown. In this subsection, we calculate the probability that at least one channel is idle, u. Without loss of generality, we associate a PU with one channel and model the activity of a PU on a channel as an ON/OFF process [72][123]. SUs can only exploit the channels when the channels are idle (i.e., in the OFF period). We assume that the buffer in each PU can store at most one packet at a time. Once a packet is stored at a buffer, it remains there until it is successfully transmitted. Thus, we assume that the OFF period of a channel follows the geometric distribution, where the probability mass function (pmf) is given by

$$\Pr(N_{OFF} = n) = p(1-p)^n, \tag{8.21}$$

where N_{OFF} is the number of time slots of an OFF period.

Let $\Omega(t)$ be the number of channels used by PUs at time slot t. The process $\{\Omega(t), t = 0, 1, 2, \cdots\}$ forms a Markov chain whose state transition diagram is given in Figure 8.3, in which the self loops are omitted. To characterize the behavior of the PU channels, we define $\mathcal{D}_\alpha^l$ as the event that l PUs finish their transmissions given that there are α PUs in the network in a time slot. We also define $\mathcal{A}_\gamma^m$ as the event that m PUs start new transmissions given that there are γ idle PUs in a time slot. Thus, the probabilities of events $\mathcal{D}_\alpha^l$ and $\mathcal{A}_\gamma^m$ are:

$$\Pr(\mathcal{D}_\alpha^l) = \binom{\alpha}{l} v^l (1-v)^{\alpha-l}, \tag{8.22}$$

$$\Pr(\mathcal{A}_\gamma^m) = \binom{\gamma}{m} p^m (1-p)^{\gamma-m}, \tag{8.23}$$

where v is the probability that a PU finishes its transmission in a slot. If the average length of a PU packet is denoted as $\bar{L}$, then $v = 1/\bar{L}$. Therefore, the state transition probability from state $\{\Omega(t) = a\}$ to state $\{\Omega(t+1) = b\}$ can be written as

$$p_{ab} = \begin{cases} \sum_{l=0}^{a} \Pr(\mathcal{D}_a^l) \Pr(\mathcal{A}_{M-a+l}^{b-a+l}), & \text{for } b \geq a \\ \sum_{l=a-b}^{a} \Pr(\mathcal{D}_a^l) \Pr(\mathcal{A}_{M-a+l}^{b-a+l}), & \text{for } b < a. \end{cases} \tag{8.24}$$

Therefore, we can obtain the steady-state probabilities of the number of busy channels in the band in a time slot, denoted as $\mathbf{g} = [g_0 \quad g_1 \quad g_2 \quad \cdots \quad g_M]^T$, where g_i denotes the steady-state probability that there are i busy channels in a time slot. Hence, $u = \sum_{i=0}^{M-1} g_i$.

8.3 The Impact of Different Channel Selection Schemes

In this section, we investigate the impact of different channel selection schemes on the performance of the spectrum handoff process in a multi-SU scenario by deriving

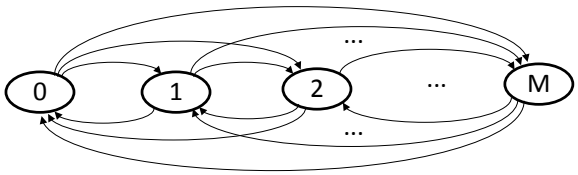

Figure 8.3: The transition diagram of the number of channels used by PUs in one time slot.

the probability of a collision among SUs, q.

8.3.1 Random Channel Selection

For the random channel selection scheme, a SU selects an available channel for access on a random basis. Thus, a collision among SUs happens if more than one SU selects the same channel. To make the analysis tractable, we assume that the SU traffic is saturated (i.e., after finishing transmitting a packet, a SU always has another packet in the buffer to send). Thus, let $\mathcal{B}(t)$, $\mathcal{T}(t)$, and $\mathcal{C}(t)$ be the number of SUs in the Backlogged, Transmitting, and *Collided* state at time slot t, respectively. Therefore, $\mathcal{B}(t)+\mathcal{T}(t)+\mathcal{C}(t)=N$. The process $\{\mathcal{B}(t),\mathcal{T}(t),\mathcal{C}(t),t=1,2,\cdots\}$ forms a Markov chain, namely the system chain. Thus, we denote the state transition probability of the system chain from (n_1,n_2,n_3) to (n_1',n_2',n_3') as $K_{((n_1,n_2,n_3),(n_1',n_2',n_3'))}$. Let $X_w(n_2)$ be the probability that w number of SUs in the $Transmitting$ state successfully finish their transmissions at time slot t given that there are n_2 SUs in the $Transmitting$ state. Then,

$$X_w(n_2)=\binom{n_2}{w}\sigma^w(1-\sigma)^{n_2-w}, \tag{8.25}$$

where σ is the probability that a SU finishes a packet transmission in a slot. Let $Y_r(n_2,w)$ be the probability that r SUs in the $Transmitting$ state collide with PU packets in the next time slot given that n_2 SUs are in the $Transmitting$ state and w

SUs out of n_2 SUs finish their transmissions. Thus,

$$Y_r(n_2, w) = \binom{n_2 - w}{r} p^r (1-p)^{n_2-w-r}. \tag{8.26}$$

Let $Z_e(n)$ be the probability that e of n_3 users transmit the last time slot of a frame in the current slot given there are n_3 SUs in the *Collided* state. Then,

$$Z_e(n_3) = \binom{n_3}{e} p_f^e (1-p_f)^{n_3-e}, \tag{8.27}$$

where p_f is the probability that the current time slot is the end of a frame. Since the frame length is c time slots, $p_f = \frac{1}{c}$. Let $T_d(n_1, \theta)$ be the probability that d SUs successfully access the channels given that there are n_1 SUs in the *Backlogged* state and θ available channels in the band. Then,

$$T_d(n_1, \theta) = \frac{S_d(n_1, \theta)}{\binom{\theta+n_1-1}{n_1}}, \tag{8.28}$$

where $S_d(n_1, \theta)$ is the number of possibilities that d of n_1 SUs select a channel that is only selected by one SU given that there are θ channels available. The denominator in (8.28) is the total number of possibilities that n_1 SUs select θ available channels. $S_d(n_1, \theta)$ can be calculated using the following iterative equation:

$$S_d(n_1, \theta) = U_d(n_1, \theta) - U_{d+1}(n_1, \theta) - \sum_{i=1}^{n_1-d} \left[\binom{d+i}{d} - \binom{d+i}{d+1} \right] S_{d+i}(n_1, \theta), \tag{8.29}$$

where $U_d(n_1, \theta) = \binom{n_1}{d} \binom{\theta+n_1-2d-1}{\theta-d}$.

We now give the proof of (8.29). $S_d(n_1, \theta)$ is the number of possibilities that d channels are selected by only one SU for each channel given that there are n_1 SUs and θ available channels. Let $\Phi_d(n_1, \theta)$ be the number of possibilities that at least d channels are selected by one SU for each channel given that there are n_1 SUs and θ available channels. Thus,

$$S_d(n_1,\theta) = \Phi_d(n_1,\theta) - \Phi_{d+1}(n_1,\theta). \tag{8.30}$$

Then, we calculate $\Phi_d(n_1,\theta)$. We first select d channels out of n_1 with one SU on each channel. The total number of possibilities is $\binom{n_1}{d}$. Then, let the remaining n_1-d SUs select the remaining $\theta-d$ channels. The total number of possibilities is $\binom{\theta+n_1-2d-1}{\theta-d}$. Thus, we denote $U_d(n_1,\theta) = \binom{n_1}{d}\binom{\theta+n_1-2d-1}{\theta-d}$. Compare $\Phi_d(n_1,\theta)$ with $U_d(n_1,\theta)$, there are many repeated counts that need to be removed. We denote the number of repeated counts as $\Gamma_d(n_1,\theta)$.

Note that for the $d+i, i>0$, channels that are selected by only one SU, the number of repeated counts is $\left[\binom{d+i}{d}-1\right] S_{d+i}(n_1,\theta)$. Thus, the total number of repeated counts is

$$\Gamma_d(n_1,\theta) = \sum_{i=1}^{n_1-d}\left[\binom{d+i}{d}-1\right] S_{d+i}(n_1,\theta). \tag{8.31}$$

Thus,

$$\Phi_d(n_1,\theta) = U_d(n_1,\theta) - \Gamma_d(n_1,\theta). \tag{8.32}$$

Compare (8.38) through (8.40), (8.29) is obtained.

Since $n_2 = N-n_1-n_3$, we can remove n_2 from the state space and reduce the state space from three dimensions to two dimensions. Thus, the system chain becomes a two-dimensional Markov chain $\{\mathcal{B}(t),\mathcal{C}(t)\}$. The state transition probability is

$$\begin{aligned} K_{((n_1,n_3),(n_1',n_3'))} = &\sum_{\theta=0}^{M}\sum_{e=0}^{n_3}\sum_{w=0}^{N-n_1-n_3} T_{n_1-n_1'+w+e}(n_1,\theta) Y_{n_3'+e-n_3}(N-n_1-n_3,w) \\ &X_w(N-n_1-n_3) Z_e(n_3)\Pr(\theta), \end{aligned} \tag{8.33}$$

where $\Pr(\theta)$ is the steady-state probability that there are θ channels available in the band which can be obtained in Chapter 8.2.3.

We further reduce the two dimensional system chain $\{\mathcal{B}(t),\mathcal{C}(t)\}$ with the state transition probability matrix $K_{((n_1,n_3),(n_1',n_3'))}$ to a one dimensional Markov chain with

the state transition probability matrix $H_{(m,m')} = K_{((n_1,n_3),(n_1',n_3'))}$, where

$$\begin{cases} m &= \frac{(2N-n_1+3)n_1}{2} + n_3 \\ m' &= \frac{(2N-n_1'+3)n_1'}{2} + n_3'. \end{cases} \tag{8.34}$$

Let π_m be the steady-state probability for state $m, 0 \leq m \leq \frac{(N+1)(N+2)}{2}$, of the one-dimensional Markov chain with the state transition probability matrix $H_{(m,m')}$. By solving the equilibrium equation $\pi_m' = \sum_{m=0}^{\frac{(N+1)(N+2)}{2}} \pi_m H_{(m,m')}$ with the condition $\sum_{m=0}^{\frac{(N+1)(N+2)}{2}} \pi_m = 1$, we can obtain the steady-state probability π_m. We denote the steady-state probability that there are k SUs in the *Backlogged* state as ρ_k. ρ_k can be calculated by adding all the π_m in which m should be:

$$m = \frac{(2N-k+3)k}{2} + j, \quad \forall j \in [0, N-k]. \tag{8.35}$$

Thus,

$$\rho_k = \sum_{m=\frac{(2N-k+3)k}{2}}^{\frac{(2N-k+3)k}{2}+N-k} \pi_m. \tag{8.36}$$

Thus, the probability that a collision occurs among SUs when they randomly select a channel for each SU is obtained by

$$q = \sum_{\theta=1}^{M} \sum_{k=1}^{N} \frac{k-1}{\theta+k-2} \rho_k \Pr(\theta). \tag{8.37}$$

We now give the proof of (8.29). $S_d(n_1, \theta)$ is the number of possibilities that d channels are selected by only one SU for each channel given that there are n_1 SUs and θ available channels. Let $\Phi_d(n_1, \theta)$ be the number of possibilities that at least d channels are selected by one SU for each channel given that there are n_1 SUs and θ available channels. Thus,

$$S_d(n_1, \theta) = \Phi_d(n_1, \theta) - \Phi_{d+1}(n_1, \theta). \tag{8.38}$$

Then, we calculate $\Phi_d(n_1, \theta)$. We first select d channels out of n_1 with one SU on each channel. The total number of possibilities is $\binom{n_1}{d}$. Then, let the remaining $n_1 - d$ SUs select the remaining $\theta - d$ channels. The total number of possibilities is $\binom{\theta+n_1-2d-1}{\theta-d}$. Thus, we denote $U_d(n_1, \theta) = \binom{n_1}{d}\binom{\theta+n_1-2d-1}{\theta-d}$. Compare $\Phi_d(n_1, \theta)$ with $U_d(n_1, \theta)$, there are many repeated counts that need to be removed. We denote the number of repeated counts as $\Gamma_d(n_1, \theta)$.

Note that for the $d+i, i>0$, channels that are selected by only one SU, the number of repeated counts is $\left[\binom{d+i}{d}-1\right] S_{d+i}(n_1, \theta)$. Thus, the total number of repeated counts is

$$\Gamma_d(n_1, \theta) = \sum_{i=1}^{n_1-d} \left[\binom{d+i}{d} - 1\right] S_{d+i}(n_1, \theta). \tag{8.39}$$

Thus,

$$\Phi_d(n_1, \theta) = U_d(n_1, \theta) - \Gamma_d(n_1, \theta). \tag{8.40}$$

Compare (8.38) through (8.40), (8.29) is obtained.

8.3.2 Greedy Channel Selection

For the greedy channel selection scheme, a SU always selects the channel which leads to the minimum service time [55]. If more than one SU pair perform spectrum handoffs at the same time, this channel selection method will cause definite collisions among SUs. Thus, the probability that a collision occurs among SUs is given by:

$$q = \begin{cases} 0 & \text{for } N \leq 2 \\ 1 & \text{for } N > 2. \end{cases} \tag{8.41}$$

Note that in this channel selection scheme, both the SU transmitter and receiver do not need to exchange information on the selected channel. Thus, the transition probability from the *Collided* states to the corresponding *Backlogged* state is $1-u$ instead of one. A part of the modified state transition diagram for the first tier is shown in Figure 8.4. The derivation of the steady-state probabilities of this modified

model can be carried out in the way as in Chapter 8.2.2.

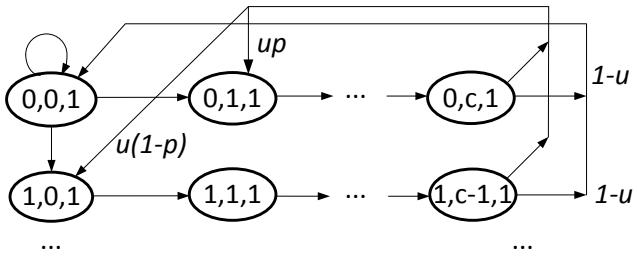

Figure 8.4: The modified Markov model based on the greedy channel selection scheme.

8.3.3 Pseudo-Random Selecting Sequence based Channel Selection

A channel selection scheme is proposed based on a pseudo-random selecting sequence [107]. When multiple SUs perform spectrum handoffs at the same time, a pseudo-random selecting sequence for each SU is generated locally. SUs need to perform spectrum handoffs following the same selecting sequence to select channels to avoid collisions. Thus, for this channel selection scheme, the probability of a collision among SUs is always zero (i.e., $q=0$).

8.3.4 Results Validation

In this subsection, we validate the numerical results obtained from our proposed Markov model using simulation. Note that when the number of SUs in the network is larger than two, the throughput using the greedy channel selection scheme for spectrum handoff is always zero because $q=1$. Thus, we first validate our numerical results in a two-SU scenario, where the number of PU channels, $M=10$. The number of frames in a SU packet, $h=1$, and the number of slots in a frame, $c=10$. We assume that the SU packets are of fixed length. Thus, $\sigma = 1/(ch)$. Figure 8.5 depicts the analytical and simulation results of the normalized SU throughput using the random channel selection scheme and the greedy channel selection scheme. It can be seen that the simulation results match extremely well with the numerical results in both schemes with the maximum difference only 3.84% for the random selection and 4.09% for the greedy selection. It is also shown that, under the same SU traffic load, the greedy channel selection scheme always outperforms the random channel selection

scheme in terms of higher SU throughput.

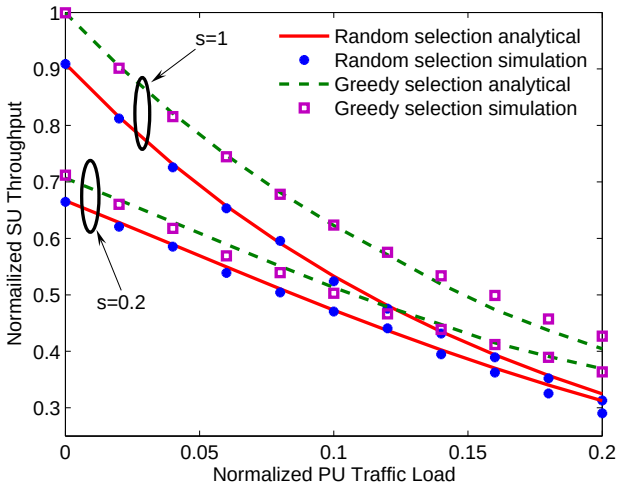

Figure 8.5: Analytical and simulation results of the normalized SU throughput in a two-SU scenario.

Then, we consider a CR network with 10 SUs in the network. We fixed the SU traffic at $s = 1$. The rest of the parameters are the same as in the two-SU scenario. Figure 8.6 shows that, under different channel selection schemes, the analytical and simulation results match well with the maximum difference only 6.14% for the random selection and 1.2% for the pseudo-random sequence selection. Figure 8.6 also indicates that the pseudo-random sequence selecion outperfoms the random selection, especially when PU traffic is high.

8.4 The Impact of Spectrum Sensing Delay

In this section, we investigate the impact of the spectrum sensing delay on the performance of a spectrum handoff process. The spectrum sensing delay considered in this chapter is defined as the duration from the moment that a collision between a SU and PU happens to the moment that the SU detects the collision (i.e., the overlapping time between a SU and PU transmission). Let T_s be the spectrum sensing delay. Therefore, a SU does not need to wait till the last time slot of a frame to realize the collision, as shown in Figure 8.1. It only needs to wait for T_s to realize that a collision with a PU packet occurs and stops the current transmission immediately. In a recent

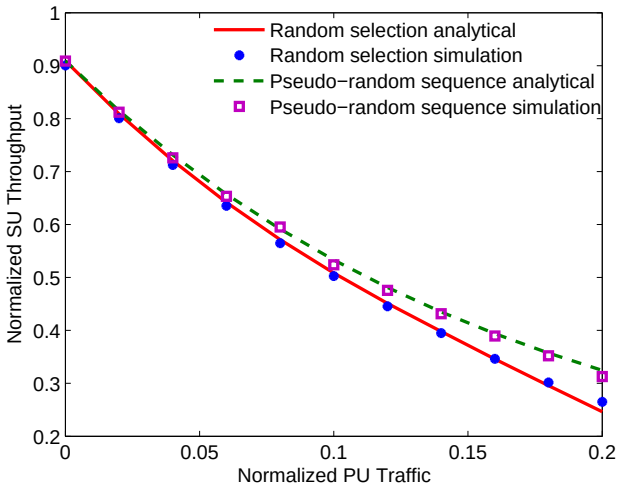

Figure 8.6: Analytical and simulation results of the normalized SU throughput under different channel selection schemes in a ten-SU scenario.

work [57], the spectrum sensing time is considered as a part of the spectrum handoff delay. However, the definition of the spectrum sensing time in [57] is different from the definition considered in this research. In [57], the spectrum sensing time only refers to the duration that a SU finds an available channel for transmission after a collision occurs. Thus, the spectrum sensing time can be as low as zero in [57]. In addition, the overlapping time of a SU and PU collision is neglected in [57]. However, the spectrum sensing delay considered in this chapter is not negligible.

The spectrum sensing delay, T_s, can be easily implemented in our proposed three dimensional Markov model with minor modifications. Figure 8.7 shows the first tier of the modified three dimensional discrete-time Markov chain when T_s equals 3 time slots. It is shown that, for a fixed $N_t(t)$, the maximum number of *Collided* states is T_s. The modified model of other tiers is similar to the first tier as shown in Figure 8.7.

Compared with the original Markov model shown in Figure 8.2, the derivation of the steady-state probabilities of the Markov model implemented with the spectrum sensing delay is exactly the same. The only difference is that the total number of the Collided states in the modified Markov model is reduced from $[c(c+1)/2]h$ in the

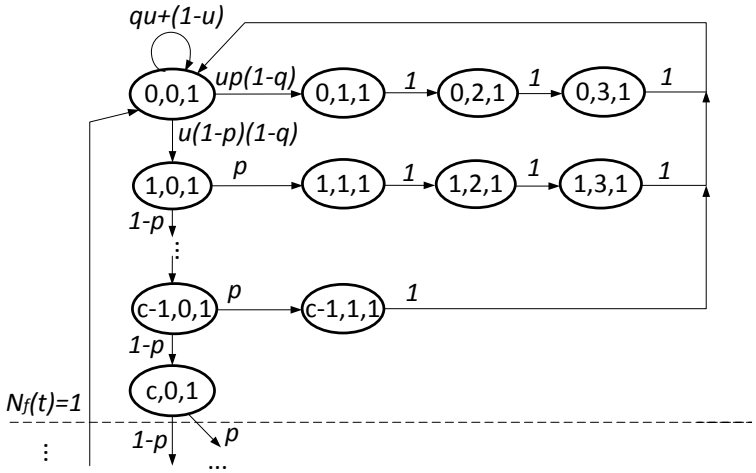

Figure 8.7: The modified Markov model based on the spectrum sensing delay when T_s equals 3 time slots.

original Markov model to $[T_s(c-T_s+1)+T_s(T_s-1)/2]h$.

8.4.1 Results Validation

Figure 8.8 shows the impact of the spectrum sensing delay on the SU throughput performance. We consider a two-SU scenario with different spectrum sensing delay using the random channel selection scheme. It is shown that the numerical results and analytical results match well with the maximum difference 1.83% for $T_s = 1$ and 4.56% for $T_s = 6$. It reveals that our proposed model can accurately predict the SU throughput.

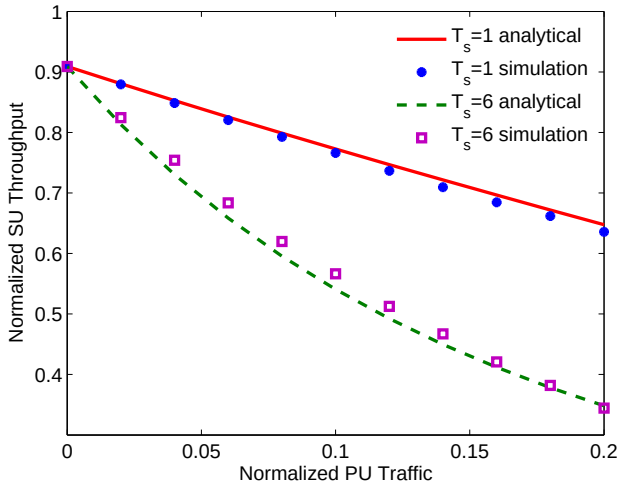

Figure 8.8: Analytical and simulation results of the normalized SU throughput under different spectrum sensing delay.

8.5 Performance Evaluation

In this section, we use our proposed Markov model to evaluate the performance of SU transmissions in spectrum handoff scenarios under various system parameters.

8.5.1 Collision Probability between SUs and PUs

Based on the proposed Markov model, the collision probability between SUs and PUs is the summation of all the steady-state probabilities of the *Collided* states. That is, $\Pr[collision] = \sum_{k=1}^{h} \sum_{i=0}^{c-1} \sum_{j=1}^{c-i} P_{(i,j,k)}$. Figure 8.9 shows the analytical and simulation results of the collision probability between SUs and PUs using the random channel selection scheme. The analytical results fit simulation results well with the maximum difference 6.26% for $N = 2$ and 3.41% for $N = 6$, respectively. It is shown that the collision probability between SUs and PUs decreases as the number of SUs increases. This is because that the number of collisions among SUs increases as the number of SUs during a spectrum handoff increases. Therefore, the probability for a SU being in the *Backlogged* states increases. Thus, the collision probability between SUs and PUs drops.

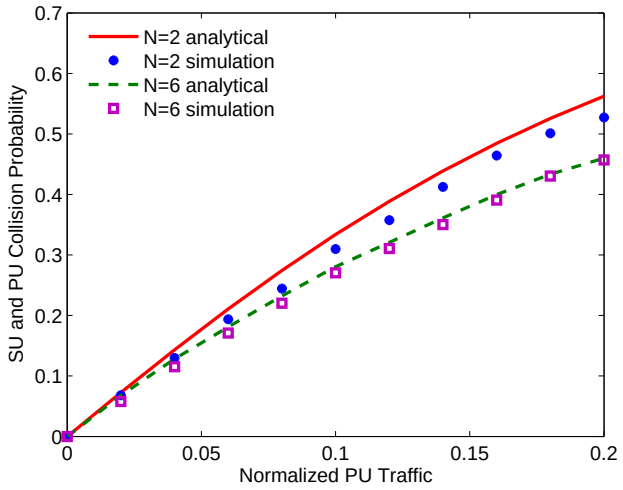

Figure 8.9: Analytical and simulation results of the collision probability between SUs and PUs.

8.5.2 Average Spectrum Handoff Delay

We denote D_s as the average spectrum handoff delay. Since the spectrum handoff delay is equivalent to the dwelling time on the *Backlogged* state, we obtain

$$D_s = \sum_{k=1}^{\infty} k p_d^{k-1}(1-p_d), \tag{8.42}$$

where $p_d = qu + (1-u)$. Figure 8.10 shows the analytical and simulation results of the average spectrum handoff delay using the random channel selection scheme. It is shown that as the number of SUs increases, the average spectrum handoff delay increases drastically.

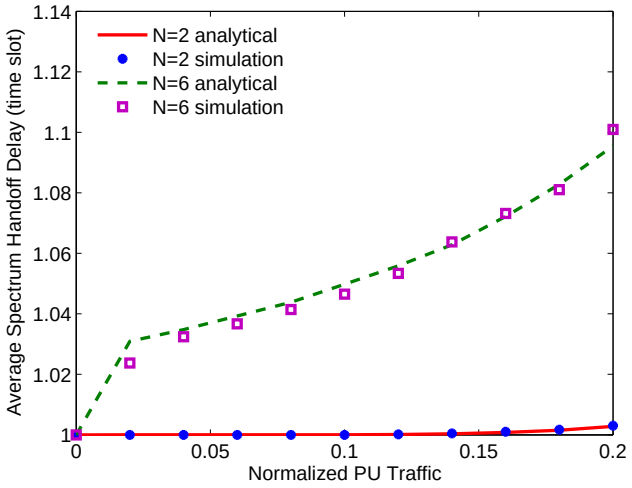

Figure 8.10: Analytical and simulation results of the average spectrum handoff delay.

CHAPTER 9: END-TO-END CONGESTION CONTROL IN CRAHNS

In this chapter, the end-to-end congestion control scheme is studied in CRAHNs. In the past decade, most of the research efforts in CR networks focus on the lower two layers (i.e., physical layer and data link layer) [125]. Despite a few routing algorithms, the transport layer issue in CR networks still remains unexplored. Although the transport layer protocol in Internet and traditional wireless ad hoc networks has been studied extensively [126, 127, 128, 129, 130], currently, there are only limited papers addressing this issue in CR networks [131, 132, 133, 134]. Due to the extremely important role of transport layer protocols in providing end-to-end communication services in a multi-hop ad hoc network (e.g., reliability, congestion control, flow control, and jitter control), in this chapter, we focus on the transport layer issue in multi-hop CR ad hoc networks.

End-to-end congestion control, aiming to find out how much traffic load offered by the source can be handled by a network, is an essential function of a transport layer protocol. Conventionally, Transmission Control Protocol (TCP) is the prevalent transport protocol to provide end-to-end congestion control on the Internet. Routers over the Internet indicate congestion by dropping packets (i.e., butter overflow). Thus, the classical TCP protocol interprets all packet losses as being congestion related. In addition, based on TCP, packet round trip timeouts (RTOs) and duplicate acknowledgments (ACKs) are used as indicators for packet losses. However, in wireless ad hoc networks, packet losses may be attributed to wireless channel errors or the change of the network topology rather than buffer overflow. If TCP reacts to these packet losses as if they were due to congestion and thus decreases the packet transfer rate, it may cause performance degradation in the end-to-end throughput. As a result, the

classical TCP is shown to perform poorly over wireless ad hoc networks [129][135]. Since RTOs and duplicate ACKs are not good indicators for congestion in wireless ad hoc networks, the Explicit Congestion Notification (ECN) mechanism is proposed to notify the source whenever congestion occurs in a wireless network [136]. In this way, the source is able to differentiate between congestion-related packet losses and non-congestion-related packet losses (e.g., channel errors) in a wireless network. Therefore, only upon the receipt of an ECN message, the source invokes the congestion control by reducing its packet transfer rate.

Generally, there are two approaches to implement the ECN mechanism: 1) the ECN is sent from the node where congestion occurs directly back to the source in a dedicated packet (e.g., an ICMP Source Quench message [131][136]); and 2) the ECN is piggybacked over data packets to the destination and then sent to the source through the ACK from the destination [129]. Despite the advantages of the ECN mechanism, there are some disadvantages. On one hand, for the first approach, more packets are added in the already congested network, which increases the network traffic load. On the other hand, for the second approach, it may take a long round trip delay for the ACK to reach the source. In fact, the initial implementation of the ECN mechanism to control network congestion for Internet has a premise that packets marked with ECN can be delivered to the source immediately so that the source knows that congestion occurs in time [136]. In traditional Internet or wireless ad hoc networks, this premise can be easily satisfied due to the existence of a common control channel (CCC) that is always available for all nodes in a network. However, in multi-hop CR ad hoc networks where a CCC usually does not exist, implementing the ECN mechanism for congestion control is a non-trivial issue.

In CR ad hoc networks, as shown in Figure 9.1, due to the non-uniformity of the secondary user (SU) channel availability, a dedicated CCC for control packet exchange may not exist. Therefore, the SU transmitting pair first needs to find a common

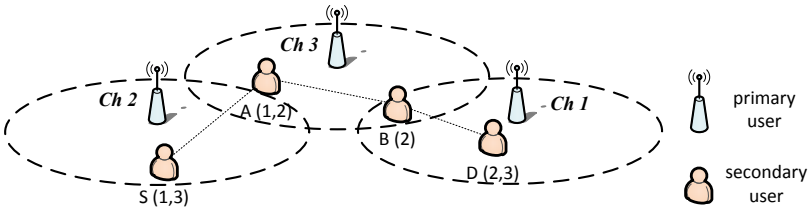

Figure 9.1: An example of a 3-hop CR ad hoc network where a common control channel does *not* exist.

available channel for communications. This process is usually not straightforward and takes a non-negligible time (the detailed process is presented in Section 9.1). In addition, due to the dynamic channel availability caused by primary user (PU) activities, the SU transmission on one channel may fail. Thus, without a CCC, it may take an excessively long time to successfully transmit an ECN message over a single hop in a CR network, let alone the delay of the ECN from the congested node to the source over multiple hops. If the delay of the ECN message is very long, the network cannot restore from the congested status quickly. Therefore, the congestion in multi-hop CR ad hoc networks cannot be properly solved by the ECN mechanism. Furthermore, since RTOs and duplicate ACKs are not used as indicators of network congestion, the end-to-end congestion control in multi-hop CR ad hoc networks is a very challenging issue.

To illustrate the impact of the delay of the ECN messages on the congestion control performance, consider a multi-hop CR ad hoc network shown in Figure 9.2. In Figure 9.2, node 2 is a "bottleneck" node whose buffer size is smaller than other nodes. If the buffer of a SU is full, additional packets sent to this node will be denied. Therefore, the "bottleneck" node is usually where the congestion occurs. We use three different ECN implementations: 1) Priority ECN with a CCC (i.e., the ECN message is sent in a dedicated packet on a CCC with the highest priority); 2) Priority ECN (i.e., the ECN message is sent in a dedicated packet on data channels with the highest priority); and 3) Piggybacked ECN (i.e., the ECN message is piggybacked in the data packets on data channels). Figure 9.3 shows the simulation results on the delay of

the ECN messages and the network performance under different ECN scenarios. We define an important performance metric, congestion control efficiency, as the ratio of the number of non-congested received packets (i.e., received packets that are not dropped due to congestion) to the total number of received packets. This metric measures the efficiency of the end-to-end congestion control scheme. From Figure 9.3(b), it is shown that if the CCC does not exist, the congestion control efficiency suffers significantly.

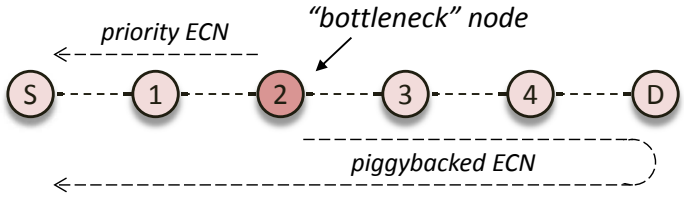

Figure 9.2: A multi-hop CR ad hoc network.

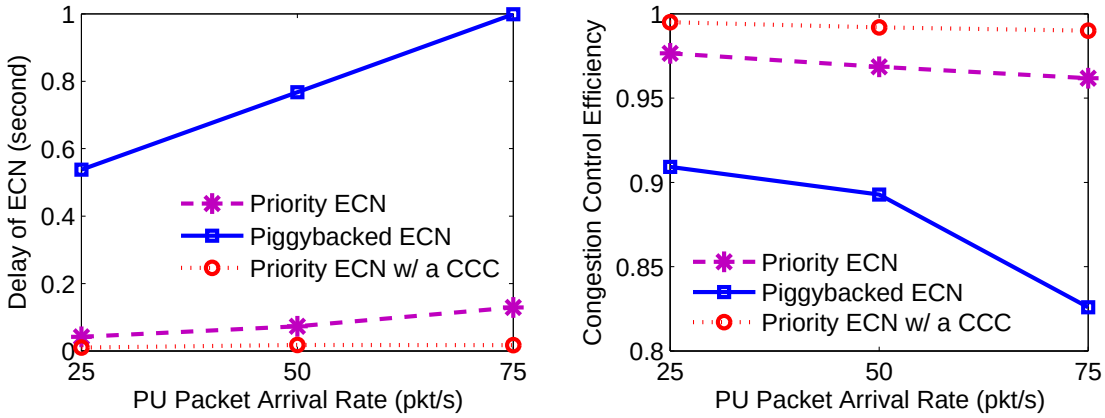

(a) Delay of the ECN messages.

(b) Congestion control efficiency.

Figure 9.3: Network performance of different ECN implementations.

In this chapter, we study the end-to-end congestion control issue in multi-hop CR ad hoc networks without a CCC. We observe that the delay of the ECN messages has a significant impact on the network performance. In addition, we show that none of the existing transport layer approaches can be simply used to solve the congestion issue in CR ad hoc networks. More specifically, the main contributions of this chapter are:

1. A comprehensive end-to-end congestion control framework is proposed in multi-hop CR ad hoc networks without a CCC.

2. The unique challenges of the end-to-end congestion control in multi-hop CR ad hoc networks without a CCC are addressed for the first time.

3. The existing methods of the end-to-end congestion control for traditional wireless ad hoc networks are studied and shown to perform poorly in CR ad hoc networks without a CCC.

To the best of our knowledge, this is the first work that investigates the end-to-end congestion control issue in multi-hop CR ad hoc networks without a common control channel.

9.1 End-to-End Congestion Control Framework in Multi-hop CRAHNs

In this section, we first introduce the related work on congestion control in CR networks and their limitations. Then, the comprehensive end-to-end congestion control framework in multi-hop CR ad hoc networks is proposed.

9.1.1 Related Work

Currently, the research effort on the transport layer issue in CR ad hoc networks is still quite insufficient. In addition, in these existing works, some unique features of CR ad hoc networks are not considered and impractical assumptions are made. In [131], a TCP-like transport protocol for CR ad hoc networks is proposed using the explicit feedback (i.e., ECN) from the intermediate nodes. However, in [131], a CCC is used to exchange the control information including the ECN messages. In [132], the authors evaluate the performance of TCP in CR ad hoc networks. However, in [132], the non-uniform channel availability of CR ad hoc networks and the complexity in finding a common available channel caused by the non-uniform channel availability on the network performance is not considered. In [133] and [134], only a single-hop CR network is studied and the end-to-end congestion control is not investigated. Furthermore, the non-uniform channel availability is still not considered. From the

above discussion, it is known that all the existing works on the transport layer issue in CR ad hoc networks cannot be used in a practical scenario where the channel availability is non-uniform and a CCC does not exist. Previous research shows that, in wireless networks, the design of the lower layer protocols (especially the data link layer) often has a significant impact on the transport layer performance [127]. Therefore, the transport layer protocol design in CR ad hoc networks should take the lower layer protocols into consideration.

9.1.2 End-to-End Congestion Control Framework

In this chapter, we propose a comprehensive end-to-end congestion control framework for multi-hop CR ad hoc networks under practical scenarios, as shown in Figure 9.4. Our proposed framework considers the interactions from the physical (PHY) layer to the transport layer in a network. More importantly, the components at each layer are necessary for SUs to work in a CR ad hoc networks without a CCC.

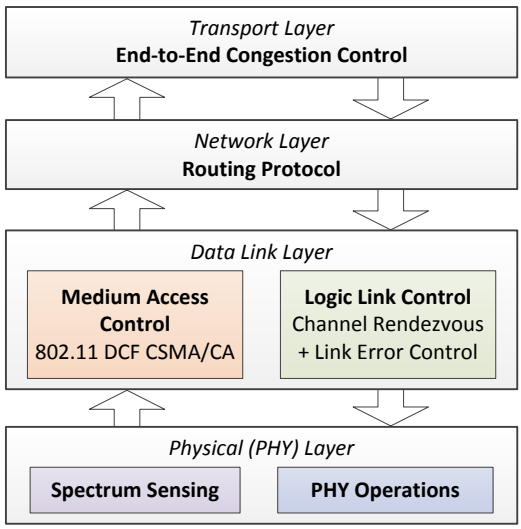

Figure 9.4: The end-to-end congestion control framework for CR ad hoc networks.

Next, we illustrate how the components at different layers are systematically integrated in the proposed framework. First of all, at the PHY layer, we use QPSK as the modulation scheme based on the IEEE 802.11 standard [120]. In addition, another major objective at the PHY layer is spectrum sensing. That is, each SU performs

spectrum sensing to obtain the availability information of the current channel as an input for the higher layers. Secondly, at the data link layer, there are two sub-layers. The first sub-layer is the medium access control (MAC) layer. In this chapter, we use the IEEE 802.11 DCF CSMA/CA as the MAC protocol [120]. The second sub-layer is called the logic link control (LLC) layer. One objective of the LLC layer is for two SUs to find a common available channel and establish a logic link for communications, namely the channel rendezvous (the channel rendezvous scheme is introduced in detail in the following paragraph). Another objective of the LLC layer is the link error control. In CR ad hoc networks, due to various reasons (e.g., channel errors, dynamic channel availability, and congestion), the SU packet transmission is prone to fail. To avoid retransmitting the unsuccessful packets constantly by the source, we incorporate the link layer error control scheme in the framework (i.e., hide link-related packet losses from the source by using local retransmissions). In this chapter, we use the stop-and-wait automatic repeat request (ARQ) protocol as the link layer error control scheme. Therefore, any unsuccessful packet will be instantaneously retransmitted over each link locally. Thirdly, at the network layer, a routing protocol for wireless ad hoc networks is used to find a path from the source to the destination. Finally, at the transport layer, the proposed end-to-end congestion control scheme is implemented.

Then, we present the operations of the channel rendezvous scheme. In this chapter, we use Common Hopping as the channel rendezvous scheme, which is a straightforward and effective scheme [89]. Figure 9.5 shows the procedure of Common Hopping, where the SU channels are time-slotted and SUs communicate with each other in a synchronous manner. Based on Common Hopping, all the SUs in a network hop through the spectrum band using the same hopping sequence (e.g., the hopping pattern cycles through channels $1, 2, \cdots, M$, where M is the number of channels). This is similar to the frequency hopping technique used in Bluetooth [113]. SUs stay on

each hopped channel for one time slot. There are two phases in a time slot. At the beginning of each time slot, the first phase is called Sensing Phase (SP): all SUs are required to perform spectrum sensing during this phase. Following the SP, the second phase is called Transmission Phase (TP): SUs may transmit packets during this phase. Therefore, if the current channel is sensed idle during a SP, SUs may use this channel for transmissions during the following TP. On the other hand, if the current channel is sensed busy, SUs cannot start transmissions during the TP. SUs need to hop on channels until an available channel is found. As we can see, in order to find a common available channel, the SU transmitting pair may need to hop several time slots, which leads to long delay of packet transmissions over a single hop.

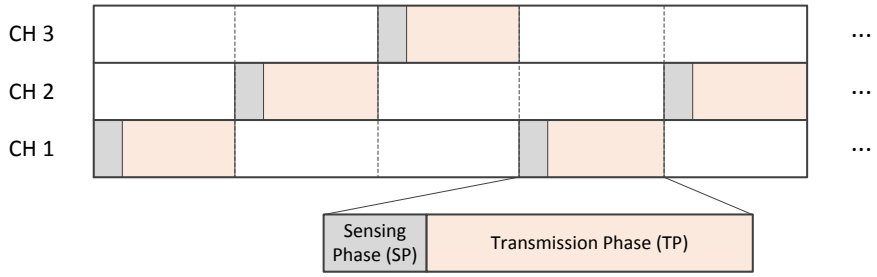

Figure 9.5: An example of the Common Hopping channel rendezvous scheme in CR ad hoc networks.

From the above description, if a SU does not have any packet to transmit, it hops through channels following the hopping sequence. If a SU has a packet in the buffer and needs to initiate a transmission, it follows the IEEE 802.11 DCF CSMA/CA and sends the request-to-send (RTS) packet to the intended receiver during the TP if the current channel is idle. Then, the receiver replies with the clear-to-send (CTS) packet on the same channel. After the transmitting pair has successfully exchanged the RTS/CTS messages, they pause the channel hopping and remain on the same channel for data transmissions, while other non-transmitting SUs continue hopping. After the data being successfully transmitted, the SU pair rejoins the channel hopping.

9.2 Challenges of End-to-End Congestion Control in Multi-hop CRAHNs

It is shown that the transport layer network performance suffers degradation when a CCC does not exist. In this section, we first introduce the network scenario considered in this chapter. Then, based on the network scenario, we further elaborate the challenges of end-to-end congestion control in multi-hop CR ad hoc networks.

9.2.1 Network Scenario

In this chapter, we consider a 5-hop CR ad hoc network with a chain-topology, as shown in Figure 9.2. The distance between the two neighboring SUs is 200 meters. PUs and SUs co-exist in a $l \times l$ area. PUs are evenly distributed within the network area. SUs opportunistically access M licensed channels. Each SU has a circular transmission range with a radius of r_c. The sensing phase length is 1 ms (the minimum spectrum sensing length using the energy detection method is 1 ms [137]). In addition, the transmission phase length is 10 ms. This length is long enough for the SU pair to exchange RTS/CTS packets. Thus, the length of a time slot is 11 ms. The normal buffer size of each SU is 50 TCP packets. That is, each SU has a queue of packets waiting for transmission that holds up to 50 packets and is managed in a drop-tail fashion. In addition, the buffer size of the "bottleneck" nodes is 5 TCP packets. Other parameters are given in Table 9.1.

In addition, each SU also has a circular sensing range with a radius of r_s. That is, if a PU is currently active within the sensing range of a SU, the corresponding SU is able to detect its appearance. Since different SUs have different local sensing ranges which include different PUs, their acquired available channels may be different. In addition, in this chapter, we model the PU channel activity as an ON/OFF process, where the length of the ON period is the length of a PU packet. Moreover, the arrival process of PU packets follows Poisson distribution. We assume that each PU randomly selects a channel from the spectrum band to transmit one packet.

Table 9.1: System Parameters

Number of PUs	80
Number of channels in the spectrum band	5
Side length of the network area	1400 m
Radius of the SU transmission range	250 m
Length of the sensing phase	1 ms
Length of the transmission phase	10 ms
Data rate of the channels	2 Mbps
Size of RTS packets	288 bits
Size of CTS packets	240 bits
Size of MAC ACK packets	240 bits
Size of SU TCP segments	1460 Bytes
Size of PHY header+MAC header+IP header	70 Bytes
Size of SU TCP ACK packets	20 Bytes
Size of dedicated packets marked with ECN	20 Bytes
Size of PU packets	1460 Bytes

9.2.2 Challenges of End-to-End Congestion Control

Currently, all the existing end-to-end congestion control mechanisms can be categorized into two classes: 1) using the explicit feedback (e.g., ECN) to notify the source when congestion occurs (usually for the wireless TCP [129][131]) and 2) using RTOs and duplicate ACKs as indicators for congestion (usually for the classical TCP), namely the RTO mechanism. In this section, we study these two types of congestion control mechanisms and show that none of them can be simply used in multi-hop CR ad hoc networks.

9.2.2.1 The ECN Mechanism in Multi-hop CR Ad Hoc Networks

We first study the ECN mechanism in multi-hop CR ad hoc networks. Since the SU channel availability is non-uniform, a dedicated CCC may not exist. Hence, control packets cannot be transmitted via a dedicated control channel that is always available. In addition, due to the dynamic channel availability, the SU transmitting pair may not always have a common available channel. If the current channel is sensed busy, they need to hop through the spectrum band to find a common available channel for their transmissions based on the channel rendezvous scheme. If PU traffic

is heavy, the SUs have to wait for a long time before they can start the transmissions, which causes an excessive delay for the ECN messages from the congested node to the source. The excessively long delay of the ECN messages results in a very serious consequence. That is, the TCP source reacts to network congestion slowly. Once the network is congested, the network cannot restore from the congested status quickly.

We still use the three ECN implementations. If the congested node is near to the source, as shown in Figure 9.2, the delay of the ECN messages using the Priority ECN is very close to the scenario where a CCC exists. Therefore, the Priority ECN has similar performance as the Priority ECN with a CCC in terms of the congestion control efficiency. In addition, the Priority ECN outperforms the Piggybacked ECN in terms of higher congestion control efficiency because it has shorter delay of the ECN. However, if the congested node is far away from the source, the results are quite different. Consider a multi-hop CR ad hoc network, as shown in Figure 9.6. In Figure 9.6, node 4 is the "bottleneck" node who is far away from the source. If congestion occurs at node 4, the priority ECN message needs to travels a long path through the network back to the source. In addition, since the Priority ECN adds more packets in the already congested network, the congestion status becomes even more critical. On the other hand, the Piggybacked ECN does not introduce any overhead in the network. Figure 9.7 shows the simulation results of the delay of the ECN messages and the congestion control efficiency under different ECN implementations. From Figure 9.7, it is shown that the Piggybacked ECN outperforms the Priority ECN in terms of higher congestion control efficiency in this scenario.

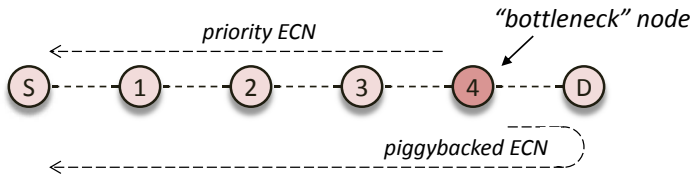

Figure 9.6: A multi-hop CR ad hoc network where the congested node is far away from the source.

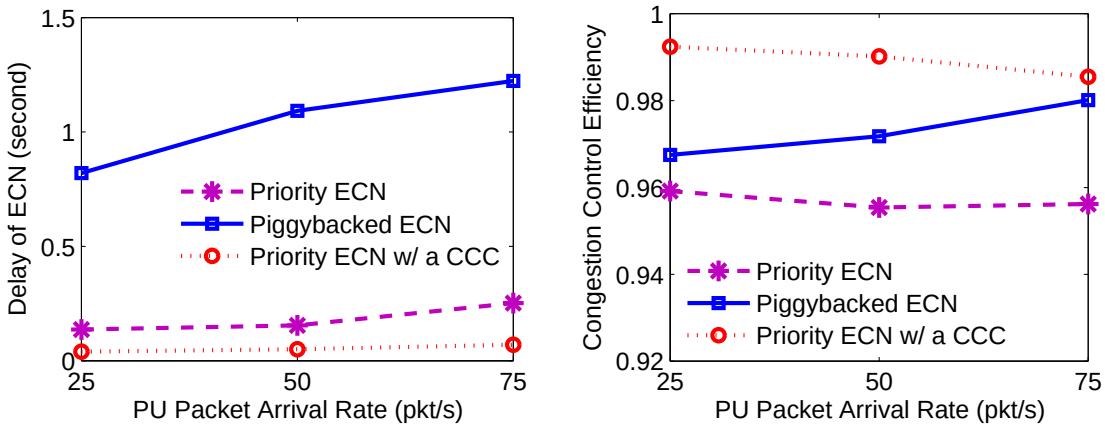

(a) Delay of the ECN messages.

(b) Congestion control efficiency.

Figure 9.7: Network performance of different ECN implementations.

As the transport protocol runs at the end nodes (i.e., source and destination), it has limited knowledge of the conditions of the intermediate nodes. That is, the source does not know the location of the "bottleneck" node. Thus, the source cannot decide which ECN implementation is used. Therefore, as we can see, without a CCC, using either the Priority ECN or the Piggybacked ECN may not be an optimal solution for multi-hop CR ad hoc networks.

9.2.2.2 The RTO Mechanism in Multi-hop CR Ad Hoc Networks

Since in our network scenario, there is only one path from the source to the destination, duplicate ACKs do not occur. Therefore, in this chapter, we only study the RTO mechanism in multi-hop CR ad hoc networks. The main idea of the RTO mechanism is that the source keeps a timer when a segment is sent. If the timer expires before the ACK of the corresponding segment comes in, the congestion control is invoked. In our considered network scenario, if congestion occurs, the dropped packet is retransmitted on each link. Therefore, this could lead to a long round trip time (RTT) of that segment. Hence, by using the timeout mechanism, the congestion is known to the source. However, to determine a RTO interval is not a trivial issue. Due to the dynamic spectrum environment of CR ad hoc networks, the RTT of SU TCP segments varies significantly. Figure 9.8 shows the cumulative distribution function

(CDF) of the SU TCP segment RTT under different PU traffic load when there is no "bottleneck" node in the network. From Figure 9.8, it is shown that, when the PU traffic is heavy (e.g., PU packet arrival rate is 75 pkt/s), the variance of the RTT is very large.

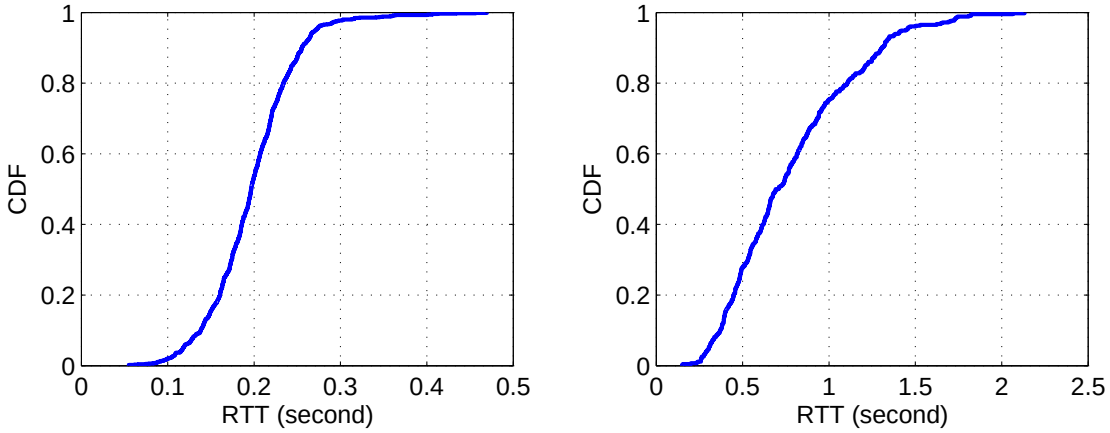

(a) PU packet arrival rate is 10 pkt/s. (b) PU packet arrival rate is 75 pkt/s.

Figure 9.8: The CDF of the SU TCP segment RTT under different PU traffic load.

In this chapter, we adopt the timeout algorithm used by TCP [138]. Based on the TCP protocol specification, the average estimated RTT can be calculated using the following equation:

$$R = \alpha R + (1 - \alpha)T, \tag{9.1}$$

where R is the average estimated RTT and T is the RTT measured from the most recent ACKed segment, respectively. In addition, α is a smoothing factor with a typical value of 0.8. Once the estimated RTT is updated, the RTO for the next segment is set to be βR. Normally, $\beta = 2$. However, we observe that if $\beta = 2$, the source seldom timeouts since the RTO is larger than the RTT with a high probability. Thus, the network cannot function properly. Therefore, in this chapter, we use $\beta = 1$. Figure 9.9 shows the simulation results of network performance of the RTO mechanism and the ECN mechanisms. From Figure 9.9(a), it is shown that the RTO mechanism outperforms the ECN mechanisms in terms of higher congestion control efficiency. In fact, using the RTO mechanism, the congestion control efficiency is always one since

there is no packet congested. On the other hand, from Figure 9.9(b), it is shown that the RTO mechanism has the lowest end-to-end throughput among the three congestion control mechanisms.

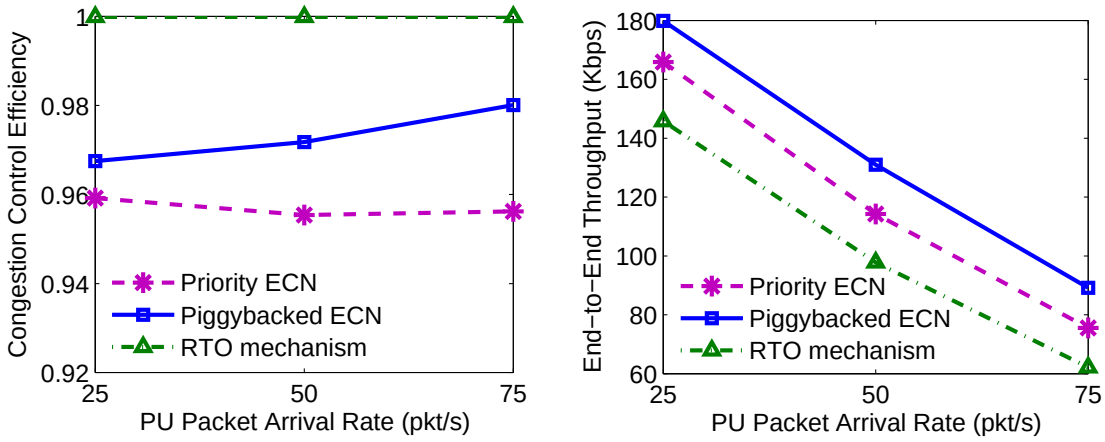

(a) Congestion control efficiency.

(b) End-to-end throughput.

Figure 9.9: Performance comparison between the ECN mechanism and the RTO mechanism.

In addition, Figure 9.10 shows the change of the congestion window in terms of the maximum segment size (MSS) under different congestion control mechanisms. From Figure 9.10, the RTO mechanism reduces the congestion window very frequently, when comparing to the Piggybacked ECN. As we can see, the congestion window using the RTO mechanism is always smaller than five MSS. This overly conservative congestion control leads to the low end-to-end throughput.

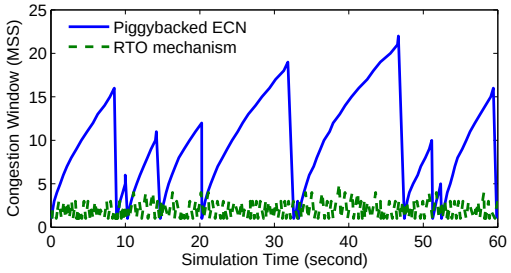

Figure 9.10: The change of the congestion window under different congestion control mechanisms.

Therefore, from the above analysis, it is known that both the ECN mechanism and the RTO mechanism have their limitations in performing the end-to-end congestion control in multi-hop CR ad hoc networks.

9.3 Performance Evaluation

In this section, we show other performance results of the existing end-to-end congestion control mechanisms in multi-hop CR ad hoc networks.

9.3.1 Performance of Packet Delay Variation

For audio and video communications, the average value the end-to-end packet delay does not have significant impact on the network performance as long as the delay is constant. However, the deviation of the packet delay is an important performance metric. In computer networking, the variance of the end-to-end packet delay is also called jitter. Even though the jitter control is a different issue in the transport layer, maintaining a small variance of the packet delay is a main objective of a good end-to-end congestion control mechanism. Figure 9.11 shows the simulation results of the jitter under different congestion control mechanisms. From Figure 9.11, it is shown that when the "bottleneck" node is far from the source and the PU traffic is heavy, the Piggybacked ECN has better performance than the Priority ECN in terms of smaller jitter. However, the RTO mechanism always has the smallest jitter among the three congestion control schemes.

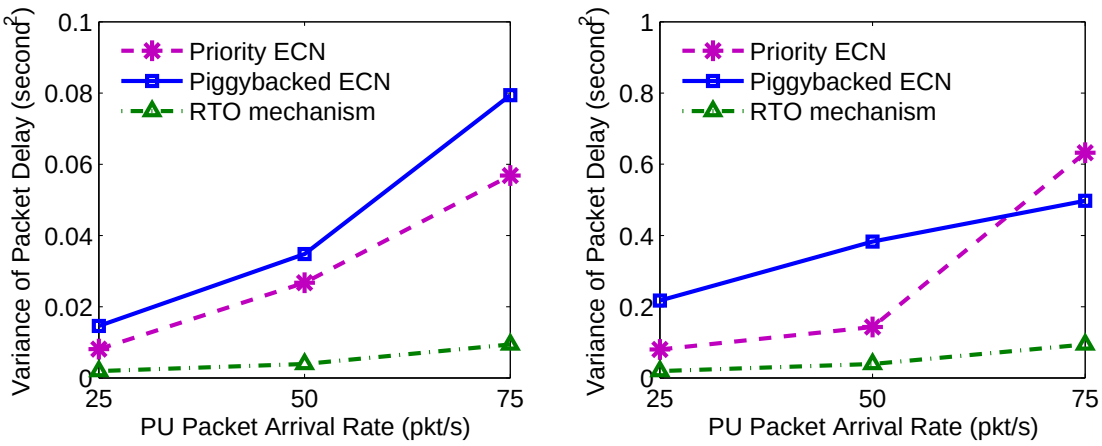

(a) Node 2 is the "bottleneck" node.

(b) Node 4 is the "bottleneck" node.

Figure 9.11: The packet delay variation under different congestion control mechanisms.

9.3.2 Impact of Channel Errors on Network Performance

As mentioned in Section 9.2, similar to traditional wireless ad hoc networks, in CR ad hoc networks, the packet loss could also be caused by wireless channel errors. If a packet cannot be successfully received by the receiver due to the lossy channel, the packet is retransmitted locally, which results in a long delay of the packet. Therefore, the channel errors may have significant effect on network performance. In this chapter, we use QPSK as the modulation scheme, the bit error rate (BER) of QPSK for an additive white Gaussian noise (AWGN) channel is

$$P_e = Q\left(\sqrt{\frac{2E_b}{N_0}}\right), \tag{9.2}$$

where $Q(\cdot)$ is the Q-function and E_b/N_0 is signal-to-noise ratio (SNR) on a channel [139]. Therefore, the probability that a packet is lost due to wireless channel error is

$$P_{loss} = 1 - (1 - P_e)^{L_s}, \tag{9.3}$$

where L_s is the size of the PHY layer packet. Figure 9.12 shows the performance results of different end-to-end congestion control mechanisms under different SNR. Similar to Figure 9.9(b), from Figure 9.12(b), it is shown that the RTO mechanism has the lowest end-to-end throughput among the three schemes. However, as we can see, for other performance metrics, the RTO mechanism achieves the best performance.

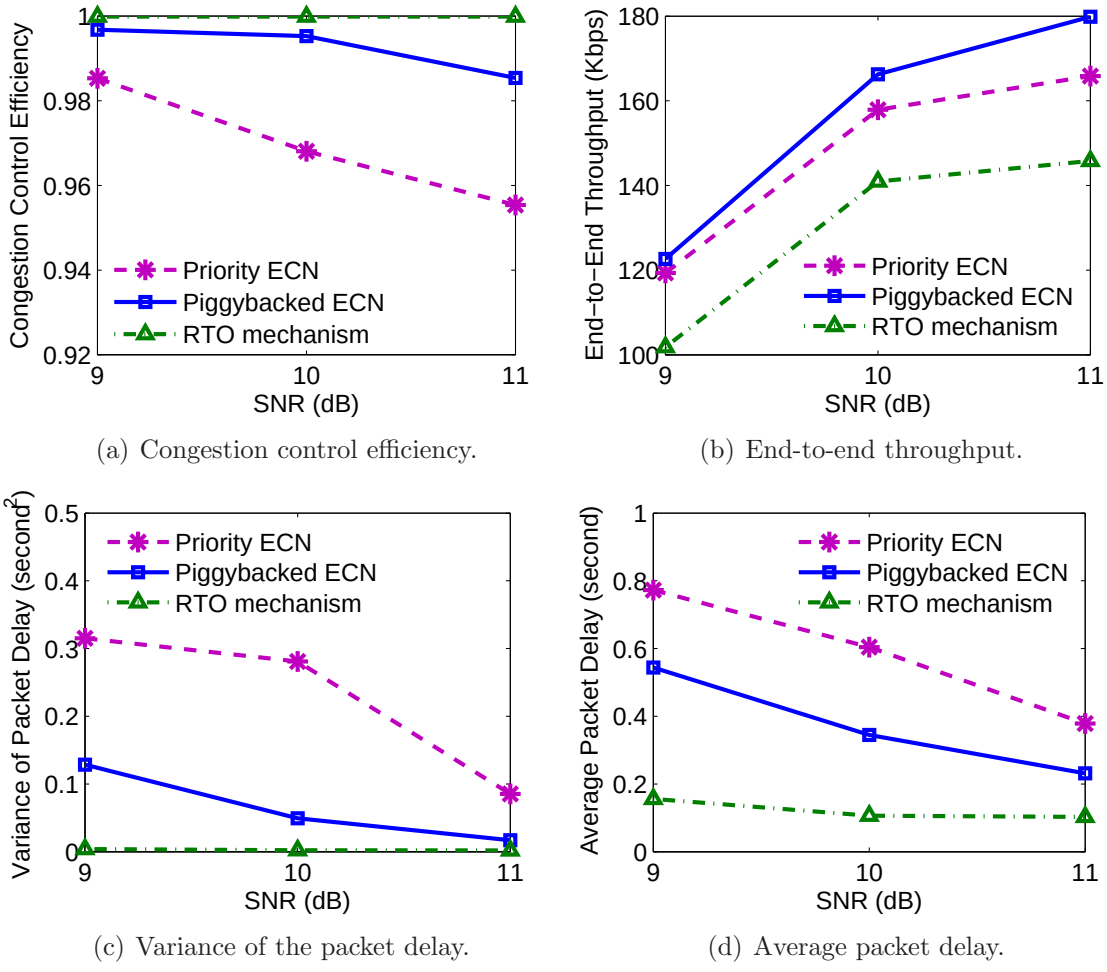

(a) Congestion control efficiency.

(b) End-to-end throughput.

(c) Variance of the packet delay.

(d) Average packet delay.

Figure 9.12: Performance results of different congestion control mechanisms under different SNR.

CHAPTER 10: OPTIMAL POWER CONTROL FOR CRAHNS

In this chapter, the optimal power control issue is studied in CRAHNs. Many challenges exist in the deployment of CR networks [4]. First of all, the transmission of CR users should not cause interference to primary (PR) users. Secondly, the throughput of CR links should be maximized for reliable quality communications. Thirdly, the robustness of CR links becomes extremely difficult to achieve under the mobility of CR users. A number of studies have been conducted in order to address these challenges.

One commonly known technique to address the above challenges is spectrum sensing, under which a CR transmitter can access the frequency band of interest only if the PR transmission is detected to be off. Through spectrum sensing, CR users can exploit unused spectrum opportunistically in a radio environment. Several spectrum detection techniques have been proposed, such as the detection of a primary transmitter through matched filter detection, energy detection, and cyclostationary feature detection [140], and the detection of local oscillator power [141].

In this chapter, we consider to achieve the above mentioned goals from a different perspective. Due to the non-zero probability of false detection and implementation complexity of spectrum sensing, we may raise a question: is there a way to achieve the goals of CR networks without spectrum sensing? Hence, we study a new sensing-free solution to enable concurrent transmissions of mobile CR users and also guarantee non-interference to PR users, thus improve the frequency reuse. With such aim, we examine a location-aware spectrum sharing scenario, where a CR ad hoc network is overlaid to a legacy network. CR users intend to operate over the same spectrum band which is licensed to PR users. The objective is to maximize the concurrent

transmission region of CR users within which they can move, while at the same time maintaining non-interference to PR communications.

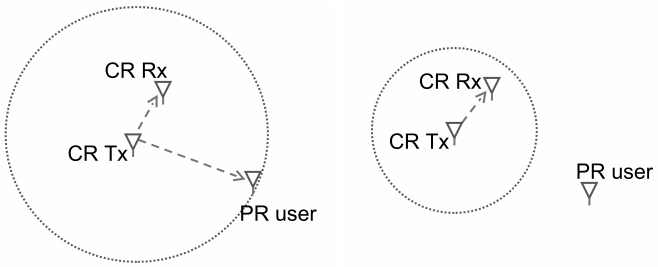

(a) Without power control (b) With power control

Figure 10.1: A spectrum sharing scenario of a two-node CR ad hoc network with a PR user.

To achieve the above objective, power control policies are important to guarantee the quality of both CR and PR communications. Figure 10.1 demonstrates the scenario of using a fixed power policy (in (a)) and the scenario of using power control (in (b)). The figure indicates that without power control, when a PR user is within the interference range of a CR transmission, concurrent transmissions are not possible. However, with power control, concurrent transmissions become feasible by reducing the transmit power of the CR transmitter to ensure non-interference to the PR user. Hence, the concurrent transmission region defined in this chapter refers to the circle within which the transmissions of CR users can be conducted without interfering PR users. The optimal power defined in this chapter refers to the transmit power which makes the concurrent transmission region of a CR user the maximum so that the bandwidth efficiency and CR link throughput can be improved. In addition, we assume that every node has its own location information in the system through Global Positioning System (GPS) or other positioning algorithms [96], and every node is able to exchange location information via a common control channel with its neighboring nodes [142][143].

Currently, related work on power control and concurrent transmissions of CR networks falls into two categories. In the first category, the power control problem is

considered in terms of either improving network energy efficiency [144, 145, 116, 146], or supporting user communication sessions in multi-hop CR networks [147], but the concurrent transmission for CR users is not considered. On the other hand, in [148], the scanning-free concurrent transmission region for CR users is considered only from a geometric point of view without taking power control into account. In addition, in this work, the CR transmitters and receivers are geographically fixed and the mobility of CR users is ignored. The concurrent transmission area defined in [148] is an irregular area which is difficult to apply in mobile scenarios. In [142], a location-assisted MAC protocol is proposed to enable concurrent transmissions for exposed nodes. In [149], the power scaling constraint of a CR transmitter is studied.

Our proposed optimal power control algorithm differs from related work in the original motivations. Most related work only considers fixed transmit power at each CR node without the power control capability [148] [150]. In this chapter, we study a mobile CR network where each CR node has the power control capability. That is, each CR node can transmit at any power in the allowable transmit power range to achieve the maximum concurrent transmission region. Our main contribution is that we propose a location-aware sensing-free optimal power control algorithm for concurrent transmissions especially in mobile CR ad hoc networks. Under such algorithm, the CR transmitter is able to conduct transmissions with the presence of the PR users while moving. Even if the CR users are in the area called "protected region" [149] in which the CR users should not transmit, if the location information of both CR and PR receivers is known to the CR transmitter, the CR transmitter can adjust its transmit power to enable the concurrent transmission.

10.1 System Model and Problem Formulation

In this section, a spectrum sharing scenario in which a cognitive radio ad hoc network overlaid to a legacy network is considered. Figure 10.2 shows the system model, where the shaded triangle and square represent the PR transmitter and receiver, re-

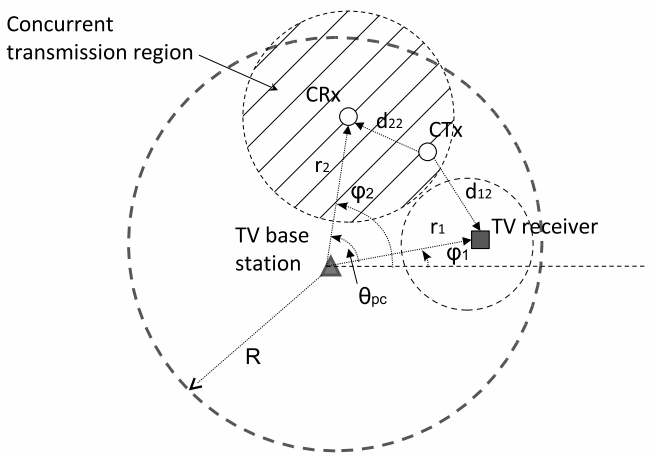

Figure 10.2: System model of a CR ad hoc network overlaid to a legacy network.

spectively. The white circles are the CR transmitter (denoted as CTx) and receiver (denoted as CRx). They form an ad hoc network to share the same spectrum band with the primary network. Without loss of generality, we assume that the PR base station is at the origin of the coordinate axes, and the PR receiver does not move. Let the location of the PR and CR receiver be (r_1, φ_1) and (r_2, φ_2), respectively. d_{12} represents the distance between the CTx and the PR receiver, and d_{22} represents the distance between the CTx and CRx. The decodable radius of the TV base station is R. Thus, the distance between the PR and CR receivers is $d_{pc} = \sqrt{r_1^2 + r_2^2 - 2r_1 r_2 \cos\theta_{pc}}$, where θ_{pc} is the relative angle of the PR and CR receivers.

Based on the two-ray ground propagation model [139][151], the received signal power P_r can be written as$P_r = \frac{P_t G_t G_r h_t^2 h_r^2}{r^\alpha}$, where P_t is the transmit power, G_t and G_r are the gains of the transmitter and receiver antennas, respectively; h_t and h_r are the heights of the transmitter and receiver antennas, respectively; r is the distance between the transmitter and the receiver; and α is the path loss factor.

In this chapter, we consider that the concurrent transmission for CR users must satisfy the co-channel signal-to-interference ratio (SIR) requirements for both PR and CR receivers. We denote the SIR thresholds for the PR and CR receivers as τ_p and τ_c, respectively; and the SIRs for the PR and CR receivers are SIR_p and SIR_c,

respectively. The optimal power control problem for concurrent transmission region maximization is formulated as follows:

Maximize: the area of concurrent transmission region

Subject to:

$$\begin{aligned} SIR_p &> \tau_p \\ SIR_c &> \tau_c \\ P_c^{min} \leq P_{ct} &\leq P_c^{max}, \end{aligned} \tag{10.1}$$

where P_{ct} is the transmit power of the CTx, P_c^{min} and P_c^{max} are the minimum and maximum allowable transmit power of the CTx, respectively.

10.2 Optimal Power Control

In this section, the proposed optimal power control algorithm for concurrent transmission region maximization is presented. We first consider the feasibility of the proposed optimal power control algorithm. Then, we consider the implementation of the algorithm in a mobility scenario. Finally, the impact of the shadowing fading effect on the optimal power control algorithm is investigated for the mobility scenario.

10.2.1 Feasibility of Optimal Power Control

We assume that the transmit power of the TV base station is P_{bs}, the gains of the transmitter and receiver antennas are unity, the heights of the antennas are the same, the path loss factors of the PR and CR transmissions are the same, and the Gaussian noise is negligible. Based on these assumptions, the SIRs at both CR and PR receivers can be written as $SIR_c = \frac{P_{ct} r_2^{\alpha}}{P_{bs} d_{22}^{\alpha}}$ and $SIR_p = \frac{P_{bs} d_{12}^{\alpha}}{P_{ct} r_1^{\alpha}}$, respectively. Since the SIRs must satisfy (10.1), we have

$$\begin{aligned} d_{22} &< r_2 (\frac{P_{ct}}{\tau_c P_{bs}})^{1/\alpha} \\ d_{12} &> r_1 (\frac{\tau_p P_{ct}}{P_{bs}})^{1/\alpha}. \end{aligned} \tag{10.2}$$

The first constraint in (10.2) means that the CTx which can concurrently transmit to the CRx must be physically within the disk centered at the CRx with a radius of $r_2(\frac{P_{ct}}{\tau_c P_{bs}})^{1/\alpha}$, as shown in Figure 10.2. The second constraint means that the CTx must not fall into the disk which is centered at the TV receiver with a radius of $r_1(\frac{\tau_p P_{ct}}{P_{bs}})^{1/\alpha}$, as shown in Figure 10.2. Therefore, the concurrent transmission region reaches the maximum when the following equation is satisfied:

$$r_1(\frac{\tau_p P_{ct}}{P_{bs}})^{1/\alpha} + r_2(\frac{P_{ct}}{\tau_c P_{bs}})^{1/\alpha} = d_{pc}. \tag{10.3}$$

Hence, given r_1, r_2, and θ_{pc}, the optimal power for concurrent transmission region maximization can be derived by solving equation (10.3).

However, considering (10.1), the solution of (10.3) may not lie in the allowable range $[P_c^{min}, P_c^{max}]$. So we consider two extreme cases by letting P_{ct} be P_c^{min} and P_c^{max}, respectively. We have the following two extreme functions of r_2 and θ_{pc}:

$$\begin{aligned} f(r_2, \theta_{pc}) =& r_1(\frac{\tau_p P_c^{min}}{P_{bs}})^{1/\alpha} + r_2(\frac{P_c^{min}}{\tau_c P_{bs}})^{1/\alpha} \\ & - \sqrt{r_1^2 + r_2^2 - 2r_1 r_2 \cos\theta_{pc}} \end{aligned} \tag{10.4}$$

$$\begin{aligned} g(r_2, \theta_{pc}) =& r_1(\frac{\tau_p P_c^{max}}{P_{bs}})^{1/\alpha} + r_2(\frac{P_c^{max}}{\tau_c P_{bs}})^{1/\alpha} \\ & - \sqrt{r_1^2 + r_2^2 - 2r_1 r_2 \cos\theta_{pc}}. \end{aligned} \tag{10.5}$$

If $f(r_2, \theta_{pc}) > 0$, as shown in Figure 10.3(a), the two disks overlap and increasing the transmit power P_{ct} cannot make these two disks separate, therefore, the optimal transmit power of P_{ct} can never be reached. Similarly, if $g(r_2, \theta_{pc}) < 0$, as shown in Figure 10.3(b), there will not be an optimal power either. Hence, the existence of the optimal P_{ct} power relies on r_2 and θ_{pc}. If the optimal power control is feasible, the two cases shown in Figure 10.3 should be avoided. That is, to let the optimal power exist, r_2 and θ_{pc} must be in the set

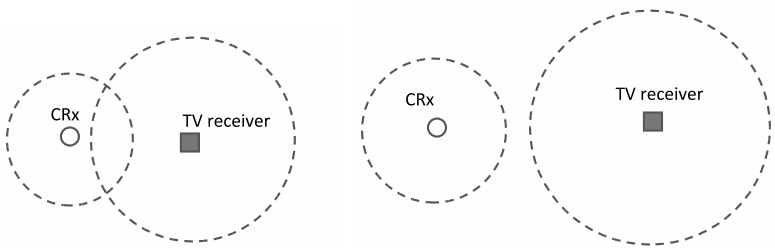

(a) (b)

Figure 10.3: Two possible cases that there will be no solution for (10.3). (a) $f(r_2, \theta_{pc}) > 0$. (b) $g(r_2, \theta_{pc}) < 0$.

$$\{(r_2, \theta_{pc}) | f(r_2, \theta_{pc}) \leq 0 \cap g(r_2, \theta_{pc}) \geq 0)\}. \tag{10.6}$$

Update r_1 , φ_1, r_2 and φ_2;

Calculate θ_{pc}, d_{22}, $f(r_2, \theta_{pc})$ and $g(r_2, \theta_{pc})$;

if $(f(r_2, \theta_{pc}) \leq 0)AND(g(r_2, \theta_{pc}) \geq 0)AND(d_{22} \leq r_{max})$

calculate optimal power; //optimal power could apply

transmit with optimal power;

else if $(g(r_2, \theta_{pc}) < 0)AND(d_{22} \leq r_{max})$

transmit with maximum power; //concurrent transmission

will not affect primary user

else if $(f(r_2, \theta_{pc}) > 0)$

stop transmitting; //concurrent transmission is not

allowed

end if

The above algorithm presents the proposed optimal power control algorithm for the scenario when the CRx is in a fixed location, where r_{max} is the maximum decodable range of the CTx. Recall that the location information of both the CR and PR receivers is available to the CTx. The proposed algorithm first evaluates the feasibility

of the optimal power control for concurrent transmissions. Then, the optimal power can be computed using any numerical method when the optimal power control is feasible. The last case checks the availability of concurrent transmissions, and the CTx will not conduct transmissions unless the condition is violated.

10.2.2 Optimal Power Control for Mobility Scenarios

We now extend our model to the scenario in which the mobility of the CRx is considered. Because of the mobility of the CRx, r_2 and relative angle θ_{pc} change with the movement of the CRx. Thus, the optimal power and the concurrent transmission region also change. Figure 10.4 shows the scenario where the concurrent transmission region evolves with the movement of the CRx from A to B.

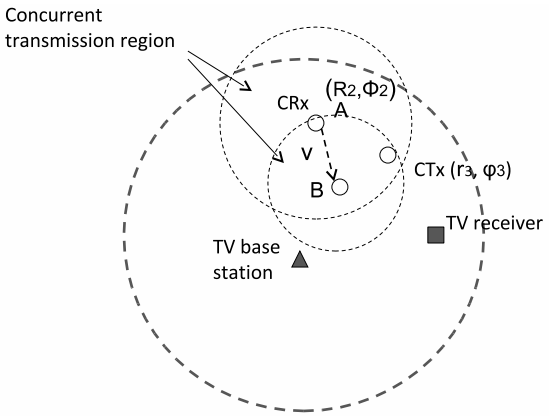

Figure 10.4: The concurrent transmission region evolves with the movement of the CRx.

Without loss of generality, we assume that the CR transmitter is static in a location (r_3, φ_3), and the CRx is moving from a starting point (R_2, Φ_2) with a velocity of $\vec{v} = s\vec{u}$, where s is the speed and $\vec{u} = (\cos\gamma, \sin\gamma)$ is the unit directional vector. Therefore, the polar coordinates of the CRx can be written as:

$$\begin{cases} r_2(t) = \sqrt{(R_2\cos\Phi_2 + st\cos\gamma)^2 + (R_2\sin\Phi_2 + st\sin\gamma)^2} \\ \varphi_2(t) = \arctan(\frac{R_2\sin\Phi_2 + st\sin\gamma}{R_2\cos\Phi_2 + st\cos\gamma}). \end{cases}$$

If the movement pattern of the CRx does not change (i.e., the direction and

velocity remain the same) or the movement pattern is deterministic, the coordinates of the CRx are just functions of time. Therefore, the CTx can "predict" the location of the CRx, thus adjust its transmit power using exactly the same optimal power control algorithm shown in Figure 4.

On the other hand, if the movement pattern of the CRx keeps changing randomly, the CRx should update its location to the CTx for computing the optimal power control. Figure 6 demonstrates the proposed optimal power control algorithm for a mobile CRx that changes movement patterns randomly, where r_{CT} is the radius of the concurrent transmission region.

Update r_1 , φ_1, R_2, Φ_2, r_3, φ_3, s and $\vec{u}$;

Calculate r_2, φ_2, θ_{pc} and d_{22};

if $(d_{22} \leq r_{CT})$AND$(d_{22} \leq r_{max})$

//the distance between CTx and CRx

is still in concurrent transmission region

transmit power remains the same;

else

calculate $f(r_2, \theta_{pc})$ and $g(r_2, \theta_{pc})$;

if $(f(r_2, \theta_{pc}) \leq 0)AND(g(r_2, \theta_{pc}) \geq 0)AND(d_{22} \leq r_{max})$

calculate optimal power;

calculate concurrent transmission radius r_{CT};

transmit with optimal power;

else if $(g(r_2, \theta_{pc}) < 0)AND(d_{22} \leq r_{max})$

transmit with maximum power;

will not affect primary user

else if $(f(r_2, \theta_{pc}) > 0)$

stop transmitting;

end if

end if

10.2.3 Shadowing Fading Effect

In this subsection, we consider the impact of the shadowing fading effect on the optimal power control algorithm. Since the antenna of the TV transmitter is usually hundreds of meters higher than that of the CR transmitter, we loose the assumption that the path loss factors of the PR user and CR user are the same, and assume $\alpha_1 < \alpha_2$, where α_1 and α_2 are the path loss factors of the PR user and CR user, respectively. Using log-distance path loss model [139], the path loss of PR transmissions can be written as:

$$PL_p(r_1)[dB] = PL_p(d_0) + 10\alpha_1 \log(\frac{r_1}{d_0}) + X_\sigma,$$

where d_0 is the reference distance and X_σ is a zero-mean Gaussian random variable with standard deviation σ which is location and distance dependent. Therefore, the received power of the PR receiver is $P_{pr}(r_1) = P_{bs} - PL_p(r_1)$, and interference from the CTx is $P_i(d_{12}) = P_{ct} - PL_c(d_{12})$. Hence, the SIR at the PR receiver is $SIR_p = P_{pr}(r_1) - P_i(d_{12})$. Similarly, the SIR at the CR receiver is $SIR_c = P_{cr}(d_{22}) - P_i(r_2)$. Since the SIRs must satisfy the constraints in (10.1), we have

$$d_{12}[dB] > \frac{P_{ct} + \alpha_1 r_1 + \tau_p + X_\sigma^{'} - P_{bs}}{\alpha_2} \tag{10.7}$$

$$d_{22}[dB] < \frac{P_{ct} + \alpha_1 r_2 - \tau_c - X_\sigma^{'} - P_{bs}}{\alpha_2}, \tag{10.8}$$

where $X_\sigma^{'} \sim N(0, \sqrt{2}\sigma)$. Similar to (10.3), the optimal power is achieved when the following equation is satisfied.

$$\begin{aligned} &10^{\frac{P_{ct}+\alpha_1 r_1+\tau_p+X_\sigma^{'}-P_{bs}}{10\alpha_2}} + 10^{\frac{P_{ct}+\alpha_1 r_2-\tau_c-X_\sigma^{'}-P_{bs}}{10\alpha_2}} \\ &= \sqrt{r_1^2 + r_2^2 - 2r_1 r_2 \cos\theta_{pc}}. \end{aligned} \tag{10.9}$$

The solution of equation (10.9) can be written as

$$P_{ct}[dB] = 10\alpha_2 \lg \left(\frac{\sqrt{r_1^2 + r_2^2 - 2r_1 r_2 \cos\theta_{pc}}}{10^{\frac{\alpha_1 r_1 + \tau_p + X'_\sigma - P_{bs}}{10\alpha_2}} + 10^{\frac{\alpha_1 r_2 - \tau_c - X'_\sigma - P_{bs}}{10\alpha_2}}} \right). \tag{10.10}$$

10.3 Performance Results

In this section, the performance of the proposed optimal power control algorithm is evaluated via simulations and compared with the power control algorithm with fixed transmit power.

10.3.1 Simulation Parameters

The parameters used in our simulations are listed in Table 10.1. We assume that the transmit power of the TV base station is 100 kW [152], the transmit power range of the CTx is [1W, 100W] [152], and the SIR thresholds for the TV and CR receivers are 30dB and 3dB, respectively.

Table 10.1: Simulation Parameters

TV base station transmit power	100kW
maximum transmit power of CTx	100W
minimum transmit power of CTx	1W
coordinates of TV receiver	$(50km, 0°)$
coordinates of CTx	$(50km, 60°)$
SIR thershold for PR receiver	30dB
SIR thershold for CR receiver	3dB
path loss factor	3
Simulation time	1000s

The mobility characteristics of the CRx are modeled using the random waypoint mobility model [112][153]. The CRx changes its movement pattern every ts seconds, where ts is uniformly distributed between 0 and 30s. The average speed of the CRx s is chosen at 10, 20, 30, 40 m/s. The heading angle of the CRx is selected to be uniformly distributed between 0 and 2π. The average pause time of the CRx is set to be 5 seconds. The starting position of the CRx is $(50km,\ 60°)$. The time-based update mechanism is used in our simulations with the time threshold 1 second.

The length of packets sent from the CTx is exponentially distributed with the mean length of 100 bytes. The packets are sent in a Poisson stream fashion with the average arrival rate of 10 packets/s.

10.3.2 Simulation Results

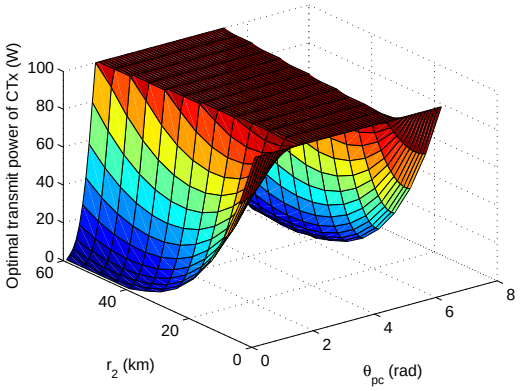

Figure 10.5: Optimal transmit power of CTx for maximum concurrent transmission.

First, from (10.3) we obtain the plane of the optimal power with respect to r_2 and θ_{pc}, as shown in Figure 10.5. It is observed that when θ_{pc} is within a certain range, the optimal power is constant at P_c^{max}. This is because that if the solution of (10.3) is greater than the maximum allowable transmit power of the CTx, the optimal power will be limited to the maximum transmit power.

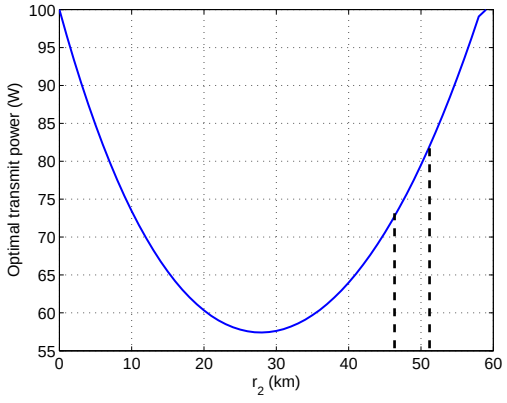

Figure 10.6: Optimal transmit power when $\theta_{pc} = 60°$.

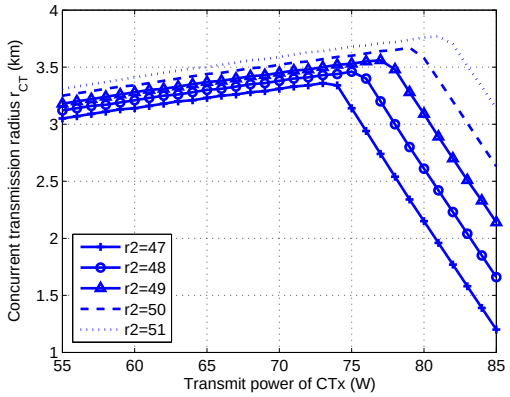

Figure 10.7: Simulation results of concurrent transmission radius vs. transmit power of CTx.

Figure 10.6 along with Figure 10.7 illustrate the relationship between the radius of the concurrent transmission region r_{CT} and the transmit power of the CTx under different r_2. Figure 10.6 is obtained from Figure 10.5 when θ_{pc} is fixed to be 60°, while Figure 10.7 is obtained through the simulation based on the constraints in (10.1). It is noted that when r_2 is in the interval [47km, 51km] as shown in Figure 10.6, the optimal power in these two figures match perfectly, which indicate the analytical and simulation results coincided well. From the proposed optimal power control algorithm shown in Figure 6, the distance between the CTx and the CRx d_{22} must be smaller than the maximum decodable radius of the CTx to let the concurrent transmission be feasible. According to (10.2), the maximum decodable radii of the CTx are 3.7km when r_2 is 47km and 4.2km when r_2 is 54km. So if r_2 is out of the neighborhood of 50km (i.e., [47km, 54km]), d_{22} is larger than the maximum decodable radius of the CTx. Hence, the concurrent transmission radius is zero, which means that the concurrent transmission is not allowed. From Figure 10.6, the radius of the concurrent transmission region increases as the transmit power of the CTx increases. When the transmit power reaches the optimal power, the concurrent transmission radius reaches the maximum, and then it decreases drastically.

Figure 10.8 shows the simulation results of packet delivery ratio of the mobile CR

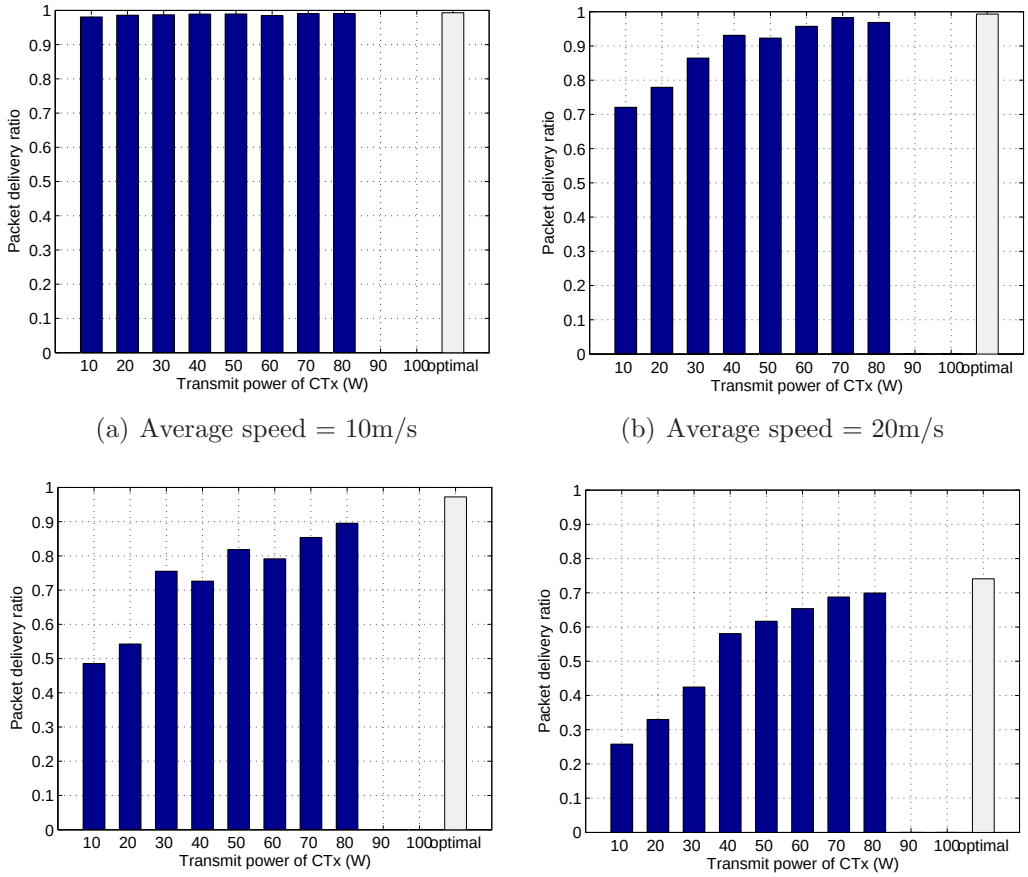

(a) Average speed = 10m/s

(b) Average speed = 20m/s

(c) Average speed = 30m/s

(d) Average speed = 40m/s

Figure 10.8: Packet delivery ratio using fixed power algorithm and the proposed power control algorithm under different average speeds.

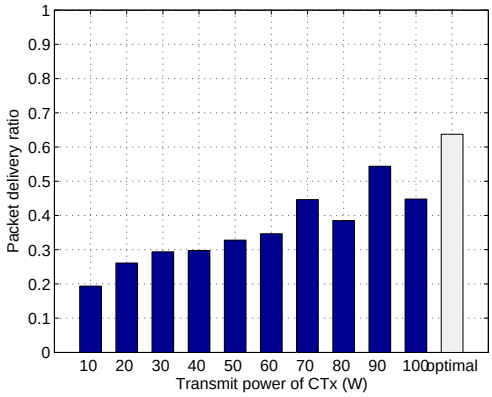

Figure 10.9: Packet delivery ratio under the shadowing fading effect (average speed = 30m/s).

ad hoc network using fixed transmit power of the CTx and the proposed optimal power control algorithm with different moving speeds of the CRx. The mobility characteristics are given in Section 10.3.1. First of all, it is observed that the overall packet delivery ratio suffers degradation as the moving speed of the CRx increases. Secondly, with the same moving speed, the packet delivery ratio increases as the transmit power of the CTx increases. When the fixed transmit power of the CTx exceeds 80W, the packet delivery ratio decreases to zero. This is because that the SIR_p can never be satisfied when the transmit power of the CTx exceeds 80W. However, it is noted that the packet delivery ratio using the proposed optimal power control algorithm is always higher than that of the fixed power algorithm at any speed.

Finally, Figure 10.9 shows the simulation results of the packet delivery ratio under different power control algorithms with the impact of the shadowing fading effect. The mobility characteristics are the same as used for Figure 10.8. The path loss factors of PR and CR transmissions are 3 and 4, respectively. The average speed of the CRx is set to be 30 m/s, and the standard deviation σ is chosen to be 6 dB. Compared to Figure 10.8(c), the overall packet delivery ratio decreases significantly. However, with the shadowing fading effect, the SIR_p can be satisfied with certain probability

when the transmit power of the CTx exceeds 80W. It is observed from the simulation results that the proposed optimal power control algorithm also outperforms the fixed power algorithm under the shadowing fading effect.

CHAPTER 11: CONCLUSION

11.1 Conclusions

In this research, the broadcasting challenges specifically in multi-hop CR ad hoc networks under practical scenarios with collision avoidance have been addressed for the first time. A fully-distributed broadcast protocol named BRACER is proposed without the existence of a global or local common control channel. By intelligently downsizing the original available channel set and designing the broadcasting sequences and broadcast scheduling schemes, our proposed broadcast protocol can provide very high successful broadcast ratio while achieving very short broadcast delay. In addition, it can also avoid broadcast collisions. Simulation results show that our proposed BRACER protocol outperforms other possible broadcast schemes in terms of higher successful broadcast ratio and shorter average broadcast delay.

The performance analysis of broadcast protocols for multi-hop CR ad hoc networks is studied. Due to the non-uniform channel availability in CR networks, several significant differences and unique challenges are introduced when analyzing the performance of broadcast protocols in CR ad hoc networks. A novel unified analytical model is proposed to address these challenges and analyze the broadcast protocols in CR ad hoc networks with any topology. Specifically, two algorithms are proposed to calculate the successful broadcast ratio and the average broadcast delay of a broadcast protocol. In addition, the derivation methods of the single-hop performance metrics for three different broadcast protocols in CR ad hoc networks under practical scenarios are proposed. Results from both the hardware implementation and software simulation validate the analysis well. To the best of our knowledge, this is the first analytical work on the performance analysis of broadcast protocols for multi-hop CR

ad hoc networks.

The optimal HELLO message exchange issue in static and mobile CR ad hoc networks is addressed for the first time. The impact of PU traffic and periodic HELLO message update on SU traffic is mathematically modeled. Based on the proposed analytical model, the trade-off between SU throughput as well as average SU waiting time and control overhead is analytically obtained. Simulation results show that our proposed optimal HELLO message exchange protocol outperforms the change-triggered scheme in terms of higher utilities. The proposed methodology and modeling techniques are enlightening for realizing and optimizing other networking protocols in CR ad hoc networks.

A new type of security threat in CR ad hoc networks called the false channel information exchange attack is investigated. Malicious nodes broadcast false channel information to neighboring nodes so that the victim nodes may make incorrect decisions about other nodes. This attack is extremely challenging to detect and may significantly deteriorate the performance for both the legacy and secondary network. By investigating the spatial correlation of the channel availability between neighboring nodes, the malicious node that sends the false channel information can be identified. Simulation results show that the proposed algorithm can achieve very high detection rate while maintaining low false alarm rate. To the best of our knowledge, this is the first work that defines and addresses the FCIE attacks in CR ad hoc networks.

In this research, a proactive spectrum handoff framework in a CR ad hoc network scenario without the existence of a CCC, ProSpect, is proposed. Compared with the sensing-based reactive spectrum handoff approach, our proposed framework can achieve fewer disruptions to primary transmissions by letting SUs proactively predict the future spectrum availability and perform spectrum handoffs before a PU occupies the current spectrum. We incorporated a single rendezvous and a multiple rendezvous network coordination scheme into the spectrum handoff protocol design,

thus our proposed spectrum handoff framework is suitable for the network scenarios that do not need a CCC. Furthermore, most of the prior work on channel selection in spectrum handoffs only considers a two-SU scenario, while the channel selection issue for a multi-SU scenario is ignored. In this dissertation, we proposed a novel fully distributed channel selection scheme which leads to zero collision among SUs in a multi-SU scenario. Simulation results show that network coordination is crucial to the performance of spectrum handoffs. Performance results also indicate that our proposed channel selection scheme outperforms the existing methods in terms of higher throughput and shorter handoff delay in multi-SU scenarios.

A novel three dimensional discrete-time Markov chain is proposed to analyze the performance of SUs in the spectrum handoff scenario in a CR ad hoc network. We performed extensive simulations in different network scenarios to validate our proposed model. The analysis shows that our proposed Markov model is very flexible and can be applied to various practical network scenarios. Thus, our analysis provides insights into the spectrum handoff process for CR networks. This allows us to obtain the throughput and other performance metrics for various design requirements. Currently, no existing analysis has considered the comprehensive aspects of spectrum handoff as what we considered in this dissertation. Finally, although we focus on the spectrum handoff scenario in CR networks, the modeling techniques developed in the dissertation are quite general and are applicable to other multi-channel scenarios with multiple interacting users.

The end-to-end congestion control issue in multi-hop CR ad hoc networks without a CCC is investigated for the first time. A comprehensive end-to-end congestion control framework is proposed for multi-hop CR ad hoc networks without a CCC. Our proposed framework considers the interactions from the physical layer to the transport layer in a network. In addition, we observe that the delay of the ECN messages has a significant impact on the network performance. Our study shows that

the existing methods of the end-to-end congestion control for traditional wireless ad hoc networks perform poorly in CR ad hoc networks.

Finally, an optimal power control algorithm for concurrent transmissions of location-aware mobile CR ad hoc networks is proposed. The proposed algorithm incorporates the mobility characteristics of the CR receiver in the algorithm design and is aimed to maximize the concurrent transmission region of CR users, hence improving the throughput of CR links. Simulation results demonstrate that the packet delivery ratio of the proposed optimal power control algorithm can be effectively improved, as compared to that of the fixed power algorithm. The impact of the shadowing fading effect on the proposed algorithm is also considered. It is shown that the proposed power control algorithm also outperforms the fixed power control algorithm under the shadowing fading effect.

11.1.1 Completed Work

In this dissertation, the following research work has been completed:

1. Two distributed broadcast protocols for cognitive radio ad hoc networks are proposed under practical constraints [23, 24, 103, 104].

2. A novel unified analytical model for performance analysis of broadcast protocols in cognitive radio ad hoc networks is developed to analyze the performance of broadcast protocols [154].

3. An optimal control information exchange scheme for cognitive radio ad hoc networks are proposed to efficiently update the control information among SUs.

4. Network security protocols to fight against false channel information exchange attacks in cognitive radio ad hoc networks are designed [155].

5. A proactive spectrum handoff framework for cognitive radio ad hoc networks is developed to realize seamless communications [89].

6. A novel 3-dimensional Markov model for performance analysis of spectrum handoff in cognitive radio ad hoc networks is proposed to analyze the performance of the

spectrum handoff protocols [88].

11.2 Future Work

In the future, I would like to direct, but not limit my future research effort, to the following research topics:

1. Cognitive radio network security algorithms design: Most of the current research efforts in cognitive radio networks still focus on pure physical layer or higher layer issues without considering the security aspects. The security issues in cognitive radio networks have drawn the attention of the research community only in recent years. Since cognitive radios can intelligently adapt to their radio environments, many unique security threats are introduced in cognitive radio networks that are different from traditional wireless networks. I am particularly interested in identifying unique malicious threats in cognitive radio networks and providing robust security solutions to defend these threats.

2. End-to-end congestion control protocol designs: In this research, we have studied the existing end-to-end congestion control schemes for multi-hop CR ad hoc networks. We have identified several challenges in these existing schemes. However, we have not proposed any new protocol to support end-to-end congestion control in CR ad hoc networks. In the future, I would like to investigate the end-to-end congestion control protocol design, which is not considered in previous works.

3. Spectrum and energy-efficient wireless systems: Spectrum and energy efficiencies are among the most important venues for technological advances in current and emerging wireless communication networks. The past decade has witnessed tremendous efforts and progress made by both the industry and academia for improving spectrum efficiency. It is known that cognitive and self-organizing networks will further increase spectrum efficiency. In recent years, energy and power efficiencies of wireless networks have become more crucial because of the steadily rising energy cost and environmental concerns. While there has been a paradigm shift from improving

spectrum efficiency to reducing energy consumption, a dilemma also arises as some energy efficiency criteria are in conflict with the spectrum efficiency objectives. I am particularly interested in the research that jointly considers spectrum and energy efficiencies using cognitive radio technologies.

REFERENCES

[1] FCC, "Notice of proposed rule making and order," December 2003.

[2] ——. (2003, November) Et docket no. 03-237. [Online]. Available: http://hraunfoss.fcc.gov/edocs_public/attachmatch/FCC-03-289A1.pdf

[3] J. M. III, "Cognitive radio: an integrated agent architecture for software defined radio," Ph.D. dissertation, KTH Royal Institute of Technology, Sweden, 2000.

[4] I. F. Akyildiz, W.-Y. Lee, M. C. Vuran, and S. Mohanty, "NeXt generation/dynamic spectrum access/cognitive radio wireless networks: A survey," *Computer Networks (Elsevier)*, vol. 50, 2006.

[5] I. F. Akyildiz, W.-Y. Lee, and K. R. Chowdhury, "CRAHNs: cognitive radio ad hoc networks," *Ad Hoc Networks*, vol. 7, no. 5, pp. 810–836, July 2009.

[6] D. Cabric, S. M. Mishra, and R. W. Brodersen, "Implementation issues in spectrum sensing for cognitive radios," in *Proc. 38hth Asilomar Conference on Signals, Systems and Computers*, vol. 1, Nov. 2004, pp. 772–776.

[7] S. Mishra, A. Sahai, and R. Brodersen, "Cooperative sensing among cognitive radios," in *Proc. IEEE ICC*, June 2006, pp. 1658–1663.

[8] FCC. (2003, November) Et docket no. 03-289 notice of proposed rule making and order.

[9] G. Resta, P. Santi, and J. Simon, "Analysis of multi-hop emergency message propagation in vehicular ad hoc networks," in *Proc. ACM MobiHoc*, 2007, pp. 140–149.

[10] I. Chlamtac and S. Kutten, "On broadcasting in radio networks — problem analysis and protocol design," *IEEE Transactions on Communications*, vol. 33, no. 12, pp. 1240–1246, Dec. 1985.

[11] S.-Y. Ni, Y.-C. Tseng, Y.-S. Chen, and J.-P. Sheu, "The broadcast storm problem in a mobile ad hoc network," in *Proc. ACM MobiCom*, 1999, pp. 151–162.

[12] J. Wu and F. Dai, "Broadcasting in ad hoc networks based on self-pruning," in *Proc. IEEE INFOCOM*, 2003, pp. 2240–2250.

[13] J. Qadir, A. Misra, and C. T. Chou, "Minimum latency broadcasting in multi-radio multi-channel multi-rate wireless meshes," in *Proc. IEEE SECON*, vol. 1, 2006, pp. 80–89.

[14] A. Qayyum, L. Viennot, and A. Laouiti, "Multipoint relaying for flooding broadcast messages in mobile wireless networks," in *Proc. HICSS*, 2002, pp. 3866–3875.

[15] Z. Haas, J. Halpern, and L. Li, "Gossip-based ad hoc routing," *IEEE/ACM Trans. Networking*, vol. 14, no. 3, pp. 479–491, June 2006.

[16] Z. Chen, C. Qiao, J. Xu, and T. Lee, "A constant approximation algorithm for interference aware broadcast in wireless networks," in *Proc. IEEE INFOCOM*, 2007, pp. 740–748.

[17] S. Huang, P.-J. Wan, X. Jia, H. Du, and W. Shang, "Broadcast scheduling in interference environment," *IEEE Transactions on Mobile Computing*, vol. 7, no. 11, pp. 1338–1348, 2008.

[18] R. Mahjourian, F. Chen, R. Tiwari, M. Thai, H. Zhai, and Y. Fang, "An approximation algorithm for conflict-aware broadcast scheduling in wireless ad hoc networks," in *Proc. ACM MobiHoc*, 2008, pp. 331–340.

[19] R. Gandhi, A. Mishra, and S. Parthasarathy, "Minimizing broadcast latency and redundancy in ad hoc networks," *IEEE/ACM Transactions on Networking*, vol. 16, no. 4, pp. 840–851, 2008.

[20] R. Ramaswami and K. Parhi, "Distributed scheduling of broadcasts in a radio network," in *Proc. IEEE INFOCOM*, 1989, pp. 497–504.

[21] Y. Kondareddy and P. Agrawal, "Selective broadcasting in multi-hop cognitive radio networks," in *Proc. IEEE Sarnoff Symposium*, 2008, pp. 1–5.

[22] C. J. L. Arachchige, S. Venkatesan, R. Chandrasekaran, and N. Mittal, "Minimal time broadcasting in cognitive radio networks," in *Proc. ICDCN*, 2011, pp. 364–375.

[23] Y. Song and J. Xie, "A QoS-based broadcast protocol for multi-hop cognitive radio ad hoc networks under blind information," in *Proc. IEEE GLOBECOM*, 2011.

[24] ——, "A distributed broadcast protocol in multi-hop cognitive radio ad hoc networks without a common control channel," in *Proc. IEEE INFOCOM*, 2012.

[25] N. Alon, A. Bar-Noy, N. Linial, and D. Peleg, "A lower bound for radio broadcast," *Journal of Computer System Science*, vol. 43, pp. 290–298, October 1991.

[26] B. Chlebus, L. Gasieniec, A. Gibbons, A. Pelc, and W. Rytter, "Deterministic broadcasting in unknown radio networks," in *Proc. ACM-SIAM Symposium on Discrete Algorithms (SODA)*, 2000, pp. 861–870.

[27] B. Williams and T. Camp, "Comparison of broadcasting techniques for mobile ad hoc networks," in *Proc. ACM International Symposium on Mobile Ad Hoc Networking & Computing (MobiHoc)*, 2002, pp. 194–205.

[28] A. Czumaj and W. Rytter, "Broadcasting algorithms in radio networks with unknown topology," *Journal of Algorithms*, vol. 60, pp. 115–143, August 2006.

[29] W. Lou and J. Wu, "Toward broadcast reliability in mobile ad hoc networks with double coverage," *IEEE Transactions on Mobile Computing*, vol. 6, no. 2, pp. 148–163, 2007.

[30] N. Theis, R. Thomas, and L. DaSilva, "Rendezvous for cognitive radios," *IEEE Trans. Mobile Computing*, vol. 10, no. 2, pp. 216–227, 2010.

[31] C. Cormio and K. R. Chowdhury, "Common control channel design for cognitive radio wireless ad hoc networks using adaptive frequency hopping," *Ad Hoc Networks*, vol. 8, no. 4, pp. 430–438, 2010.

[32] Y. Zhang, Q. Li, G. Yu, and B. Wang, "ETCH: Efficient channel hopping for communication rendezvous in dynamic spectrum access networks," in *Proc. IEEE INFOCOM*, 2011, pp. 2471–2479.

[33] Z. Lin, H. Liu, X. Chu, and Y.-W. Leung, "Jump-stay based channel hopping algorithm with guaranteed rendezvous for cognitive radio networks," in *Proc. IEEE INFOCOM*, 2011.

[34] K. Bian, J.-M. Park, and R. Chen, "Control channel establishment in cognitive radio networks using channel hopping," *IEEE JSAC*, vol. 29, no. 4, pp. 689–703, April 2011.

[35] C. E. Perkins, E. M. Belding-Royer, and S. Das, "Ad hoc on-demand distance vector (AODV) routing," Request for Comments (RFC) 3561, Internet Engineering Task Force (IETF), July 2003.

[36] T. Clausen and P. Jacquet, "Optimized link state routing protocol (OLSR)," IETF Request for Comments (RFC) 3626, October 2003.

[37] B. Karp and H. T. Kung, "GPSR: greedy perimeter stateless routing for wireless networks," in *Proc. ACM MobiCom*, 2000, pp. 243–254.

[38] C. Cordeiro and K. Challapali, "C-MAC: A cognitive MAC protocol for multi-channel wireless networks," in *Proc. IEEE DySPAN*, April 2007, pp. 147–157.

[39] L. Cao and H. Zheng, "Distributed rule-regulated spectrum sharing," *IEEE Journal on Selected Areas in Communications (JSAC)*, vol. 26, no. 1, pp. 130–145, January 2008.

[40] K. R. Chowdhury and M. Di Felice, "SEARCH: A routing protocol for mobile cognitive radio ad-hoc networks," in *Proc. IEEE Sarnoff Symposium*, 2009, pp. 1–6.

[41] J. Zhao and G. Cao, "Robust topology control in multi-hop cognitive radio networks," in *Proc. IEEE INFOCOM*, march 2012, pp. 2032–2040.

[42] J. Mo, H.-S. W. So, and J. Walrand, "Comparison of multichannel MAC protocols," *IEEE Trans. on Mobile Computing*, vol. 7, no. 1, 2008.

[43] I. D. Chakeres and E. M. Belding-Royer, "The utility of hello messages for determining link connectivity," in *Proc. International Symposium on Wireless Personal Multimedia Communications*, 2002, pp. 504–508.

[44] P. Samar and S. B. Wicker, "On the behavior of communication links of a node in a multi-hop mobile environment," in *Proc. ACM MobiHoc*, 2004, pp. 145–156.

[45] V. C. Giruka and M. Singhal, "Hello protocols for ad-hoc networks: overhead and accuracy tradeoffs," in *Proc. IEEE WoWMoM*, June 2005, pp. 354–361.

[46] F. Ingelrest, N. Mitton, and D. Simplot-Ryl, "A turnover based adaptive hello protocol for mobile ad hoc and sensor networks," in *Proc. MASCOTS*, Oct. 2007, pp. 9–14.

[47] T. C. Clancy and N. Goergen, "Security in cognitive radio networks: Threats and mitigation," in *Proc. International Conference on Cognitive Radio Oriented Wireless Networks and Communications (CrownCom)*, 2008, pp. 1–8.

[48] J. L. Burbank, "Security in cognitive radio networks: The required evolution in approaches to wireless network security," in *Proc. International Conference on Cognitive Radio Oriented Wireless Networks and Communications (CrownCom)*, May 2008, pp. 1–7.

[49] R. Chen, J.-M. Park, and J. H. Reed, "Defense against primary user emulation attacks in cognitive radio networks," *IEEE Journal on Selected Areas in Communications (JSAC)*, vol. 26, no. 1, pp. 25–37, January 2008.

[50] R. Chen, J.-M. Park, Y. T. Hou, and J. H. Reed, "Toward secure distributed spectrum sensing in cognitive radio networks," *IEEE Communications Magazine*, vol. 46, no. 4, pp. 50–55, April 2008.

[51] B. Wang, Y. Wu, K. J. R. Liu, and T. C. Clancy, "An anti-jamming stochastic game for cognitive radio networks," *IEEE Journal on Selected Areas in Communications (JSAC)*, vol. 29, no. 4, pp. 877–889, April 2011.

[52] J. Zhao, H. Zheng, and G. Yang, "Spectrum sharing through distributed coordination in dynamic spectrum access networks," *Wireless Communications and Mobile Computing*, vol. 7, pp. 1061–1075, November 2007.

[53] H. Ma, L. Zheng, X. Ma, and Y. Luo, "Spectrum aware routing for multi-hop cognitive radio networks with a single transceiver," in *Proc. International Conference on Cognitive Radio Oriented Wireless Networks and Communications (CrownCom)*, May 2008, pp. 1–6.

[54] D. Willkomm, J. Gross, and A. Wolisz, "Reliable link maintenance in cognitive radio systems," in *Proc. IEEE International Symposium on New Frontiers in Dynamic Spectrum Access Networks (DySPAN)*, November 2005, pp. 371–378.

[55] C.-W. Wang and L.-C. Wang, "Modeling and analysis for proactive-decision spectrum handoff in cognitive radio networks," in *Proc. IEEE ICC*, June 2009, pp. 1–6.

[56] Y. Zhang, "Spectrum handoff in cognitive radio networks: Opportunistic and negotiated situations," in *Proc. IEEE ICC*, June 2009, pp. 1–6.

[57] C.-W. Wang and L.-C. Wang, "Modeling and analysis for reactive-decision spectrum handoff in cognitive radio networks," in *Proc. IEEE GlobeCom*, 2010, pp. 1–6.

[58] L. Yang, L. Cao, and H. Zheng, "Proactive channel access in dynamic spectrum networks," *Physical Communication (Elsevier)*, vol. 1, pp. 103–111, June 2008.

[59] T. Clancy and B. Walker, "Predictive dynamic spectrum access," in *Proc. SDR Forum Technical Conference*, Orlando, Florida, USA, November 2006.

[60] S. Yarkan and H. Arslan, "Binary time series approach to spectrum prediction for cognitive radio," in *Proc. Vehicular Technology Conference (VTC)*, October 2007, pp. 1563–1567.

[61] C. Song and Q. Zhang, "Intelligent dynamic spectrum access assisted by channel usage prediction," in *IEEE INFOCOM Conference on Computer Communications Workshops*, 2010, pp. 1–6.

[62] S. Geirhofer, J. Z. Sun, L. Tong, and B. M. Sadler, "Cognitive frequency hopping based on interference prediction: theory and experimental results," *ACM SIGMOBILE Mobile Computing and Communications Review*, vol. 13, no. 2, pp. 49–61, 2009.

[63] S. Geirhofer, L. Tong, and B. Sadler, "Cognitive medium access: Constraining interference based on experimental models," *IEEE Journal on Selected Area in Communications*, vol. 26, no. 1, pp. 95–105, 2008.

[64] S. Huang, X. Liu, and Z. Ding, "Optimal transmission strategies for dynamic spectrum access in cognitive radio networks," *IEEE Transactions on Mobile Computing*, vol. 8, no. 12, pp. 1636–1648, 2009.

[65] S.-U. Yoon and E. Ekici, "Voluntary spectrum handoff: A novel approach to spectrum management in CRNs," in *Proc. IEEE International Conference on Communications (ICC)*, 2010.

[66] C. R. Stevenson, G. Chouinard, Z. Lei, W. Hu, S. J. Shellhammer, and W. Caldwell, "IEEE 802.22: The first cognitive radio wireless regional area network standard," *IEEE Communications Magazine*, vol. 47, no. 1, pp. 130–138, January 2009.

[67] K. Challapali, C. Cordeiro, and D. Birru, "Evolution of spectrum-agile cognitive radios: first wireless Internet standard and beyond," in *Proc. International Wireless Internet Conference (WICON)*, 2006.

[68] J. Neel, "Analysis and design of cognitive radio networks and distributed radio resource management algorithms," Ph.D. dissertation, Virginia Polytechnic Institute and State University, September 2006.

[69] S. Sengupta and M. Chatterjee, "Designing auction mechanisms for dynamic spectrum access," *Mobile Network and Applications*, vol. 13, no. 5, pp. 498–515, 2008.

[70] D. Niyato and E. Hossain, "Competitive pricing for spectrum sharing in cognitive radio networks: Dynamic game, inefficiency of nash equilibrium, and collusion," *IEEE Journal on Selected Areas in Communications*, vol. 26, no. 1, pp. 192–202, January 2008.

[71] H. Zheng and L. Cao, "Device-centric spectrum management," in *Proc. IEEE International Symposium on New Frontiers in Dynamic Spectrum Access Networks (DySPAN)*, November 2005, pp. 56–65.

[72] S. Wang, J. Zhang, and L. Tong, "Delay analysis for cognitive radio networks with random access: A fluid queue view," in *Proc. IEEE INFOCOM*, 2010, pp. 1–9.

[73] A. Laourine, S. Chen, and L. Tong, "Queuing analysis in multichannel cognitive spectrum access: A large deviation approach," in *Proc. IEEE INFOCOM*, 2010, pp. 1–9.

[74] L. Lazos, S. Liu, and M. Krunz, "Spectrum opportunity-based control channel assignment in cognitive radio networks," in *Proc. IEEE SECON*, 2009, pp. 1–9.

[75] J. Zhao, H. Zheng, and G. Yang, "Spectrum sharing through distributed coordination in dynamic spectrum access networks," *Wireless Communications and Mobile Computing*, vol. 7, pp. 1061–1075, November 2007.

[76] C. Campolo, A. Molinaro, A. Vinel, and Y. Zhang, "Modeling prioritized broadcasting in multichannel vehicular networks," *IEEE Transactions on Vehicular Technology*, vol. 61, pp. 687–701, February 2012.

[77] X. Ma, J. Zhang, X. Yin, and K. S. Trivedi, "Design and analysis of a robust broadcast scheme for VANET safety-related services," *IEEE Transactions on Vehicular Technology*, vol. 61, pp. 46–61, January 2012.

[78] Q. Yang, J. Zheng, and L. Shen, "Modeling and performance analysis of periodic broadcast in vehicular ad hoc networks," in *Proc. IEEE GLOBECOM*, 2011, pp. 1–5.

[79] J. Chen, "AMNP: ad hoc multichannel negotiation protocol with broadcast solutions for multi-hop mobile wireless networks," *IET Communications*, vol. 4, no. 5, pp. 521–531, 26 2010.

[80] Y. Wan, X. Chen, and J. Lu, "Broadcast enhanced cooperative asynchronous multichannel MAC for wireless ad hoc network," in *Proc. WiCOM*, 2011, pp. 1–5.

[81] L. Lin, W. Jia, and W. Lu, "Performance analysis of IEEE 802.16 multicast and broadcast polling based bandwidth request," in *Proc. IEEE WCNC*, 2007, pp. 1854–1859.

[82] J. Qadir, C. T. Chou, A. Misra, and J. G. Lim, "Minimum latency broadcasting in multiradio, multichannel, multirate wireless meshes," *IEEE Transactions on Mobile Computing*, vol. 8, no. 11, pp. 1510–1523, November 2009.

[83] F. Hu, S. Wang, and Z. Cheng, "Secure cooperative spectrum sensing for cognitive radio networks," in *Proc. IEEE Military Communications Conference (MILCOM)*, 2009, pp. 1–7.

[84] J. Wei and X. Zhang, "Two-tier optimal-cooperation based secure distributed spectrum sensing for wireless cognitive radio networks," in *Proc. IEEE INFOCOM Workshops*, 2010, pp. 1–6.

[85] P. Kaligineedi, M. Khabbazian, and V. K. Bhargava, "Malicious user detection in a cognitive radio cooperative sensing system," *IEEE Transactions on Wireless Communications*, vol. 9, no. 8, pp. 2488–2497, August 2010.

[86] A. S. Rawat, P. Anand, H. Chen, and P. K. Varshney, "Collaborative spectrum sensing in the presence of byzantine attacks in cognitive radio networks," *IEEE Transactions on Signal Processing*, vol. 59, no. 2, pp. 774–786, Feburary 2011.

[87] C. Gao, Y. Shi, Y. T. Hou, H. D. Sherali, and H. Zhou, "Multicast communications in multi-hop cognitive radio networks," *IEEE Journal on Selected Areas in Communications (JSAC)*, vol. 29, no. 4, pp. 784–793, April 2011.

[88] Y. Song and J. Xie, "Performance analysis of spectrum handoff for cognitive radio ad hoc networks without common control channel under homogeneous primary traffic," in *Proc. IEEE INFOCOM*, 2011, pp. 3011–3019.

[89] ——, "ProSpect: A proactive spectrum handoff framework for cognitive radio ad hoc networks without common control channel," *IEEE Transactions on Mobile Computing*, vol. 11, no. 7, pp. 1127–1139, July 2012.

[90] F. Gebali, *Analysis of Computer and Communication Networks*. Springer, 2008.

[91] T. Camp, J. Boleng, and V. Davies, "A survey of mobility models for ad hoc network research," *Wireless Communications and Mobile Computing*, vol. 2, pp. 483–502, August 2002.

[92] B. H. Wellenhoff, H. Lichtenegger, and J. Collins, *Global Positions System: Theory and Practice*, 5th ed. Springer, 2001.

[93] N. Bulusu, J. Heidemann, and D. Estrin, "GPS-less low cost outdoor localization for very small devices," *IEEE Personal Communications*, vol. 7, no. 5, pp. 28–34, Oct. 2000.

[94] A. Savvides, C.-C. Han, and M. B. Strivastava, "Dynamic fine-grained localization in ad-hoc networks of sensors," in *Proc. ACM MobiCom*, 2001, pp. 166–179.

[95] T. He, C. Huang, B. M. Blum, J. A. Stankovic, and T. Abdelzaher, "Range-free localization schemes for large scale sensor networks," in *Proc. ACM MobiCom*, 2003, pp. 81–95.

[96] H. Celebi and H. Arslan, "Cognitive positioning systems," *IEEE Transactions on Wireless Communications*, vol. 6, no. 12, pp. 4475–4483, Dec. 2007.

[97] O. Duval, A. Punchihewa, F. Gagnon, C. Despins, and V. K. Bhargava, "Blind multi-sources detection and localization for cognitive radio," in *Proc. IEEE GLOBECOM*, 2008, pp. 1–5.

[98] S. Liu, Y. Chen, W. Trappe, and L. J. Greenstein, "Non-interactive localization of cognitive radios based on dynamic signal strength mapping," in *Proc. International Conference on Wireless On-Demand Network Systems and Services (WONS)*, 2009, pp. 85–92.

[99] Y. Wang, L. Zhou, and R. Wang, "A novel frequency sense solution for cognitive radio based on tracing localization," in *Proc. IEEE International Conference on Communications (ICC)*, 2011, pp. 1–5.

[100] M. Marina and S. Das, "Performance of route caching strategies in dynamic source routing," in *Proc. International Conference on Distributed Computing Systems Workshop*, 2001, pp. 425–432.

[101] S.-J. Lee and M. Gerla, "Split multipath routing with maximally disjoint paths in ad hoc networks," in *Proc. IEEE ICC*, vol. 10, 2001, pp. 3201–3205.

[102] C. Perkins, E. Royer, S. Das, and M. Marina, "Performance comparison of two on-demand routing protocols for ad hoc networks," *IEEE Personal Communications*, vol. 8, no. 1, pp. 16–28, Feb. 2001.

[103] Y. Song and J. Xie, "QB2IC: A QoS-based broadcast protocol under blind information for multi-hop cognitive radio ad hoc networks," *submitted to IEEE Transactions on Vehicular Technology*, 2013.

[104] ——, "BRACER: A distributed broadcast protocol in multi-hop cognitive radio ad hoc networks with collision avoidance," *submitted to IEEE Transactions on Mobile Computing*, 2012.

[105] X. Wang, "Power efficient time-controlled CSMA/CA MAC protocol for lunar surface networks," in *Proc. IEEE GLOBECOM*, 2010, pp. 1–5.

[106] "IEEE Standard for Information Technology - Telecommunications and Information Exchange Between Systems - LAN/MAN Specific Requirements - Part 11: Wireless LAN Medium Access Control (MAC) and Physical Layer (PHY) Specifications," IEEE Std 802.11-2012 (Revision of IEEE Std 802.11-2007), 2012.

[107] Y. Song and J. Xie, "Common hopping based proactive spectrum handoff in cognitive radio ad hoc networks," in *Proc. IEEE GLOBECOM*, 2010, pp. 1–5.

[108] L. Kleinrock, *Queueing System, Volume I: Theory.* John Wiley & Sons, 1975.

[109] A. W. Min, K.-H. Kim, J. P. Singh, and K. G. Shin, "Opportunistic spectrum access for mobile cognitive radios," in *Proc. IEEE INFOCOM*, April 2011, pp. 2993–3001.

[110] W.-Y. Lee and I. F. Akyildiz, "Spectrum-aware mobility management in cognitive radio cellular networks," *IEEE Transactions on Mobile Computing*, vol. 11, no. 4, pp. 529–542, April 2012.

[111] N. Srinivas and K. Deb, "Multiobjective optimization using nondominated sorting in genetic algorithms," *Evolutionary Computation*, vol. 2, pp. 221–248, 1994.

[112] T. Camp, J. Boleng, and V. Davies, "A survey of mobility models for ad hoc network research." *Wireless Communications and Mobile Computing*, vol. 2, pp. 483–502, 2002.

[113] E. Ferro and F. Potorti, "Bluetooth and Wi-Fi wireless protocols: a survey and a comparison," *IEEE Wireless Communications*, vol. 12, no. 1, pp. 12–26, Feb. 2005.

[114] H. W. So and J. Walrand, "McMAC: A multi-channel MAC proposal for ad-hoc wireless networks," in *Proc. of IEEE Wireless Communication and Networking Conference (WCNC)*, 2007.

[115] F. Sivrikaya and B. Yener, "Time synchronization in sensor networks: a survey," *IEEE Network*, vol. 18, no. 4, pp. 45–50, July-August 2004.

[116] H. Su and X. Zhang, "Cross-layer based opportunistic MAC protocols for QoS provisionings over cognitive radio mobile wireless networks," *IEEE Journal on Selected Areas in Communications (JSAC)*, vol. 26, no. 1, pp. 118–129, January 2008.

[117] ——, "Channel-hopping based single transceiver MAC for cognitive radio networks," in *Proc. 42nd Annual Conference on Information Sciences and Systems (CISS)*, 2008, pp. 197–202.

[118] Y. Song and J. Xie, "Optimal power control for concurrent transmissions of location-aware mobile cognitive radio ad hoc networks," in *Proc. IEEE GLOBECOM*, 2009, pp. 1–6.

[119] ——, *Cognitive Radio Mobile Ad Hoc Networks*. Springer, 2011, ch. On the Spectrum Handoff for Cognitive Radio Ad Hoc Networks without Common Control Channel.

[120] *Wireless LAN Medium Access Control (MAC) and Physical Layer (PHY) Specification*, IEEE Std. 802.11b, 2012.

[121] M. Blum, "On the sums of independently distributed pareto variates," *SIAM Journal on Applied Mathematics*, vol. 19, no. 1, pp. 191–198, July 1970.

[122] S. Tang and B. L. Mark, "Modeling and analysis of opportunistic spectrum sharing with unreliable spectrum sensing," *IEEE Transactions on Wireless Communications*, vol. 8, no. 4, pp. 1934–1943, 2009.

[123] H. Su and X. Zhang, "Cross-layer based opportunistic MAC protocols for QoS provisionings over cognitive radio wireless networks," *IEEE Journal on Selected Areas in Communications (JSAC)*, vol. 26, no. 1, pp. 118–129, January 2008.

[124] Y. Song and J. Xie, "Proactive spectrum handoff in cognitive radio ad hoc networks based on common hopping coordination," in *INFOCOM IEEE Conference on Computer Communications Workshops , 2010*, march 2010, pp. 1–2.

[125] B. Wang and K. J. R. Liu, "Advances in cognitive radio networks: A survey," *IEEE Journal of Selected Topics in Signal Processing*, vol. 5, no. 1, pp. 5–23, Feb. 2011.

[126] S. Floyd and V. Jacobson, "Random early detection gateways for congestion avoidance," *IEEE/ACM Transactions on Networing*, vol. 1, no. 4, pp. 397–413, Aug. 1993.

[127] H. Balakrishnan, V. N. Padmanabhan, S. Seshan, and R. H. Katz, "A comparison of mechanisms for improving TCP performance over wireless links," *IEEE/ACM Transactions on Networking*, vol. 5, pp. 756–769, 1997.

[128] S. Floyd and K. Fall, "Promoting the use of end-to-end congestion control in the Internet," *IEEE/ACM Transactions on Networking*, vol. 7, no. 4, pp. 458–472, Aug. 1999.

[129] J. Liu and S. Singh, "ATCP: TCP for mobile ad hoc networks," *IEEE Journal on Selected Areas in Communications*, vol. 19, no. 7, pp. 1300–1315, 2001.

[130] S. Kunniyur and R. Srikant, "End-to-end congestion control schemes: utility functions, random losses and ECN marks," *IEEE/ACM Transactions on Networking*, vol. 11, no. 5, pp. 689–702, Oct. 2003.

[131] K. R. Chowdhury, M. D. Felice, and I. F. Akyildiz, "TP-CRAHN: a transport protocol for cognitive radio ad-hoc networks," in *Proc. IEEE INFOCOM*, 2009, pp. 2482–2490.

[132] M. D. Felice, K. R. Chowdhury, and L. Bononi, "Modeling and performance evaluation of transmission control protocol over cognitive radio ad hoc networks," in *Proc. ACM International Conference on Modeling, Analysis and Simulation of Wireless and Mobile Systems (MSWiM)*, 2009.

[133] T. Issariyakul, L. S. Pillutla, and V. Krishnamurthy, "Tuning radio resource in an overlay cognitive radio network for TCP: greed isn't good," *IEEE Communications Magazine*, vol. 47, no. 7, pp. 57–63, July 2009.

[134] D. Sarkar and H. Narayan, "Transport layer protocol for cognitive radio networks," in *Proc. IEEE INFOCOM Workshops*, 2010.

[135] K. Sundaresan, V. Anantharaman, H.-Y. Hsieh, and R. Sivakumar, "ATP: A reliable transport protocol for ad hoc networks," *IEEE Transactions on Mobile Computing*, vol. 4, no. 6, pp. 588–603, 2005.

[136] S. Floyd, "TCP and explicit congestion notification," *ACM SIGCOMM Computer Communication Review*, vol. 24, no. 5, pp. 8–23, Oct. 1994.

[137] H. Kim and K. G. Shin, "In-band spectrum sensing in IEEE 802.22 WRANs for incumbent protection," *IEEE Transactions on Mobile Computing*, vol. 9, no. 12, pp. 1766–1779, Dec. 2010.

[138] V. Jacobson, "Congestion avoidance and control," in *Proc. ACM SIGCOMM '88*, 1988, pp. 314–329.

[139] T. S. Rappaport, *Wireless Communications: Principles and Practice*, 2nd ed. Prentice Hall, 2002.

[140] A. Fehske, J. Gaeddert, and J. Reed, "A new approach to signal classification using spectral correlation and neural networks," in *Proc. IEEE International Symposium on New Frontiers in Dynamic Spectrum Access Networks (DySPAN)*, November 2005, pp. 144–150.

[141] B. Wild and K. Ramchandran, "Detecting primary receivers for cognitive radio applications," in *Proc. IEEE DySPAN*, November 2005, pp. 124–130.

[142] S. M. Hur, S. Mao, Y. T. Hou, K. Nam, and J. H. Reed, "Exploiting location information for concurrent transmissions in multihop wireless networks," *IEEE Trans. Vehicular Technology*, vol. 58, no. 1, pp. 314–323, January 2009.

[143] X. Zhang, K. Shin, D. Saha, and D. Kandlur, "Scalable flow control for multicast ABR services in ATM networks," *IEEE/ACM Transactions on Networking*, vol. 10, no. 1, pp. 67–85, February 2002.

[144] L. Qian, X. Li, J. Attia, and Z. Gajic, "Power control for cognitive radio ad hoc network," in *Proc. IEEE Workshop on Local and Metropolitan Area Networks*, 2007, pp. 7–12.

[145] X. Li, J. Chen, and J. Hwu, "Secondary transmission power of cognitive radios for dynamic spectrum access," in *Proc. of ChinaCom*, 2008, pp. 1211–1215.

[146] J. Tang and X. Zhang, "Cross-layer-model based adaptive resource allocation for statistical QoS guarantees in mobile wireless networks," *IEEE Transactions on Wireless Communications*, vol. 7, no. 6, pp. 2318–2328, June 2008.

[147] Y. Shi and Y. T. Hou, "Optimal power control for multi-hop software defined radio networks," in *Proc. of IEEE INFOCOM*, May 2007, pp. 1694–1702.

[148] L.-C. Wang and A. Chen, "Effect of location awareness on concurrent transmissions for cognitive ad hoc networks overlaying infrastructure-based systems," *IEEE Trans. Mobile Computing*, vol. 8, no. 5, pp. 577–589, May 2009.

[149] N. Hoven and A. Sahai, "Power scaling for cognitive radio," in *Proc. of International Conference on Wireless Networks, Communications and Mobile Computing*, 2005, pp. 250–255.

[150] A. Behzad and I. Rubin, "Impact of power control on the performance of the ad hoc wireless networks," in *Proc. of IEEE INFOCOM*, March 2005, pp. 102–113.

[151] J. Tang and X. Zhang, "Quality-of-service driven power and rate adaptation for multichannel communications over wireless links," *IEEE Transactions on Wireless Communications*, vol. 6, no. 12, pp. 4349–4360, December 2007.

[152] FCC, "Unlicensed operation on the tv broadcast bands," May 2004.

[153] X. Zhang, J. Tang, H.-H. Chen, S. Ci, and M. Guizani, "Cross-layer-based modeling for quality of service guarantees in mobile wireless networks," *IEEE Communications Magazine*, vol. 44, no. 1, pp. 100–106, January 2006.

[154] Y. Song, J. Xie, and X. Wang, "A novel unified analytical model for broadcast protocols in multi-hop cognitive radio ad hoc networks," *to appear in IEEE Transactions on Mobile Computing*, 2013.

[155] Y. Song and J. Xie, "Finding out the liars: Fight against false channel information exchange attacks in cognitive radio ad hoc networks," in *Proc. IEEE GLOBECOM*, 2012, pp. 1–5.

APPENDIX A: PUBLISHED AND SUBMITTED WORKS

1. **Y. Song**, J. Xie and X. Wang, "A Novel Unified Analytical Model for Broadcast Protocols in Multi-hop Cognitive Radio Ad Hoc Networks, " to appear in IEEE Transactions on Mobile Computing (TMC), 2013.

2. **Y. Song** and J. Xie, "A Distributed Broadcast Protocol in Multi-hop Cognitive Radio Ad Hoc Networks without a Common Control Channel, " in Proc. IEEE INFOCOM, March, 2012.

3. **Y. Song** and J. Xie, "ProSpect: A proactive spectrum handoff framework for cognitive radio ad hoc networks without common control channel, " IEEE Transactions on Mobile Computing (TMC), 2012.

4. **Y. Song** and J. Xie, "Finding Out the Liars: Fight Against False Channel Information Exchange Attacks in Cognitive Radio Ad Hoc Networks," in Proc. IEEE GLOBECOM, 2012.

5. **Y. Song** and J. Xie, "A QoS-based broadcast protocol for multi-hop cognitive radio ad hoc networks under blind information," in Proc. IEEE GLOBECOM, pp. 1-5, December, 2011.

6. **Y. Song** and J. Xie, "Performance Analysis of Spectrum Handoff for Cognitive Radio Ad Hoc Networks without Common Control Channel under Homogeneous Primary Traffic, " in Proc. IEEE INFOCOM, April, 2011.

7. **Y. Song** and J. Xie, "On the Spectrum Handoff for Cognitive Radio Ad Hoc Networks without Common Control Channel," Book Chapter of Cognitive Radio Mobile Ad Hoc Networks, Eds. Springer.

8. **Y. Song** and J. Xie, "Common Hopping Based Proactive Spectrum Handoff in Cognitive Radio Ad Hoc Networks," in Proc. IEEE GLOBECOM, pp. 1-5, December, 2010.

9. **Y. Song** and J. Xie, "Proactive Spectrum Handoff in Cognitive Radio Ad Hoc Networks Based on Common Hopping Coordination," in Proc. IEEE INFOCOM Workshops, pp. 1-2, 2010.

10. **Y. Song** and J. Xie, "Optimal Power Control for Concurrent Transmissions of Location-aware Mobile Cognitive Radio Ad Hoc Networks," in Proc. IEEE GLOBECOM, pp. 1744-1749, December, 2009.

11. **Y. Song** and J. Xie, "BRACER: A Distributed Broadcast Protocol in Multi-hop Cognitive Radio Ad Hoc Networks with Collision Avoidance, " under Major Revision for IEEE Transactions on Mobile Computing (TMC), 2012.

12. **Y. Song** and J. Xie, "QB2IC: A QoS-based Broadcast Protocol under Blind Information for Multi-hop Cognitive Radio Ad Hoc Networks," submitted to IEEE Transactions on Vehicular Technology, 2012.